Late Cretaceous and Tertiary Evolution of the Zambezi Delta Basin, Mozambique.

Francisco Vieira.

Thesis submitted to the University of Edinburgh for the degree of Doctor of Philosophy, 1998.

Volume I

This volume contains the main text of the Thesis. Excluded from this volume are isochron and isopach maps derived from seismic data, large tables, well log examples referred to in the main text and some interpreted seismic sections, which are presented as appendices in Volume II of this thesis.

Abstract

The Zambezi Delta Basin is situated in central Mozambique at the present day Zambezi River mouth and extends from onshore to the offshore in a NW-SE direction into the waters of the Mozambique Channel over an estimated area of about 350,000 square kilometres both on- and offshore to the 2500m isobath.

The analyses of approximately 21,700km of 2D seismic reflexion profiles and a well log suite for nine exploration wells supplied by the state oil company of Mozambique (ENH) has enabled an improved seismic stratigraphic model of the late Cretaceous and Tertiary evolution of the Zambezi Delta Basin to be made.

It is demonstrated in this work that sedimentation alternated along a SW-NE zone between two main depocentres separated by the Beira Basement High during their Tertiary development. These depocentres are the Zambezi Delta southwestern depocentre which is bounded to the southeast by the Beira Basement High and the East African Rift Active Extension in the northeast also bounded to the southwest by the Beira Basement High. The latter is suspected to be an active E-W graben structure. This finding is supported by seismological data studied here.

Generally, periods of sedimentation in one depocentre mean a period of non-deposition and erosion in the other depocentre with sediment bypass, reworking and redeposition in the deeper parts of the basin (not covered by seismic data used in this study). Moreover sedimention is controlled by onshore tectonics controlling sediment sources onshore with tectonics, eustatic sea level variations and sediment load controlling basin subsidence and accommodation space in the basin offshore.

Sedimentation generally was restricted to small areas which with time become widespread in the depocentres and at times cover the whole basin. This was the case during the early stages of major depositional cycles. Lithofacies relationships are very complex in the basin due to the sedimentary architecture

produced by the interplay between sea level variation, basin subsidence and sediment supply. The resulting along-strike variability mapped in the Zambezi Delta Basin in this work has the potential not only to impact upon existing sequence stratigraphic models for deltaic settings but also on existing interpretation methods, for example the implications for the recognition of depositional sequences and "systems tracts".

There is evidence of listric growth faulting of Middle Eocene age affecting turbidite deposits in the southwestern part of the basin while long wavelength folding observed in the deeper part of the sedimentary succession raises questions over the possibilities of evaporites or mobile shales underneath the sediment pile. Deltaic sedimentation switched from one depocentre to the other via distributary channels producing marked along-strike variability in the NE-SW direction. Generally sedimentation was more active in the southwestern part of the basin in late Cretaceous until late Middle Miocene when deposition moved into channel deposition in the northeastern part of the basin. From early late Miocene to Recent times various basinward prograding, southwestward-migrating depositional cycles with relatively high sedimentation and basin subsidence rates have characterized the evolution of the basin.

Gravity and magnetic data supplied by GETECH (Leeds University) are used to derive crustal structure and to estimate the depth to magnetic basement beneath the basin. The Free-Air gravity model achieved in this study is a variant of the usual model achieved when crustal thinning and accumulated sediments extend seaward from the coastal area at a rifted passive continental margin. In view of the fact that oceanic magnetic anomalies lie 300km away to the south, thin crust beneath the Zambezi Delta Basin sediments is thought to be continental in origin and stretched immediately prior to breakup in middle Jurassic times.

Acknowledgement

I would like first to thank Dr. Roger A. Scrutton, Prof. John R. Underhill and Dr. Robert Pearce for agreeing to supervise this project, and for providing me with excellent advice throughout the course of the project. No words can express how thankfull I am to them for their help and support throughout the project and during the write up of this thesis.

Special thanks go to Prof. John Underhill and Dr. Sarah Davis for organising and leading an excellent field trip to the Namurian basin of County Clare in western Ireland, where I learned a lot in a very short time.

I also would like to extend my thanks to Peter Nixon (retired Professor and former Director of the Institute of African Geology at Leeds University) for making the necessary arrangements to secure the grant for this study from ODA (The British Overseas Development Agency) and the British Council. Special thanks go to Mrs. Carolyn ffrench Blacke, former director of the British Council office in Maputo for all the efforts she made to ensure that this grant was awarded in 1992.

I thank the ODA for fully funding this research program and the British Council for providing excellent administrative services to the program. I would like to specially thank Mr. Roy White, this program coordinator, from the British Council office in Manchester, for, amongst many things, being very supportive at the critical times when this program had to be extended to allow time to ensure its successful completion. My thanks also go to the University Eduardo Mondlane, in Maputo, Mozambique, for giving me six years leave from my work there to complete this study in the UK.

This project would not have been possible without the generous provision of data from a number of bodies. In particular, I must thank ENH, the state oil company of Mozambique, NPD, the Norwegian petroleum Directorate, especially Dr. Per Blaisted, INTERA, the National Directorate of Geology of Mozambique, GETECH at Leeds University and SGP, the Geological Survey of Portugal in Lisbon for all the geological and geophysical data they provided.

My thanks also go to the departmental computing support team: Ian Chisholm, Shane Voss, Justin McNeil and Chung Lau of the Seismic and Sequence Stratigraphy Group. Special thanks however go to Dan and Christine Bishop for kindly giving me an introduction into the basic and most important features of ZYCOR, the software used to digitise, manipulate interpreted 2D seismic data and produce most of the maps displayed in this thesis.

I also would like to thank the University of Edinburgh's excellent administrative and other internal support services, academic staff and students for providing an excellent working environment and thus making this department a perfect home for me. Thanks to Gerry White for beautifully drafting most pictures displayed in this work. I thank John Turner for running my well data through his subsidence analysis program and for some useful comments on the manuscript of the thesis.

Last but not least, I would like to thank and dedicate this piece of work to my parents and my family for all they mean to me, especially my late father for his encouragement and support through his life. He became my main source of inspiration for big tasks like this. My wife Teresa for being a wonderful mother and an excellent friend of mine, she is my ultimate source of inspiration. My son Francisco Junior for being so nice to his mother and for my daughter Ana for accepting my absence from home for the last five years to allow the completion of the present study. Thanks to my sister in law Albertina Marilia for being a perfect caretaker for Francisco Junior and allowing Teresa to carry on with her duties in Stockholm. To all of them my profound sense of gratitude.

Contents

1 Introduction and project rationale. **1**

1.1 General introduction. 1

1.2 Depositional processes and delta development. 8

1.3 Project rationale and aims. 13

1.4 Structure of the thesis. 14

2 Background. **17**

2.1 Introduction. 17

2.2 The modern Zambezi Delta. 18

2.3 Evolution of the Zambezi River catchment area. 20

2.4 Basin development and sedimentation. 28

2.4.1 Introduction. 28

2.4.2 Rift and drift tectonics. 32

2.4.3 Stratigraphy and Sedimentation. 47

2.5 Continental margin evolution and geology. 58

3 Data description. **61**

3.1 Introduction and exploration history. 61

3.2 Gravity and magnetic data set. 63

3.3 Bathymetric and topographic data. 65

3.4 Seismic and well data set. 66

3.5 Discussion of data quality. 74

3.5.1 Gravity and magnetic data. 74

3.5.2 Bathymetric and topographic data base 75

3.5.3 Seismic and velocity data. 75
3.5.4 Well log data. 76
3.6 Summary. 76

4 Basin evolution and sedimentation. 78
4.1 Introduction. 78
4.2 Well log interpretation and correlation. 80
4.2.1 Foundations for well log interpretation. 80
4.2.2 Well log interpretation and correlation. 83
4.2.3 Well tie to seismic. 95
4.3 Subsidence history. 96
4.3.1 Background. 96
4.3.2 Interpretation of subsidence history data. 97
4.3.3 Summary and discussion. 108
4.4 Structural interpretation of seismic data. 109
4.4.1 Fault distribution. 116
4.4.2 Folding. 119
4.4.3 Structural controls on sedimentation. 119
4.5 Seismic stratigraphic interpretation. 121
4.5.1 Basic principles of seismic and sequence stratigraphy. . . . 121
4.5.2 Definition of boundaries. 122
4.5.3 Sequence boundary types. 124
4.5.4 Methodology used in this work. 130
4.6 Results. 133
4.6.1 Introduction. 133
4.6.2 The Top Basement to Top Cenomanian succession. 136
4.6.3 The Turonian megasequence. 137
4.6.4 The Senonian and Maastrichtian megasequence. 137
4.6.5 The Palaeocene megasequence. 138
4.6.6 The Lower and Middle Eocene megasequence. 138
4.6.7 The Upper Eocene megasequence. 139
4.6.8 The Oligocene megasequence. 139

4.6.9 The Lower and Middle Miocene megasequence. 140
4.6.10 The Upper Miocene megasequence. 142
4.6.11 The Pliocene megasequence. 145
4.6.12 The Quaternary succession. 148
4.7 Rms-velocity and depth conversion. 149
4.8 Relative sea level changes in the southeastern African region. . . 153
4.9 Summary and discussion of results. 157

5 Interpretation of gravity and magnetic data. 160
5.1 Introduction. 160
5.2 Methodology. 162
5.3 Controls on models. 163
5.4 Interpretation of gravity anomaly maps. 164
5.4.1 The Free-Air anomaly map. 165
5.4.2 The Bouguer anomaly map. 167
5.5 Interpretation of the magnetic anomaly map. 169
5.5.1 Regional magnetic anomalies. 169
5.5.2 Integration of gravity and magnetic. 171
5.5.3 2D interpretation of magnetic anomalies. 173
5.6 Gravity data modelling. 180
5.6.1 The standard earth crust model. 180
5.6.2 Gravmag program features. 184
5.6.3 2D gravity modelling. 185
5.7 Summary and discussion of results. 190

6 Controls on Late Mesozoic and Cenozoic basin development. 192
6.1 Introduction. 192
6.2 Late Cretaceous and Cenozoic basin development. 194
6.2.1 The Beira basement high and the East African Rift active extension. 203
6.2.2 Basin depositional architecture. 203
6.2.3 Distributary Channels. 205

6.2.4 Upper slope instability. 208
6.3 Strike variability of depositional units. 209
6.3.1 General characteristics. 209
6.3.2 Zambezi Delta along-strike variability. 211
6.4 Implications for basin stratigraphy, reservoir facies distribution and quality. 218
6.5 Hydrocarbon prospectivity. 220
6.6 Comparison of the Zambezi Delta Basin to other delta basins around the world. 221
6.6.1 Introduction. 221
6.6.2 The Mississippi Delta *(U.S Gulf Coast)*. 223
6.6.3 The Niger Delta *(West Africa)*. 228
6.6.4 The Beaufort-Mackenzie delta *(Alaska-Canada)*. 232
6.6.5 The Western Irish Namurian Basin *(Southwest Ireland)*. . . . 237
6.6.6 Summary and comparison of regional geology. 245
6.6.7 Summary of similarities and differences. 249

7 Conclusions and recommendation for further work. 251
7.1 Summary of main findings. 251
7.2 Comparison with previous work. 254
7.3 Further work. 256

Bibliography 258

List of Figures

1.1 Map summarising surface geology and schematically, the main tectonic elements, showing the main geological provinces of Mozambique. 2

1.2 Schematic W-E geologic and structural section of the Mozambique and Zambezi Delta Basins, crossing just north of Beira. 4

1.3 Map of important geographical reference points and of Mozambique main sedimentary basins (redrawn and modified from Coster *et al.*, 1989). 5

1.4 Schematic map of main structural elements of South East Africa, redrawn and modified from Coster *et al.* (1989). 7

1.5 Ternary diagram of delta types, based on the regime of the delta-front, redrawn and modified from Elliott (1986). 9

1.6 Schematic diagram displaying some variations in delta morphology and facies distribution resulting from variations in the ratio of sedimentation (Rd) to rate of basin subsidence (Rs), redrawn and modified from Curtis (1970). 12

2.1 Geological map of the modern Zambezi Delta (onshore). 19

2.2 Schematic diagrams showing the Zambezi River catchment area (upper diagram) and redrawn and modified after Moore (1988) and Nugent (1989). *Key: Blue lines for rivers.* ***A) Rapids and falls:*** *1 - Chavuma; 2 - Gonya; 3 - Katima Molilo; 4 - Mambova; 5 - Katombora; 6 - Victoria falls.* ***Rift structures and gorges:*** *B - Batoka Gorge; G - Middle Zambezi Basin (Gwembe); K - Kariba Gorge; X - Mana Pools Basin; M - Mupata Gorge; c - Lower Zambezi Basin; CB - Cabora Bassa Gorge.* ***B), blue lines for rivers:*** *1b - Zambezi; 2b - Limpopo; 3b - Cuando; 4b - Chobe; 5b - Cuito-Okavango; 6b - Shire; 7b - Orange; 8b - Olifants; 9b - Cunene.* ***C)*** *1c to 4c - are equivalent to rivers in 2.2b; 5c - Cuito; 9c - Okavango; 10c - Boteti; 11c - Motloutse; 12c - Shashi and Mg - Makgadigadi pans complex.* . 21

2.3 Four diagrams displaying ten curves each showing the variation of the average discharge at the Lupata station in central Mozambique between 1930 and 1969. Series 1 to 10 correspond to years 1930-39, 1940-49, 1950-59 and 160-69 respectively, with line colour corresponding to the discharge variation for each year. 24

2.4 Two diagrams displaying (above) four curves showing variation of the average of the monthly discharge for four ten years periods, recorded between 1930 and 1969 and (below) three curves showing the variation of the overall average, maximum and minimum discharge at the Lupata station. Series 1 to 4 and line colour correspond to the curves for decades 1930-39, 1940-49, 1950-59 and 1960-69 average discharges in the diagram above and series 1 to 3 correspond to the mean, maximum and minimum per month in the diagram below for the time period between 1930-69. 25

2.5 Two diagrams displaying 6 curves each (October to March on the curve above and April to September on the curve below) showing the yearly variation of the monthly average discharge recorded for the Zambezi River at the Lupata station in central Mozambique between 1930 and 1973. Series 1 to 6 and line colours correspond to months from October to March in the diagrame above and series 1 to 6 and line colours correspond to months from April to September in the diagram below. 26

2.6 Diagram displaying three curves showing the variation of the overall yearly average, maximum and minimum discharge recorded for the Zambezi River at the Lupata station in central Mozambique between 1930 and 1973. Series 1 to 3 and line colours correspond to the yearly average, maximum and minimum for the time period between 1930-73. 27

2.7 Plate reconstruction of Gondwanaland by du Toit, redrawn and modified from du Toit (1937). Red lines showing fault distribution. 29

2.8 Plate tectonic reconstruction for the Early Jurassic *(Pliensbachian)* displaying the close fit aproach for plate tectonic reconstruction, redrawn and modified from Scotese (1991). Bold lines are fault lineaments of the East African Rift system and those related to the colison of India against Asia, printed in this diagram only for reference. 30

2.9 Map of types of sedimentary basins in Africa, redrawn and modified from Clifford (1986) and Petters (1991). 31

2.10 The Karoo Rift System in South-east Africa, redrawn and modified from Castaing (1991). 33

2.11 Plate tectonic reconstruction for the Early Cretaceous *(Aptian)*, redrawn and modified from Scotese (1991). Bold lines are fault lineaments. 35

2.12 Plate tectonic reconstruction for the Middle Cretaceous *(Cenomanian)*, redrawn and modified from Scotese (1991). Bold lines are fault lineaments. 36

2.13 Plate tectonic reconstruction for the latest Cretaceous *(Maastrichtian)*, redrawn and modified from Scotese (1991). Bold lines are fault lineaments. 37

2.14 Gondwana break-up rift phase in South-east Africa *(Middle Jurassic - late Cretaceous)*, redrawn and modified from Castaing (1991). . . . 38

2.15 A simplified geotectonic sketch of the East African margin and surrounding ocean basins. Shown are the inferred ocean-continent boundary (dashed line), major fracture zones and associated magnetic anomalies, redrawn and modified from Mascle *et al.* (1987). 40

2.16 Plate tectonic history of southeastern Africa, redrawn and modified from Coster *et al.* (1989). 41

2.17 The East African Rift System, the eastern and western rift branches displaying the main graben and half graben systems and transcurrent fault lineaments (compiled from Darracott *et al.*, 1973; Mougenot *et al.*, 1985; 1986a; b; c; 1989; Petters, 1991; Castaing, 1991). 42

2.18 The topographic expression of the East African Rift System (onshore). Offshore, the sea bed expression of the main lineaments produced by the movement of Madagascar and India and of Antartica and Australia south and southeastwards respectively (courtesy of BP). 43

2.19 The East African Rift System (southern end), redrawn and modified from Castaing (1991). 45

2.20 Structural model of the Lower Zambezi graben, redrawn and modified from Coster *et al.* (1989). 46

2.21 Pan-African orogenic systems and pre-Karoo and Karoo basins of central and southern Africa, redrawn and modified after Lawrence (1989). 49

2.22 Generalized Karoo stratigraphy in the Morondava Basin of western Madagascar, redrawn and modified from Wescott (1988). 50

2.23 Geological schematic map of southeast Africa and the southwestern Indian Ocean, highlighting the main structural elements offshore, compiled from Scrutton *et al.* (1981) and Coffin and Rabinowitz (1987). 52

2.24 Summary of the stratigraphy of the Mozambique Basin, redrawn and modified from Salman and Abdula (1995). 54

2.25 Development and distribution of the Red Beds and the Lupata formations *(Late Jurassic)* in the Mozambique Basin, redrawn and modified from Salman *et al.* (1995). 56

2.26 Reservoir rock formations development and distribution in the Mozambique Basin *(Early Cretaceous - Middle Tertiary)*, redrawn and modified from Coster *et al.* (1989). 57

2.27 A three step model for the development of fracture zones at a passive continental margin, redrawn and modified after Scrutton (1982a,b). 60

3.1 Map of the main geological provinces of Mozambique, highlighting the study area. 62

3.2 Gravity data coverage map for the Zambezi Delta basin and adjacent areas. Data compiled from several vintages and supplied by GETECH, Leeds University. 64

3.3 Magnetic data coverage (shaded)of the study area. Data supplied by GETECH, Leeds University. 65

3.4 Topographic data points distribution onshore and contour data points offshore in the study area. Topographic data are digitised from topographic maps of the study area 66

3.5 Location of the seismic and well data in the study area. This figure includes some wells not used in this work. 67

3.6 A typical stacking velocity profile. Black dots represent velocity sampling points. Average velocity sampling interval, 100 shot-points (2500 m) along the seismic section. 73

4.1 Schematic gamma ray log and spontaneous potential (SP) log curves against depth, illustrating how the sand line and the shale base line are derived, redrawn and modified after Selley, 1992. Sand grain size can be calibrated where core or well cuttings are available. . . 82

4.2 Grain size profiles for nine wells derived from Gamma ray and SP-log, well completion reports. 84

4.3 Key for well logs lithostratigraphic interpretations used in this thesis. 85

4.4 Well to well correlation of geologic time boundaries (geological well tops) SW-NE in the Zambezi Delta Basin. Profile location shown by red line on Fig. 4.5. 88

4.5 Location map of four well to well correlation profiles numbered one to four and of three seismic sections GMC-B, GMC-074 and GMC-080 in the Zambezi Delta Basin. 91

4.6 Well to well correlation of geologic time boundaries SW-NE in the southeast Zambezi Delta Basin. Profile location shown by black line on Fig. 4.5. 92

4.7 Well to well correlation of geologic time borndaries NW-SE in the southeast Zambezi Delta Basin. 93

4.8 Well to well correlation of geologic time boundaries NW-SE in the central part of the Zambezi Delta Basin. 94

4.9 Total subsidence (blue) and sedimentation rate (red) curves for the well Nhanguazi-1 (onshore). 98

4.10 Total subsidence (blue) and sedimentation rate (red) curves for the well Micaune-1 (onshore). 99

4.11 Total subsidence (blue) and sedimentation rate (red) curves for the well Zambezi-1 (offshore). 100

4.12 Total subsidence (blue) and sedimentation rate (red) curves for the well Zambezi-3 (offshore). 101

4.13 Total subsidence (blue) and sedimentation rate (red) curves for the well Sangussi Marine-1 (offshore). 103
4.14 Total subsidence (blue) and sedimentation rate (red) curves for the well Sengo Marine-1 (offshore). 104
4.15 Total subsidence (blue) and sedimentation rate (red) curves for the well Sofala-1 (offshore). 105
4.16 Total subsidence (blue) and sedimentation rate (red) curves for the well Nemo-1 (offshore). 106
4.17 Total subsidence (blue) and sedimentation rate (red) curves for the well Divinhe-1 (onshore). 107
4.18 Schematic display of the top basement fault map derived from seismic data showing the Beira uplift to the south-west and the East African Rift active extention (active graben structure) as defined in this study. 111
4.19 Top Cenomanian fault map derived from seismic data. 112
4.20 Top Turonian fault map derived from seismic data. 113
4.21 Top Cretaceous fault map derived from seismic data. 114
4.22 Top Palaeocene fault map derived from seismic data. 115
4.23 Seismicity map of Mozambique and neighbouring regions (1964-1997) highlighting the southern end of the south-western branch of the East African Rift System. Seismic event body wave magnitude (Mb) 2.0 to 6.8. Size of circles in the map is proportional to body wave magnitude. Data source: ISC (International Seismological Centre) catalogue. 118
4.24 Sketch map of main sediment basins, basement highs and fracture lineaments in existence prior to the breakup of west Gondwana (Late Jurassic), showing the Lower Zambezi graben and the Zambezi Cone, from Dingle and Scrutton (1974). 120
4.25 Relationship of strata to boundaries of depositional sequences, redrawn and modified from Mitchum, *et al.* (1977a). 122

4.26 Seismic patterns that are used in seismic and sequence stratigraphic interpretation to indicate eustatic sea level changes. Types of reflection terminations from Vail (1987). 123

4.27 Type 1 and type 2 unconformities and the condensed section as defined by Vail *et al.* (1984). 125

4.28 Schematic diagram illustrating the definition of systems tracts, from Vail (1987). 126

4.29 Schematic illustration of the concept of seismic facies using typical seismic reflection patterns often observed in seismic sections. Redrawn from Mitchum *et al.* (1977b). 128

4.30 Schematic depositional sequence displaying relationships between seismic architecture and depositional environments and showing the three major controls on stratigraphic architecture (Vail, 1987). 132

4.31 Chronostratigraphic diagram along dip offshore the Zambezi Delta basin, summarized from seismic interpretation. Colours in this diagram have no geological meaning. 134

4.32 Chronostratigraphic diagram in the strike direction offshore the Zambezi Delta basin, summarized from seismic interpretation. . . 135

4.33 Rms velocity contour map of line GMC-064. Contour interval 200 m/sec from 1500 m/s at the sea floor. 150

4.34 Chronostratigraphic diagram in the dip direction offshore the Zambezi Delta basin, summarizing depositional units derived from seismic interpretation. Colour bars express relative lateral extent of depositional units along the NW-SE direction where the colour fill does not bear any geological meaning. 154

4.35 Chronostratigraphic diagram in the strike direction offshore the Zambezi Delta basin, drawn in a way to emphasize the depositional hiatuses and the along-strike vaiability during Neogene times. Colour bars express relative lateral extent of depositional units along the SW-NE direction where the colour fill does not bear any geological meaning. 156

5.1 The Free-Air anomaly map (offshore) of the study area joined with the Bouguer anomaly (onshore) at the coast line. Red line is the modelled gravity profile. A-A and B-B are trends in the gravity field and C and D are positive gravity anomalies 166
5.2 The Bouguer anomaly map, on- and offshore the study area. . . . 168
5.3 The magnetic anomaly map of the study area highlighting the main magnetic anomaly trends in the study area. Red line for positive anomaly trends and green line for negative anomaly trends. 170
5.4 Sketch map summarizing the main structural features mapped from gravity and magnetic data of the study area. 172
5.5 Graphic illustration of the parameters used in the slope and half slope methods for depth estimates from a magnetic anomaly curve, after Telford, Geldart and Sheriff (1990). 175
5.6 The magnetic anomaly map of the study area showing a regional gravity profile (red line) and five magnetic profiles (purple lines) numbered 1 to 5. 176
5.7 Magnetic profile number 2 across the northern part of the East African Rift active extension, interpreted after the empirical maximum slope and half slope methods. 177
5.8 Magnetic profile number 3 across the Beira basement uplift, interpreted after the empirical maximum slope and half slope methods. 178
5.9 The combined topographic and bathymetric map joined at the coast line. Red line is the gravity profile. 181
5.10 The standard crust thickness of the study area derived from topography and bathymetry. 183
5.11 A three step crustal reconstruction of the geological profile modelled with Gravmag. 187
5.12 A Free-Air anomaly profile across the Zambezi Delta Basin, southwestern depocentre. 188
5.13 2D gravity model, generated with Gravmag for a Free-Air profile across the Zambezi Delta Basin. 189

6.1 A schematic geological cross-section across the Zambezi Delta Basin along dip, summarizing the main geological features of the basin, highlighting the stratigraphic subdivision introduced in this study. Offshore part derived from seismic (this study) and onshore part of the section from Salman (Pers. comm. 1997; BP unpublished inhause data). For location see Fig. 6.2. 196

6.2 Schematic top basement fault map derived from seismic data shown on a map summarizing the regional geology of Mozambique and regional fault trends on- and offshore Mozambique. Sections A-A' and B-B' refer to Figs. 6.3; 6.1, respectively. 197

6.3 A schematic geological cross-section across the Zambezi Delta Basin along strike, summarizing the main geological features of the basin, highlighting the stratigraphic subdivision introduced in this study. For location see Fig. 6.2. 199

6.4 Total subsidence and sedimentation rate curves derived from well data for nine wells used in this study. 201

6.5 Tectonic subsidence curves derived from well data for nine wells used in this study. 202

6.6 Map of ocean water circulation in the Mozambique Channel and south-western Indian ocean, redrawn and modified after Martin (1984). 204

6.7 Fault map of top Cretaceous unconformity, displaying the Zambezi Delta slope slumps involving turbidity deposits. Figure zoomed from Fig. 4.21. 208

6.8 Conceptual diagram of delta lobes that creates oppositely arranged stacking patterns depending on location within the depositional system, after Martinsen and Helland-Hansen (1995). 210

6.9 Approximate position of shoreline for various stages of deposition between Turonian and the present day. 212

6.10 Approximate position of strandlines during transgression (Beaupaw transgression) in Montana, northwest United States, after Gill and Cobban (1973). Arrows showing the direction of strandline movement. Shaded area is the complex strandline cross-over zone. 214

6.11 Approximate position of strandlines during the initial phase of regression (Fox Hills regression), after Gill and Cobban (1973).Barbs show the direction of strandline movement. Cross-section AB not shown here. 215

6.12 The maximum basinward shoreline progradation during highstand of ten sequences recognized in the Marsdenian/Yeadonian, redrawn from Church and Gawthorpe (1997). Key: **(a)** R. gracile to R. bilingue (late) sequence highstand shorelines, **b** R. superbilingue to G.cancellatum sequence highstand shorelines and **c** G. cumbriense and G. subcrenatum sequence highstand shorelines. Vertically hatched areas indicate non-deposition of highstand.Horizontal dashes in the far northwest and southeast represent the limits of Marsdenian/Yeadonian outcrop and deposition respectively. Diagonal dashes to the north and east of Derby represent the top Namurian subcrop to Permian. FH, Foston High; SHP, South Humberside Platform; D, Derby; L, Lincoln; M, Manchester; S, sheffield. 217

6.13 Schematic cross-section in dip direction summarizing offshore stratigraphy of the Zambezi Delta Basin. *Arrows represent estimated average summation of aggradation and progradation for distinctive sediment sets.* . . 219

6.14 Location maps of the Mississippi (Gulf coast), Niger, Beaufort-Mackenzie and the Western Irish Namurian Basin. 222

6.15 Schematic tectonic map of the Gulf Coast area, displaying major structural features, salt basins and the Lower Cretaceous shelf edge, and major growth-fault trends (after Curtis, 1986). The cross-section along AA' is displayed on Fig. 6.30. 224

6.16 Schematic conceptual diagrams showing successive stages in development of counter-regional dip and shale uplift during syndepositional faulting, redrawn and modified from Curtis (1970). 225

6.17 Generalized stratigraphic map of the Gulf Coast (from Curtis 1986).226
6.18 Generalized geological map of the west African Coast, including the Niger Delta (after Allen, 1970). 228
6.19 Schematic geological map of the Niger Delta area (after Curtis, 1986). 229
6.20 Generalized stratigraphic map of the Niger Delta (after Curtis, 1986).230
6.21 Map of the main sedimentary environments of the Niger Delta (after Allen, 1970). 231
6.22 Schematic structural cross-sections of the Beaufort-Mackenzie Delta (after Dixon *et al.,* 1992). Cross-section A, across the western part and B, across the southern part of the Beaufort-Mackenzie basin. 234
6.23 Generalized stratigraphic map of the Beaufort-Mackenzie Delta, modified from Curtis (1986). 236
6.24 Schematic geological map of southwest County Claire, western Ireland, after Pulham (1989). 239
6.25 Mud diapir exposed off the coast of western Ireland. 240
6.26 Syn-depositional soft sediment deformation (erosion and folding) in the Namurian Delta in western Ireland. 241
6.27 Syn-depositional soft sediment deformation (erosion growth faulting and folding) in the Namurian Delta in western Ireland. 242
6.28 Syn- and post-depositional deformation features including normal and listric growth faults and sediment folding in the western Ireland Namurian basin. 243
6.29 Syn- and post-depositional deformation features including normal and listric growth faults and sediment folding in the western Ireland Namurian basin. 244
6.30 Schematic dip cross-sections of the Mississippi (A), Niger (B) and Beaufort-Mackenzie (C) after Huff (1980) and Curtis (1986). No horizontal scale is given for B and C. See Fig. 6.15 for the geographic location of section (A). 245

6.31 Schematic map of sediment depocentres of the Gulf Coast area showing eastward and seaward migration of sediment depocentres (after Curtis, 1986). 248

6.32 Paleogeographic map of Tertiary evolution of the Niger Delta (after Short and Staeuble, 1967). 249

List of Tables

3.1 Summary of the recording parameters used for the survey by GECO, 1982. 68

3.2 Summary of the processing flow and main parameters applied to the seismic data by GECO, UK, 1982. 69

3.3 Summary of well log data used in this work, data supplied by ENH and INTERA. 71

4.1 Summary of calculated rms-interval velocity values and of velocity derived geologic interval average densities for the Zambezi Delta Basin. 152

5.1 Summary of measured and of calculated parameters for five 2D magnetic profiles across the Zambezi Delta Basin. 179

Chapter 1

Introduction and project rationale.

Chapter 1 gives a general introduction about the scope of the present study, followed by an outline of the most important depositional processes involved in the development of deltaic systems. The rationale and aims of the present study are then outlined and a brief outline and justification of the structure and order of the thesis is given at the end of the Chapter.

1.1 General introduction.

The Mozambique Basin, of which the Zambezi Delta Basin is part, is a major Mesozoic-Cenozoic basin in southeastern Africa. It extends from latitude $14°S$ south of Pemba in northern Mozambique, where it is a narrow basin, to the south and southwest, widening towards Zululand in South Africa. It includes present day on- and offshore areas of both Mozambique and east South Africa. Fig. 1.1 shows the onshore extent of the Mozambique Basin sedimentary fill generally thickening from west to east towards the Indian Ocean and reaching an estimated maximum sediment thickness of 12km in the Zambezi Delta Basin (Fortes and

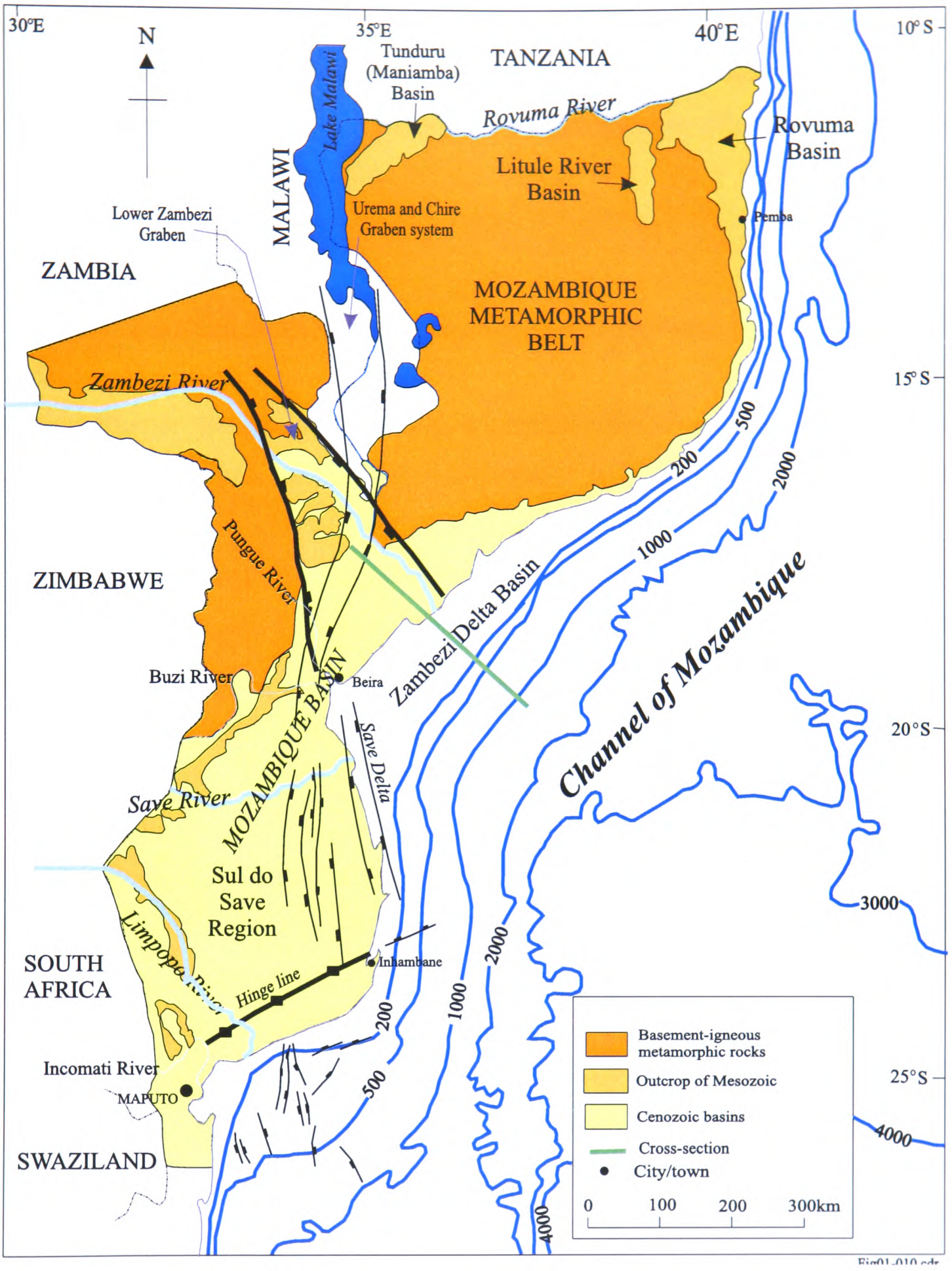

Figure 1.1: Map summarising surface geology and schematically, the main tectonic elements, showing the main geological provinces of Mozambique.

Kihle 1983; Salman *et al.*, 1985; Coster *et al.*, 1989; Salman and Abdula 1995) before thinning once more in an easterly direction into the deep waters of the Mozambique Channel (Fig. 1.2). To the north and northwest the Mozambique

Basin is bounded by the outcroping Precambrian basement and by the Zimbabwe craton respectively, to the west by the Lebombo volcanics of eastern South Africa (Fig. 1.3) and to the east and southeast sediment thickness decreases at the base of the continental slope at about 3000m isobath. Fig. 1.2 is a schematic cross-section designed to show the general picture of the Meso- Cenozoic sediment pile of the Mozambique Basin.

The Mozambique Basin is usually subdivided into four sedimentary provinces (Salman *et al.*, 1985, Coster *et al.*, 1989), the lower Zambezi and Urema Grabens (Fig. 1.1), the "Sul do Save" Region, which includes all the area onshore south of the Save River and the Zambezi Delta Basin (Fig. 1.3) which is the subject of the present study.

The Zambezi Delta Basin is situated at the present day Zambezi River mouth and it extends from onshore to the offshore in a mainly NW-SE direction into the deep waters of the Mozambique Channel (see Figs. 1.1; 1.3). It represents a major accumulation of mainly Jurassic to Recent sediments in which local depocentres varied in importance along depositonal strike through geologic history. Sedimentation has been controlled by the availability of inland sediment sources, the distribution of sediment transport pathways and also by basin subsidence and structural controls during and after the main phases of rifting. Eustatic sea level and climatic changes both became more important in controlling basin sedimentation from Late Jurassic as the basin underwent post-rift thermal relaxation.

It is important to first understand the regional tectonic history of southeast Africa, namely the Karoo Rifting, the break-up of the Gondwana continent and the movement of Madagascar southwards to its present position, and the East African Rift System whose main structural trends and sedimentary basins are summarized in Fig. 1.4. These three tectonic episodes are the most important factors responsible for basin creation and development in eastern Africa. The chronology of these three main tectonic events is very important as the events gave rise to inland and offshore basins and determined the actual position of the various sediment source rocks relative to the basins through time. Associated

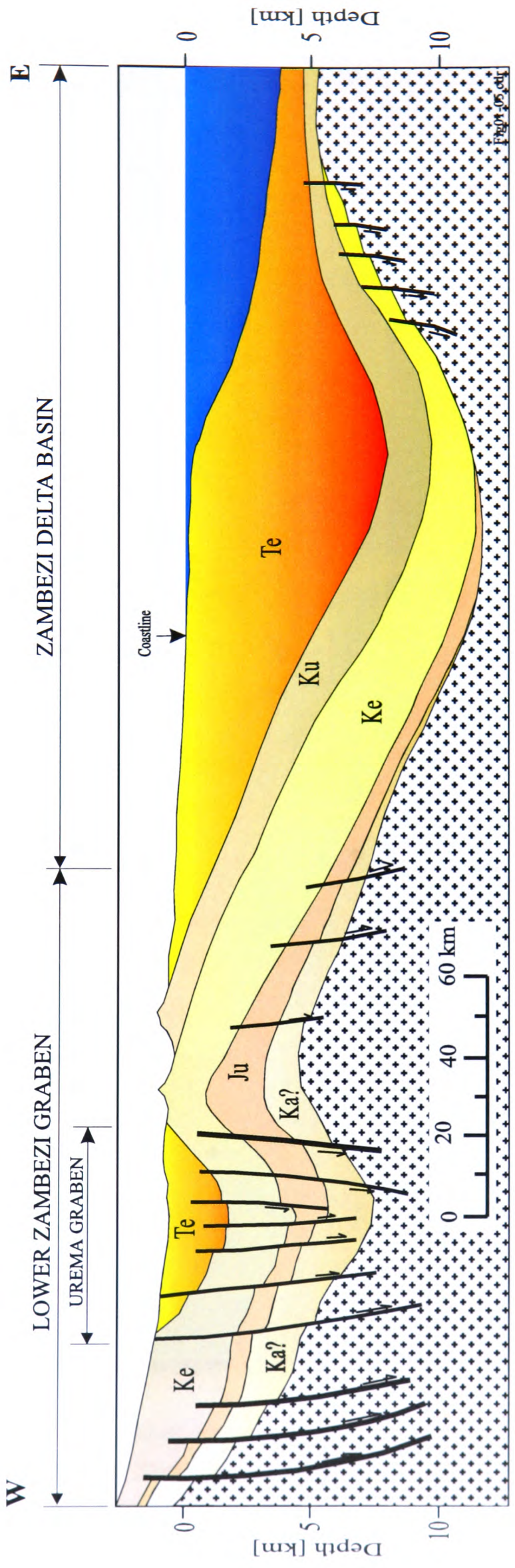

Figure 1.2: Schematic W-E geologic and structural section of the Mozambique and Zambezi Delta Basins, crossing just north of Beira. Key: Ka? - inferred Karoo strata; Ju - Jurassic; Ke - Lower Cretaceous; Ku - Upper Cretaceous; Te - Tertiary and Recent.

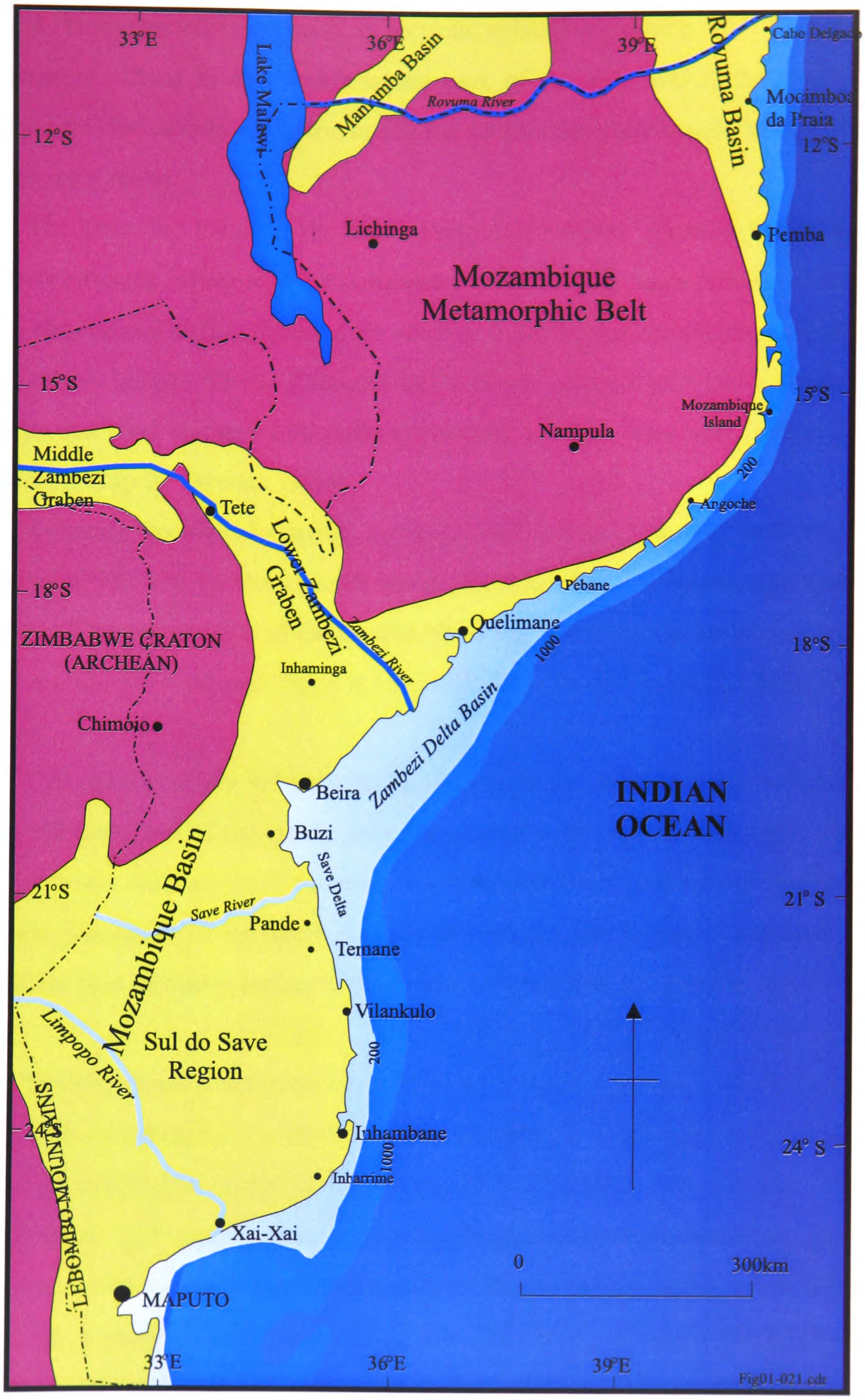

Figure 1.3: Map of important geographical reference points and of Mozambique main sedimentary basins (redrawn and modified from Coster *et al.*, 1989).

vertical crustal movements, such as tectonic subsidence during and after the latest stage of rifting in the northeastern part of the Zambezi Delta Basin (this study) provided accommodation space for sediments while uplift produced sediment source areas.

The interplay between the above tectonics, climatic (onshore) and eustatic sea level changes (offshore) and sediment supply are the main factors which produced the sedimentation patterns we observe today in the various on- and offshore sedimentary basins. In the Zambezi Delta Basin tectonic and basin subsidence, eustatic sea level changes and sediment supply are the dominant factors during deltaic buildup in Tertiary times.

Accurate geological dating, mapping and interpretation of sedimentation patterns is the key to the correct reconstruction of the sedimentary history of a basin. The recognition of facies distributions, sedimentary environments and basin architecture through time is the basis for a better understanding of basin history.

The present study is based on the reinterpretation of well and seismic data in the offshore part of the study area, integrated with onshore well data. Gravity and magnetic data are used to assist in estimating the depth to the Precambrian volcanic basement to establish structural settings and extend structural interpretation into onshore parts of the basin not covered by seismic data studied here.

The objective of this study is to improve present knowledge about the structural and stratigraphic evolution of the Zambezi Delta Basin by producing a seismic-stratigraphic model of the evolution of the basin and a robust tectono-stratigraphic and depositional environments and facies distribution model. Two important deltaic depocentres, displaying evidence of along-strike variability through geological history emerge from this study. The study assesses the relative role of the continental breakup phase versus East African Rift structural trends in controlling and modifying sediment dispersal in and around the Zambezi Delta Basin. Based on results achieved in the present work, the Zambezi Delta Basin is compared to other delta settings around the world in an attempt to establish

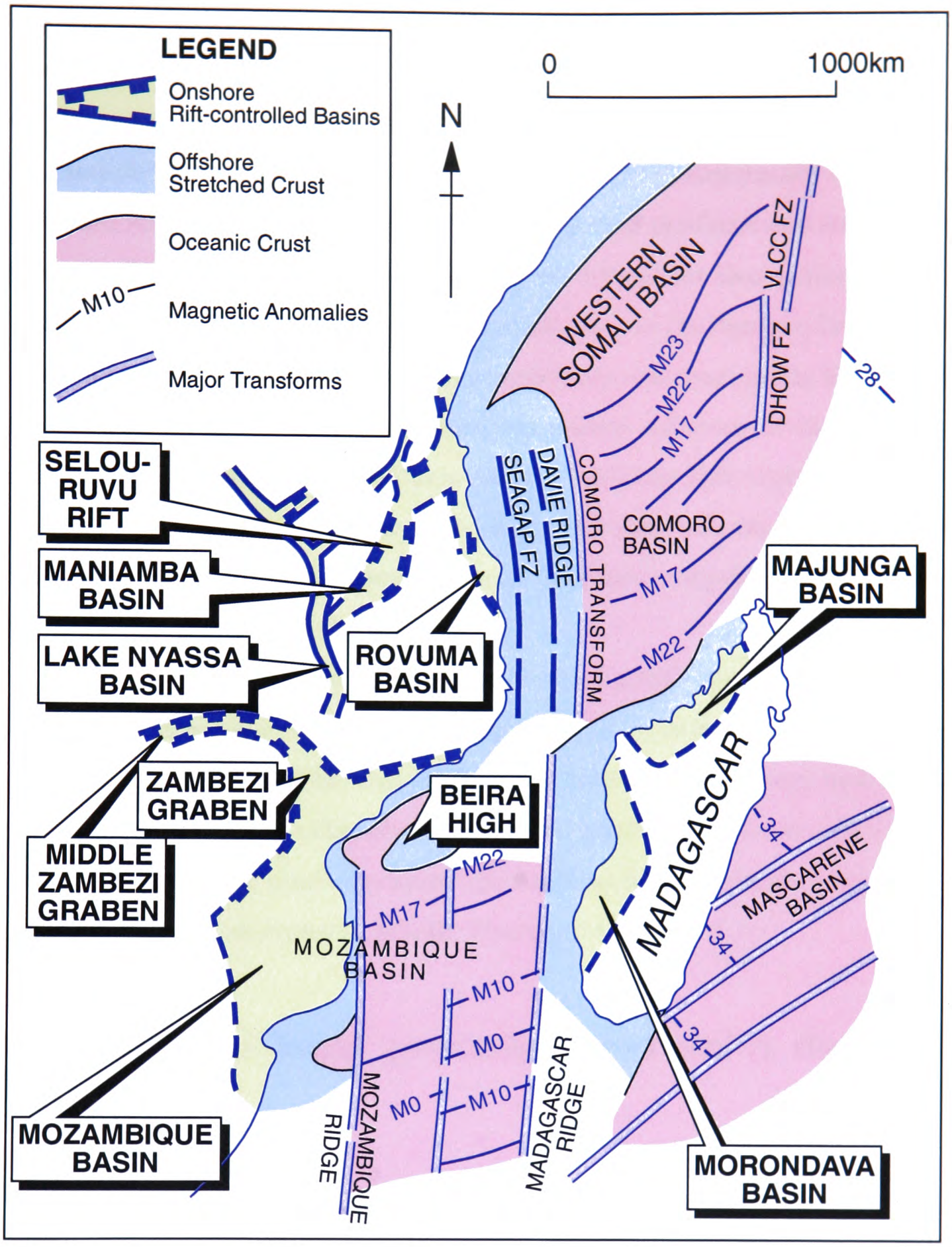

Figure 1.4: Schematic map of main structural elements of South East Africa, redrawn and modified from Coster *et al.* (1989).

similarities and differences in deltaic development and tectonic evolution. Information from wells in and around the area is crucial in providing geological age

and other attributes used to interpret processes leading to facies and depositional environments characterisation.

In summary an improved basin model has been produced and suggests a basin sud-division into two main deltaic depocentres, both structurally controlled. A detailed stratigraphy of the Upper Tertiary has been produced and shows varying sedimentation rates at the two depocentres throughout that period of time. The structural model produced suggests a subdivision of the Zambezi Delta Basin into: i) a southwestern depocentre constrained to the southeast by the Beira basement uplift, and ii) a still active extensional graben structure to the northeast with an E-W orientation, named here the East African Rift (EAR) active extension, accommodating the main sedimentary depocentre in the Zambezi Delta Basin for late Tertiary and Recent sediments and thus controlling sedimentation and erosion in this part of the basin.

It will be demonstrated that the pre-Middle Tertiary stages of basin development were dominated by sediments supplied through pathways located west or southwest of the basin. The East African rift produced the Urema and Chiure Graben system, striking obliquely to the Lower Zambezi graben in a N-S direction. These structural elements caused the Zambezi River to change course to its present day path sometimes in Middle Tertiary times (Fig. 1.1).

1.2 Depositional processes and delta development.

The Zambezi Delta Basin contains a major deltaic depositional system, creating a passive continental margin depocentre in much the same way as the Niger or the Rhone Delta. From studies of deltaic systems worldwide attempts have been made to describe and classify these systems using generic depositional features. In this section a review of this literature is presented.

Considering the delta front, which includes the shoreline and the seaward dipping profile extending offshore, and the delta plain, which is behind the delta front, the two basic components of a delta, a ternary diagram can be used (Fig.

1.5) to define fields of fluvial-, wave- and tide-dominated deltas which can be used to characterize and classify deltas after the most dominant process during deposition (Galloway, 1975; Elliott, 1986). In taking this approach it is important to note that: *(i)* the depositional regime of the delta front is used to define delta type and not the regime of the delta plain; *(ii)* factors other than physical regime are often important in the formation and the nature of deltas (e.g. sediment grain size, water depth and the position of the delta shelf edge); *(iii)* it must be considered that as deltas prograde into the basin, they may evolve through a series of different delta types as the regime, sediment load, climate, basin subsidence or basin configuration (accommodation space) changes; *(iv)* the range of modern delta types known to date may not resemble some ancient deltas not yet studied which may not fit into the modern delta type classification.

The three main depositional processes interacting in deltaic deposition are fluvial, wave and tidal processes. Fluvial processes are a function of the fluvial regime which is determined by the hinterland drainage basin and the fluvial

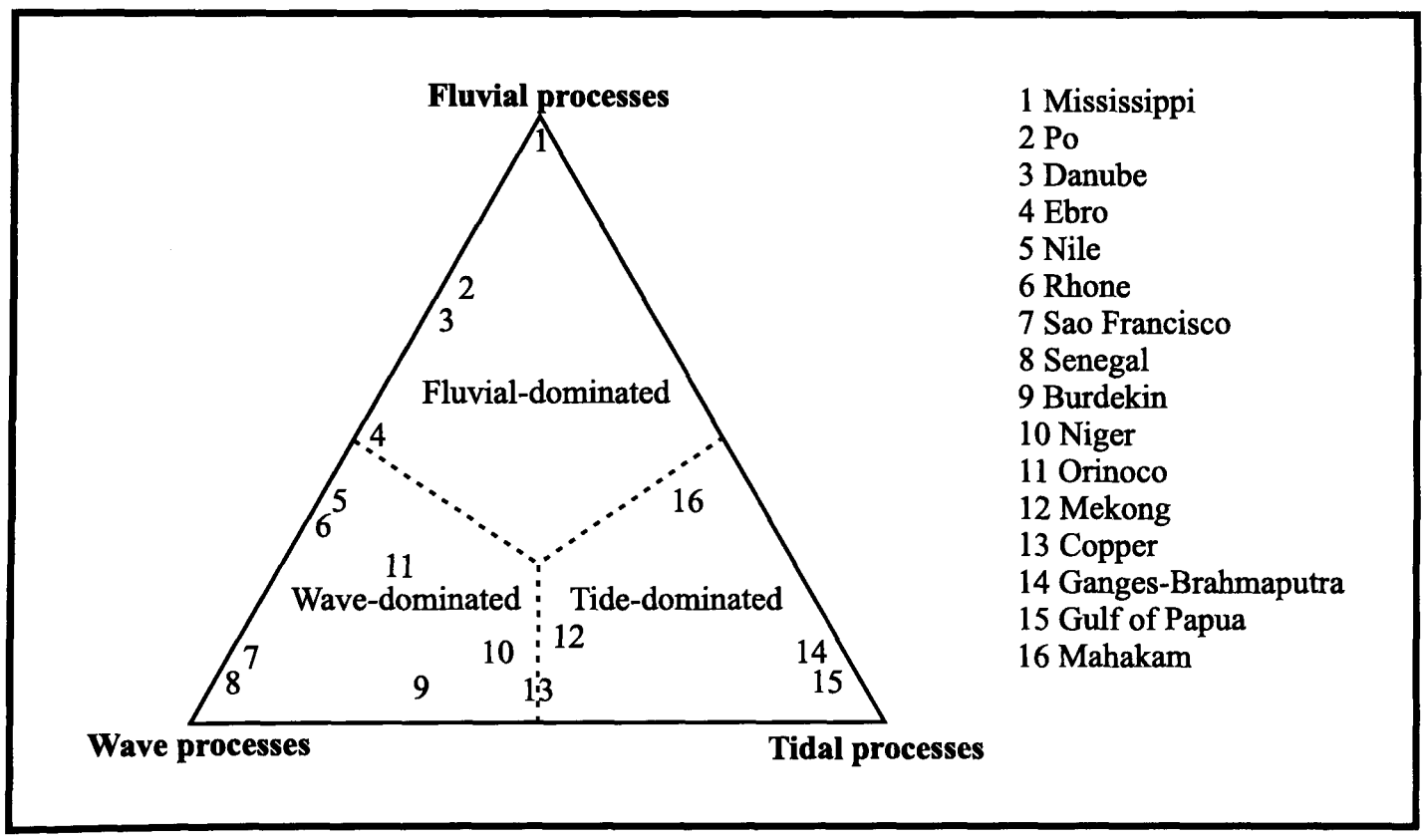

Figure 1.5: Ternary diagram of delta types, based on the regime of the delta-front, redrawn and modified from Elliott (1986).

drainage system, which are both influenced by the interaction of relief, geology and climatic and tectonic behaviour. Important features which influence the fluvial regime in deltas are the relation between the total amount of sediments supplied to the basin and the sediment-reworking ability of basinal processes (wave and wave-induced and tidal processes), the level of sediment supply, discharge fluctuations which can influence the level of sediment supply, tectonic and climatic behaviour in the hinterland and the timing of fluctuations in fluvial discharge in relation to fluctuations in basinal energy regime. Tectonic events can be of major influence to the source position and may substantially modify the fluvial drainage patterns and affect the level of sediment supply.

The development of deltas is influenced by the sediment receiving basin characteristics, such as water depth and salinity, bathymetry, the shape, size and energy regime of the basin, sea-level fluctuations, basin subsidence and tectonics. Salinity of the receiving water body is an important factor determining the relative density of river discharge and basin waters, which controls the manner in which the sediment-laden river discharge is dispersed in the basin.

For rivers entering fresh water basins, depending on the relative density of the river discharge and the receiving basin water body, either an immediate mixing of the water bodies can occurs at the river mouth or the river discharge will flow beneath the basin waters as a density current (river discharge density greater than the density of the receiving water body). In the case of rivers entering saline basins the river discharge, in contrast, may extend into the basin as a buoyantly supported plume because of the higher density of the sea water.

In fluvial dominated delta fronts (Mississippi delta type), delta front sedimentation is dominated by fluvial processes with insignificant interference from basinal processes. Sediment deposition generally occurs at each mouth of a distributary channel and constructs discrete mouth bars which project into the basin. A delta regime of this kind generally results in a fluvial-dominated, birdfoot delta type like the Mississippi Delta of the U.S Gulf Coast.

Wave and tidal processes are part of the basinal regime, as well as semi-permanent, bottom and ocean-surface currents and wind effects which may tem-

porarily raise and lower sea-level. Wave-dominated delta deposition takes place when, at the receiving end, wave processes are capable of reworking and redistributing the sediment load supplied to the delta front. Deltas of this type are wave-dominated deltas characterized by regular beach shorelines with only a slight deflection at the distributary mouth and a relatively steep delta slope. No mouth bar formation takes place and bathymetric contour lines generally are parallel to the shoreline with generally slow progradation involving the entire delta front.

Tide-dominated deltas are characterized by an ill-defined system of tidal current ridges, channels and islands which may extend considerably offshore before giving way to the formation of the delta front slope. Tidal current ridges generally radiating as a funnel-shaped delta distributary system are the main features of this delta type.

However, often tidal currents operate in conjuction with wave processes at the delta front whereby tidal processes remain confined to distributary mouth areas whilst wave processes operate in the remainder of the delta front. As a result, the shoreline is composed of wave-produced beaches, also known as cheniers, separated by tide-dominated distributary channels and mouth areas with the bathymetric contours offshore paralleling the shoreline, e.g. Niger, Burdekin, Orinoco and Mekong deltas (Elliott, 1986) (Fig. 1.5). Fluvial and wave processes might interact if the basinal energy regime is not strong enough to redistribute the discharged sediments and there proceeds only a partial sediment redistribution. This results in an cuspate or arcuate shoreline with localized protuberances in the vicinity of the distributary channel mouths, composed of subdued mouth bars flanked by beach ridge complexes. Examples of deltas of this type are the Danube, Ebro, Nile and Rhone deltas, all of which are located in enclosed seas with moderate wave action.

The resulting vertical and lateral facies geometry in deltaic stratigraphy for a particular geographical and geological setting is effected by the interaction of the river system and waves and tides and the interrelation of variable rates of sediment supply and basin subsidence. Through their interaction these factors produce many variations in delta morphology (Fig. 1.6). Nevertheless the interrelation

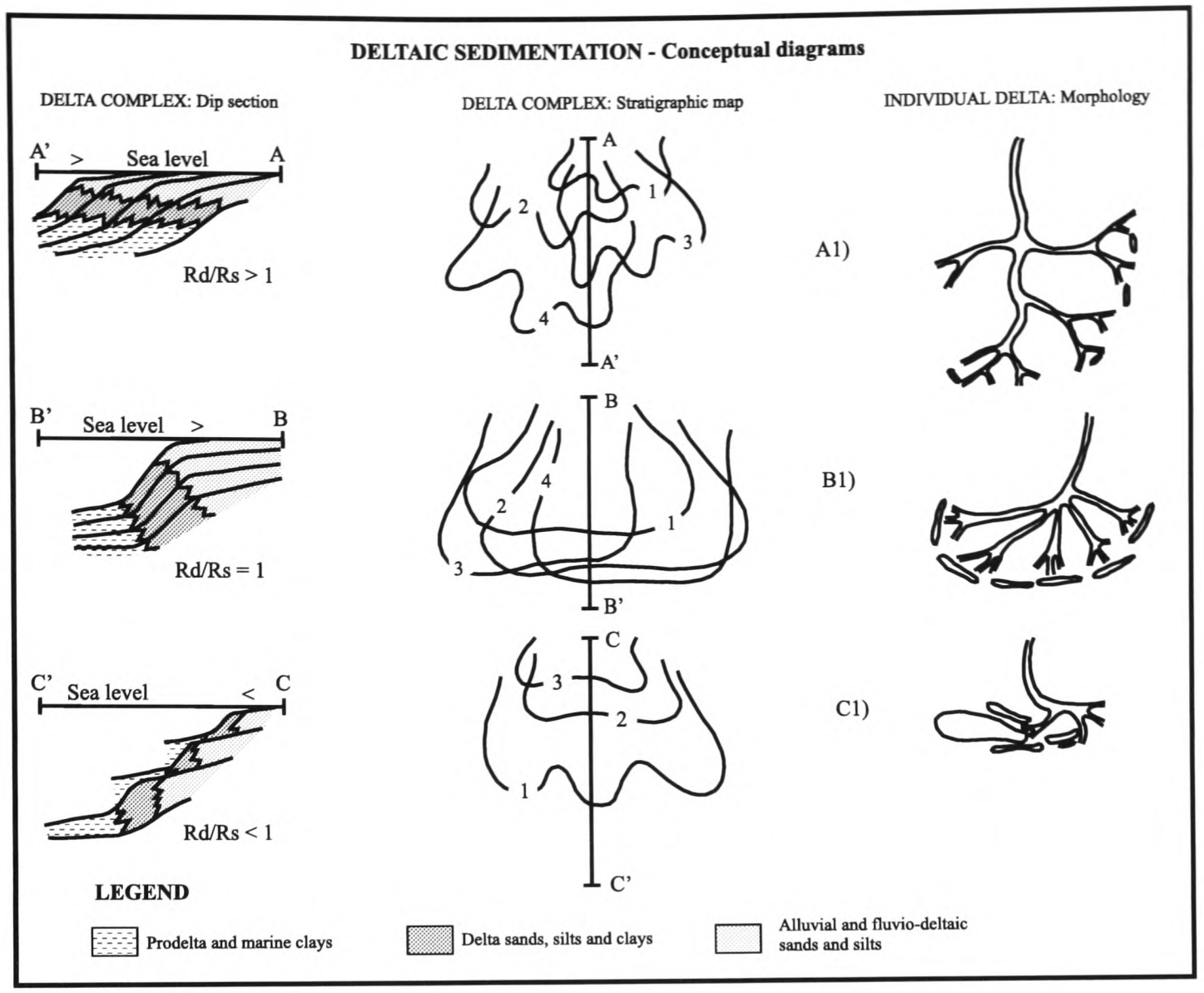

Figure 1.6: Schematic diagram displaying some variations in delta morphology and facies distribution resulting from variations in the ratio of sedimentation (Rd) to rate of basin subsidence (Rs), redrawn and modified from Curtis (1970).

between sedimentation and basin subsidence through geological time remains the most important factor in the development of the three dimensional delta geometry.

Birdfoot delta systems and dip-orientated sand bodies deposited in distributary channels systems are characteristic of river-dominated delta systems.

Arcuate-shaped deltas with along-strike orientated sand bodies, beaches, bars and delta fringe deposits are the product of a wave and tide dominance over the river system. When sedimentation exceeds the rate of basin subsidence basinward regression (seaward progradation) takes place with river dominated deposits emphasized. The lithofacies (formations) of a sequence of this type can be diachronous with basinward younging lithological units. However, sediments

tend to accumulate vertically (aggradation) rather than prograde basinward when sediment supply keeps pace with the rate of basin subsidence through geological time. The lithofacies boundaries of the almost vertically stacked lithofacies in this case can be subvertical. A third variation is obtained when neither aggradation nor progradation takes place, when the rate of sedimentation remains less than the rate of basin subsidence. This situation produces regressive sediment sequences which tend to be retrogradational and a net effect of lateral accretion, with the sand facies forming the base of the sequence and marine shaley facies on top. The sequence, in effect, appears transgressive.

The modern Zambezi Delta morphology is one of a tidal dominated delta complex. However, it will be demonstrated later in this thesis, that the Zambezi Delta, as many other deltas in the world, evolved through varios delta types amongst which the river- and wave-dominated environments were the most important.

1.3 Project rationale and aims.

The Zambezi Delta Basin stratigraphy ranges from Late Jurassic to Recent. Despite its size and long geological history, the basin stratigraphy is often described only within the context of the major Mozambique Basin (Fortes and Kihle 1983; Salman *et al.*, 1985; Coster *et al.*, 1989; Salman and Abdula 1995), which has a north-south extension exceeding 1500km, with only a little mention of its deltaic setting. This approach does not allow an appropriate geological understanding and description of the Basin taking into consideration local events triggered by local and/or sub-regional tectonic and sea level events.

This work is an attempt to improve the understanding of the local and regional geo-history of the area using available geological and geophysical information and using improved seismic stratigraphic interpretation techniques, with a view to establishing an improved basin stratigraphy and petroleum geology for the Zambezi Delta Basin. This is achieved through a detailed study of seismic sections, through mapping of erosional surfaces, channels and channel valleys and

studying lateral channel migration through geological time.

21700km of seismic sections are tied to existing well information in the study area for Upper Cretaceous to Recent sediments. Special attention is paid to the mapping of erosional surfaces, unconformities channels and channel valleys in order to try to predict the most likely distribution of reservoir sands in the basin. This exercise is also crucial in establishing the location of major depositional breaks and their timing and significance in the geological record.

Well data from nine wells in and around the basin will be reinterpreted with the aim of producing a simple stratigraphic framework which will be integrated with seismic data to construct the Zambezi Delta Basin stratigraphic framework. Broad subsidence analysis has been carried out on the nine wells with the aim of assessing the effect of tectonics and sediment load on basin geohistory.

Gravity and magnetic data modelling has been carried out on some profiles across the basin with the aim of estimating depth to geologic basement based on the Airy isostatic compensation and limiting depth assumptions respectively. Results are discussed in Chap. 5 in an attempt to establish the nature of the underlying crust.

Results achieved in this work will be discussed in the context of the main geologic events in the East African region with the aim of assessing the role of main controls on basin evolution. Geologic cross-sections and chronostratigraphic templates will be produced with the aim of illustrating similarities and differences between the results of this work and previous knowledge. Based on the findings of this study, the Zambezi Delta Basin will be compared and contrasted with better known and well described deltaic systems around the world with the aim of drawing similarities and differences in tectonic setting, depositional and evolutionary styles.

1.4 Structure of the thesis.

This thesis is presented in seven chapters and their order is designed to facilitate the reader in following the account from the presentation of the prob-

lem through the data and methodology used, to the results obtained and their discussion.

Chapter 1 has given a general introduction with regard to the scope of the present work, followed by an outline of the most important depositional processes involved in the development of deltaic systems. The rationale and aims of the present study are then outlined and a brief outline and justification of the structure and order of the thesis is given at the end of the Chapter.

Chapter 2 gives a summary of the background regional tectonics and geology of south and eastern Africa and a summary of the main tectonic events in the area and the general basin evolution in East Africa including a brief summary of syn- and post-rift sedimentation in southern east Africa.

Chapter 3 describes the data available to this study, data coverage, quality and reliability, and how these factors will determine the quality of the results of the present work.

Chapter 4 is devoted to the seismic and sequence stratigraphic study and introduces a basin development model for Cretaceous and Tertiary basin evolution. Structural maps have been derived from seismic data and the results are used to constrain and refine gravity and magnetic models generated and discussed in Chapter 5. They also help discuss and constrain the main controls on basin evolution and sedimentary basin architecture in Chapter 6. A relative onlap curve based on mapped events has been produced for the region. Subsidence analysis is carried out on nine wells and discussed in the context of Late Cretaceous and Cenozoic basin development.

Chapter 5 describes how gravity and magnetic data can assist in investigating and modelling deep geologic structures and in estimating depth to geologic basement at depths not penetrated by seismic and well data.

Chapter 6 discusses the controls on basin evolution and sedimentary architecture based on the seismic sequence stratigraphic and well interpretation and gravity and magnetic modelling of Chapters 5 and 4. Finally the implications of present results to basin stratigraphy and reservoir rock distribution are discussed.

Chapter 7 discusses and summarises the main findings of the present work

in the context of other delta basins sited on passive continental margins, draws conclusions and makes some recommendations for further work.

Chapter 2

Background.

This chapter introduces the modern Zambezi Delta and discusses the evolution of the Zambezi River catchment area. A summary of the background information on the most important aspects of regional tectonics and geology of south and east Africa relevant to the present study is presented.

2.1 Introduction.

The Zambezi Delta Basin in central Mozambique is the most important deltaic basin of the coast of Mozambique. There are three more deltaic basins of the coast of Mozambique. These are the Limpopo Delta Basin in the south, the Save Delta Basin, just southwest of the Zambezi Delta Basin, and the Rovuma Delta Basin on the northeast of the country.

According to Salman and Abdula (1995), the Limpopo and the Zambezi Deltas developed at almost the same time and it is believed from this study that the Save Delta may have started to develop earlier some time in Early or Middle Cretaceous times, ceasing some time in Middle Tertiary just after the onset of the East African Rift activity. Sediment supply cut off to the Save River Delta Basin is thought to have happened in Neogene times possibly due to tectonic factors related to the East African Rift in the source area onshore afecting the Save River drainage system, as will be discussed later in the following section.

Parts of the onshore of the Save River Delta located on the flanks of the southern Urema and Chire Graben system (Fig. 1.1) will have been uplifted during the the East African Rift. Evidence gathered in this work shows that there was interference between the sediment units deposited during the late stages of the Save River Delta with those deposited during the early stages of deltaic development in the Zambezi in late Cretaceous and early Tertiary times.

Three major tectonic phases are of great importance for basin creation and evolution in south and eastern Africa. They are the Karoo rift of Permo-Carboniferous age, the continental breakup and sea floor spreading in Middle Jurassic and finally the East African Rift tectonics in Middle Tertiary. These tectonic phases controlled basin formation and stratigraphic development in the on- and offshore of south and eastern Africa between Permian and Recent times.

2.2 The modern Zambezi Delta.

The Zambezi Delta, which is believed from this study to have developed from late Cretaceous (Senonian/Maastrichtian), covers onshore areas north and northeast and west and southwest of thepresent day Zambezi River mouth in central Mozambique (Fig. 2.1). To the offshore the delta extends south and eastwards into the Mozambique Channel building a large continental platform, where the sedimentary strata is thickest, then thinning onto the continental slope and rise in the deep waters of the Mozambique Channel.

The Zambezi Delta is bounded to the north and northeast by the outcroping Mozambique Metamorphic Belt, which is the acoustic basement to the Zambezi Delta Basin. To the west and northwest the N-S striking Urema and Chire Graben system separate the younger deltaic sedimentary units to the east and southeast from the Zimbabwe Craton (Archean) and the outcropping Upper Lupata Formation sandstones respectively.

Geologically the modern Zambezi Delta is characterized by southeastwards younging exposures of sedimentary rock formations, which range from Cenozoic sandstones and sandy chalk to aeolian and fluvial sands, chains of interior stable

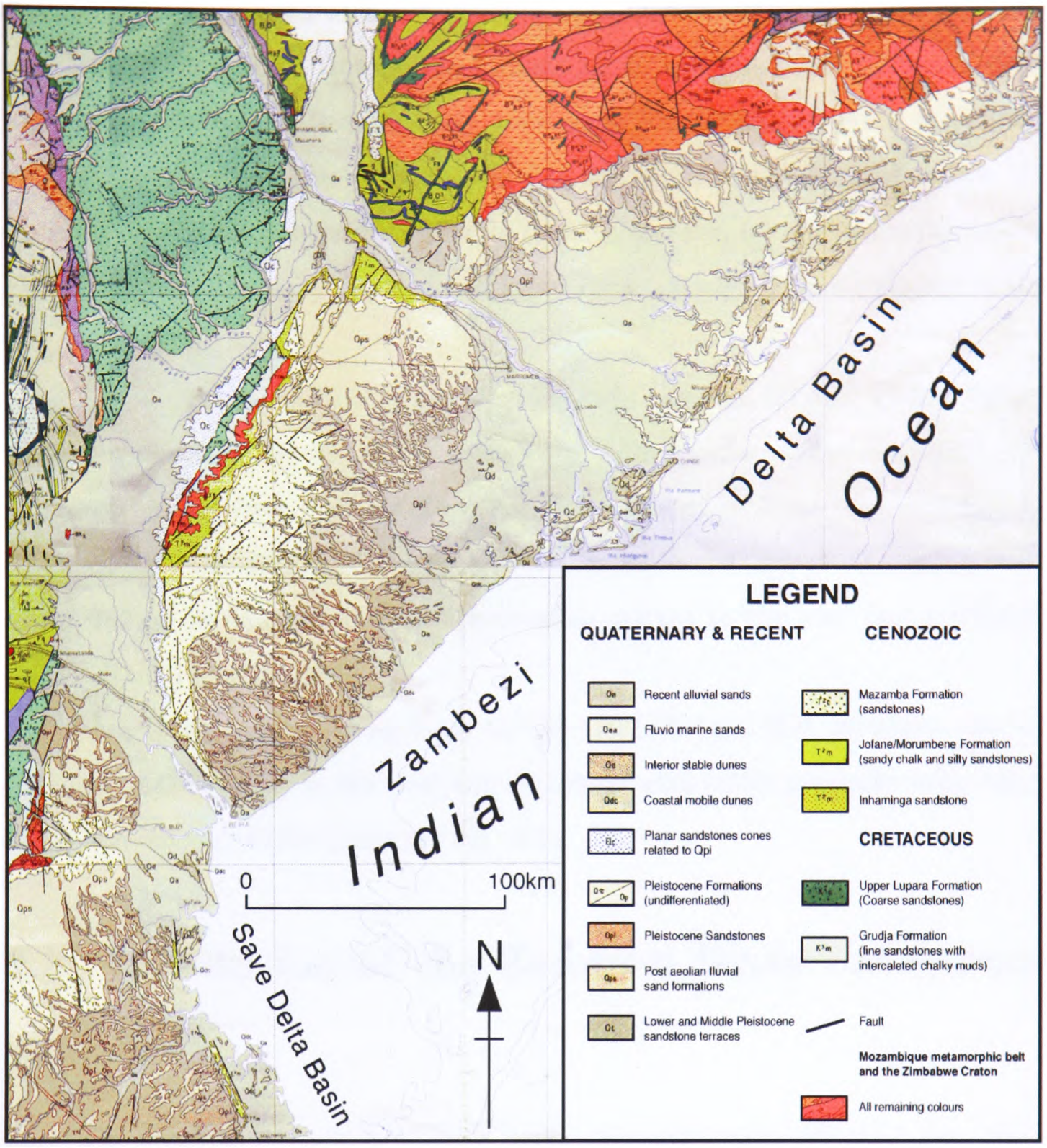

Figure 2.1: Geological map of the modern Zambezi Delta (onshore).

dunes, sandstone terraces with fluvio-marine sands and coastal mobile dunes in the nearshore. To the southwest on Fig. 2.1, Cenozoic and Quaternary formations of the Save River Delta emerge. The Save River Delta deposition interfered at times with sedimentary units deposited from the north and northwest in the Zambezi Delta as is discussed later in this thesis.

Onshore surface geology of the Zambezi Delta Basin shows a significant difference between the southwest and the east and northeast. The southwest is

characterized by an area with outcropping Upper Cretaceous sandstones and volcanics and Cenozoic to Recent sandstones, chalk and fluvio-deltaic formations. The east and northeast is extensively covered by Recent aluvial sands with Quaternary fluvio-marine sands, interior stable and coastal mobile sand dunes. In addition, fluvio-marine sands, and both interior and coastal dunes are characteristic of the east and northeastern coast and they are very little developed in the southwest coast.

In the offshore the delta platform extends between 50 and 120km before the water depth in the shelf area reaches the 200m isobath in the northeast and southwest respectively. While the delta platform widens from the northeast to the southwest the continental slope and rise widen in the opposite direction from about 180km in the southwest to more than 300km in the east and northeast (DNG, IGM 1999, in press).

Structural trends dating back to the East African Rift tectonics can be observed at the surface in the west and northwest with faults generally subparallel to the Urema and Chire grabens (Fig. 2.1).

2.3 Evolution of the Zambezi River catchment area.

The Zambezi River is the fourth largest river and one of the most important rivers of the African continent. It originates in northeastern Angola and flows through Angola, Zambia, Namibia, Botswana, Zimbabwe and Mozambique where it enters the Indian Ocean (Fig. 2.2A). In its course of about 2000km, the Zambezi River drains an area of about 1540000km^2 in southern central Africa between northeastern Angola and the Indian Ocean in central Mozambique (Drummond, 1978, Nugent, 1989, 1991). However, by evaluating the evolution of the Zambezi River catchment area, it soon becomes clear that for a large river system like the Zambezi, various interacting factors become of great importance and must be

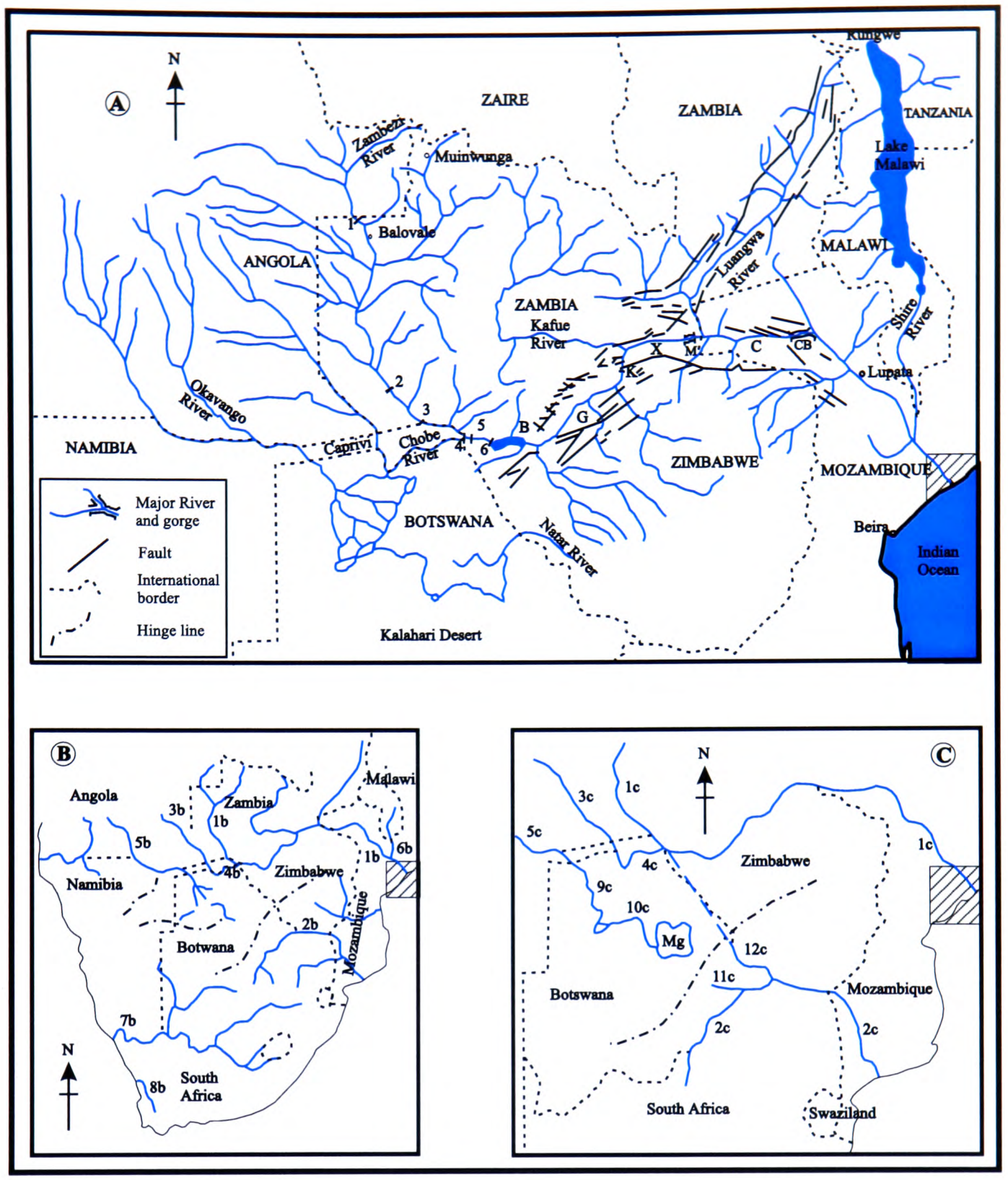

Figure 2.2: Schematic diagrams showing the Zambezi River catchment area (upper diagram) and redrawn and modified after Moore (1988) and Nugent (1989). *Key: Blue lines for rivers.* ***A) Rapids and falls:*** *1 - Chavuma; 2 - Gonya; 3 - Katima Molilo; 4 - Mambova; 5 - Katombora; 6 - Victoria falls.* ***Rift structures and gorges:*** *B - Batoka Gorge; G - Middle Zambezi Basin (Gwembe); K - Kariba Gorge; X - Mana Pools Basin; M - Mupata Gorge; c - Lower Zambezi Basin; CB - Cabora Bassa Gorge.* ***B), blue lines for rivers:*** *1b - Zambezi; 2b - Limpopo; 3b - Cuando; 4b - Chobe; 5b - Cuito-Okavango; 6b - Shire; 7b - Orange; 8b - Olifants; 9b - Cunene.* ***C)*** *1c to 4c - are equivalent to rivers in 2.2b; 5c - Cuito; 9c - Okavango; 10c - Boteti; 11c - Motloutse; 12c - Shashi and Mg - Makgadigadi pans complex.*

considered. Amongst the most important are the tectonic evolution of the catchment area, climatic change and the possible interaction between adjacent river systems due to tectonics through geologic time (du Toit, 1933; Wellington 1955; Moore 1988; Nugent 1989, 1991).

The Zambezi River system, according to its geographical and tectonic evolution is subdivided into three main sections. These are the upper, middle and lower Zambezi (Moore 1988). The Lower Zambezi river system which has the Luangwa and the Chire rivers as the main tributaries, is known to have stayed fairly consistent river system through time, while the middle and the upper Zambezi river systems at times have been separated from the lower Zambezi section at times when landscape deformation due to tectonic uplift caused the drainage systems to reshape. During periods of separation between the three sections of the river system, there is evidence that the upper Zambezi river system has been part of the Limpopo river system (Fig. 2.2B,C). This was the case during some stages of the Limpopo Delta development prior to the onset of the East African Rift which produced several topographic features (hinge lines) in southern central Africa, one of which caused the upper Zambezi section to separate from the Limpopo, thus causing a relative slowdown in sedimentation due to diminished sediment supply to the Limpopo Delta (Fig. 2.2B,C) (Moore 1988).

The Okavango River system just west of the upper Zambezi section, flows into the Okavango Lake in Botswana northwest of the Kalahari desert and is known to have joined the the Zambezi river system during periods of severe rains in southern central Africa which may have caused the lake to overspill and flood adjacent areas. These periods may possibly correlate with periods of high sedimentation rates in the Zambezi Delta during post East African Rift onset or in the Limpopo Delta prior to the East African Rift.

However, since human intervention to the environment began with terrain cultivation, deforestation and dam building amongst other activities, the behavior of river systems and their drainage and catchment areas became significantly affected by such activities. Therefore, it is important to incorporate the possible effects to the drainage system evaluation using drainage and discharge data

collected during the last few centuries.

Data collected from the Zambezi River at the Lupata station, downstream the Cabora Bassa Dam in northwestern Mozambique between 1930 and 1973, are used here to assess the Zambezi river behaviour during the above period with a view to making some inference into the past. However, it must be acknowledged that three major dams (Kariba in Zimbabwe, Kafue in Zambia and Cabora Bassa in Mozambique) were build at three location in the river and its tributaries, which will have affected sediment discharge downstream and caused artificially low discahrge values at the Lupata station. Therefore it is important to note that the Kariba, the first dam to be build on the Zambezi, began filling up in December, 1958. This is the reason why the monthly average discharges at the Lupata station are relatively low for the entire 1958/59 rainy season, compared to previous and subsequent years (Fig. 2.3).

The Kafue and the Cabora Bassa Dams began filling in January 1971 and December 1974 respectively and fall outside the period considered for most of the analysis undertaken here.

At the Lupata station, most of the discharge (about 51%) is from the Kariba Dam with an estimated drainage area of $518000km^2$, followed by the Cabora Bassa Dam contributing about 23% drained from an estimated area of $231000km^2$, with the Kafue Dam contributing about 15% from a drainage area of about $151000km^2$. The area drained into these three dams is $900000km^2$ about 89% of the total drainage area of the Zambezi of about $1017000km^2$. The remaining 11% are contributed by the drainage basin downstream the Lupata station, mainly as part of the Chire River drainage system which links the Lake Malawi and the Zambezi River.

From Fig. 2.3, a complex picture of the Zambezi River discharges at the Lupata station emerges for the period between 1930 and 1969. However, it is clear from the above diagram that during this time period the rainy season varyed between November and May with some irregular behavior during the sixties decade. It is also clear from Fig. 2.3 and Fig. 2.4 that the peak of the rainy season over

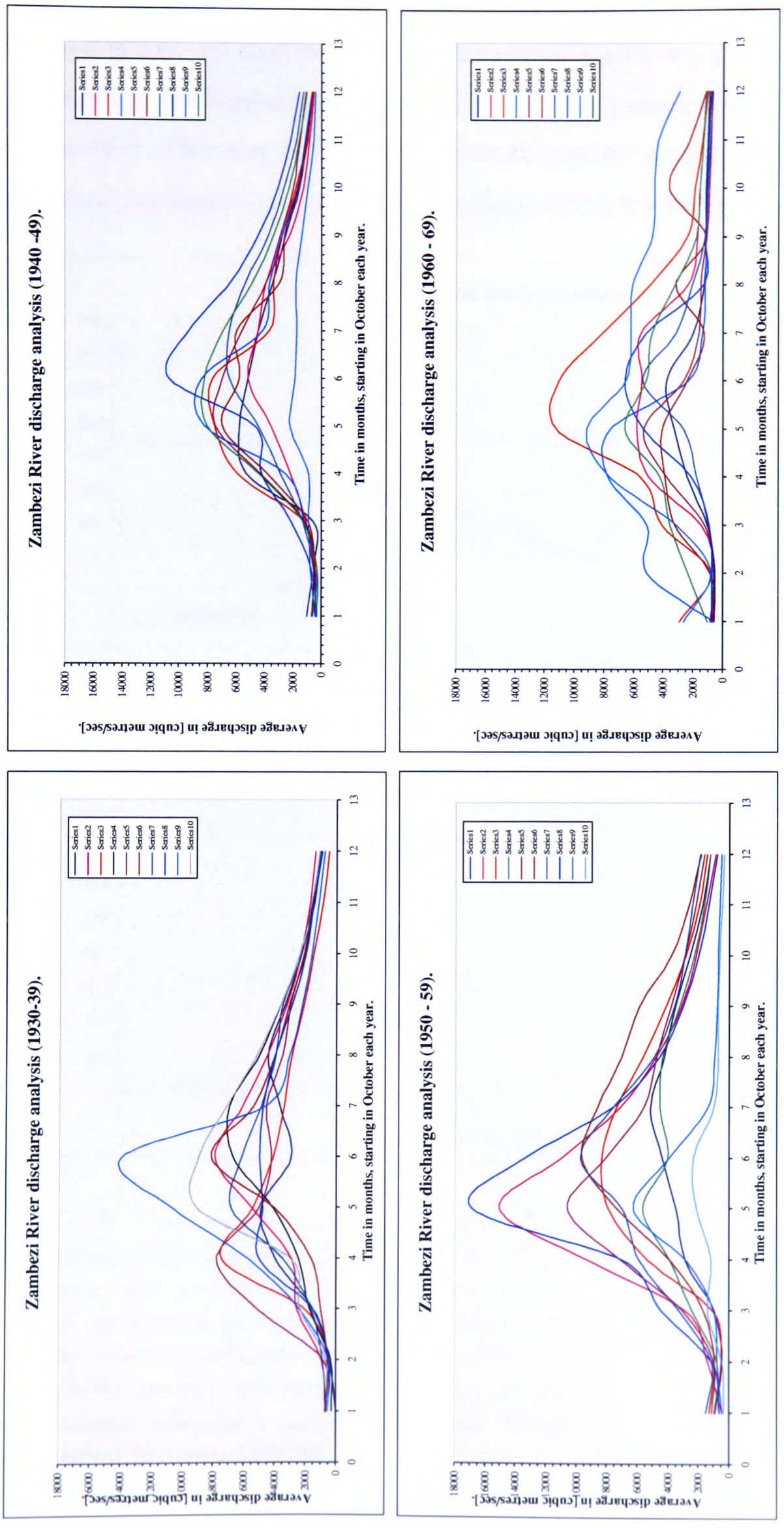

Figure 2.3: Four diagrams displaying ten curves each showing the variation of the average discharge at the Lupata station in central Mozambique between 1930 and 1969. Series 1 to 10 correspond to years 1930-39, 1940-49, 1950-59 and 160-69 respectively, with line colour corresponding to the discharge variation for each year.

the fourty years period lies betwen November and May. However, it can be observed in Fig. 2.5 that within the rainy period March is a month during which generally low discharges have been recorded at the Lupata station over a fourty years period. This may be due to a relatively consistent pause in rain fall in the hinterland catchment area which may indicate relatively stable over the period of

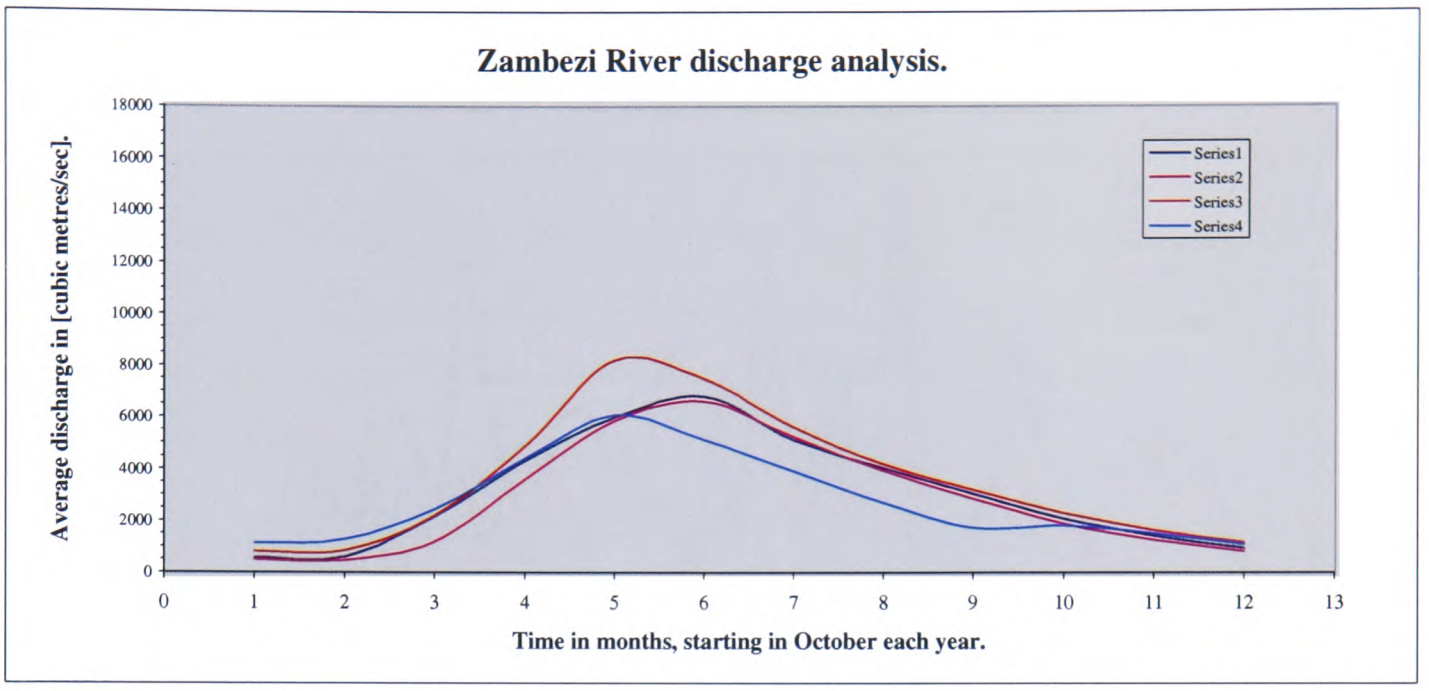

Figure 2.4: Two diagrams displaying (above) four curves showing variation of the average of the monthly discharge for four ten years periods, recorded between 1930 and 1969 and (below) three curves showing the variation of the overall average, maximum and minimum discharge at the Lupata station. Series 1 to 4 and line colour correspond to the curves for decades 1930-39, 1940-49, 1950-59 and 1960-69 average discharges in the diagram above and series 1 to 3 correspond to the mean, maximum and minimum per month in the diagram below for the time period between 1930-69.

observation. Minimum discharge at the Lupata station is generally observed between July and October and corresponds to the dry season for most of the drainage basin.

From Fig. 2.4 it can be said that for the fourty years period a seasonal discharge variation is observed related to dry and rainy seasons each year. However,

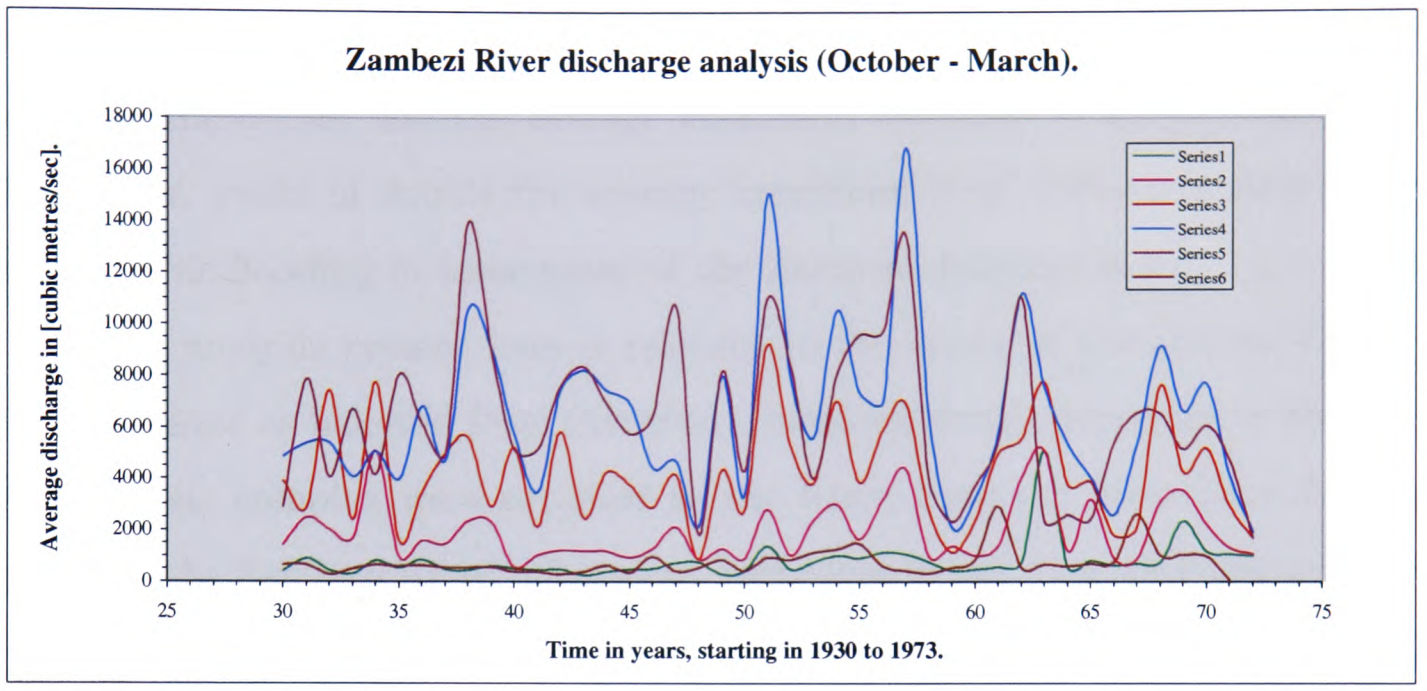

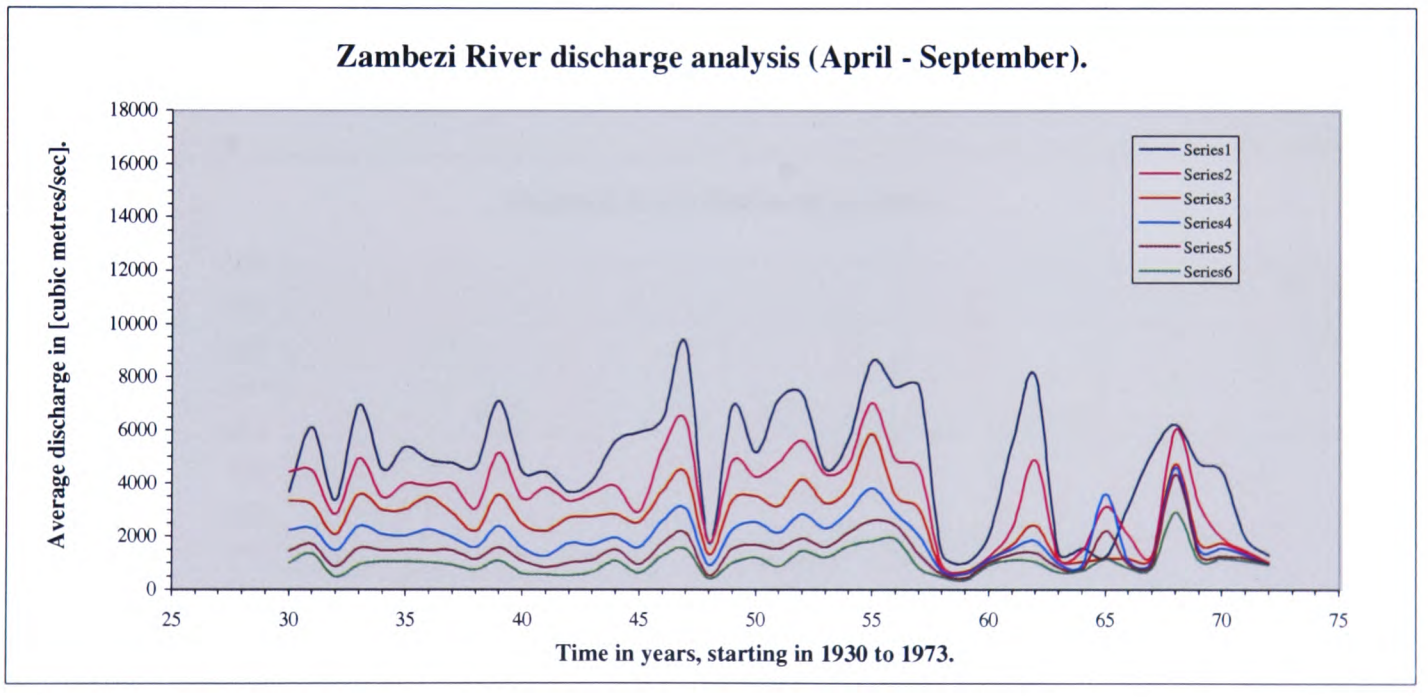

Figure 2.5: Two diagrams displaying 6 curves each (October to March on the curve above and April to September on the curve below) showing the yearly variation of the monthly average discharge recorded for the Zambezi River at the Lupata station in central Mozambique between 1930 and 1973. Series 1 to 6 and line colours correspond to months from October to March in the diagrame above and series 1 to 6 and line colours correspond to months from April to September in the diagram below.

in Fig. 2.6 the yearly average and maximum discharge curves reveal periodical discharge peaks and lows, probably indicating possible cyclic climatic variations which considerably affected discharges of the Zambezi River throughout time. These may correspond to cyclic dry and rainy seaons with a perodicity of three up to seven years well known in various parts of central and southern Africa through cyclic records of poor agricultural results during the drought years and flooding disasters during years of heavy rains. The average minimum discharge is about $100m^3/sec$ and the average maximum discharge is about $9000m^3/sec$. Thereafter, peaks of double the average maximum (Fig. 2.6) are a clear sign of catastrophic flooding in some areas of the Zambezi drainage basin.

The analysis present here is relevant to the study of the ancient Zambezi Delta because as believed from this study, most sediments deposited in the Zambezi Deltaic complex were supplied to the basin from the hinterland drainage basin via the Zambezi River. Therefore, variations in the river discharges through geologic time will have been of great significance in producing the sedimentation pattern we observe today. The strike variability of depositional sequences, one

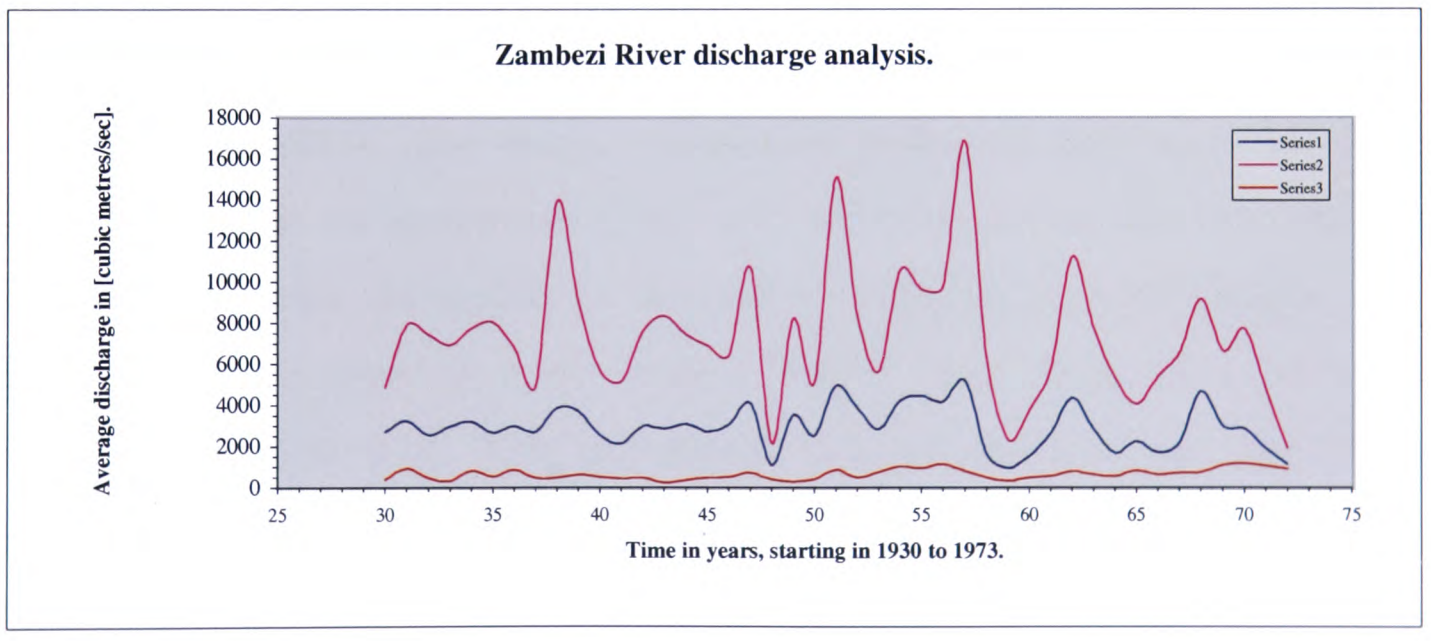

Figure 2.6: Diagram displaying three curves showing the variation of the overall yearly average, maximum and minimum discharge recorded for the Zambezi River at the Lupata station in central Mozambique between 1930 and 1973. Series 1 to 3 and line colours correspond to the yearly average, maximum and minimum for the time period between 1930-73.

of the main results of this study, discussed later in chapter 4, is a direct result of tectonics and climatic variation in hinterland source area, causing spacial and temporal variation of sediment supply in the basin. For example Zambezi deltaic deposition was most affected by tectonic events in the Zambezi River catchment area in Tertiary to Recent times.

Although the observation period at the Lupata station is relatively short to be used to infer back to Tertiary and Quaternary time, future detailed studies on Recent sediments of the delta top will point to the way sediments have been distributed in the past in older sections of the delta basin.

2.4 Basin development and sedimentation.

2.4.1 Introduction.

Most offshore basins of east Africa developed during continental breakup, which started in Middle Jurassic. Plate tectonics history of eastern Africa has been a focus for discussions for many years, chiefly surrounding the controversy on Madagascar's position prior to continental breakup and later drift in Middle Jurassic times.

Du Toit (1937), after some considerable geological field work, produced the plate tectonic reconstruction (Fig. 2.7) which would became the centre of attention for further discussions on the matter. Subsequent improvements to du Toit's model were made by many workers (Flores, 1970; King, 1973; Al-Kasim *et al.,* 1985; Mascle *et al.,* 1987 and others) as more geological and geophysical data became available in the Indian Ocean. Smith and Hallam (1970) produced a computerized reassembly of Gondwanaland using the 500m isobath for best fit of the plates, but it failed because it overlooked the geological evidence for a looser continental fit (King, 1973).

Some workers, for lack of offshore geologic and geophysical evidence, argued for a fit of Madagascar close to the eastern coast of Mozambique, advocating a later southeastwards movement of Madagascar from Africa to its present position.

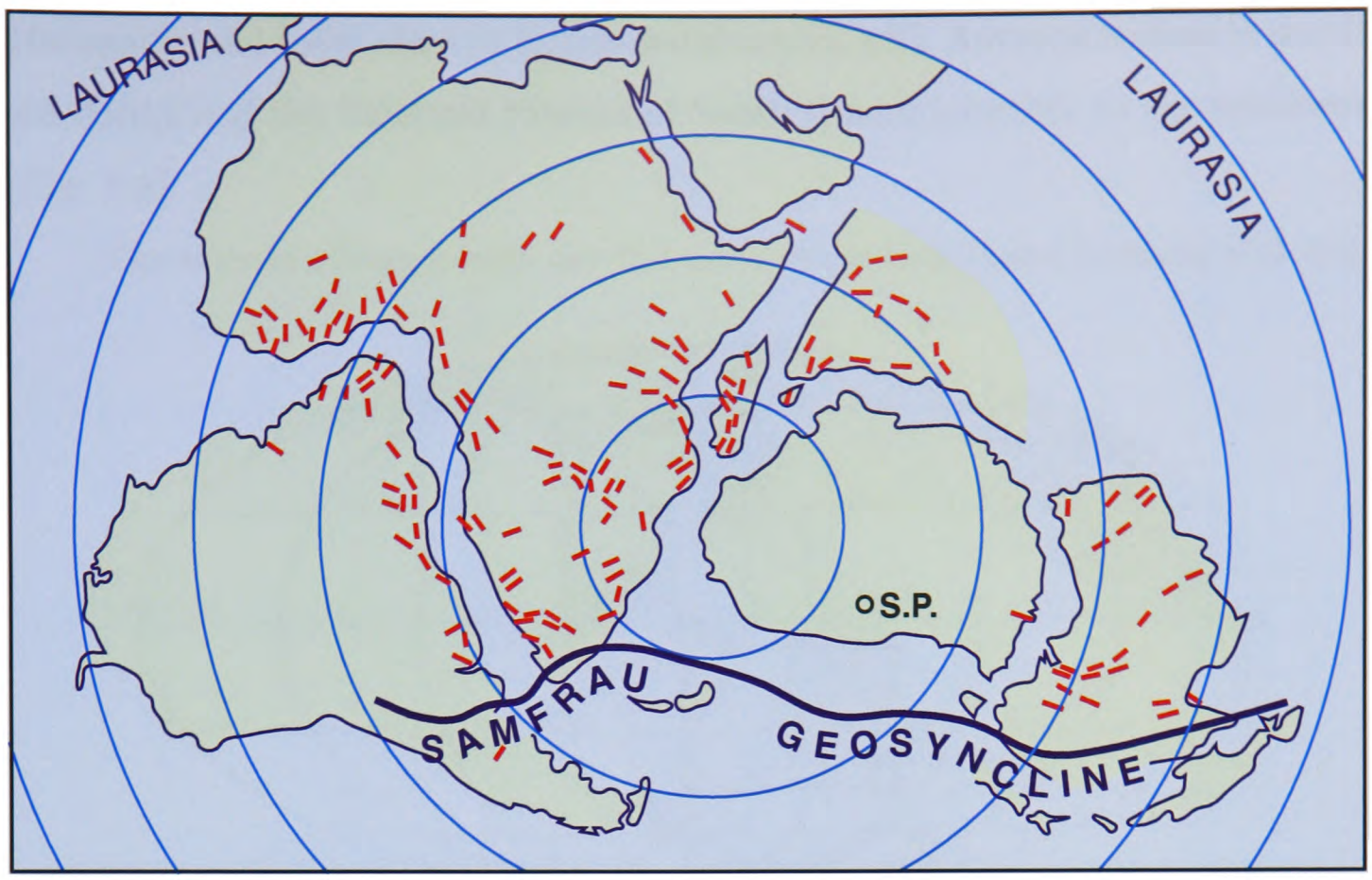

Figure 2.7: Plate reconstruction of Gondwanaland by du Toit, redrawn and modified from du Toit (1937). Red lines showing fault distribution.

But as more geological and geophysical data from the Mozambique Channel and the Indian Ocean became available it would be proved (Scrutton, 1978; Rabinowitz *et al.,* 1981; Al Kasim *et al.,* 1985; Coster *et al.,* 1989; Scotese, 1991; Salman *et al.,* 1995) that actually Madagascar's position prior to Gondwanaland breakup and plate dispersal was east of Kenya and Somalia in the north.

Despite the various subsequent attempts made to improve du Toit's plate tectonic model from 1937 the present day model of consensus still supports to some extent the early suggestions of du Toit (1937), that prior to continental breakup Madagascar was positioned east of the coast of Kenya and Somalia,with India and the Seychelles to its northeast and Antartica and Australia to the south and southeast. Scotese (1991) produced a set of plate tectonic reconstruction maps of the earth which discuss the most important tectonic events between early Jurassic and late Cretaceous in eastern Africa, including the opening of the Indian Ocean and the closure of the Neotethys ocean in northeast Africa.

His reconstruction at early Jurassic time (Pliensbachian), 195 Ma, shows

Madagacar and India close to Kenya and Somalia, with Antarctica close to southern Africa and the Falkland Plateau of South America further to the southwest (Fig. 2.8).

Three main rifting events are the most important Post-Devonian tectonic

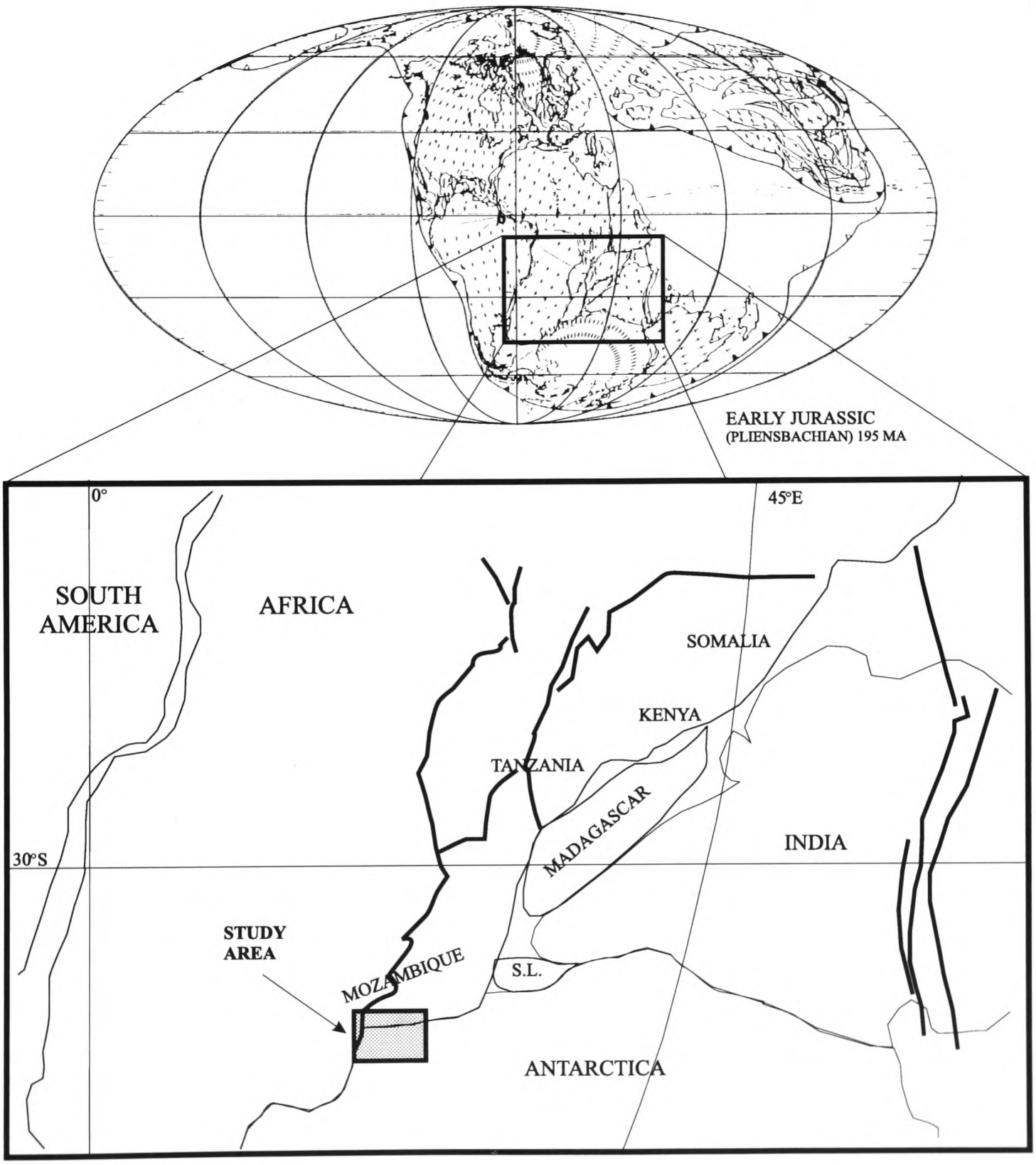

Figure 2.8: Plate tectonic reconstruction for the Early Jurassic *(Pliensbachian)* displaying the close fit aproach for plate tectonic reconstruction, redrawn and modified from Scotese (1991). Bold lines are fault lineaments of the East African Rift system and those related to the colison of India against Asia, printed in this diagram only for reference.

events relevant to basin development in east Africa: **1)** the Karoo rift; **2)** the Gondwana continent breakup and plate separation including the opening of the Indian Ocean and of the Mozambique Channel and **3)** the East African Rift system.

Basin history is determined by critical stages of the plate tectonic cycle (Wilson Cycle): **(i)** rifting; **(ii)** drifting and sagging; and **(iii)** subduction and

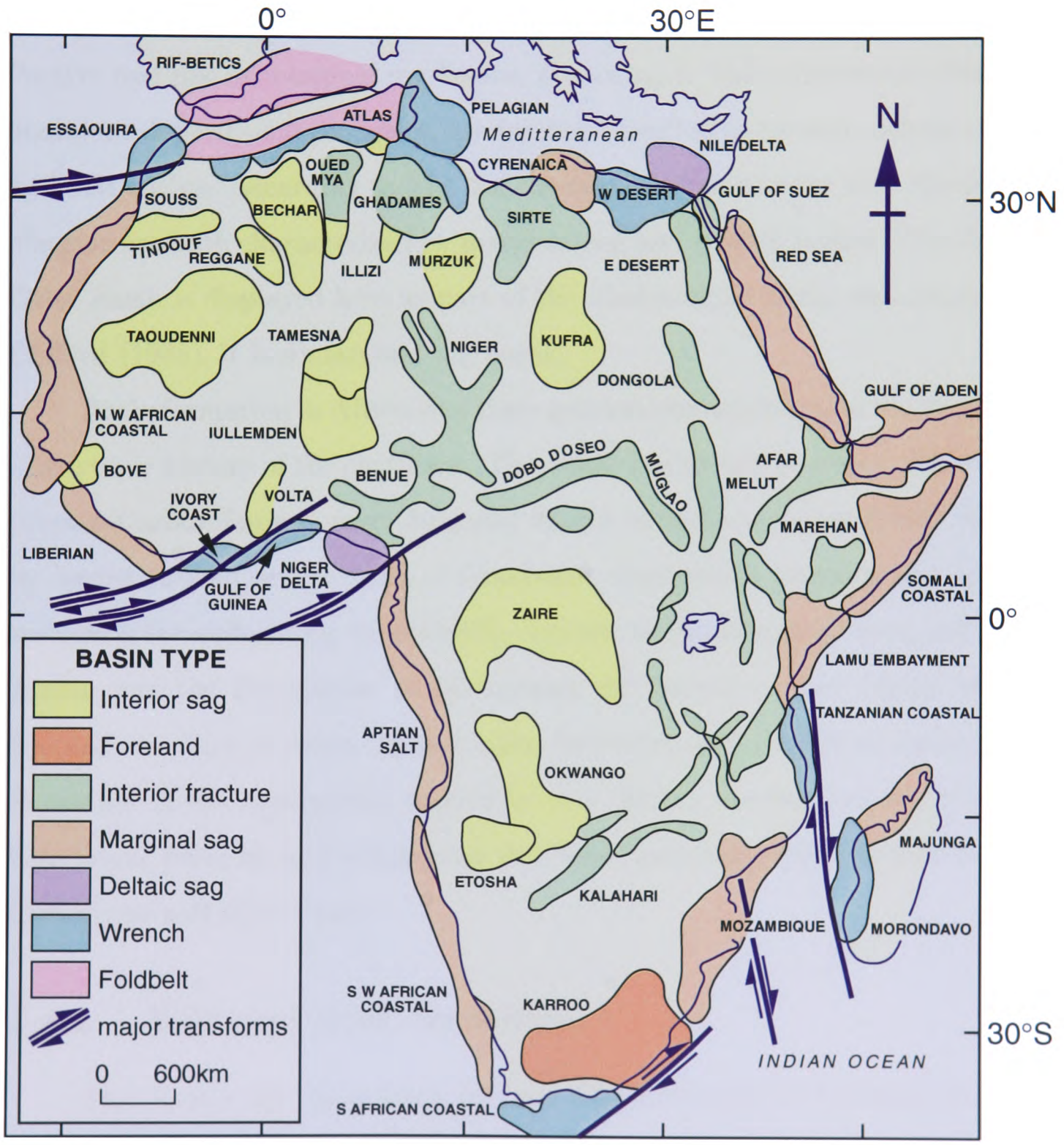

Figure 2.9: Map of types of sedimentary basins in Africa, redrawn and modified from Clifford (1986) and Petters (1991).

continental collision. Most basins in Africa evolved through various plate tectonic cycles from one basin type to another.

African basins were regrouped by Clifford (1984; 1986) into four basin types as follows: divergent passive margins; intracratonic sag; intracratonic fracture and cratonic foreland basins (Fig. 2.9). Later Picha (1988) studied 243 African basins and foldbelts and grouped them into five classes according to basin plate tectonic history: (1) intracontinental basins; (2) convergent margins; (3) divergent margins; (4) oceanic basins; and (5) orogenic belts and associated basins. Passive margins or marginal sag basins, according to their structural setting and dominant depositional processes, are further classified as wrench, deltaic sag and fold belt basins. According to Fig. 2.9 the east African and the west Madagascar margins are both characterized by marginal sag and wrench basins. The Zambezi Delta Basin is displayed here as part of the Mozambique Basin and according to Clifford (1986), it is a marginal sag basin.

Basin formation in Africa is of three generations according to the three phase geotectonic history of the continent. The oldest basins are the result of Karoo rifts (Permo-Carboniferous - early Jurassic) known in south and east Africa, followed by basins formed at the time of Gondwana continental breakup and sea floor spreading through rifting from Middle Jurassic to Palaeocene in west and central Africa, and the Palaeogene to Quaternary rift basins in east Africa, the Red Sea and the Gulf of Aden. Ocean basin formation and evolution, including the formation of the continental margin in east Africa, are intrinsically related to Gondwana breakup and subsequent sea floor spreading from Jurassic to Early Cretaceous and later times.

2.4.2 Rift and drift tectonics.

The Karoo rift dates back to Late Carboniferous to Permian times. It resulted in the opening of several inland basins in extensional settings of graben and half graben structures (Fig. 2.10). These basins were filled with continental aeolian and fluvio-deltaic sediments and this phase of rifting was terminated

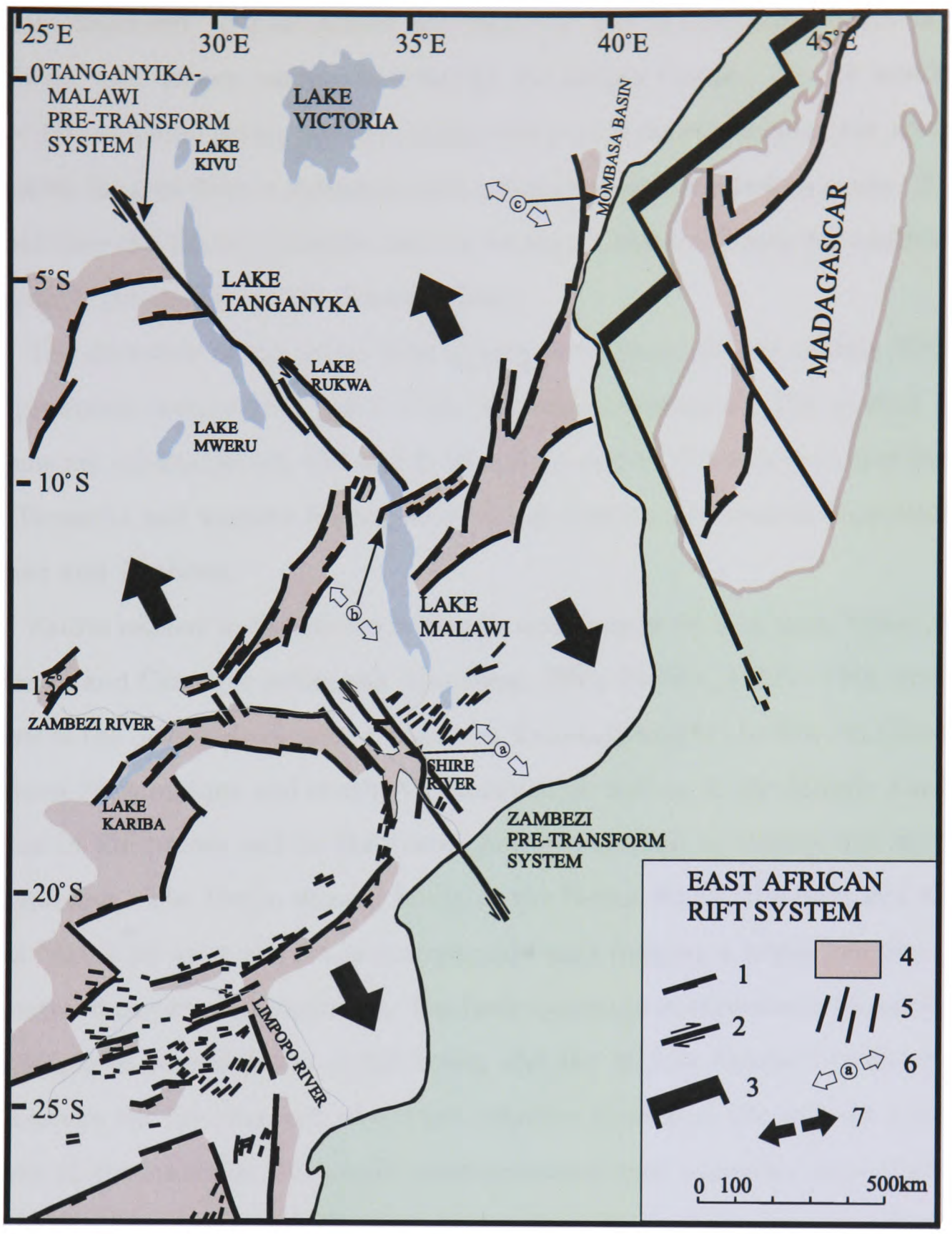

Figure 2.10: The Karoo Rift System in South-east Africa, redrawn and modified from Castaing (1991). Key: 1= Karoo boundary normal faults; 2 = pre-transform faults; 3 = opening of the proto-Indian Ocean; 4 = Karoo deposits; 5 = Karoo dolerite dykes; 6 = direction of extension (a = Lengwe and Mwabvi basins, b = Livingstonia basin, c = Mombasa basin); 7 = general extension.

by an extensive phase of volcanism with basaltic and rhyolite lava topping the Karoo stratigraphy in many of the basins (Salman and Abdula 1995). In south-western Mozambique this phase is represented by the Lebombo mountain chain, which runs along the border between Mozambique and South Africa in the south, extending well into Zimbabwe to the north. The Lebombo rhyolites form the

acoustic basement to post-Karoo sediments of the Mozambique Basin in the southwest and deepen eastwards towards the Indian Ocean. To the southeast of the Mozambique Basin, basaltic rocks take over from rhyolites as the acoustic basement for post-Karoo sediments and extend beneath the Indian ocean. It can be said that the Karoo rifting in eastern Africa set the conditions for continental breakup beginning in Middle Jurassic times.

The direction of the stress field during the Karoo rift was mainly NW-SE and produced transcurrent faults with the same orientation. The normal fault systems are orientated NE-SW and E-W and generate the Karoo basins of Kenya and Tanzania and western Madagascar and of western and central Mozambique, Malawi and Zimbawe.

Faults related to the Karoo rifting in most places lie very deep below thick Mesozoic and Cenozoic sediments (Castaing, 1991; Petters, 1991). They are well known in the Selous Ruvu area of southern Tanzania and in the Rovuma Basin in northern Mozambique and southern Tanzania, as well as in the Middle Zambezi graben in Zimbabwe and in the Lower Zambezi graben in central and western Mozambique. The Karoo normal faults at the Selous Ruvu, Rovuma and Maniamba basins are part of a set of extensional faults froming a triple junction with its centre in eastern Dar-es-Salam. The fault system in northwestern Mozambique comprising of normal faults of the Lower and the Middle Zambezi Grabens and the Luanga rift are also part of a triple junction located in the western province of Tete of Mozambique. The triple junction centres may represent some of several hot spots which might have been active in the region causing tensional forces in the crust to increase.

The second rift phase is mainly known as the phase of continental breakup associated with the fragmentation of the great Gondwana continent into various plates in Middle Jurassic. Gondwana continent assemblage was still complete in Early Jurassic times (Fig. 2.8). In Late Jurassic, 152 Ma, continental extension and the opening of the north Atlantic Ocean was underway between North Africa and North America. At the same time in northeast Africa, Madagascar could be seen detaching from Africa and moving southwards.

In Early Cretaceous *(Aptian)* sea floor spreading continued between North America and North Africa and an additional spreading centre was initiated between eastern and western Gondwana which signalled the begining of the opening of the South Atlantic Ocean (Fig. 2.11). Madagascar, India, Antartica and Australia also continued their journey south and southeast of Africa and the

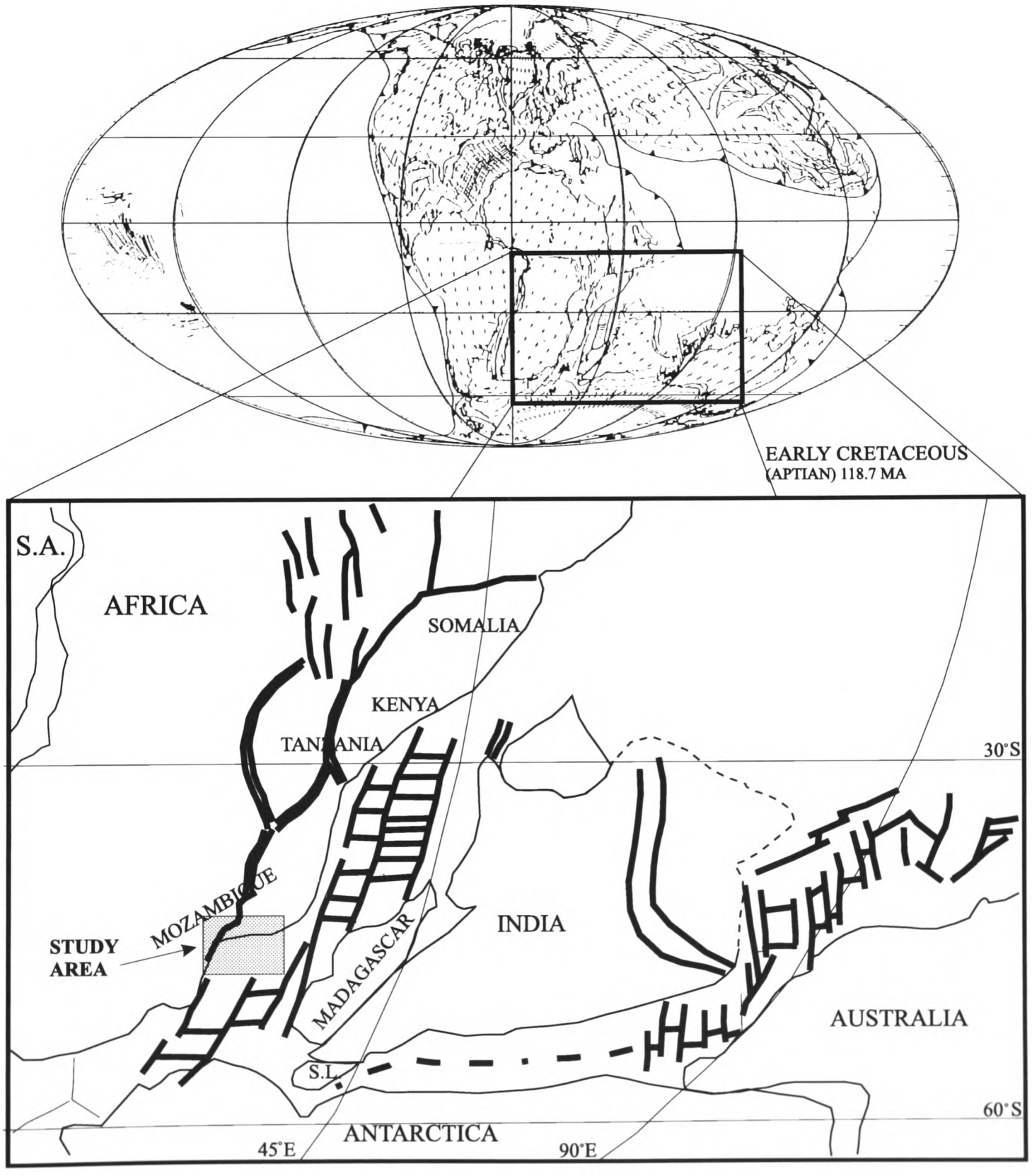

Figure 2.11: Plate tectonic reconstruction for the Early Cretaceous *(Aptian)*, redrawn and modified from Scotese (1991). Bold lines are fault lineaments.

Mozambique Channel was open at the time. However, so far there is no geological evidence of marine sedimentation prior to Early Cretaceous times in the Mozambique Basin.

At Middle Cretaceous times *(Cenomanian)* the opening of the North and South Atlantic Oceans was underway and sea floor spreading centres in both oceans were active (Fig. 2.12). In southern east Africa (north of Madagascar) sea floor spreading aborted in Middle Cretaceous when Madagascar was at its

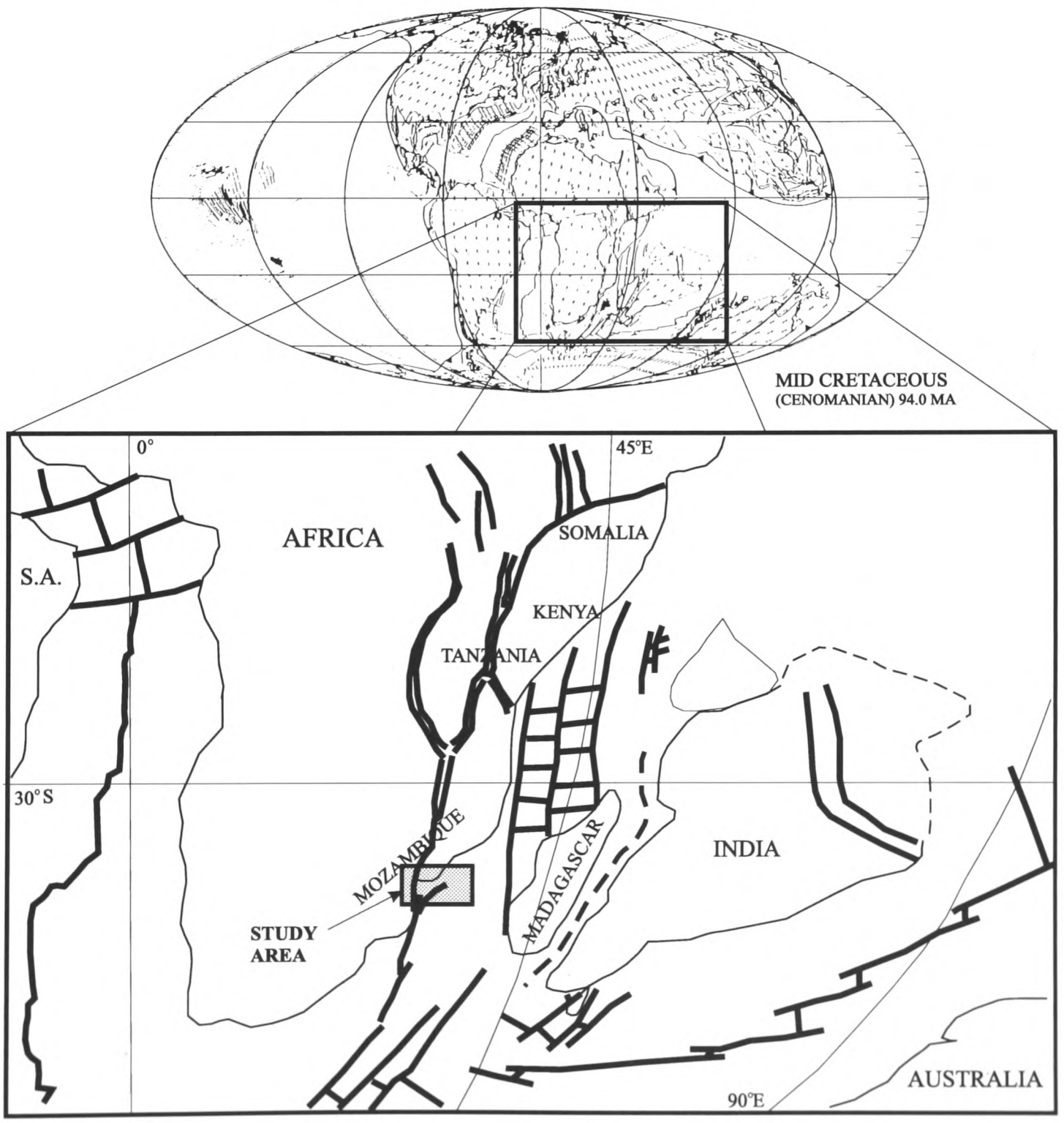

Figure 2.12: Plate tectonic reconstruction for the Middle Cretaceous *(Cenomanian)*, redrawn and modified from Scotese (1991). Bold lines are fault lineaments.

present position but sea floor spreading continued east of Madagascar, and India separated from Madagascar and moved north closing the Tethys Ocean and heading towards collision with Eurasia. Antartica and Australia continued

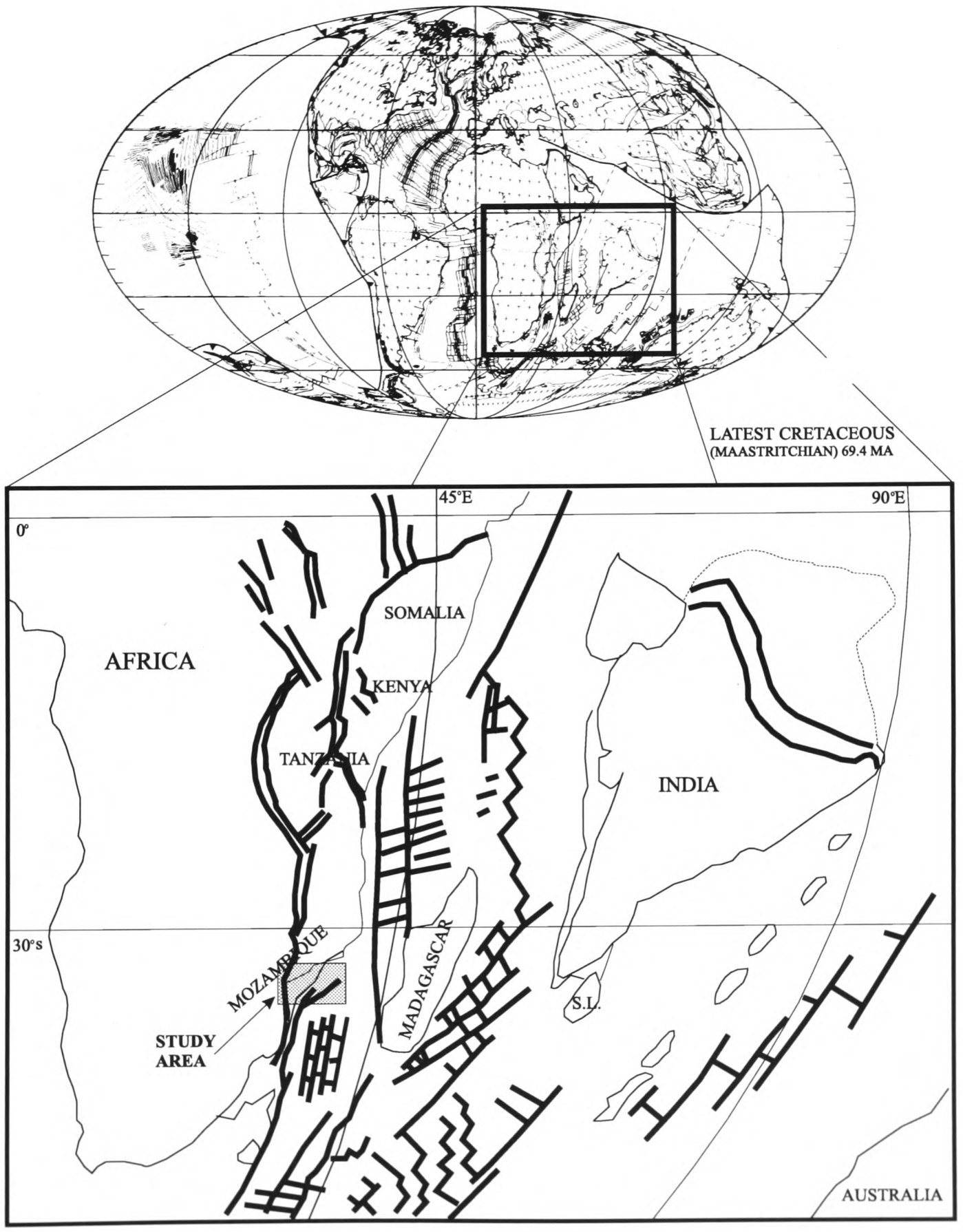

Figure 2.13: Plate tectonic reconstruction for the latest Cretaceous *(Maastrichtian)*, redrawn and modified from Scotese (1991). Bold lines are fault lineaments.

moving south and southwest respectively, thus opening the southern Indian Ocean. India continued moving north during the Late Creataceous (Fig. 2.13), leaving behind Madagascar and the Seychelles in the Indian Ocean. It finally collided with Eurasia in Tertiary times. Spreading centres continued to develop in both

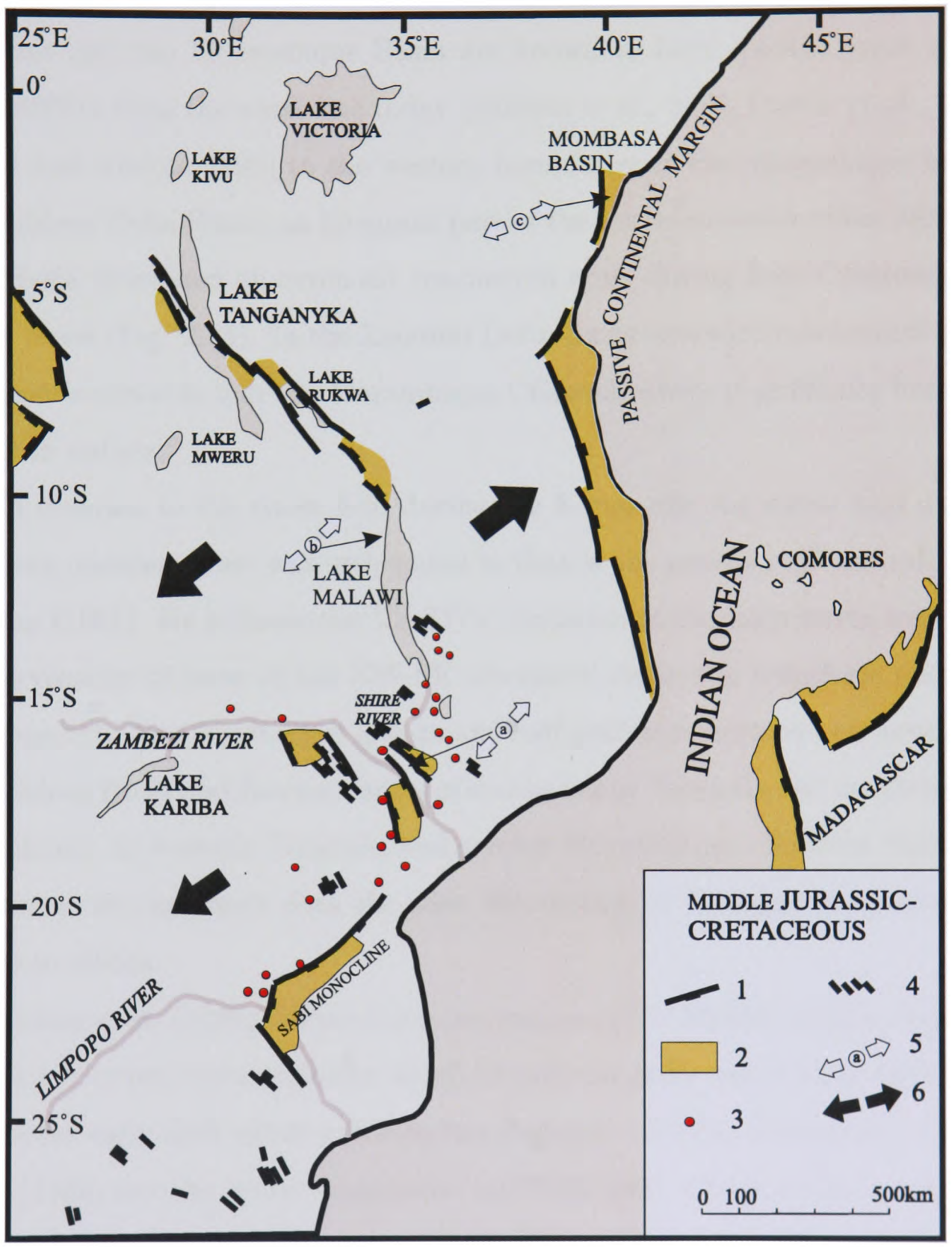

Figure 2.14: Gondwana break-up Rift phase in South-east Africa *(Middle Jurassic - late Cretaceous)*, redrawn and modified from Castaing (1991). Key: 1 = Cretaceous boundary normal faults; 2 = Cretaceous deposits; 3 = igneous centres (Cilwa Alkaline Province); 4 = NW-SE dykes; 5 = direction of extension (a = Lengwe and Mwabvi basins, b = Livingstonia basin, c = Mombasa basin); 6 = general extension.

the North and South Atlantic Oceans and in the southern Indian Ocean.

This sequence of events created the Mozambique Channel and the Indian Ocean in eastern Africa and the North and South Atlantic Oceans. It also marked the beginning of the development of the East African continental margin and of offshore basins in eastern Africa. After the opening of the Indian Ocean, marine incursions into the Mozambique Basin are known to have reached areas about 200 to 350km from the coast line today (Salman *et al.*, 1985, Coster *et al.*, 1989, Salman and Abdula 1995) to the western boundaries of the Mozambique basin. The Zambezi Delta Basin, an integrant part of the northern sector of the Mozambique Basin developed on extended continental crust during Late Cretaceous to Recent times (Fig. 2.15). In the Zambezi Delta Basin extended continental crust thins southeastwards into the Mozambique Channel, where it gradually becomes oceanic in nature.

In contrast to the stress field during the Karoo rift, the stress field during this ocean opening phase was orthogonal to that of the previous rift according to Castaing (1991). He believes the NE-SW orientation of the main stress triggered the reactivation of some of the NW-SE orientated strike-slip transform faults of the Karoo rift. As a result a few graben and half graben structures were produced in the Selous Ruvu and Rovuma areas of southeastern Tanzania and northeastern Mozambique, in western Tanzania and central Mozambique. However this does not seem to be consistent with the stike slip motion of Madagascar southwards relative to Africa.

Coster *et al.* (1989) discuss the stress regime of the Middle Jurassic to Early Tertiary rift in two distinct phases which he calls the early and the late drift (Fig. 2.16).In the early drift phase *(Middle/late Jurassic - Middle Cretaceous)*, Coster *et al.* (1989) set the stress orientation to NNW-SSE. These stresses are then responsible for the opening of interior fractures, passive margins and sheared margins in eastern Africa, the later becoming the transform zones during sea floor spreading. The late drift phase is characterized by stresses orientated NE-SW as discussed by Castaing (1991), and this might imply that the graben and half graben structures in Fig. 2.14 were produced during Coster's late drift phase

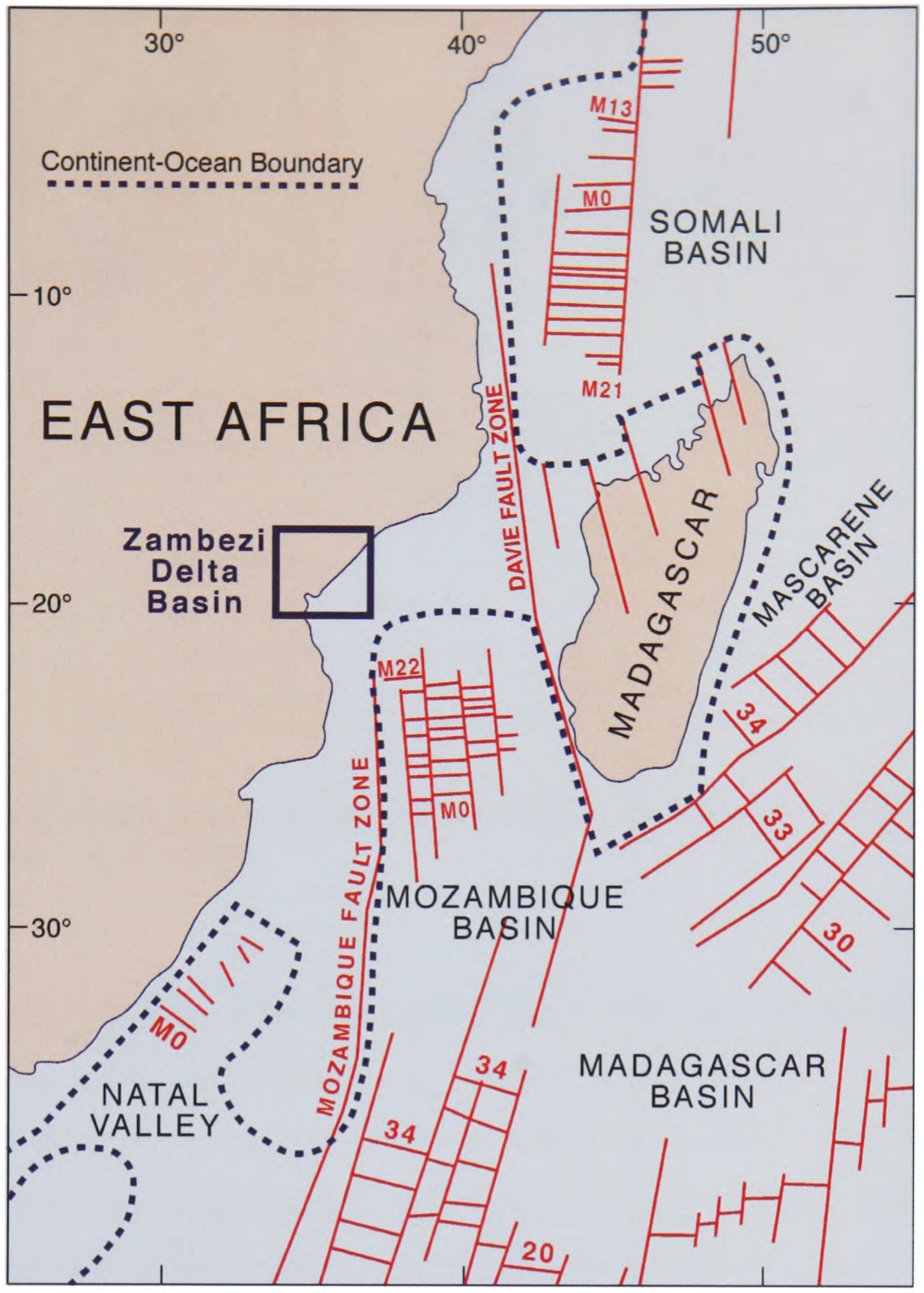

Figure 2.15: A simplified geotectonic sketch of the East African margin and surrounding ocean basins. Shown are the inferred ocean-continent boundary (dashed line), major fracture zones and associated magnetic anomalies, redrawn and modified from Mascle *et al.* (1987).

(Middle Cretaceous - Early Tertiary). The change in plate kinematics at around mid-Cretaceous time would be in accord with a change in stress direction at that time.

The breakup rift phase in onshore eastern Africa carries relatively little significance in terms of basin creation. It was, though, very important in developing

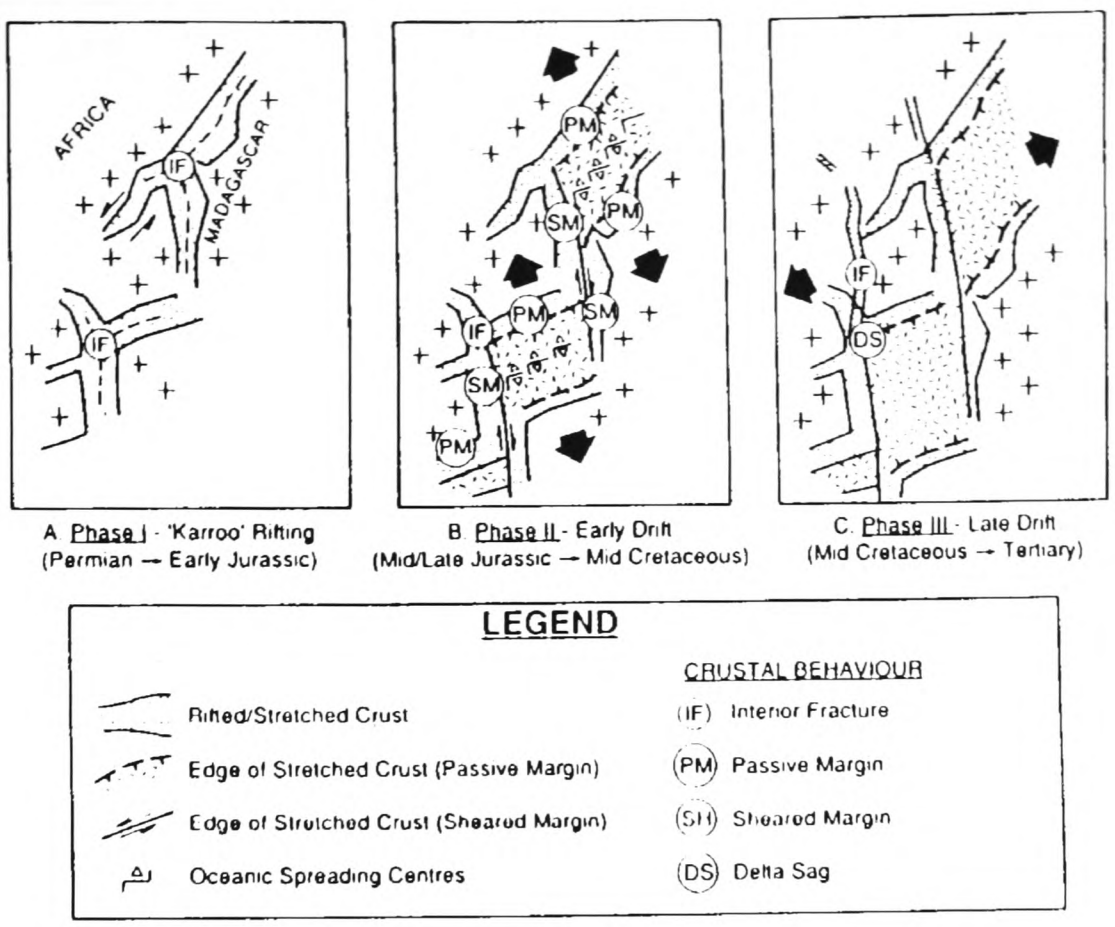

Figure 2.16: Plate tectonic history of southeastern Africa, redrawn and modified from Coster *et al.* (1989).

ocean basins in eastern Africa (the Somali Basin in the north and the Mozambique Basin in the south) and in both margins of the Atlantic Ocean.

The third phase of rifting in eastern Africa dates back to Middle Tertiary times *(Eocene)* and is well known as the East African Rift system. Regionally, it is part of a much greater system of rifts that cuts through the Middle East and northeast Africa and enters East Africa in northern Ethiopia. This rift system extends southwards with two distinct fault branches, the eastern and the western branches of graben and half graben structures (Fig 2.17). Figure 2.17 outlines the main regional tectonic features (onshore) produced by the latest rift phase in eastern Africa and offshore displays the main transform and boundary faults.

The eastern branch, also known as the Gregory Rift (Petters, 1991), extends from northwestern Ethiopia in the Afar rift triangle through eastern Uganda, Kenya and Tanzania extending southwestwards into Lake Malawi where it ends and meets the western branch. This rift branch runs through areas of basement

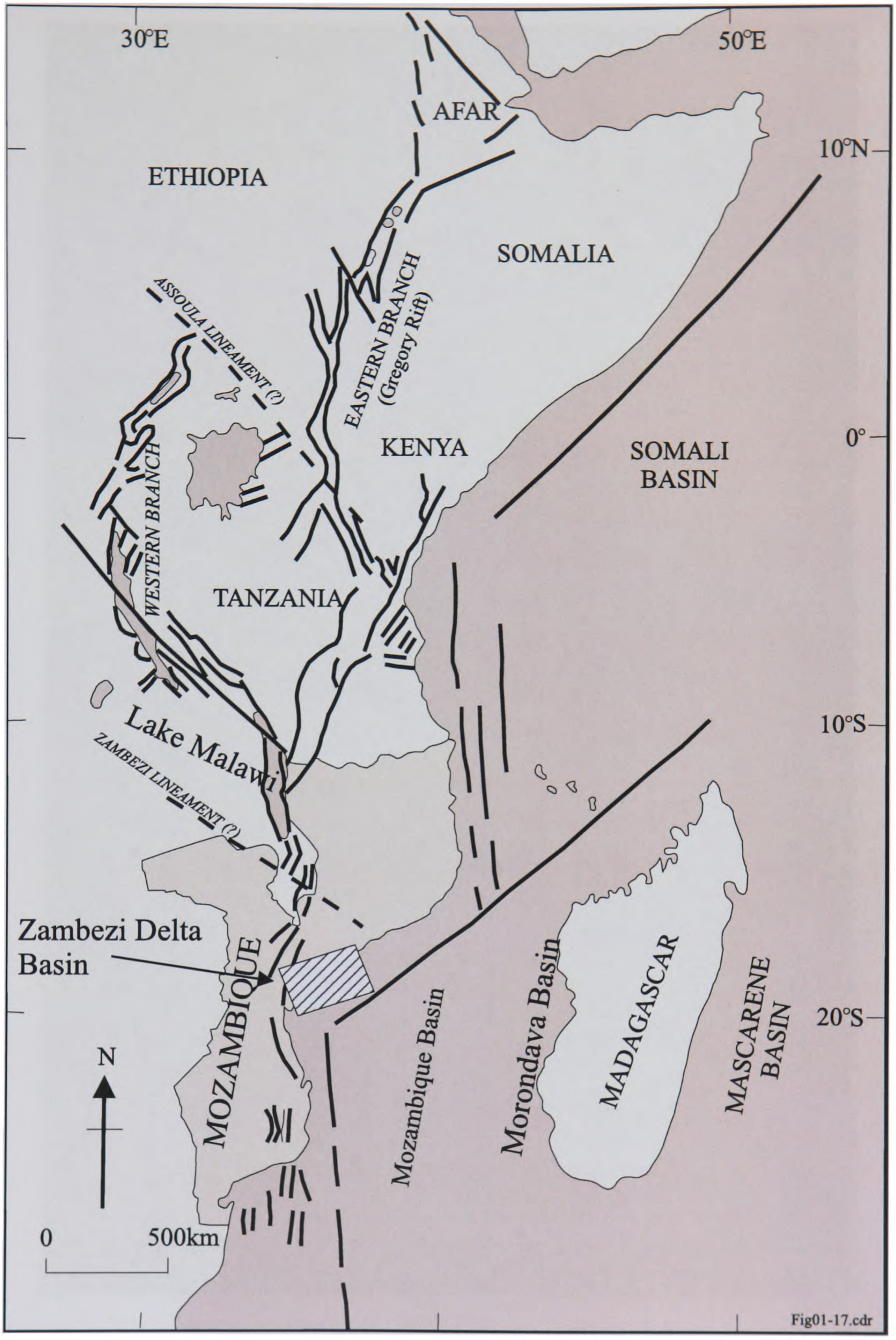

Figure 2.17: The East African Rift System, the eastern and western rift branches displaying the main graben and half graben systems and transcurrent fault lineaments (compiled from Darracott *et al.*, 1973; Mougenot *et al.*, 1985; 1986a; b; c; 1989; Petters, 1991; Castaing, 1991).

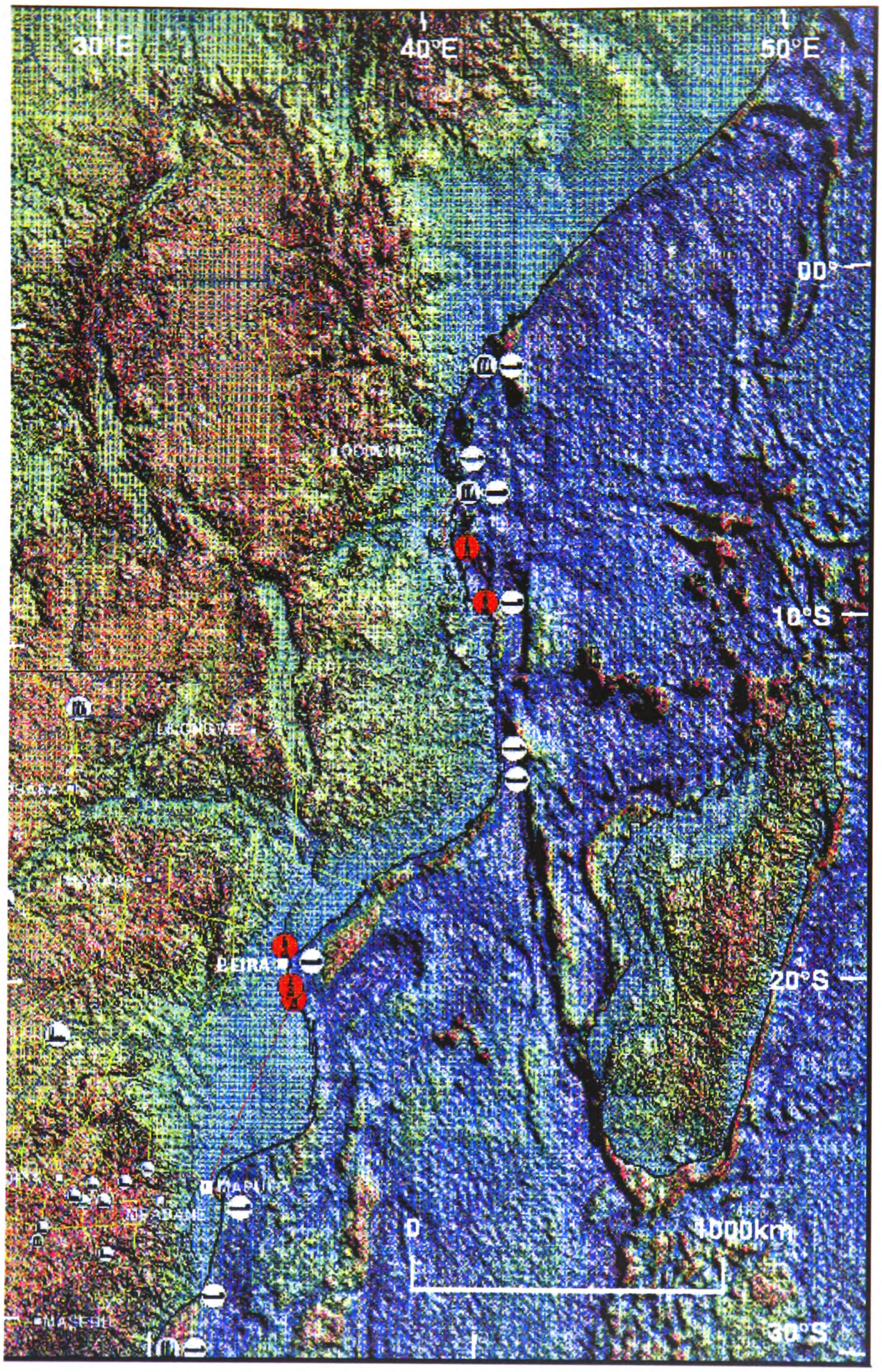

Figure 2.18: The topographic expression of the East African Rift System (onshore). Offshore, the sea bed expression of the main lineaments produced by the movement of Madagascar and India and of Antartica and Australia south and southeastwards respectively (courtesy of BP).

uplifts in Ethiopia and Kenya, which reflect broad uplifts of the lithosphere-asthenosphere boundary producing a topography sometimes as high as 3000 m (Petters, 1991). Fig. 2.18 is a satellite photograph displaying topography (onshore) and bathymetry (offshore) resulting from the main rift stages and subsequent erosion. Most interesting is the clear expression of the main East African Rift features (the graben system and mountain ranges) onshore and of the Davie Fracture Zone and the Mozambique Ridge offshore (Figs. 2.17 and 2.18).

In northern Tanzania the eastern rift branch displays a triple junction, splitting the rift branch into two rift arms one striking southwest and the second striking southeast into the Indian Ocean. This southeasterly striking rift arm is also known as the failed rift arm of the Selous Ruvu rift in Tanzania (Al-Kasim *et al.*, 1985, Kajato, 1986 and Kajato, 1994) and might reach the Indian Ocean somewhere east of Dar-es-Salam.

The western branch first strikes NNE-SSW from the Aswa shear zone through Lake Mobutu to Lake Tanganyika where its strike direction changes to become NNW-SSE down into Lake Malawi. It then extends through the lake and becomes the Lower Zambezi graben (Chiure and Urema grabens) in central and southeastern Mozambique, continuing towards the Indian Ocean with a series of inland and offshore graben and half graben structures, some of which cut through older Karoo rift structures.

Although the rift structures became difuse in central and southeastern Mozambique, it has been suggested (DNG, 1987, Salman and Abdula 1995), based on geophysical evidence, that the rift system's southernmost end might reach the Indian Ocean at Palmeira and Xai-Xai in southern Mozambique (Figs. 1.1; 2.17). Iliffe *et al.* (1986), Iliffe *et al.* (1991) and Nairn *et al.* (1991) mapped a complex graben and half graben structure striking NNW-SSE there. The inference that the western branch of the East African Rift system strikes through onshore southern Mozambique and that the Palmeira and Xai-Xai graben systems are its southern expression is suported by the interpretation of gravity and aeromagnetic data acquired during the last decade in southern Mozambique.

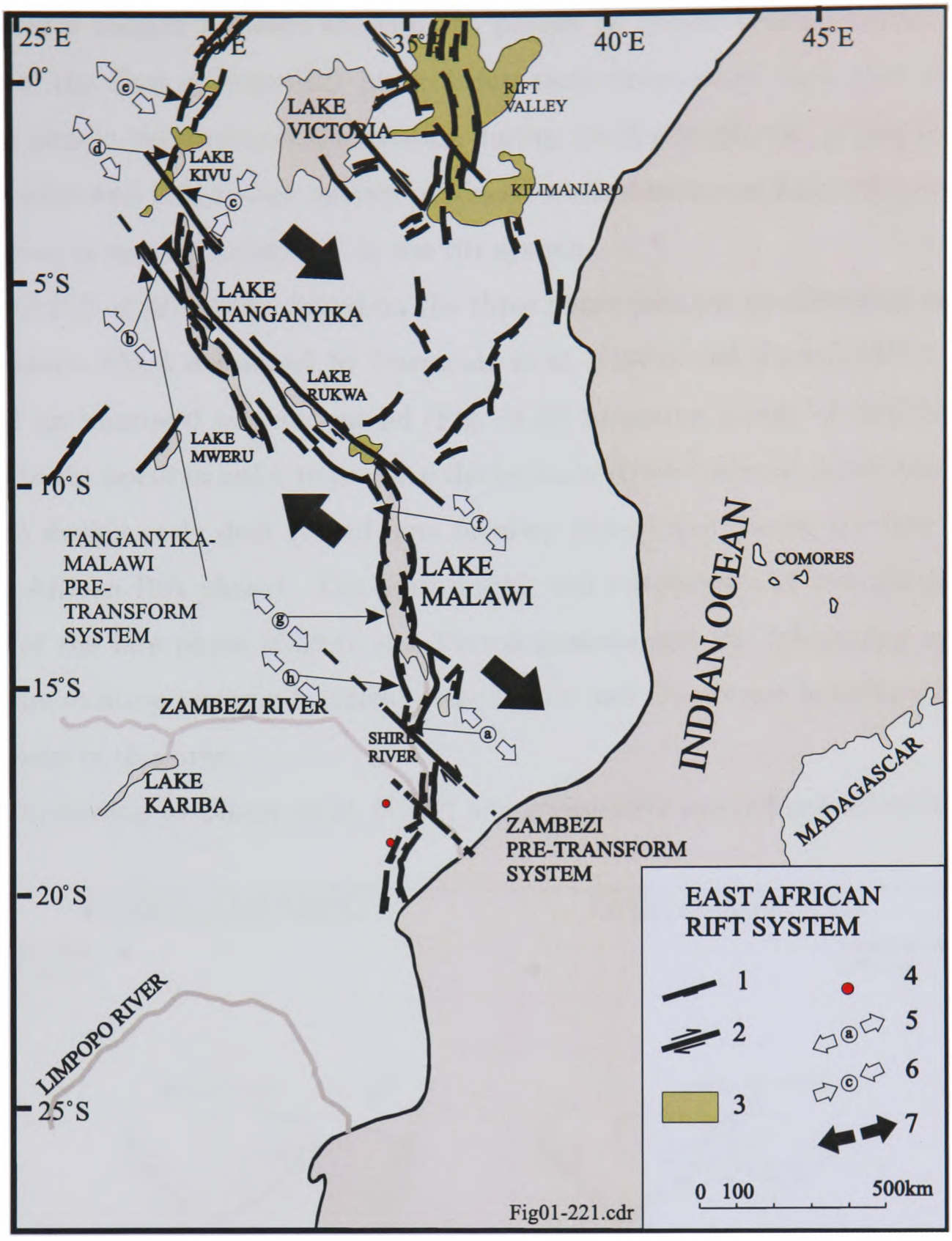

Figure 2.19: The East African Rift System (southern end), redrawn and modified from Castaing (1991). Key: 1 = Rift boundary normal faults; 2 = pre transform faults; 3 = Cenozoic and Recent volcanics; 4 = Cenozoic granites; 5 = direction of extension (a = Lengwe and Mwabvi basins, b-h = microtectonic observations between Lake Edward and Lake Malawi); 6 = direction of compression; 7 = general extension.

The East African Rift is segmented in several places by transcurrent faults, striking NW-SE, suggesting an extensional stress regime in the strike direction (Fig. 2.17). Transcurrent fault systems acted as pre-transform faults both during the Karoo rifting and the East African rift phases when they were reactivated (Figs. 2.10; 2.17; 2.19), and they controlled extensional tectonics at those times.

Differences though between the two rift phases lie in the transtensional character of the East African Rift phase being more pronounced than that of the Karoo phase: the direction of extension during the Karoo rift was orthogonal to the graben and half graben system produced while during the East African Rift extension is approximately 45° to the rift system.

Coster *et al.* (1989), based on the three phase tectonic development model for eastern Africa developed by Darracott *et al.* (1973) and Flores (1973), suggested an improved tectonic model (Fig. 2.20) assigning a pole of rotation located to the north in order to produce the tectonic styles observed in the Zambezi graben during early drift (Gondwana breakup phase) and during the late drift (East African Rift phase). The overprinting and interference of tectonic signatures of the late phase (Chiure and Urema grabens and the Inhaminga uplift) onto pre-existing tectonic features of the Karoo and Gondwana breakup phases is evident in this area.

According to Coster *et al.* (1989) a northwesterly located pole of rotation

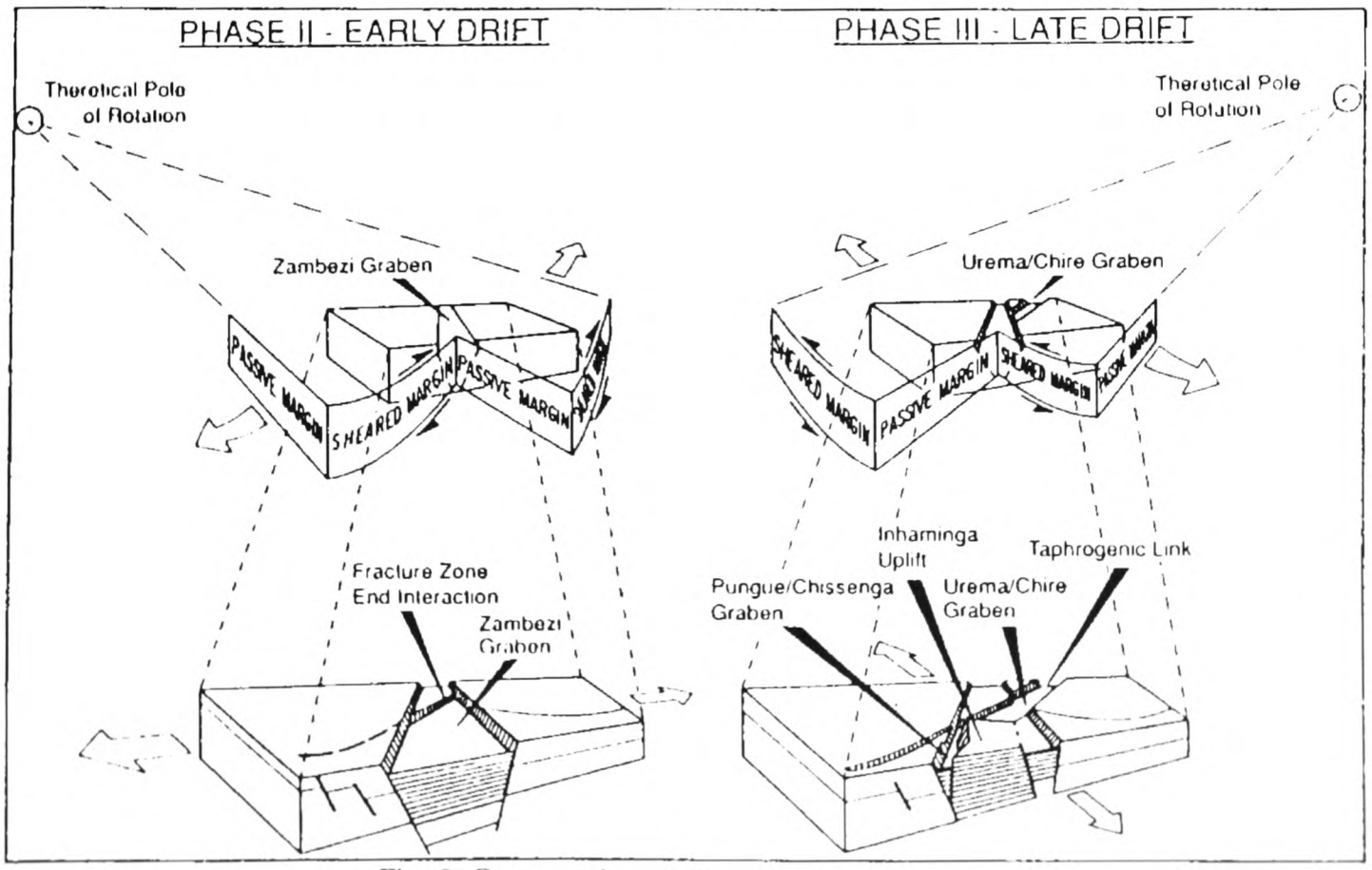

Figure 2.20: Structural model of the Lower Zambezi graben, redrawn and modified from Coster *et al.* (1989).

during the early drift phase is required to produce the rotation of two blocks at a shear zone in central Mozambique, opening the Zambezi graben. Similarly during the late drift phase a northeasterly located pole of rotation caused newly formed fault blocks across the Zambezi graben to generate a new set of graben structures (Fig. 2.20). The graben structure resultant from the early drift phase (the Lower Zambezi graben) is an important control as the main sediment conduit for inland sediments into the Mozambique Basin for the period between the early and the late drift phases. The late drift phase structures are relevant in reshaping sediment pathways feeding the newly positioned Zambezi Delta Basin after the late drift phase.

2.4.3 Stratigraphy and Sedimentation.

This section aims at outlining the stratigraphy and sedimentation of south-eastern Africa. A short description of the Karoo is given because it is believed here that it is present in the deeper parts of the Zambezi Delta Basin. However, it is recognized that the most important section of stratigraphy for hydrocarbon generation and accummulation in the basin is post breakup. Continental karoo sediments are known for their coal content in varios karoo basins and they may be important for gas generation.

Karoo rifting and volcanism gave way to the formation of inland basins in Late Carboniferous times. This rifting phase affected south and east Africa and Madagascar (Fig. 2.10) at the time when the latter could be found east of Somalia, Kenya and Tanzania.

Gondwana formations of which Karoo deposits are part are paleontologically world-famous for their content of Glossopteris flora and rich reptilian faunas with pre-mammalian terrestrial vertebrates (Petters, 1991). The greatest vertebrate diversity used for the correlation of Karoo strata is found in South Africa (Petters, 1991).

Karoo successions in general begin with tillites followed by coal seams, fan-deltaic clastic wedges which usually interfinger with lacustrine sediments, fluvial and aeolian sediment beds with extensive basalt and rhyolite flows on top of the

succession (Tankard *et al.,* 1982; Salman *et al.,* 1985; Daly and Unrug 1982; Nicols and Daly 1989; Coster *et al.,* 1989; Lawrence, 1989 and Petters, 1991).

Karoo basins according to their tectonic setting can be subdivided in three basin types (Petters, 1991): (1) the main Karoo Foreland Basin of South Africa to the south; (2) the western intracratonic basins in South Africa, Botswana, Namibia, Congo and Gabon and; (3) the eastern Karoo basins in Kenya, Uganda, Zambia, Tanzania, Zimbabwe, Mozambique and Madagascar (Figs. 2.10; 2.21). The third basin type is made of relatively narrow grabens, half-grabens and troughs (Al-kasim *et al.,* 1985; Coster *et al.,* 1989; Lawrence, 1989; Petters, 1991).

The lithostratigraphy of the Karoo Supergroup (Late Carboniferous to Early Jurassic) of widespread non-marine deposits ranges from glacial through coarse sediments and braided streams, deltaic, distal flysch to aeolian deposits in the Karoo Foreland Basin of South Africa. Essentially, the above depositional environments can be grouped in four major lithostratigraphic units: the Dwyka Formation followed by the Ecca Group, the Beaufort Group and the Molteno, Elliot, Clarens Formations on top. The strata of the above sedimentary units are toped by massive outpouring of the Drakensberg basaltic lava of late Triassic to Jurassic age which ended the Karoo depositional cycle.

Judging from the sedimentary succession in the various other Karoo sedimentary basins of south and eastern Africa, climatic and paleotectonic changes happened at almost the same time for most of the Karoo period. The South African Karoo favoured more fauna and animal diversity which so far has helped in dating and correlating South African Karoo strata with other Karoo occurences in eastern Africa, Madagascar and other parts of the world.

The Morondava Basin of western Madagascar (Fig. 2.17) has the thickest Karoo strata of all basins of about 12km which Besaire (1972) subdivided into three groups: the basal Sakoa Group (Late Carboniferous to Early Permian) followed by the Sakamena Group (Late Permian to Early Triassic) with the Isalo Group (Late Triassic to early Jurassic) on top of the succession. The three groups

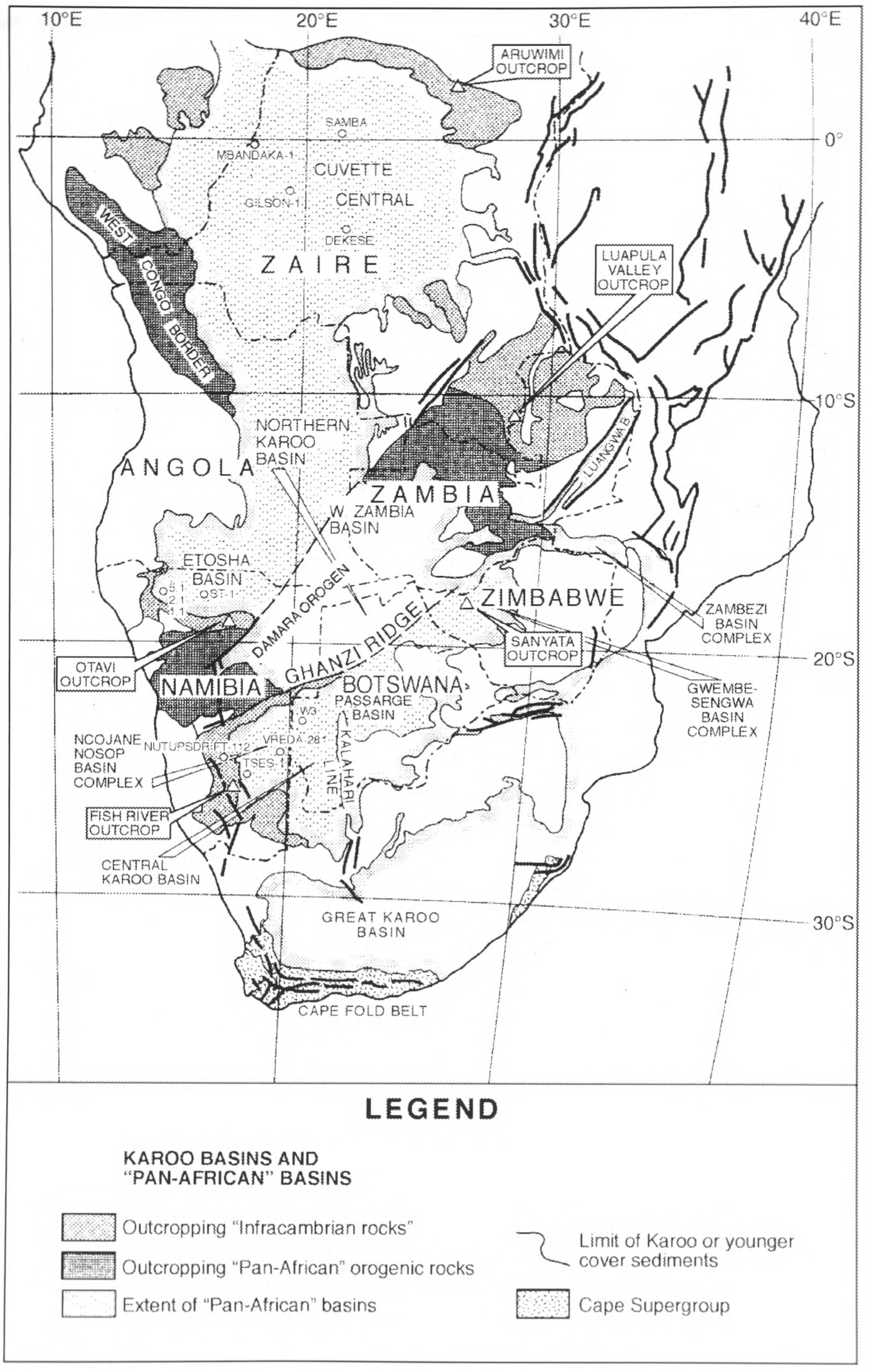

Figure 2.21: Pan-African orogenic systems and pre-Karoo and Karoo basins of central and southern Africa, redrawn and modified after Lawrence (1989).

are separated by unconformities and during deposition the Morondava basin was tectonically tilted to the west towards a lake basin. The Sakoa Group sits direct onto the Precambrian basement with coarse sediments at the base followed by sandy, muddy and carbonaceous sediments on top (Fig. 2.22). It is unconformably oversteped in the northern part of the basin and overlain by the Sakamena Group of about 4km thickness. The deposition of the Sakamena Group was preceded by the uplift and erosion of the underlying Sakoa Group. The base of Sakamena is characterized by coarse sediments reflecting renewed tectonic activity along border faults followed by braided-stream sandstones, lithoral clastics, limestones of lagoonal, algal reef and shallow shelf origin. In the middle, the Sakanema Group is of predominantly fossiliferous mudstones, siltstones and fine sandstones deposited in a shallow marine environment during the Early Triassic

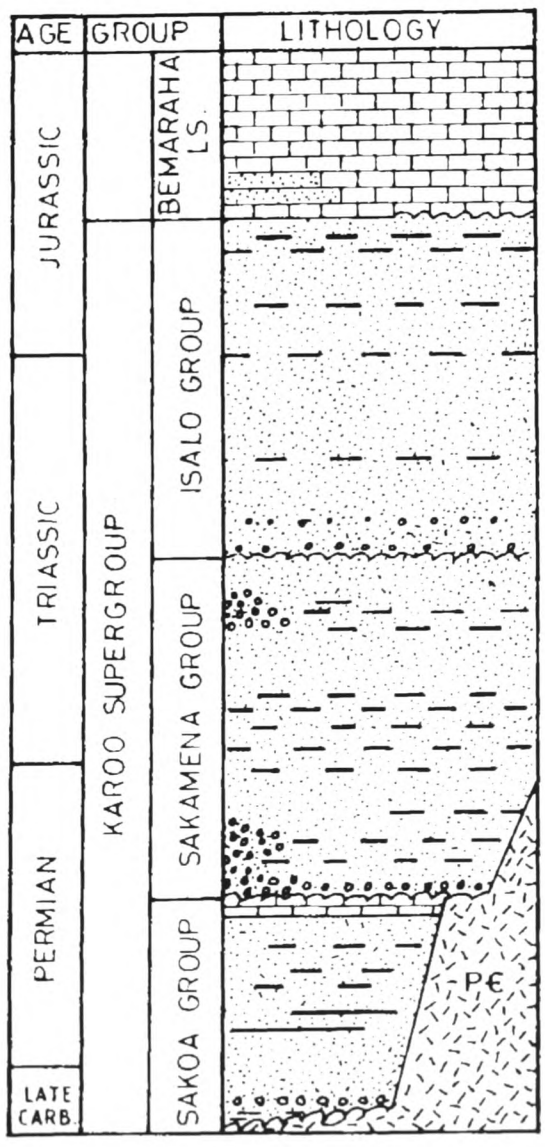

Figure 2.22: Generalized Karoo stratigraphy in the Morondava Basin of western Madagascar, redrawn and modified from Wescott (1988).

transgression (Wright and Askin, 1987). Fluvial deposition resumed in the late stages of deposition of the Sakamena Group, with the deposition of cross-bedded gravelly sandstones and mudstones. The Isalo Group is 5-6km thick, and was characterized by continuing deposition of alternating cross-bedded gravelly sandstone and sandy mudstones.

A serious constraint to correlation of the Karoo successions is the lack of a common terminology and subdivision of stratal groups for the various Karoo basins. A data base of biostratigraphic data should be made as an important step towards a common stratigraphic framework for the Karoo Supergoup.

Karoo rifting was followed by the breakup of the Gondwana continent. The drift of the Antarctic and Australian plates to the south and southeast, and of India and Sri Lanka to the north, gave way to the opening of the Indian ocean and the creation of major offshore basins. The drift of the Madagascar plate southwards with Antarctica, and the opening of the Mozambique Channel was a significant step in the formation of the Somali offshore basin in northeast Africa and of the Mozambique Basin in the southeast. It allowed marine incursions to flood large areas of coastal land in eastern Africa. At this time marine sedimentation began to dominate over continental and fluvio-deltaic sedimentation in most foreland and coastal basins of the region. Karoo sedimentation, mainly of fluvial and lacustrine sediments in coastal and foreland areas, was superceded by more predominantly marine lagoonal and fluvio-deltaic sedimentation. This scenario, characteristic of Late Jurassic to Early Cretaceous time, gradually changed basin stratigraphy in most coastal basins from a more coal-bearing continental sediment setting into marine and coastal deltaic, more hydrocarbons prone sediments.

The East African Rift system with its two distinct rift branches, the Eastern Rift branch and the Western Rift branch, represents the latest significant tectonic event in basin formation and structural evolution in the region.

The structural features which resulted from these major tectonic events, some of which are displayed in Fig. 2.23, controlled basin evolution and basin position relative to sediment source, as well as sediment source availability in

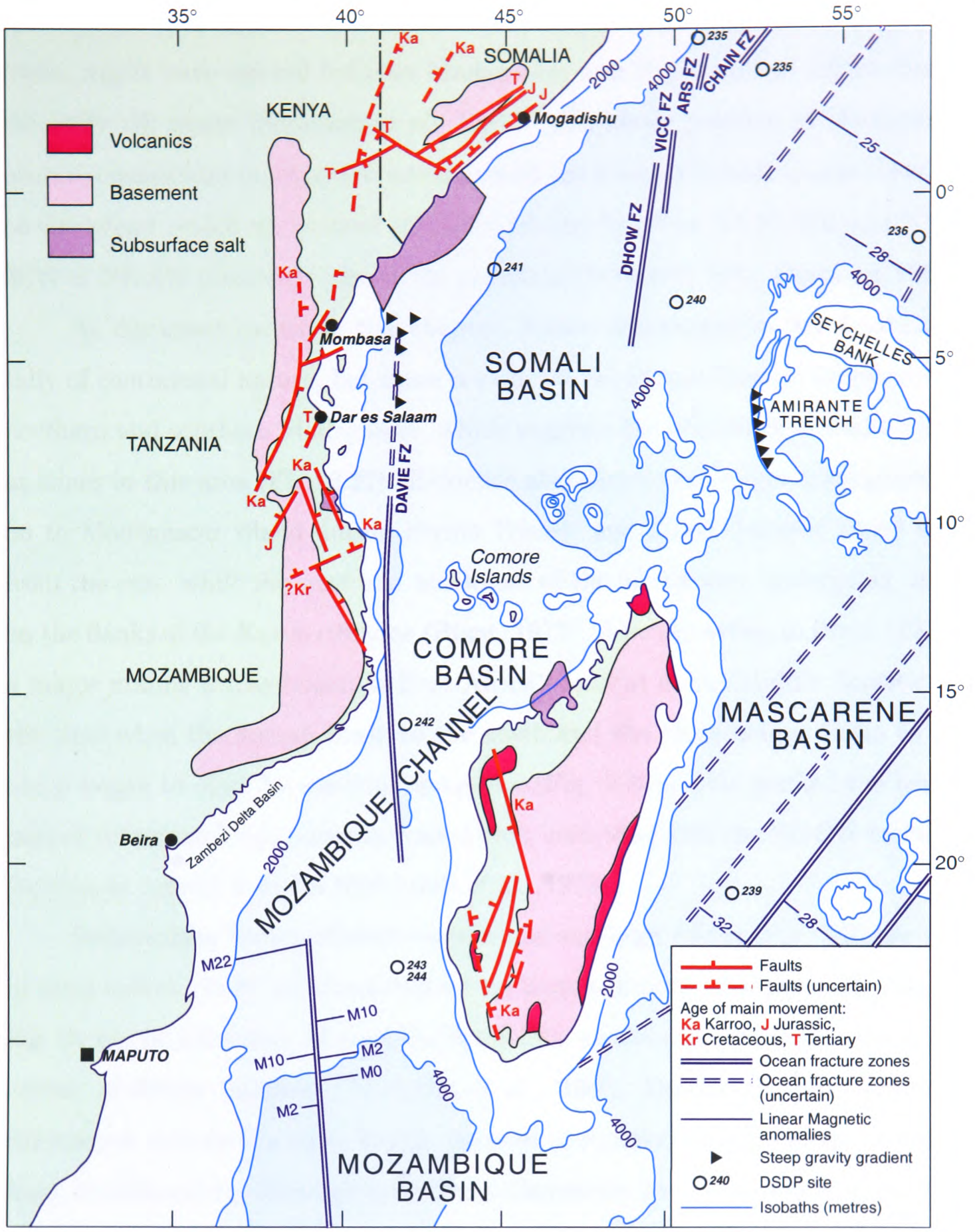

Figure 2.23: Geological schematic map of southeast Africa and the southwestern Indian Ocean, highlighting the main structural elements offshore, compiled from Scrutton *et al.* (1981) and Coffin and Rabinowitz (1987).

Mesozoic and Cenozoic times. Changes in drainage patterns due to tectonics onshore added to the factors which affected basin evolution and sedimentation through time in the various basins on- and offshore.

Madagascar's position prior to Early to Middle Jurassic was at about 300 km

off the coast of Kenya and Somalia, then a wide Karoo rift zone, an epicontinental basin, might have existed between Madagascar and the mainland Africa during the early rift phase (Scrutton *et al.,* 1981). The above position of Madagascar prior to continental breakup is consistent with the Karoo rift fault trends observed on the island, which are rotated 16° anticlockwise from the NNW-SSE and NNE-SSW or NE-SW observed today in the mainland (Scrutton, 1981; Castaing, 1991).

As discussed earlier in this chapter, Karoo sedimentation was fundamentally of continental nature, but there is evidence for Permo-Triassic limestones in northern and southern Madagascar, which suggests the occurence of shallow seas at times in this area (Fig. 2.22). Evidence also shows that major transgressions on to Madagascar island during Permo-Triassic and Lower Jurassic times were from the east, while the west and northwest of the island were undergoing uplift on the flanks of the Karoo rift zone (Blant, 1973). Also according to Blant (1973), a major marine transgression in East Africa occurred in the Middle Jurassic, at the time when the Somali Basin to the north and the Mozambique Basin to the south began to open by sea-floor spreading (Fig. 2.23). This marked the beginning of continental separation in East Africa, coincided with the NE-SW trending faulting in coastal Somalia (Beltrandi *et al.,* 1973).

Sedimentary basins offshore eastern and southern Africa (Fig. 2.9) are vast in areal extent. They are characterized by large sediment piles generally exceeding 10 km in thickness, of post-Carboniferous sediments, which in some areas consist of deltaic buildout (Al-Kasim *et al.,* 1985). Despite the large sediment thicknesses recorded in these basins, decades of exploration have made no significant oil discoveries, although several gas discoveries have been made in the Red Sea offshore Sudan, in Ethiopia, Somalia, Tanzania, Madagascar, Mozambique and South Africa. This suggests that the post-Middle Jurassic progradational sediment prism is poor in oil generating organic matter (eg. marine plankton), but rich, or at least contain, gas generating organic matter. It is also possible that some of the gas is a by-product of deep buried Karoo coal seems.

In the Mozambique Basin (Fig. 2.24), the Dwyka and Ecca Series represent

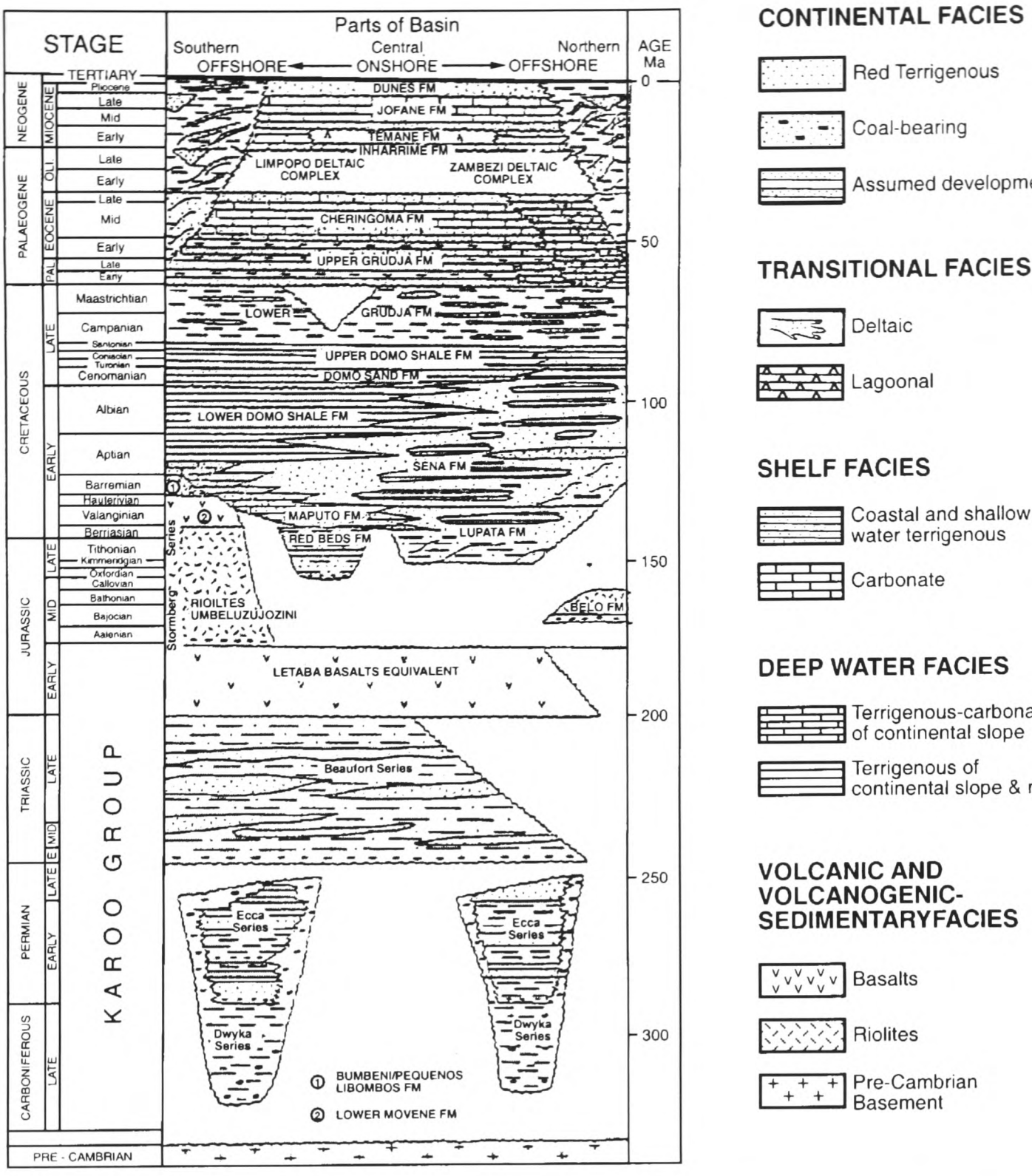

Figure 2.24: Summary of the stratigraphy of the Mozambique Basin, redrawn and modified from Salman and Abdula (1995).

the oldest sedimentary succession lying unconformably on top of the Precambrian basement. Above they are separated from the sediment series of Triassic age, which comprise the Beaufort Series, by a regional unconformity. These sediments are then unconformably overlain by basalts of the end-of-Karoo volcanism, the Letaba Basalts equivalents. These basalts are widespread over the southern offshore and central onshore parts of the Mozambique Basin but are not found in the northern offshore part of the basin. Volcanism continued during Middle and Late Jurassic times with the rhyolitic build up of the Lebombo Mountains

in the southwestern part of the basin probably because the wells drilled are too shallow. This was generally a period of relatively little or no sedimentation in the Mozambique Basin, a depositional hiatus.

The Carboniferous to Jurassic period in the geologic record of the Mozambique Basin, some 170-180my, is followed by a period of relatively continuous deposition from Early Cretaceous until Recent times. At this time a marine transgression is reported to have reached the western, southwestern and northern boundaries of the Mozambique Basin (Salman *et al.*, 1985 and Coster *et al.*, 1989) where marine sedimentation began to interfinger with continental and later with fluvio-deltaic sedimentation. The Red Beds with over 900 m thickness is the first rock formation deposited in the Lower Zambezi graben and in the Palmeira, Chidenguele and Changani graben systems in the southern part of the Mozambique Basin after the Early Jurassic unconformity (Fig. 2.25). It was followed by the deposition of the Lupata, Maputo, Sena and Lower Domo sand and shale formations in Early Cretaceous (Figs. 2.24; 2.26).

The Maputo and Sena Formations are widespread over the Mozambique Basin were they are recognized as potential reservoir rocks. The Maputo Formation is of littoral and shallow-marine sediments, while the Sena Formation, which reaches 1359 m thickness southwest of the Pande and Temane gas fields south of the Save River, is continental.

According to Salman and Abdula (1995) (Fig. 2.24), Lower Domo Shales were followed by a semi-regional unconformity, also mapped in this work, which preceded the deposition of the Domo Sand Formation in a series of submarine fans south of Beira and east and south of Inhambane. This is followed by the Upper Domo Shale Formation. In Late Cretaceous times the Lower Grudja formation was deposited composed mainly of shales and marine carbonates followed by a regional end-Cretaceous unconformity. During Late Cretaceous times beach and chenier barrier systems developed in central Mozambique and the Limpopo deltaic system started to develop in southern Mozambique (Fig. 2.25). The beach and chennier barrier systems in central Mozambique were followed by the steady

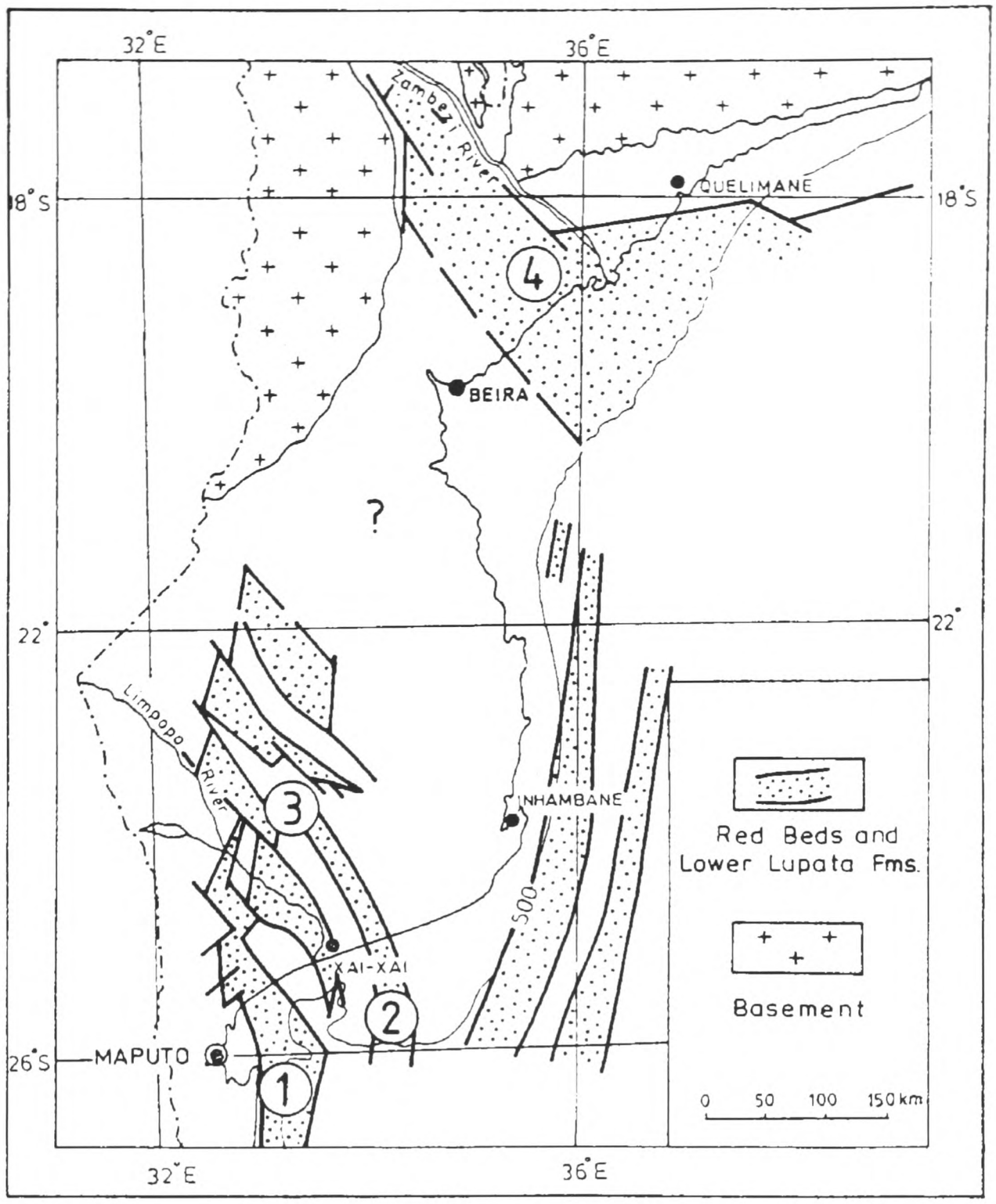

Figure 2.25: Development and distribution of the Red Beds and the Lupata formations *(Late Jurassic)* in the Mozambique Basin, redrawn and modified from Salman and Abdula (1995). Key: **1**- Palmeira graben; **2** - Chidenguele graben; **3** - Changani graben system; **4** - Lower Zambezi graben.

development of the Oligo-Miocene Zambezi Delta at a time when the deposition of the Cheringoma Formation, mainly of widespread carbonate deposits, in Eocene times. The deposition of these two rock formations in the central onshore parts of the Mozambique Basin is coincident with the early stages of development of the Limpopo Deltaic Complex in the south and the Zambezi Deltaic Complex in the central on- and offshore basin in Oligocene times. Three mainly carbonate formations were deposited in Miocene times, the Inharrime, Temane and Jofane

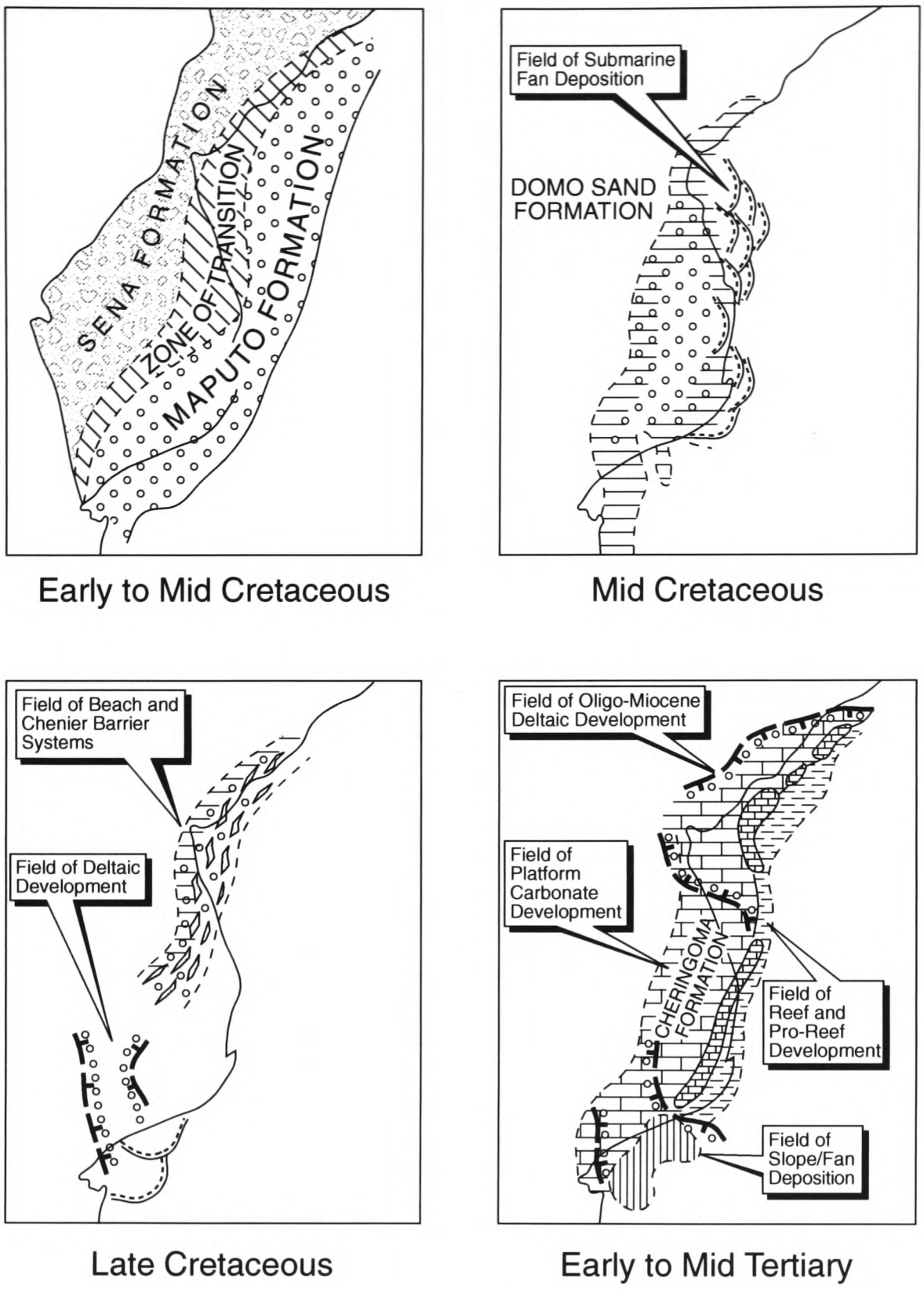

Figure 2.26: Reservoir rock formations development and distribution in the Mozambique Basin *(Early Cretaceous - Middle Tertiary)*, redrawn and modified from Coster *et al.* (1989).

formations. A formation composed of sand dunes onshore closes the stratigraphic sequence of the basin.

Post-Karoo sediments are of particular significance for hydrocarbons prospectivity in various areas of the Mozambique Basin where significant accumulations of Mesozoic and Cenozoic sediments can be found. Of particular interest is the

Zambezi Delta Basin with sediment accummulate in excess of 12-15km (Salman *et al.,* 1985; Coster *et al.,* 1989; Salman and Abdula 1995). To the southwest, Zambezi Delta sediments interfinger with deposits from the Save River Delta in the early stages of deltaic sedimentation in the Zambezi Delta Basin (this work). To the southeast the Zambezi Delta Basin is bound by the offshore Beira Basement Uplift, also called Beira High by Salman *et al.,* (1985) and Coster *et al.,* (1989) (Fig. 1.4).

The Beira Uplift is a geologic feature only mapped on seismic data and can be infered from gravity and magnetic data (Chap. 3). This geologic feature is discussed in more detail in Chapter 4 and 6 of this thesis.

2.5 Continental margin evolution and geology.

Continental margins are important areas of basin development and active sedimentation. Sediments drained from high ground in tectonically uplifted areas inland are often deposited in foreland and offshore basins which evolved during periods of tectonic activity. It is at continental margins that major sediment accumulations, often related to large hydrocarbon accumulations, are found.

Continental margins result from relative motions between lithospheric plates. Of particular importance are convergent, divergent and transform plate motions (Mascle *et al.,* 1987). These three types of plate motion are responsible for producing the main types of continental margins observed around the world today. Convergent plate motions lead to the generation of active continental margins with eventual subduction or collision zones characterized by increased earthquake activity and crustal accretion due to the development of accretionary wedges and igneous activity. Divergent plate motions produce rifted passive margins, while transform motions (strike slip) generate transform or sheared margins (Scrutton, 1976a,b).

A passive continental margin is not a plate margin today, but represents an area of continental split prior to sea floor spreading and is generally characterized by a thick and relatively undisturbed sediment accumulation. Passive

margins can be further subdivided into rifted and sheared margins in accordance with the geotectonic mechanism which brought them about, divergence or transform (strike-slip) motion (Mascle, 1976; Scrutton, 1976a). Transform motions are known to be tectonically responsible for inducing the development of characteristic structures such as shear folds and pull-apart grabens (Scrutton, 1979; Mascle *et al.*, 1987). Pull-apart grabens are important basinal structures, which subsequently become areas of active sedimentation. In pull-apart basins, sedimentation may take place at the same time as thermal exchanges between oceanic and continental lithospheres occurs, thus controlling basin subsidence. This has important implications for preservation of deposited organic matter.

A set of three possible stages in the development of fracture zones proposed by Scrutton *et al.* (1981) can lead to the formation of rifted and sheared margins, marginal plateau areas and microcontinents and spreading centres (Fig.2.27). In stage 2 of the model a sheared margin may develop with the possibility of marginal plateaus developing at conjugate margins. Stage 3 represents the situation in which a jump in sea floor spreading may lead to isolation of a microcontinent between an old abandoned spreading centre and the newly developing spreading centre. According to Scrutton (1981), marginal plateau areas and microcontinents can be formed at the intersection of rifted and sheared margin segments.

Relative to the formation of the East African continental margin, stage 3 of the model in Fig. 2.27 can be used to explain the development of at least some of the structural features of the western Indian Ocean and of the east African margin. 1 and 3 of stage 3 of the model represent the Western Somali Basin and the Zambezi Delta Basin respectively, 2 and 5 representing the Davie Fracture Zone and the Mozambique Ridge, 4 the mid-ocean ridge and M Madagascar Island.

In the context of the model, the origin of the Beira basement uplift (south-east of the Zambezi Delta Basin), could be basement deformation due to a crustal hot spot during early stages of continental breakup, which subsequently cooled down, causing the high to subside to its present depth. Alternatively, it could be a structural high or horst produced during the rifting process.

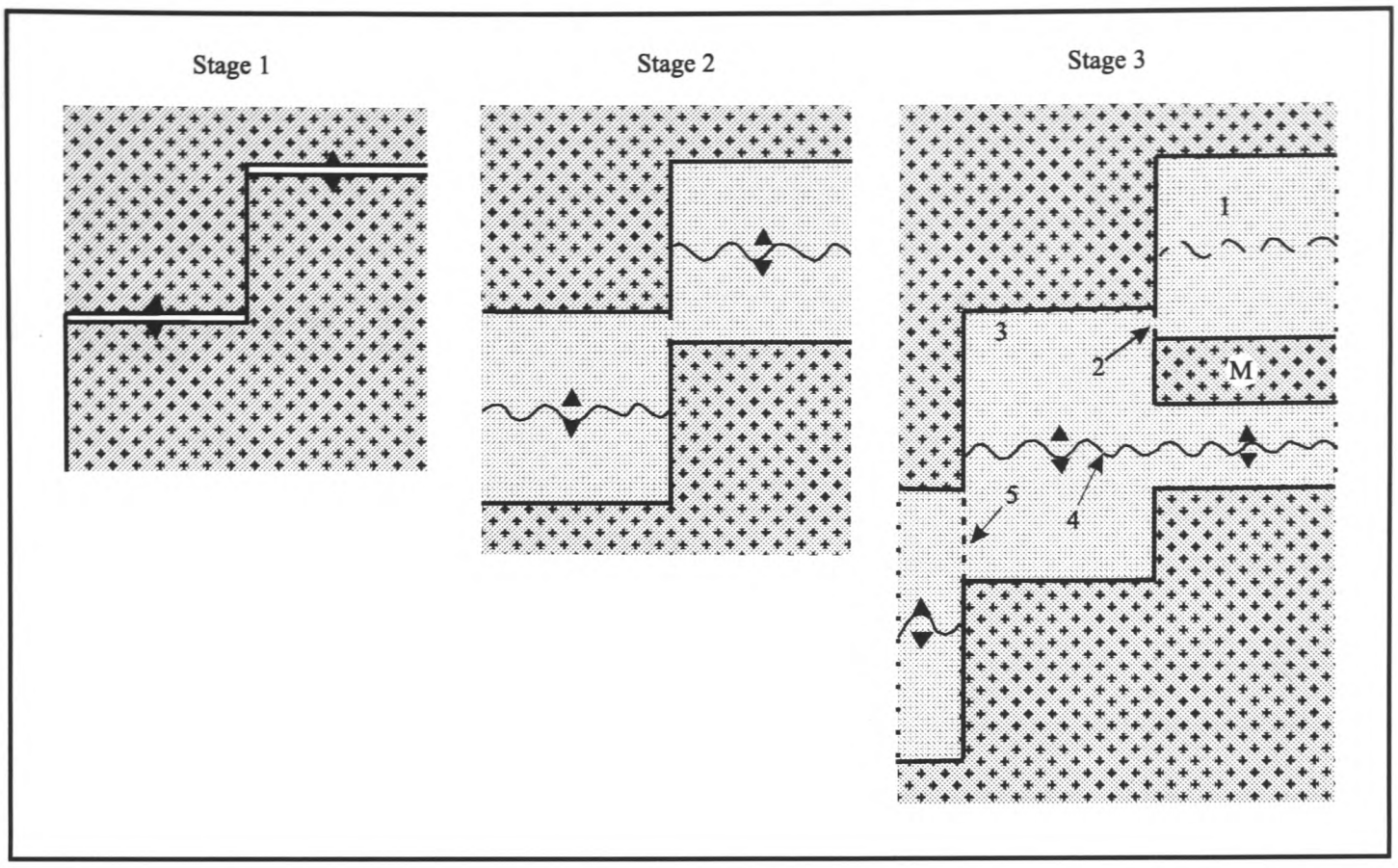

Figure 2.27: A three step model of the three possible stages in the development of fracture zones at a passive continental margin, redrawn and modified after Scrutton (1982). *Key: Stage 1 - rifting, stage 2 - development of a sheared margin, stage 3 - development of a spreading centre jump which may cause a microconinent (M) to be isolated. 1 and 3 - possible basins, 2 and 5 - transform faults and 4 is a possible mid-ocean ridge.*

Passive continental margins are important economically because of their connection to the most important hydrocarbons occurrences known in the world today. Major sediment accumulations develop at rifted margins where graben and associated structural settings provide accommodation space for sediments drained from adjacent uplifted areas during rifting. A large percentage of the world's oil and gas reserves are in Tertiary terrigenous reservoir sands on passive continental margins. Some of these reserves accumulated in large late Mesozoic and Tertiary deltaic basins on passive margins, of which the Gulf Coast (USA), Niger (West Africa), Beaufort-Mackenzie (Alaska-Canada) and the Amazon (northeast Brazil) Delta Basins represent some of the most significant accumulations of this type.

Chapter 3

Data description.

This chapter describes the data used in this study. Data coverage, quality and reliability, and how these factors will determine the quality of the results of the present work are discussed.

3.1 Introduction and exploration history.

Although oil exploration in Mozambique started around 1906 (Coster *et al.,* 1989) it was not until a few years after the end of the Second World War that exploration activities intensified. At that time, gravity and magnetic data were acquired and a few relatively shallow but unsuccessful exploratory wells were drilled. However these activities did realise some economic potential since some coal seams within the Karoo succession were discovered in the northwestern province of Tete.

Exploration activities continued until Mozambique became independent from Portugal in 1975. By 1972, most of the seismic data that exist for offshore parts of the Mozambique Basin south-eastern of Beira, had been acquired by Western Geophysical and a few wells drilled. Most oil companies operating in Mozambique pulled out of Mozambique around 1975 for fear of the political uncertainty ahead. Exploration activities only resumed in Mozambique in 1981 with extensive offshore non-exclusive seismic surveys by Western Geophysical to the south of Beira and in 1982 by GECO-Norway, mainly offshore the Zambezi Delta

Basin, with some regional extension to offshore the Rovuma basin to the north after "Empresa Nacional de Hidrocarbonetos" (ENH), the State Oil Company of

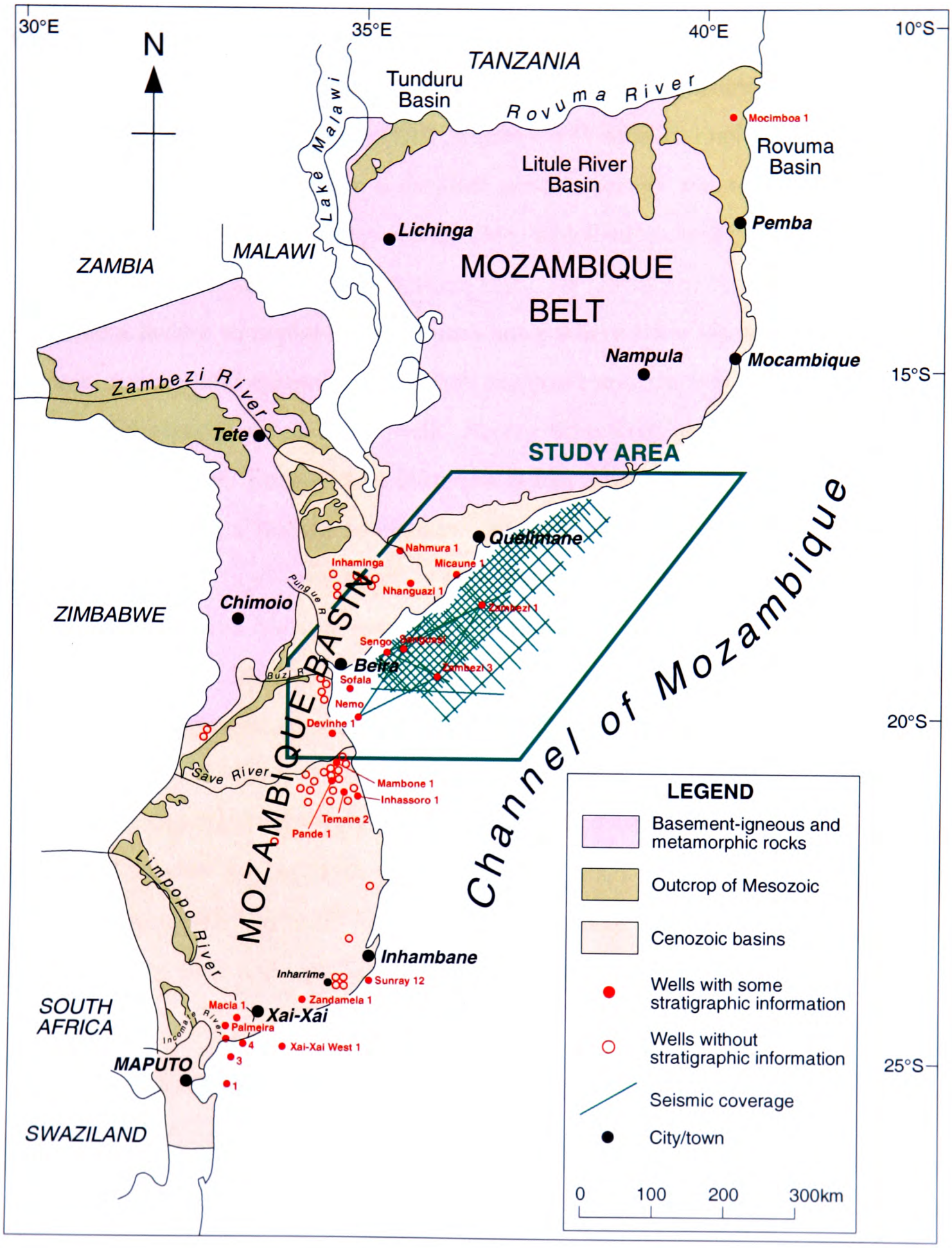

Figure 3.1: Map of the main geological provinces of Mozambique, highlighting the study area.

Mozambique was established.

These activities marked the return of exploration interest to the country with some growing interest in the development of the Pande gas field in north-eastern Inhambane province and two relatively small fields, the Temane gas field to the south of Pande and Buzi gas fields to the north in southern Sofala province.

In 1985 British Petroleum (BP) acquired a licence for exploring the offshore western Xai-Xai graben where a detailed seismic survey was undertaken, which ended with the drilling of a dry well in 1988, which supposedly missed the target and was therefore an invalid structural test. At about the same time EXXON acquired a licence to explore the Rovuma basin where a few kilometres of onshore seismic, gravity and magnetic data were acquired and the well Mocimboa-1 was drilled and abandoned as a dry well. Recent activities have been concentrated around the Pande, Temane and Buzi gas fields, Fig. 1.3. It was only in 1995 that BP acquired a licence to explore the Zambezi Delta Basin including the deep water sector, and Lohnropet, a subsidiary of Lohnro, acquired a licence to explore the Rovuma basin in northern Mozambique.

So far more than 65 wells have been drilled in Mozambique as result of hydrocarbon exploration and no oil has been found. Generally the quality of the data acquired reflects the state of acquisition and processing techniques over time. Data quality is relatively good for data acquired after 1980 and of poor to very poor quality for the data acquired before 1972. Seismic data used in this study are from the 1982 GECO survey and are good to poor quality. Well data are of poor to very poor quality and all were acquired before 1972.

3.2 Gravity and magnetic data set.

The gravity data set was supplied in two files for both the Bouguer anomaly, on- and offshore, and the Free-Air anomaly offshore only (but merged at the coast line with the Bouguer anomaly onshore). Both files consist of a 1km by 1km grid and are made up of a compilation of various data sets acquired on several occasions on- and offshore central and northern Mozambique. Original station

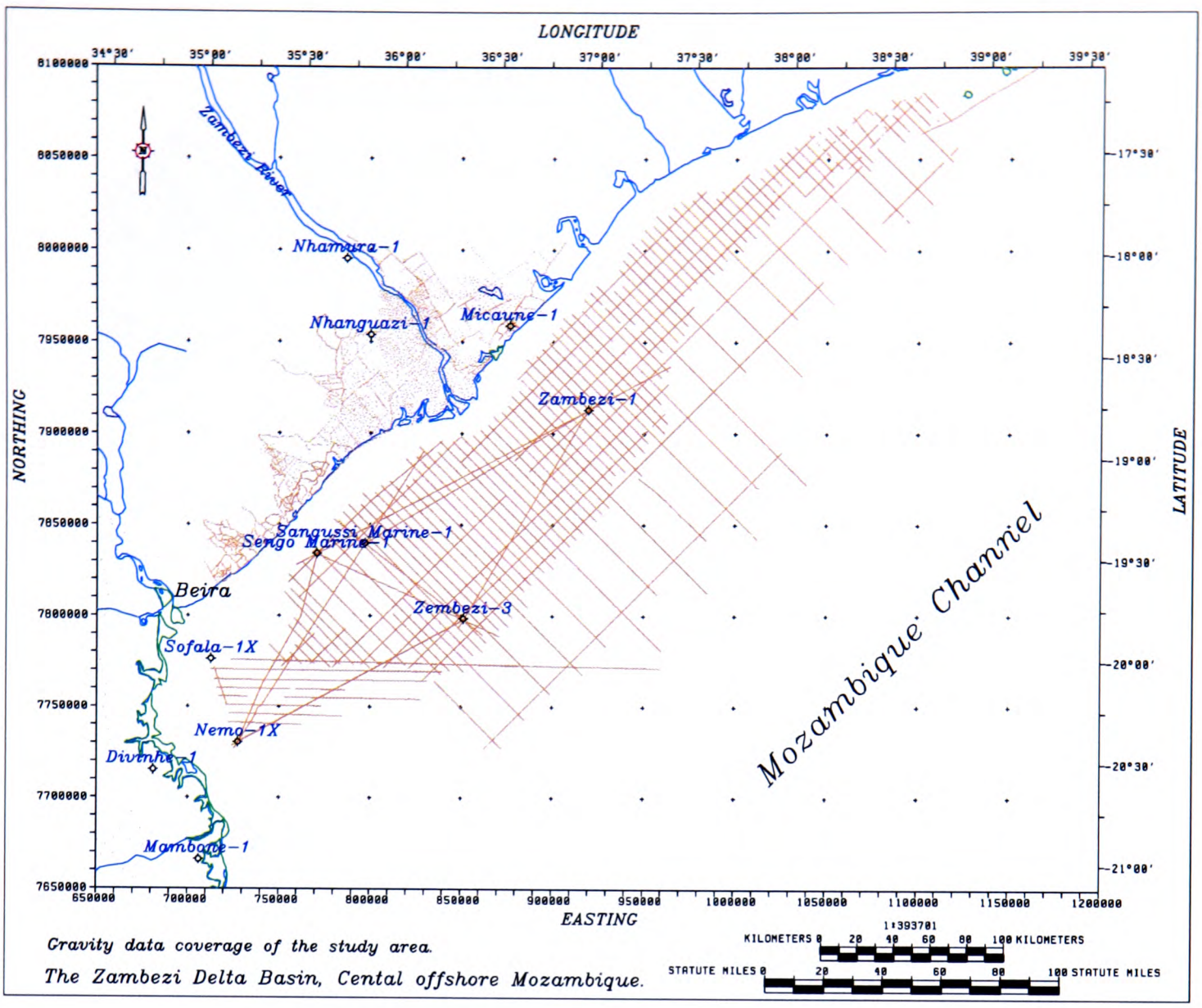

Figure 3.2: Gravity data coverage map for the Zambezi Delta basin and adjacent areas. Data compiled from several vintages and supplied by GETECH, Leeds University.

distribution is very irregular and is best in areas where gravity surveying was undertaken along seismic lines during seismic surveying, generally in offshore areas.

Figure 3.2 shows the gravity data stations on- and offshore in the study area. Offshore gravity data were acquired along seismic traverses during seismic surveying while onshore gravity measurements were undertaken at discrete points along onshore seismic surveying traverses and along the main access roads to the south-west.

The original magnetic data set consists of a series of data points on- and offshore. The magnetic grid is an irregular data grid with relatively dense measurement points in some areas but with no measurements at all in others. Offshore

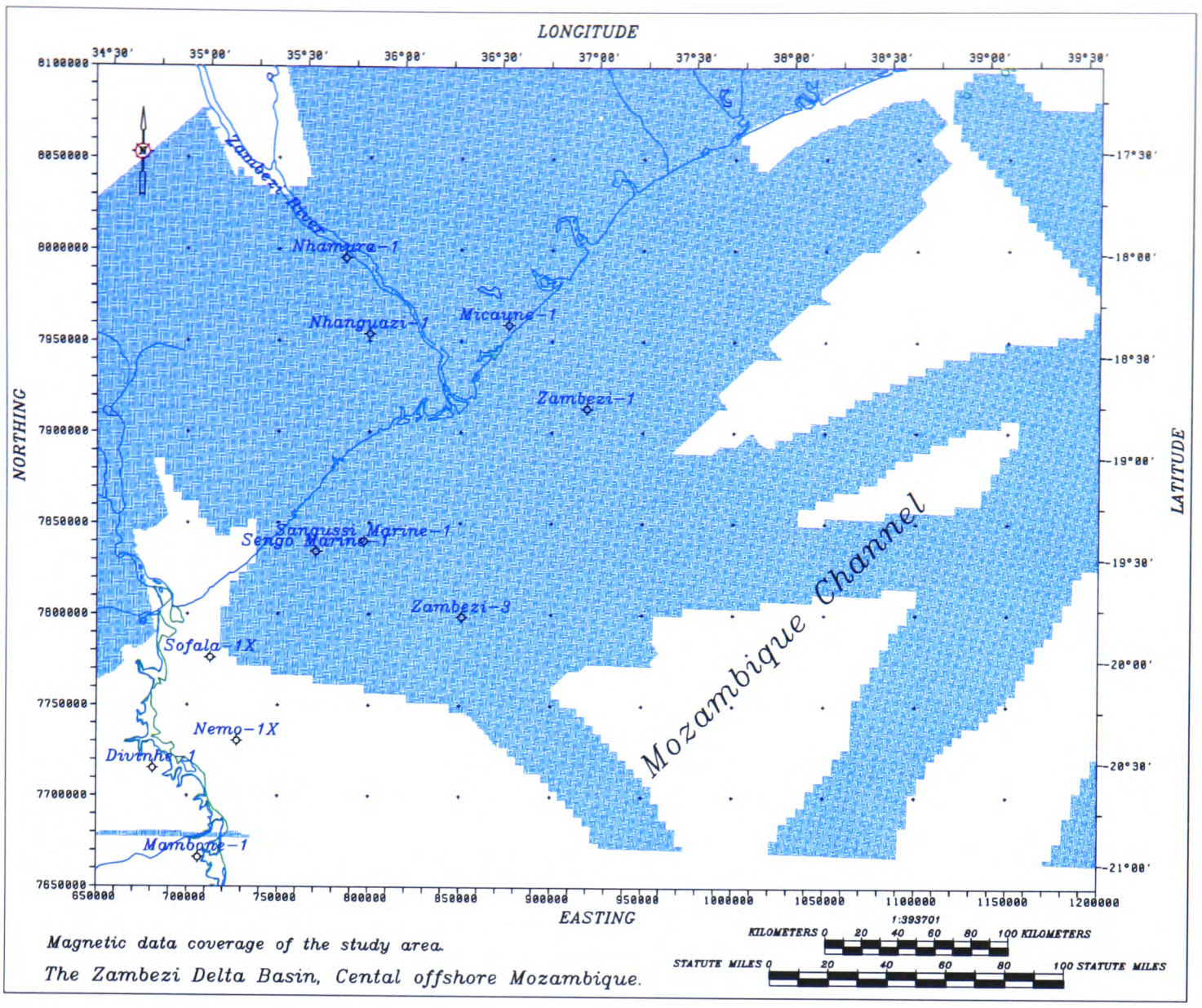

Figure 3.3: Magnetic data coverage (shaded)of the study area. Data supplied by GETECH, Leeds University.

magnetic measurements were taken at points along regional seismic survey lines while onshore aeromagnetic survey provided most of the available data with some scattered land measurements. Fig. 3.3 shows the area covered by a 5'x5' data grid supplied by GETECH for this project. The original measurement points for magnetic data were not made available to the project.

Both the gravity and magnetic data sets were supplied as regularly gridded data with the anomalies reduced to mean sea level. These data were re-gridded and contoured to produce the maps used in Chapter 5.

3.3 Bathymetric and topographic data.

The bathymetric base map was supplied by SGP ("Servicos Geologicos de

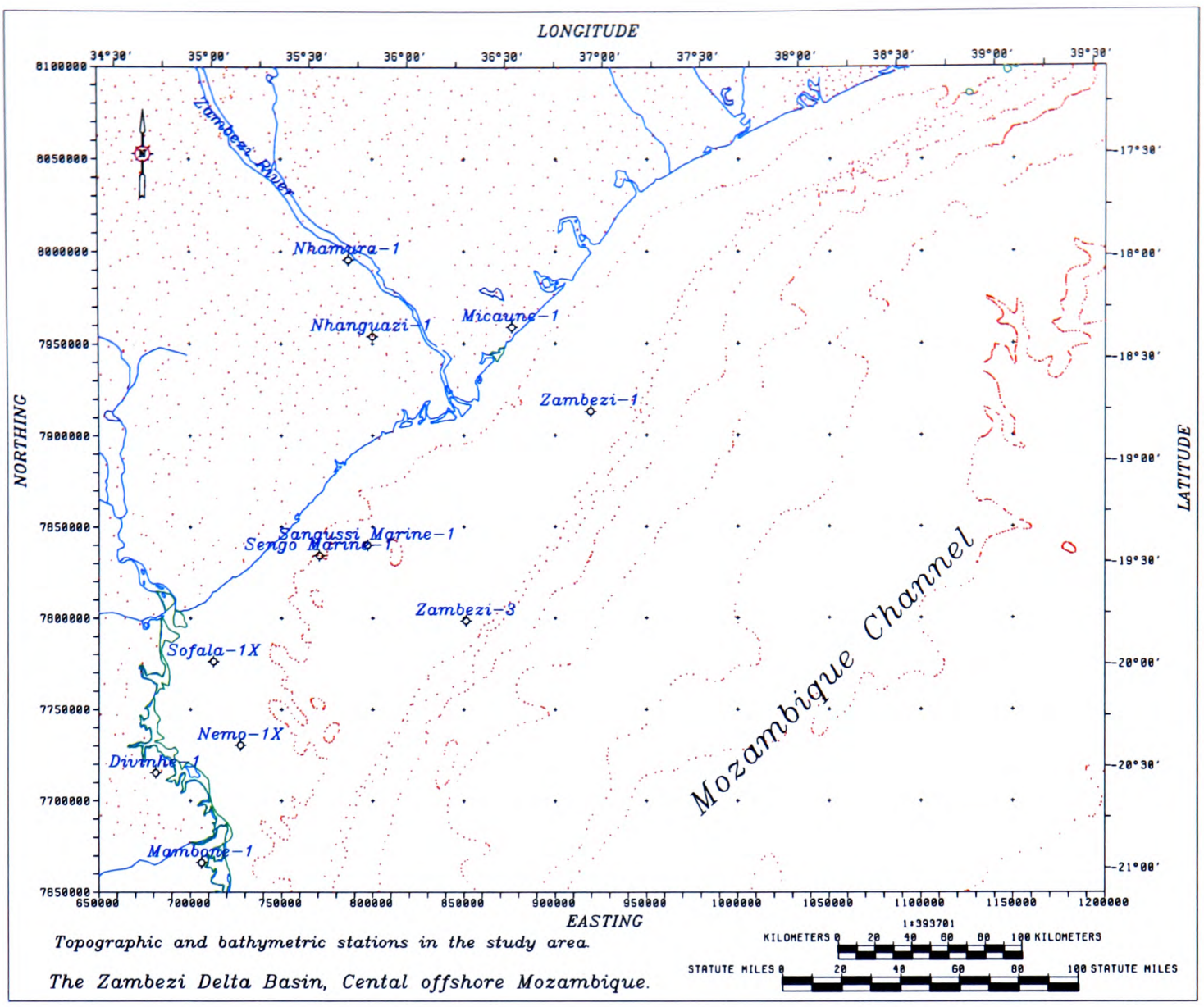

Topographic and bathymetric stations in the study area.

The Zambezi Delta Basin, Cental offshore Mozambique.

Figure 3.4: Topographic data points distribution onshore and contour data points offshore in the study area. Topographic data are digitised from topographic maps of the study area

Portugal") in ASCII format of digitised contour data points, out of a bathymetric data compilation made by the author at SGP in Lisbon in 1990. The original offshore data was obtained from various published bathymetric maps of the Indian Ocean. This data set was merged with the topographic data digitised from a set of topographic maps from the onshore part of the study area to produce the integrated topographic and bathymetric base map used in Chapter 5 (Fig. 3.4).

3.4 Seismic and well data set.

The seismic data set consist of 97 dip lines and line segments, 17 strike lines and line segments and 10 well tie lines from a semi-detailed regional seismic

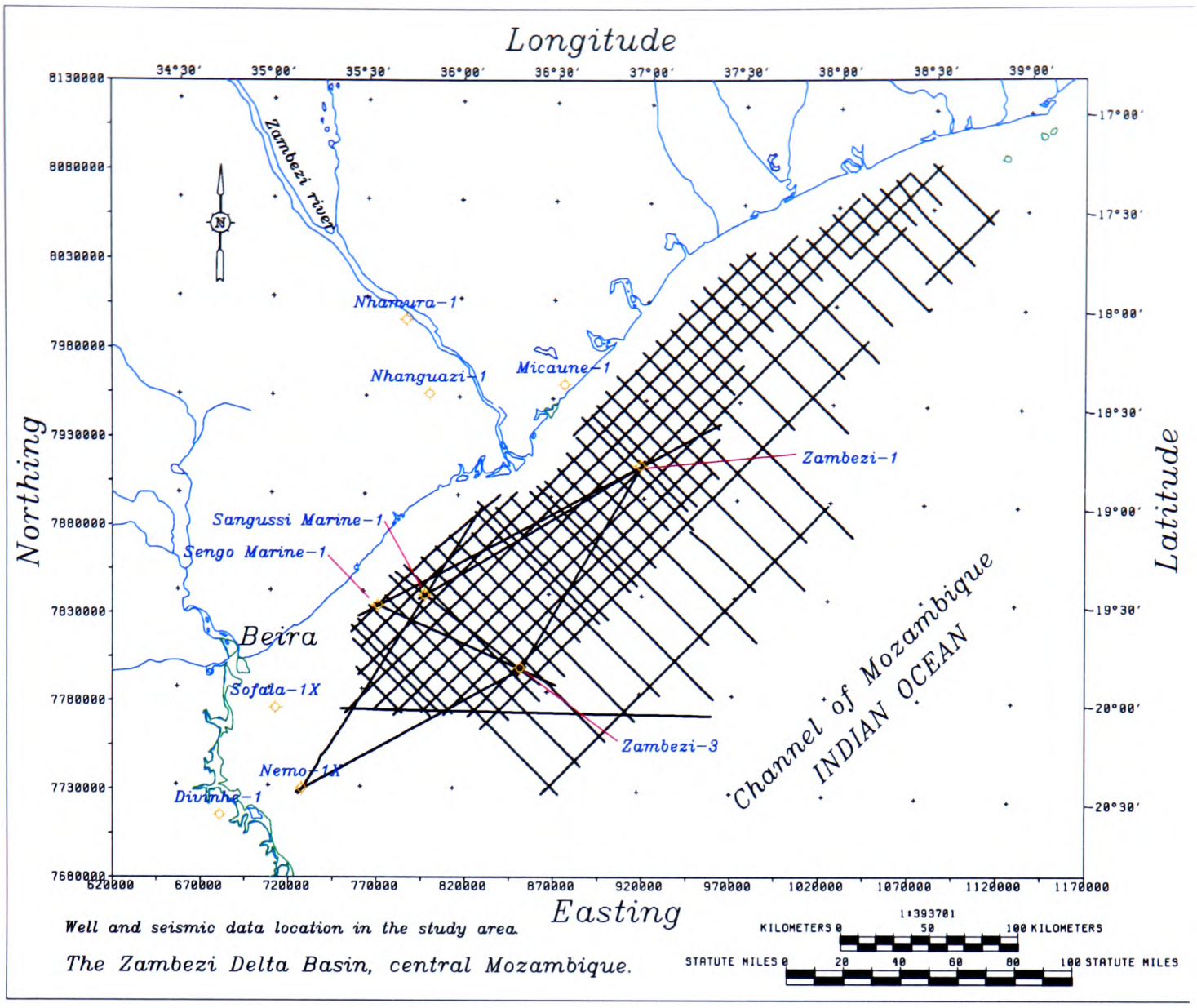

Figure 3.5: Location of the seismic and well data in the study area. This figure includes some wells not used in this work.

survey carried out by GECO, Norway, in February and March 1982 over the Zambezi Delta Basin offshore central Mozambique. These lines together have a total length of 21700 km and they make up a regional seismic data grid of generally 10km line spacing. Figure 3.5 shows the location of the seismic lines and the wells within the study area, while Table 3.1 summarises the recording parameters used during seismic acquisition.

The seismic data were processed by GECO, UK according to the processing parameters summarised in Tab. 3.2. The seismic sections available to this work were all migrated sections and were available only as paper copies with a horizontal scale of 1:50000 and a vertical scale of 5cm/s. The polarity used shows positive numbers on tape plotted on paper as black peaks and the shot point annotation coincides with the source position.

Table 3.1: Summary of the recording parameters used for the survey by GECO, 1982.

Seismic data recording parameters

SHOT BY		GECO A. S.
DATE		Feb. - March, 1982
BOAT		MV GECO DELTA
	Navigation system	Magnavox
	Fold of recording	48
ENERGY SOURCE		Conventional Airgun array
	Total volume	3101 cu ins
	Pop interval	25m
	Shot point interval	25m
	Source depth	7.5m
CABLE		PRAKLA HSSN
	Number of groups	96
	Geophone per group	32
	Near trace offset	283.5m
	Group interval	25m
	Far trace offset	2658.5m
	Cable depth	10m
INSTRUMENTS		DSS V, DFS V
	Format	Seg B, 1600 bpi
	Sample rate	2ms
	Record length	6.0s
	Low cut filter	5.3Hz, 18dB/Octave slope
	High cut filter	128Hz, 72dB/Octave slope
	Gain mode	1 F.P.
POLARITY		Positive acoustic pressure produces a negative number.

The well data set consists of five wells, Nemo-1, Sengo Marine-1, Sangussi Marine-1, Zambezi-1 and Zambezi-3 located within the seismic data grid, and five additional wells drilled adjacent to the study area. These are Divinhe-1, Sofala-1, Micaune-1, Nhamura-1 and Nhanguazi-1 (see Fig. 3.5 for well location). All

Table 3.2: Summary of the processing flow and main parameters applied to the seismic data by GECO, UK, 1982.

Seismic data processing sequence

PROCESSED BY		GECO UK
DATE		April, 1982
INITIAL PROCESSING		
	Processing record length	6-8s
	Processing sample rate	4ms
	Demultiplex	
	Gain recovery	
	Trace sum	2-fold
	Editing	
	Spherical divergence compensation	
DECONVOLUTION		
	Type	Predictive
	Total operator length	200ms
	Prediction lag	16ms
	Number of operators	1
	Auto-correlation design window	3000ms
	Design start	Near trace W.B. + 200ms, approx. offset variant
CORRECTIONS		
	Static corrections	Shot and streamer static + 12ms
	Datum	Sea level
Velocity for NMO corrections derived from GECO's contoured velocity spectra.		
COMMON DEPTH POINT STACKING		fold 48
RUNNING MIX		3 trace, weighted 1 2 1
DECONVOLUTION		
	Type	predictive
	Total operator length	200ms
	Prediction lag	24ms
	Number of operators	1
	Auto-correlation design window	W.B. + 100ms - W.B. + 4100ms

..... table continues next page .....

WAVE EQUATION MIGRATION

Finite difference approximation. Interval velocities for migration derived from the stacking velocities, smoothed and applied over user specified zones, consistent with geological boundaries.

SPACE AND TIME VARIANT BANDPASS FILTERING

These times are approximate for shallow water data.	TIME (s)	LC (Hz)	HC (Hz)	Slopes (dB/Oct)
	0.5	20	60	30/60
	1.0	15	50	30/60
	2.5	15	50	30/60
	3.0	10	40	30/60
Time variant equalisation	4.0	8	35	30/60

these wells were drilled between 1956 and 1972. The datum to which depth measurements refer vary from well to well. This problem is accounted for in Chap. 4 where well data interpretation and correlation is carried out.

Geological well tops are established using all sources of information available to this study, which are reconciled with each other to overcome discrepancies in data quality. Where well tops coincide with major depositional breaks (unconformities), these can be correlated through the five wells located within the seismic grid and then tied to the seismic sections to establish the stratigraphic framework used in this work (Chap. 4).

Well completion reports were available for some of the wells and well log data are also available for various well log types on paper copies plotted at a scale of 1:200. Table 3.3 summarises the well log information for the wells used in this study. Gamma ray and Sonic logs of wells Zambezi-1, Zambezi-3 (Fig. G.1), Sangussi Marine-1 and Divinhe-1 (Fig. G.2) are displayed in Appendix G in Volume II to ilustrate some of the problems concerning data quality discussed in this Chapter and later in the subsequent Chapters.

The only reliable source of seismic velocities in this work was the stacking velocity panels displayed on the seismic section which were digitised point by point for each velocity analysis shot-point for each line segment (see Fig. 3.6).

Table 3.3: Summary of well log data used in this work, data supplied by ENH and INTERA.

Well log data summary

Well name and location	Logging company and scale	Log sinature and well report	Depth range (feet) and total depth	Drilling company and date
Divinhe-1 X = 34 44 17 E Y = 20 39 13 S **(onshore)**	Schlumberger 1:200	- Sonic log - Gamma ray log - Neutron log - Electrical log . SP - . 8" Lateral . 64" Normal . 16" Normal - Caliper log	505-12593 12593 (3840.0 m) (Sena) **Neocomian - Cenomanian**	Mozamboque Gulf Oil Co. **(Gulf AMOCO)** 20/08/1962
Micaune-1 X = 36 33 40 E Y = 18 25 43 S **(onshore)**	Schlumberger 1:200	- Sonic log -Gamma ray log Neutron log	40-15110 15110 (4607.7m) **Turonian**	Mozambique Gulf Oil Co. **(Gulf AMOCO)** 19/11/1966
Nemo-1 X = 35 10 53 E Y = 20 30 44 S **(offshore)**	Schlumberger 1:200	- Sonic log - Gamma ray log - Sidewall neutron log - Electrical log . SP . Short normal . Induction log . Conductivity log - Caliper log - Density log - Bit size	547-13482 13482 (4125.0 m) (Basalt) **Neocomian - Cenomanian**	Mozambique Gulf Oil Co. **(Gulf AMOCO)** 04/03/1970
Nhamura-1 X = 35 42 38 E Y = 18 06 45 S **(onshore)**	Sclumberger 1:200	- Sonic log - Gamma ray log - Sidewall neutron log - Electrical log . SP . Short normal . Induction log	10-17914 17914 (5490.0 m) **Pre-Cambrian**	Mozambique Gulf Oil Co. **(Aquitaine)** 26/02/1972

... table continues next page ...

... table continued from previous page ...

Well name and location	Logging company and scale	Log sinature and well report	Depth range (feet) and total depth	Drilling company and date
Nhanguazi-1 X = 799959 (UTM) Y = 7953789 (UTM) **(onshore)**	Schlumberger 1:200	- Sonic log - Gamma ray log - Sidewall neutron log - Electrical log . SP . Short normal . Induction log - Caliper log - Bit size	87-10986 10986 (3350.0 m) (Sena) **Neocomian - Cenomanian**	Mozambique Gulf Oil Co. **(Aquitaine)** 17/08/1971
Sangussi Marine-1 X = 35 49 51 E Y = 19 30 50 S **(offshore)**	Schlumberger 1:200	- Sonic log - Gamma ray log - Electrical log - . SP . Short normal . Induction log	533-12014 12014 (3664.0 m) **Turonian**	Mozambique Gulf Oil Co. **(Aquitaine)** 30/12/1971
Sengo Marine-1 X = 35 34 50 E Y = 19 34 09 S **(onshore)**	Schlumberger 1:200	- Sonic log - Gamma ray log - Sidewall neutron log - Electrical log . SP . Short normal . Induction log - Caliper log - Bit size	534-14052 14052 (4286.0 m) (Sena) **Neocomian - Cenomanian**	Mozambique Gulf Oil Co. **(Aquitaine)** 26/11/1971
Sofala-1 X = 35 02 02 E Y = 20 06 00 S **(offshore)**	Schlumberger 1:200	- Sonic log - Gamma ray log - Sidewall neutron log - Caliper log - Bit size	493-3460 10588 (3232.0 m) (Lower Domo) **Albian - Aptian**	Mozambique Gulf Oil Co. **(Gulf AMOCO)** 10/04/1970

... table continues next page ...

... table continued from previous page ...

Well name and location	Logging company and scale	Log sinature and well report	Depth range (feet) and total depth	Drilling company and date
Zambezi-1 X = 36 58 40 E Y = 18 50 00 S **(offshore)**	Sclumbreger 1:200	- Sonic log - Gamma ray log - Electrical log . SP . Short normal . Induction log - Conductivity log.	75-15222 15222 (4656.0 m) **Upper Cretaceous**	Mozambique Gulf Oil Co. **(Hunt)** 13/02/1971
Zambezi-3 X = 36 21 09 E Y = 19 52 44 S **(offshore)**	Sclumberger 1:200	- Sonic log - Gamma ray log - Electrical log . SP . Short normal . Induction log - Conductivity log	810-14798 14798 (4501.0 m) **Upper Cretaceous**	Mozambique Gulf Oil Co. **(Hunt)** 06/09/1971

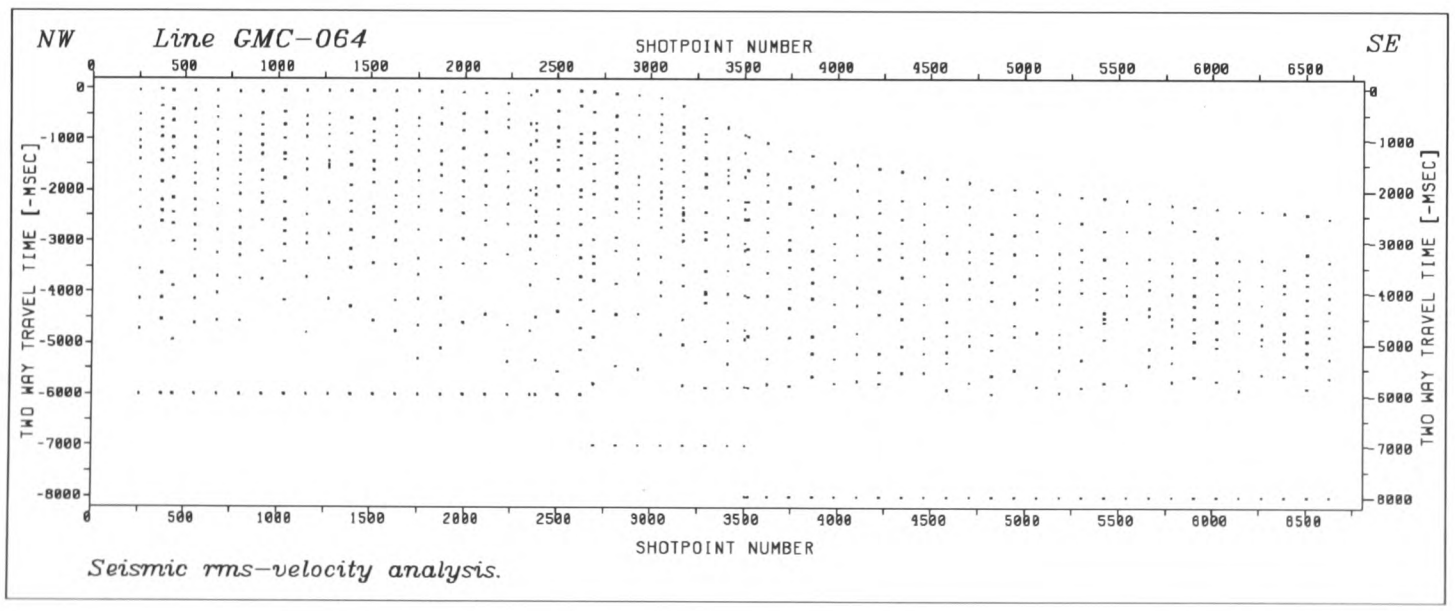

Figure 3.6: A typical stacking velocity profile. Black dots represent velocity sampling points. Average velocity sampling interval, 100 shot-points (2500 m) along the seismic section.

The digitised velocity data were then gridded and used to calculate rms-velocities

along interpreted horizons and rms interval velocities for enclosed geologic intervals between two horizons as discussed in Chapter 4.

3.5 Discussion of data quality.

3.5.1 Gravity and magnetic data.

Gravity data coverage for the Zambezi Delta Basin is good for a continental margin over the GECO survey but generally poor elsewhere, as Fig. 3.2 shows. It was only measured offshore along the seismic surveying lines at very close, non specified intervals. The onshore data were collected along seismic traverse and on land surveys of several vintages, the later ones mainly collected for mineral exploration purposes. Offshore gravity only covers parts of the present delta top and delta slope (water depth generally between 20 and 500 m), with the remaining parts of the slope and pro-delta are uncovered.

Magnetic data coverage in turn is in some areas better than gravity but its coverage of the offshore part of the study area is generally poorer than gravity data coverage and magnetic data onshore is very much affected by magnetic high frequency anomalies caused by strong magnetic anomalies which are more accentuated in areas to the north and north-east where the Mozambique Metamorphic Belt of Precambrian age outcrops.

Both gravity and magnetic data were merged and gridded by GETECH in Leeds during the course of the African Gravity and Magnetic projects. Because of poor data coverage of the study area some features on the maps used in this work merely represent the effect of the interpolation method employed for gridding the data in the areas between measurements and might not represent real geological structures. Therefore the knowledge of the original data coverage maps is very useful for a rational interpretation of the anomaly maps produced and used for both gravity and magnetic modelling in Chapter 5. The poor data coverage in some parts of the study area limits the use of the available maps for deriving and interpreting geologic structures, unless they are used in addition to other geological and geophysical information in the area.

3.5.2 Bathymetric and topographic data base .

The two data types merged together produce a good coverage of the study area. This data was then gridded to produce a combined bathymetric-topographic map displayed in Chapter 5 which was used to calculate Airy isostatic models necessary for gravity modelling also carried out in Chapter 5.

3.5.3 Seismic and velocity data.

The quality of the seismic data is generally good for the purpose of this study. The upper 4.0 - 4.5 sec of seismic record is generally of good quality while the section below is generally poor to very poor in quality which unfortunately prohibits accurate seismic stratigraphic interpretation in the deeper stratigraphic section. The presence of unsuppressed multiple reflections from the sea bed is responsible for the worsening quality of seismic data at areas below the upper slope. This makes the correlation of geologic marker horizons interpreted in this study particularly difficult in this area.

The seismic data grid with line spacing of about 10km in both dip and strike is too great to be appropriate for mapping and studying short wavelength features like distributary channels and the channel valleys visible on some of the individual seismic sections studied. This is likely to be crucial for future exploration because these features are critical in locating and describing sedimentary environments and facies, as well as predicting lowstand fans of reservoir quality sands and establishing trapping conditions through the mapping of seals deposited on top of the lowstand sands during subsequent transgression. Obtaining an infill grid of seismic lines with extended recording time in the deeper stratigraphic parts of the basin is one of the main suggestions to arise from the current study.

The stacking velocities, which provide the only reliable seismic velocity information available to this study, are generally well sampled in the upper 4.0 - 4.5 sec of the seismic record, being poor to bad in the section below. This of course has direct implications for the quality of the depth conversion procedure performed in Chapter 4 with the general effect of producing exaggerated depth

values. Exaggerated depths reflect the fact that stacking velocities are generally higher than check-shot velocities (Al-Chalabi, 1974) (not available in this study), which are the best seismic velocities for use in depth conversion procedure. Check shots can be used to calibrate seismic stacking velocities in areas of sparse well information before using the latter for depth conversion. Figure 3.6 shows a typical velocity sampling profile, where it can be clearly seen how the velocity picking worsens with seismic two-way travel time (TWT).

3.5.4 Well log data.

Well log data quality tends to vary with the well contractor and therefore it tends to vary from well to well and, in a single well, the quality of the well log signature may vary considerably from one logging method to another. The available well completion reports are characterized by differing quality and very often information is inconsistent and inconclusive within the reports.

The greatest problem often seems to be dubious reference depth or height to which measurements are tied, which in turn is crucial in tying well data to seismic marker horizons. The geologic age information reported in the completion well reports is often inconsistent with the geologic age given in well logs for the same well. This and other important aspects are discussed in more detail in Chapter 4. These inconsistencies cause problems in performing well-to-well correlation and in producing a consistent well to seismic tie. This makes an attempt to establish a age dated chronological interpretation of geologic events throughout the basin a difficult task. Nevertheless a few wells (Sengo Marine-1, Sangussi Marine-1 and Zambezi-3) with relatively consistent geologic age information have been used to calibrate the others and the best possible correlation has been achieved for this work.

3.6 Summary.

Gravity data provide a good coverage of the continental margin over the Zambezi Delta Basin. The Free-Air anomaly map offshore, merged with the

Bouguer anomaly at the coast line, provides a good basis for gravity modelling along a profile in the dip direction carried out in Chapter 5. In contrast, discontinuous magnetic data coverage (Fig. 5.2) resulted in a discontinuous magnetic anomaly map which did not allow the same sort of modelling to be carried out with the gravity anomaly. Major magnetic anomaly trends are generally obvious and two dimensional interpretation of isolated anomalies is attempted in Chapter 5.

The combined topographic and bathymetric map provided a good basis for the calculation of Airy isostasy based models for the study area also carried out in Chapter 5.

The seismic data set is of good quality in the upper part of the section (4.0 -4.5 sec) and poor to bad below. A grid with a line spacing of 10 km did not allow short wavelength features such as erosion Channels and Channel valleys to be studied on an areal basis, instead a broad picture was achieved. The stacking velocity data were also good to poor in the upper 4.0 -4.5 sec and very poor to bad below. As the only source of velocity information in the area, it was used to depth-convert some dip and some strike seismic sections which provided some information about the depth to mapped geologic events.

Well data from wells tied to the seismic and from others in surrounding areas provided a fair to good basis for erecting the stratigraphic framework necessary for the interpretation of seismic data in Chapter 4. The discontinuous logging at several wells for some well log types is addressed by using several log types to achieve the correct lithologic interpretation at those wells see Table 3.3.

Wells adjacent to the study area and geological and geophysical information in and around the area were also useful in achieving some improvement in the interpretation carried out in the offshore part of the basin, allowing extension to its onshore part and adjacent areas.

Chapter 4

Basin evolution and sedimentation.

The main aims of Chapter 4 are to study seismic and well data in order to produce a basin development model for Cretaceous and Tertiary basin evolution. The results achieved in this chapter enable the gravity models to be refined and discussed in Chapter 5 although the chief purpose is to help discuss and constrain the main controls on basin evolution and sedimentary architecture in Chapter 6.

4.1 Introduction.

The Zambezi Delta Basin is a large sedimentary basin extending about 300km from onshore to offshore into the Mozambique Channel in a NW-SE direction and covers an estimated area of about 75,000 square kilometres. It is poorly explored with only a few wells drilled by various oil companies over a period of more than 40 years (Kihle, 1983; Fortes and Kihle 1983).

Modern seismic surveying was first acquired in the offshore part of the basin by GECO, Norway, in 1982 as the first step of modern oil exploration of the Mozambique Basin. The data acquired has since been available for interpretation by a consultancy group from the Russian Petroleum Institute in Moscow led by

Salman and working for ENH, the State Oil Company of Mozambique and by ECL (currently Intera Information Technologies Limited) also working for ENH and by the Norwegian Petroleum Directorate in Stavanger, Norway.

One common character of all interpretations produced so far is the focus on deep and old (Jurassic and Cretaceous) structures as the main objective during the mapping of potential petroleum plays in the basin.

Whilst the present study has attempted to define pre-Tertiary structures it is recognised that the constraints imposed by the quality of the data largely limit accurate interpretation to the upper part of the sedimentary section encompassing Upper Cretaceous and Tertiary sedimentary successions. A comprehensive sedimentary geo-history of the Tertiary stratigraphic section of the basin has resulted from this study.

Although lack of accurate biostratigraphic and core data does not allow this study to carry out a detailed sequence stratigraphic interpretation, the seismic data has enabled a comprehensive seismic stratigraphic interpretation to be conducted. The latter is based on the mapping of surfaces defined by reflector terminations. The deposited units thus defined have been constrained by ties to all available well data all across the seismic grid.

To accomplish the above task, well logs from nine wells have been interpreted and well tops reconciled with each other to overcome discrepancies caused by varying data quality as already alluded to in Chapter 3. A stratigraphic framework is erected based on well tops correlation. Several well correlation panels are produced to describe stratigraphic relationships according to well stratigraphy in various directions within the delta basin. Most of the well tops are coincident with major unconformities mapped on seismic data. This allow the definition of ten megasequences in the Upper Cretaceous (Top Albian) to Recent times.

The unconformity-defined megasequences separate geneticaly related sediments deposited and preserved between major hiatuses as discussed later in this chapter and in Chapter 6. A detailed seismic stratigraphic interpretation is conducted for the three upper megasequences and a set of two-way travel time (TWT) isochron and isopach maps are produced showing in some detail delta develop-

ment and architecture throughout geologic time. All isochron and isopach maps are included in Volume II of this thesis.

Velocity analysis was conducted to assess the quality of the seismic velocities for use in depth conversion. However, this proved inconclusive due to large misties (errors) at crossovers caused by velocity anisotropy in dip and strike which would have to be accounted for before these data could be used for depth conversion.

Subsidence analyses was performed to assess basin subsidence due to sediment loading (Allen and Allen, 1992). A qualitative evaluation of the effect of eustatic sea level variation is made and the effect of the deep sea currents of the Mozambique Channel is assessed. The last is of general importance for the assessment of sediment dispersal in the Mozambique Basin as a whole.

Chronostratigraphic diagrams were produced which emphasise the upper section of basin stratigraphy. They show that during ealy stages of the Zambezi Delta Basin, sediment buildup (Early Tertiary) was dominated by sediment supplied from the southwest through the Lower Zambezi Graben and the Save River. This was gradually superceded and dominated by sediment inputs from the northwest, from a moving position which occasionally matched the present day geographic location of the Zambezi River mouth. The sedimentary patterns to the far northeast suggest possible early activity of the Zambezi River tributaries to the north, or of other streams which might have predominated at some stage of delta development in the northeast. Onshore seismic data would be required to explain the exact situation.

4.2 Well log interpretation and correlation.

4.2.1 Foundations for well log interpretation.

Well drilling provides the geologist with crucial geological information about the penetrated rock formations, particularly when core samples are taken from extensive lengths of the borehole. This is not very often in practice because of the very high costs of core sampling.

Well logging was developed over years of oil exploration practice and is a

good alternative to core sampling. When applied, this provides more information about the penetrated rock formations by measuring geophysical parameters such as the formation resistivity, sonic velocity, density, radiometry and the angle of dip of rock contacts. From these measurements interpretations may lead to the determination of the lithology and formation porosity of the penetrated rock formations and the quantity of fluids (gas, oil or water) within the pore space. However they do not give any direct information on the lateral extent of the rock formations penetrated by the borehole nor its age. Nevertheless lateral well to well stratigraphic correlations are very common and are achieved by making assumption based on similarities observed in adjacent wells and additional geological and geophysical knowledge.

Geophysical well logs measure geophysical properties of the strata adjacent to the borehole wall by passing a series of electrical devices of various designs through the borehole. These devices record physical and chemical properties of the sediment rock formation, including resistivity, electric potential difference, radioactivity, density and sonic velocity.

Depositional systems tend to form characteristic sequences of grain size and sedimentary structures, represented by distinguishable sequences of grain size profiles. Some geophysical log responses are indirectly related to sediment grain size, which allows them to be used to produce vertical grain size profiles. The Gamma Ray log and the Self-Potential or Spontaneous Potential (generally known as the SP log) are the two geophysical well logs mainly used to derive vertical grain size profiles for boreholes (Selley, 1976; Serra, 1986; Selley, 1992).

The gamma log records the rock formation radioactivity as the sonde is passed through the borehole. The radioactivity measured is a measure of the amount of clay present in the rock formation if no other radioactive minerals are enclosed. Gamma values are generally greater in formations composed of clay minerals and it tends to increase in proportion to the amount of clay present in the sediment and with decreasing sediment grain size, i.e. in shales.

A handicap is the occurrence of radioactive minerals other than those present in clay minerals, particularly the presence of large amounts of mica, glauconite

or zircon, which can make a sand abnormally radioactive and appear fine and shaley on the gamma log. The use of core where available can aid in removing uncertainties.

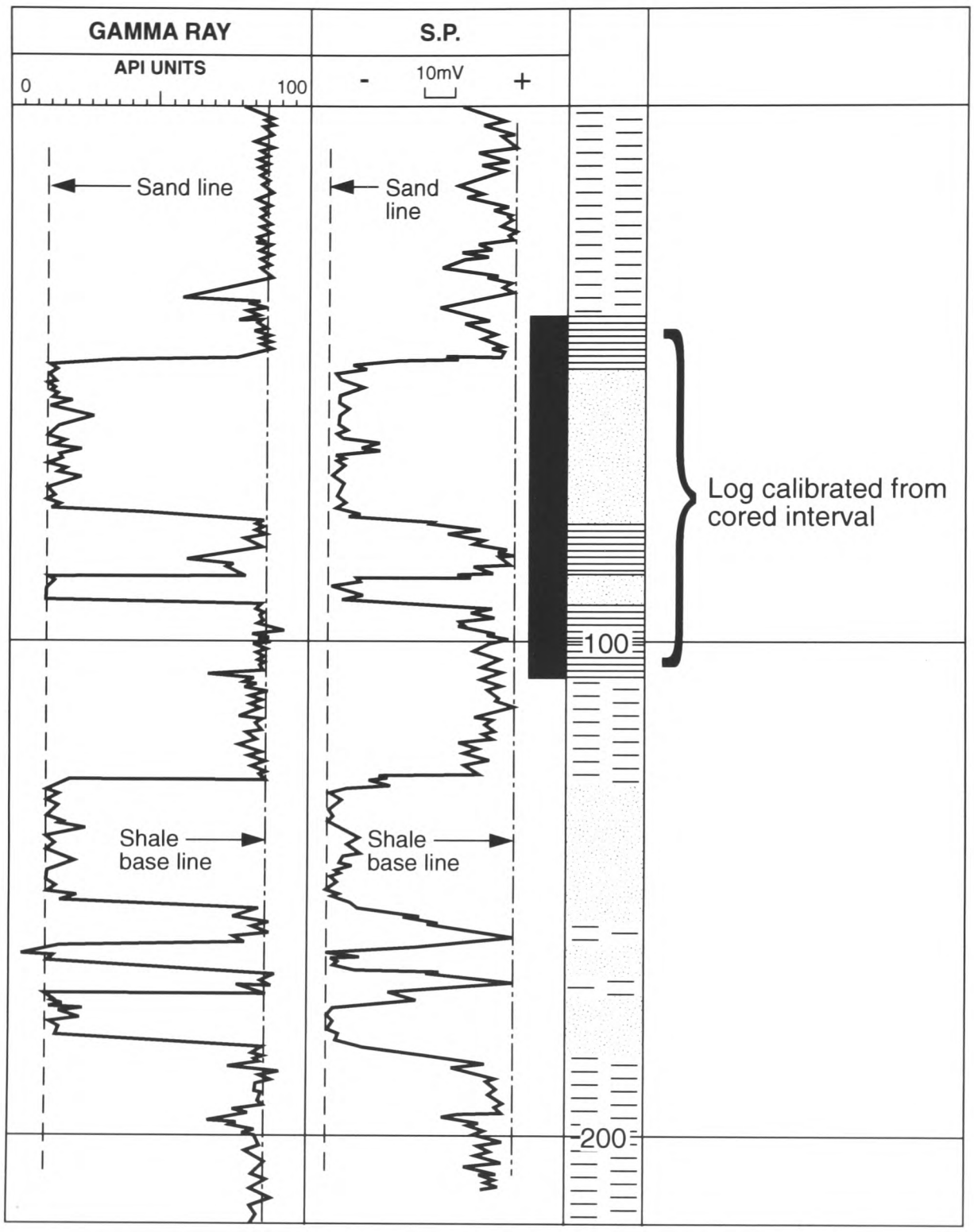

Figure 4.1: Schematic gamma ray log and spontaneous potential (SP) log curves against depth, illustrating how the sand line and the shale base line are derived, redrawn and modified after Selley, 1992. Sand grain size can be calibrated where core or well cuttings are available.

The SP log record gives the electrical potential difference between the potential of an electrode moved through the borehole and the fixed potential of

an electrode placed at the surface. The potential difference varies with electrochemical properties of the strata adjacent to the borehole and are both related to formation permeability. Generally shales are impermeable and sands are permeable.

In sands permeability tends to decrease with grainsize due to the increasing amount of clay minerals present in the fine sand matrix. Nonetheless the SP log essentially records permeability and because permeability is generally related to grain size, the SP log can also be used to derive vertical grain size profiles for boreholes.

For both tools a sand line and a shale base line can be established from the two extreme values of each curve and thus calibrated to particle size (Fig. 4.1). For the SP log, calibration can be achieved since the sand line corresponds to the coarsest sand penetrated by the borehole. Core sampled borehole intervals can also be used to calibrate the borehole logs.

Limitations to the use of both methods exist. Known relationship between permeability and grain size is only valid for sediments with primary intergranular porosity and we know that most rock formations penetrated by boreholes have undergone diagenesis and compaction with some degree of cementation, thus showing reduced or secondary porosity.

4.2.2 Well log interpretation and correlation.

Gamma and SP logs are qualitatively interpreted and vertical grain size profiles for nine wells drilled between 1962 and 1972 in on- and offshore areas of the Zambezi Delta Basin and adjacent areas are produced (Fig. 4.2 and Appendix G). The profiles produced show vertical lithological variation for each well according to the depositional cyclicity at each well location. Obvious major geologic breaks recorded on log signatures are infered in the stratigraphic column derived for all wells studied on- and offshore the Zambezi Delta Basin and adjacent areas.

The interpretation of the wireline logs is aided by the well completion reports and by the composite logs (available only for a few wells) provided. In interpreting

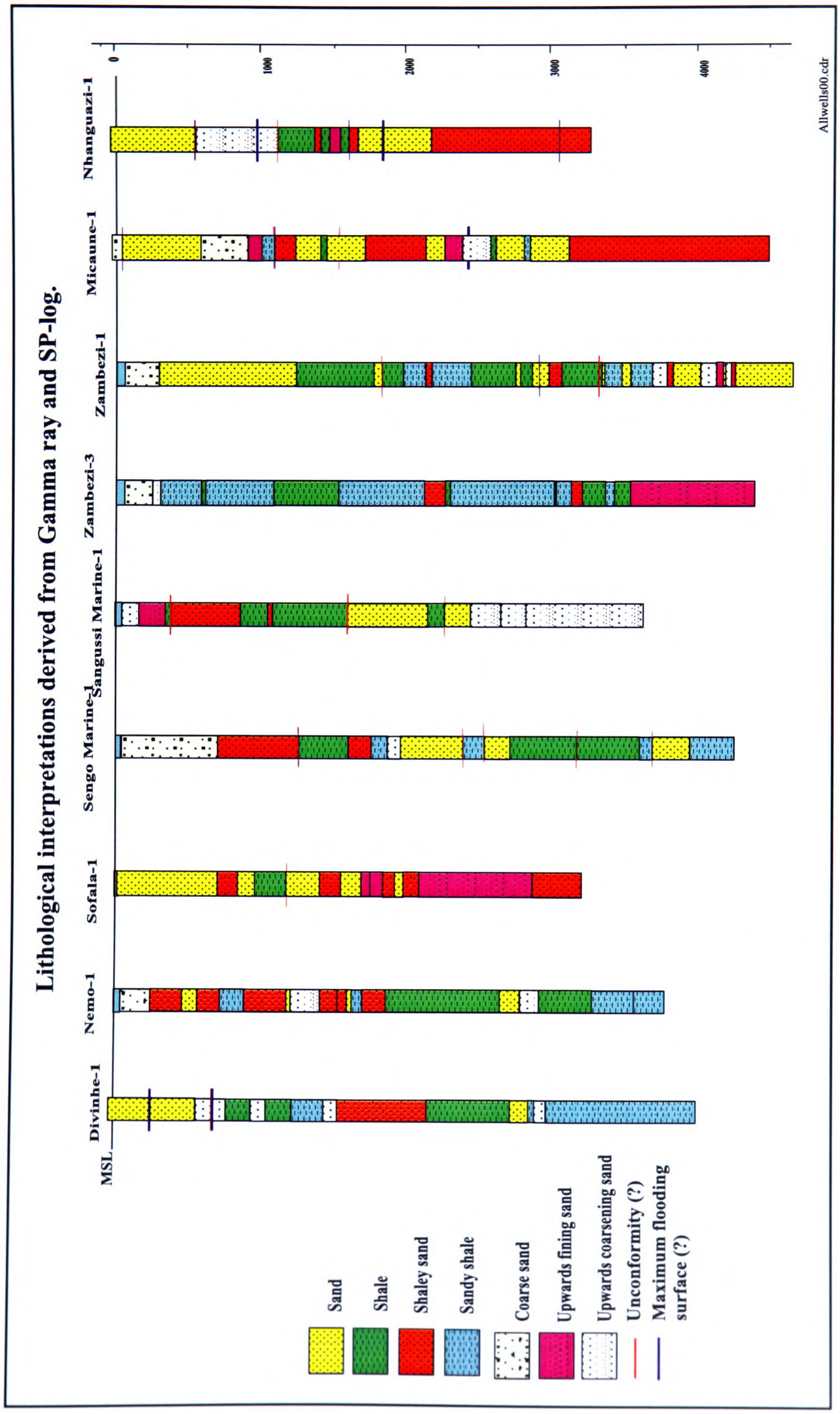

Figure 4.2: Grain size profiles for nine wells derived from Gamma ray and SP-log, well completion reports.

Key for well logs lithostratigraphic interpretations

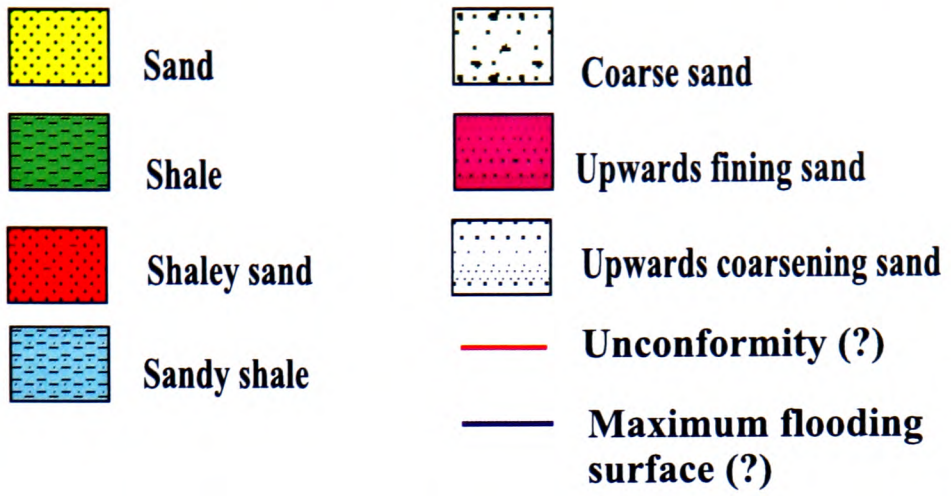

Note: - Gamma ray log displayed in first column on wells Divinh-1, Sofala-1, Sengo Marine-1, Sangussi Marine-1, Zambezi-1, Zambezi-3, Micaune-1 and Nhanguazi-1.

- SP-log displayed in first column on well Nemo-1.

- Sonic, Neutron, short normal, sidewall neutron, conductivity and induction logs are alternatively displayed alongside the Gamma ray log and SP-log.

- Maximum flooding surfaces (mfs) and unconformities are defined using total Gamma ray log, (eg. High Gamma ray for mfs and low Gamma ray for unconformity).

See also section 4.2 for discussion.

Figure 4.3: Key for well logs lithostratigraphic interpretations used in this thesis.

the Gamma ray and the SP logs the sand line and shale base line are established, aided by the composite log where it is available. Five lithologies are defined according to grain size as coarse sand, sand, shaley sand, sandy shale, shale, together with units of upwards fining and upwards coarsening sand.

For sediment sequence deposited steadily under the influence of gravity, heavy sediments would be deposited first and more close to the sediment source while lighter sediments will be carried further from the source and deposited last. The interpretation of the Gamma ray and SP logs as well as the derrived grain

size profiles may also lead to interpretations on basinal energy regime as well as depositional environments throughout geological time at a well site and in the basin. Therefore in a marine sequence prograding seaward coarse sand will preceed sand and fine sand which will be followed by shaley sand, sandy shale and muds (shale).

Sediment grain size can also be related to depositional environments in a similar way as greater grain size will be related to coastal and shallow depositional environments while fine sediments and muds generally belong to deep water depositional systems. Depositional units are also fashioned by tectonic and eustatic sea level variations, the rate of sediment supply and accommodation space to create their overall shape and physical properties.

Well to well correlation is carried out for four profiles across wells in the Zambezi Delta Basin. Two profiles strike SW-NE, along strike, and two strike NW-SE, in the dip direction. In all four profiles, formation tops, as derived from well reports are correlated through the wells. Subsequently a lithological correlation is attempted only with the purpose of assessing the degree of complexity of basin fill throughout geological time.

The result gives a general picture of a complex basin fill mainly dominated by various channels (as observed on seismic data) acting as sediment sources at different locations throughout geologic time. This picture is confirmed for the Tertiary section section where a detailed interpretation is carried out later in this Chapter.

Profile one (Fig. 4.4) connects wells Divinhe-1, Sofala-1, Sengo Marin-1, Sangussi Marin-1 Zambezi-1, Micaune-1 and Nanguazi-1 and trends northerly in the central area of the basin. Profile two (Fig. 4.6), trends more southerly in the central area of basin connecting instead the wells Divinhe-1, Nemo-1, Zambezi-3, Zambezi-1, Micaune-1 and Nhanguazi-1. Profile three (Fig. 4.7) connects wells Sengo Marin-1, Sangussi Marin-1 and Zambezi-3 and profile four in the northeast (Fig. 4.8) connects wells Nhanguazi-1, Micaune-1 (onshore) and Zambezi-1 (offshore). The geologic age data as well as the well tops are both derived from

well reports.

The correlation of well formation tops for profile one provides a picture of a northeastwards thickening sedimentary succession for Cenomanian and Turonian. For the Senonian there is a thining to well Sengo and then thickening and thinning again of the succession towards well Zambezi-1, suggesting a SW-NE sediment source at the time, probably from the Save River. Generally successions of Senonian to Palaeocene age thicken from both northeast and southwest and thin somewhere in the middle suggesting two sediment sources active during the same time period, one in the northeast (possibly the Zambezi River itself) and another in the southwest, (possibly the Save River) as seismic evidence show (discussed later this Chapter). For post-Palaeocene formations thickening is towards the centre of the basin. Lithological correlation however suggest a more channel dominated deposition at times both in the southwest and in the northeast, with periods of steady and abundant sedimentation.

Correlation of formation tops for profile two resulted in a picture generally simillar to that of profile one in terms of thickness trends of the sedimentary strata but with significant thickness increase towards the well Zambezi-3, suggesting a basinwards stratal thickening or progradation from the southwest.

Profiles one and two start at the same well in the southwest and go through the same three wells in the northeast. The two profiles differ in the middle section where profile one is more coastal through wells Sofala-1, Sengo Marin-1 and Sangussi Marin-1, while profile two is through deeper parts of the basin through wells Nemo-1 and Zambezi-3.

Cenomanian, Turonian and Senonian deposition is well-constrained by well geological tops only in the southwestern part of the basin. In this part of the basin Cenomanian strata thickens from just about 100m in the Divinhe-1 well to just over 300m in the well Sengo Marin-1. It is made of upwards coarsening sand at Divinhe-1, upwards fining sand at Sofala-1 and of sand in Nemo-1 and of sand in the base followed by shales on top in Sengo Marin-1.

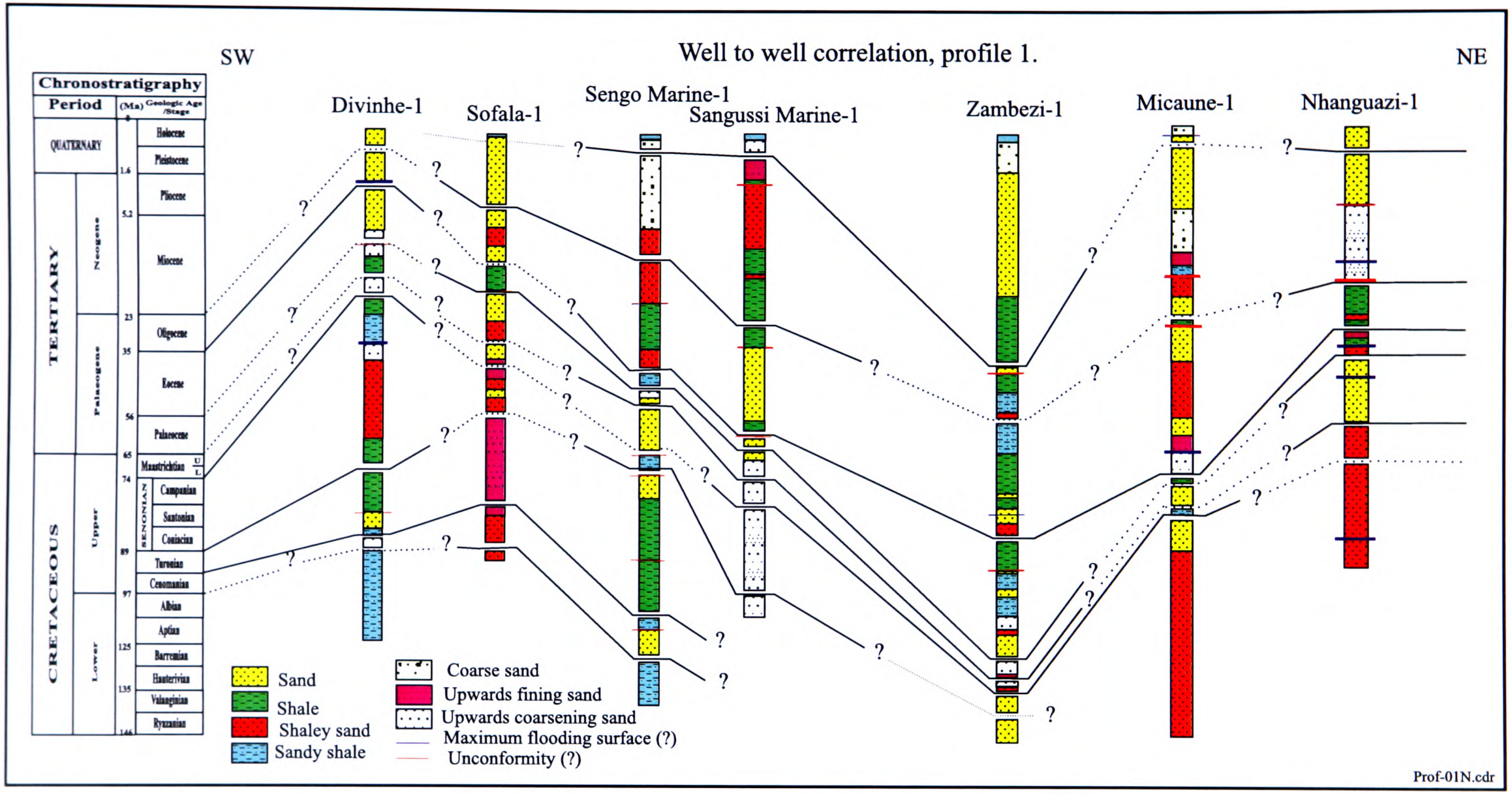

Figure 4.4: Well to well correlation of geologic time boundaries (geological well tops) SW-NE in the Zambezi Delta Basin. Profile location shown by red line on Fig. 4.5.

The lithological sequence observed in the four wells drilled trough Cenomanian lead to the interpretation of separate depositional settings for wells Divinhe-1 and Nemo-1. Upwards coarsening sand may gradually become a sand to the east from Divinhe-1 to Nemo-1 in a progradational sequence set of delta front facies. The upwards fining sand in Sofala-1 may be a fluvial channel overbank facies (as can be infered from seismic data) related or even unrelated to the sand and shale succession of well Sengo Marin-1.

Turonian is only constrained in the same wells as Cenomanian. It is thickest at well Sengo Marin-1 with about 1080m and generally thins to the southwest, suggesting progradation in this direction. This succession is basically made up of shales with some occasional sands at wells Divinha and Sengo Marin-1.

The Senonian succession is probably made of sediments entering the basin at the time from two separate localities and producing two interfingering sediment sets. It is thickest at well Divinhe-1 with about 1230m and thins in Sengo Marin-1 and then thickens again to some 230m at well Sangussi Marin-1. The southwestern succession seems to be part of the Save River Delta in the southwest with some shale in the base followed by upwards fining and then upwards coarsening sand. There is sandy shale and shale on top at well Divinhe-1. The upwards coarsening succession at well Sangussi Marin-1 seems to be part of a separate depositional set of basinwards prograding successions from the northwest.

The Maastrichtian sediment succession is generally thin all over the basin and is made of sands. Its thickness varys between a few tens and a few hundreds of metres.

Through the section where profiles one and two differ, it can be observed that for example the Palaeocene succession which is very thin on profile one is thickest at well Zambezi-3 and thins again towards well Zambezi-1. Inspection of the Palaeocene succession on profile three shows a basinwards thickening succession. This suggests that the Palaeocene succession might have been deposited mainly from a northwesterly sediment source with possible sediment inputs from the west. The Palaeocene basin in the northeast is relatively starved, as results

of seismic data interpretation show (see section on results, this chapter).

The Eocene succession thins from both sides of profiles one and two towards wells Sangussi Marin-1 and Zambezi-3. On profile three the succession is more or less uniform in thickness while on profile four it shows some significant increase in thickness to well Zambezi-1. The general picture suggests a transgressive sequence set with possibly two point sources, one source in the northeast with a significant sediment input into the basin and another source of relatively little significance in the southwest (see section on results below, this Chapter).

Oligocene, Miocene and Pliocene to Recent successions seem to be steady basinwards progradational successions as seen on well correlations. They possibly are deposited within the sceanrio of various sediment sources switching location with geologic time (see section on results below, this Chapter). This could include fluvial channel deposition within the main deltaic progradation. During this time it seems that massive diachronous sands are deposited in the delta paltform and delta front with shales possibly deposited in deeper parts of the basin.

Technical details for well logs used here are given for each well in Table F.1, Appendix F in Volume II of this thesis. The quality of the well logs varies for each well and some log signature do not cover the whole length of the borehole.

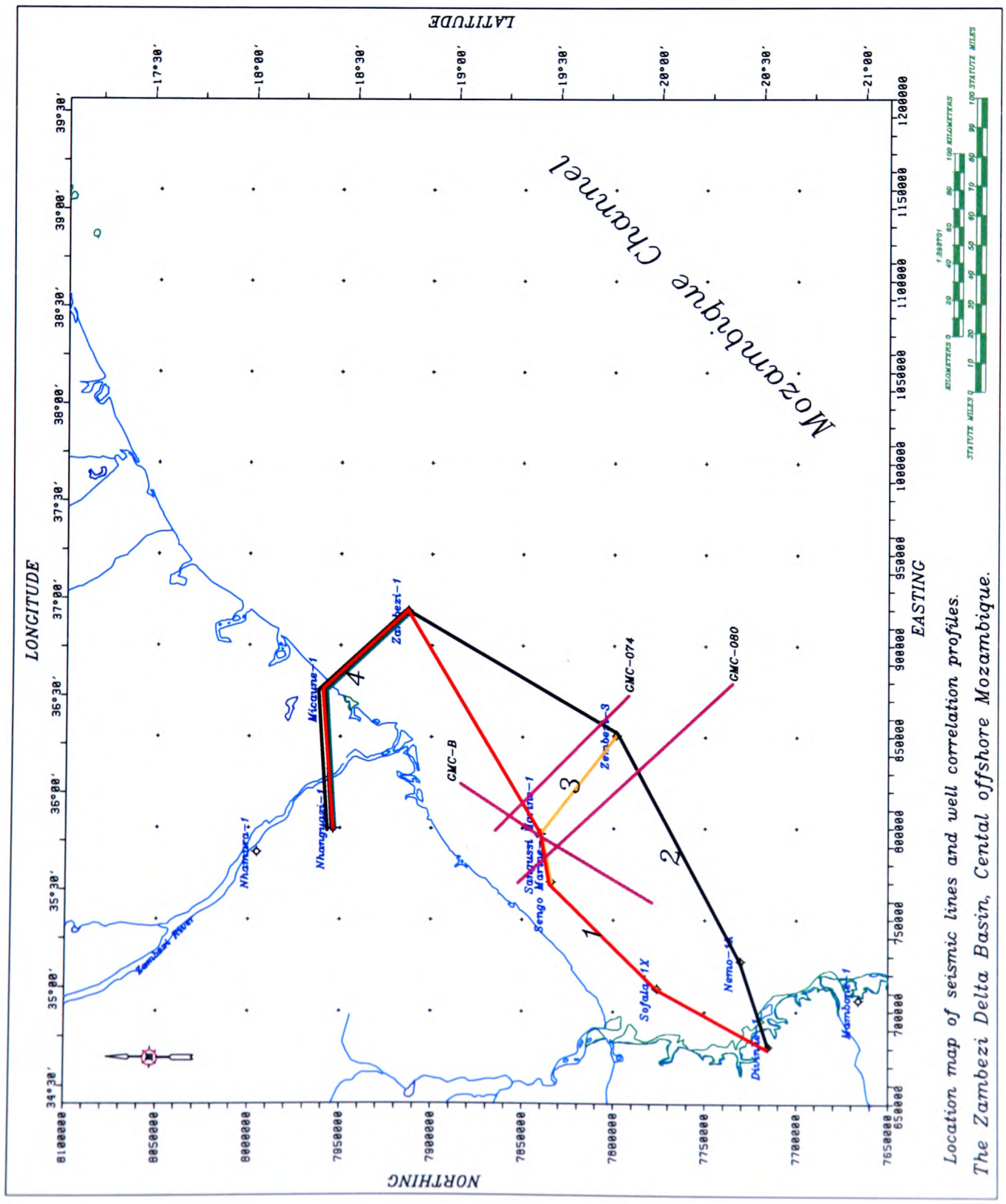

Figure 4.5: Location map of four well to well correlation profiles numbered one to four and of three seismic sections GMC-B, GMC-074 and GMC-080 in the Zambezi Delta Basin.

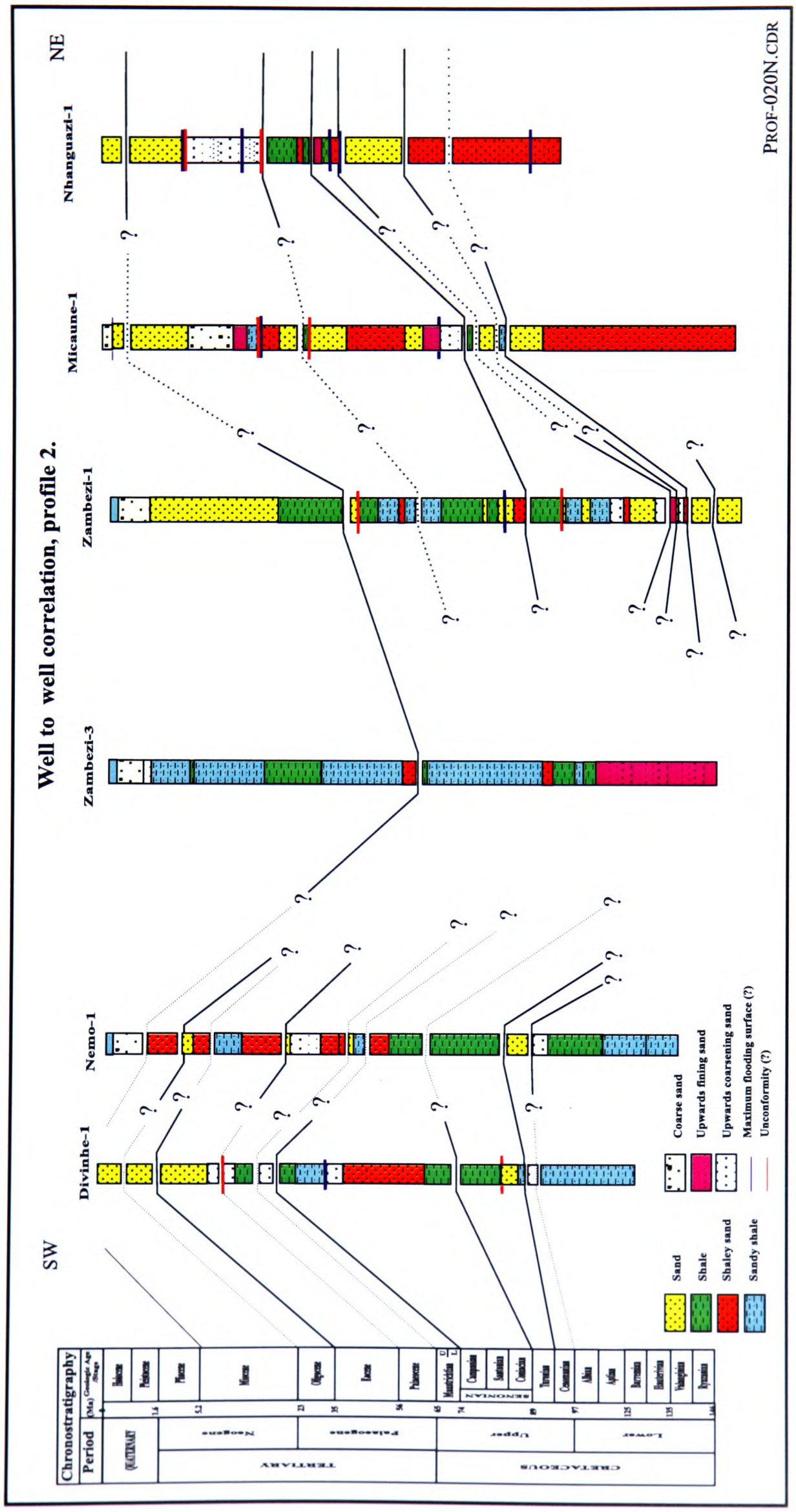

Figure 4.6: Well to well correlation of geologic time boundaries SW-NE in the southeast Zambezi Delta Basin. Profile location shown by black line on Fig. 4.5.

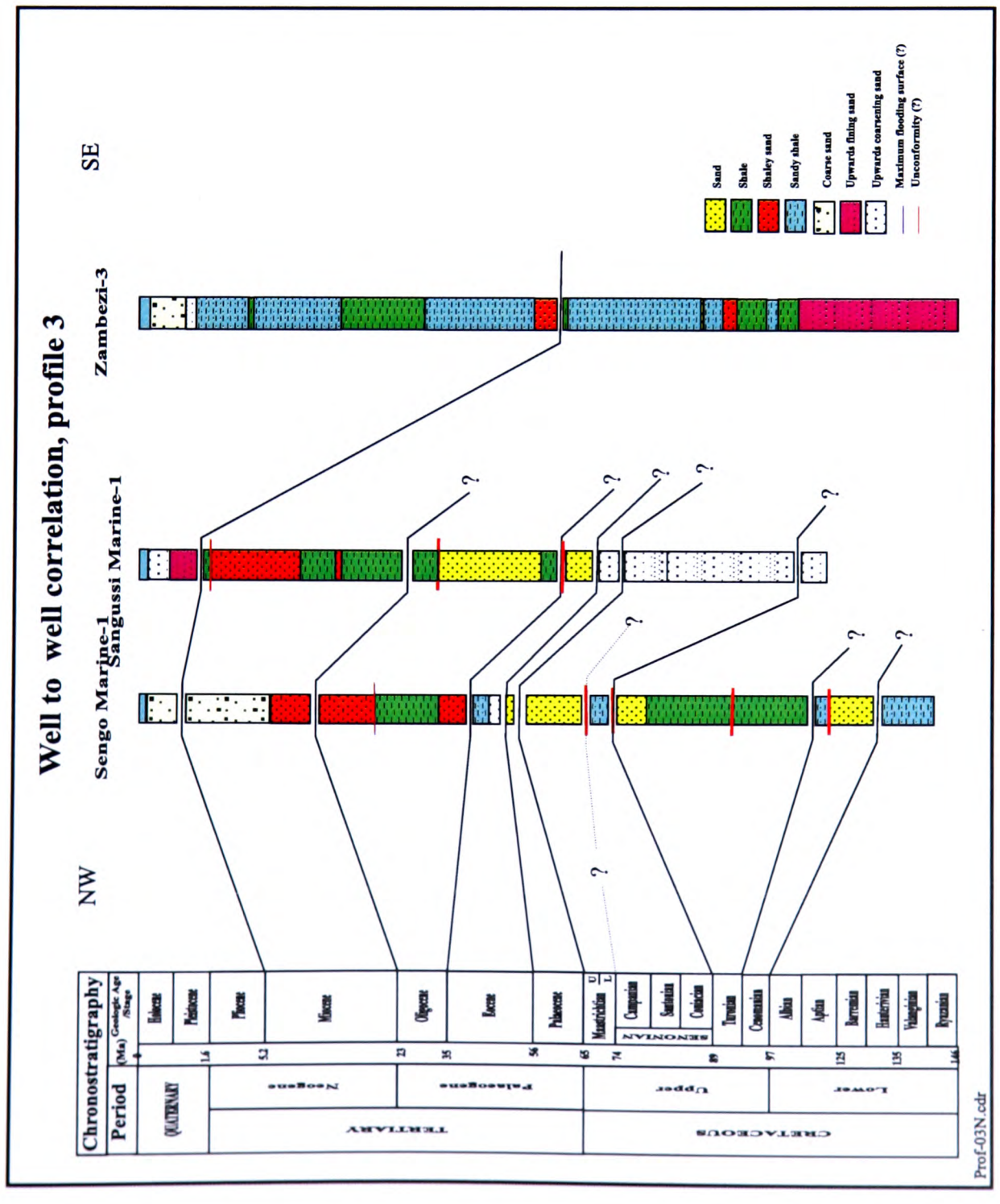

Figure 4.7: Well to well correlation of geologic time boundaries NW-SE in the southwest Zambezi Delta Basin. Profile location shown by brown line on Fig. 4.5.

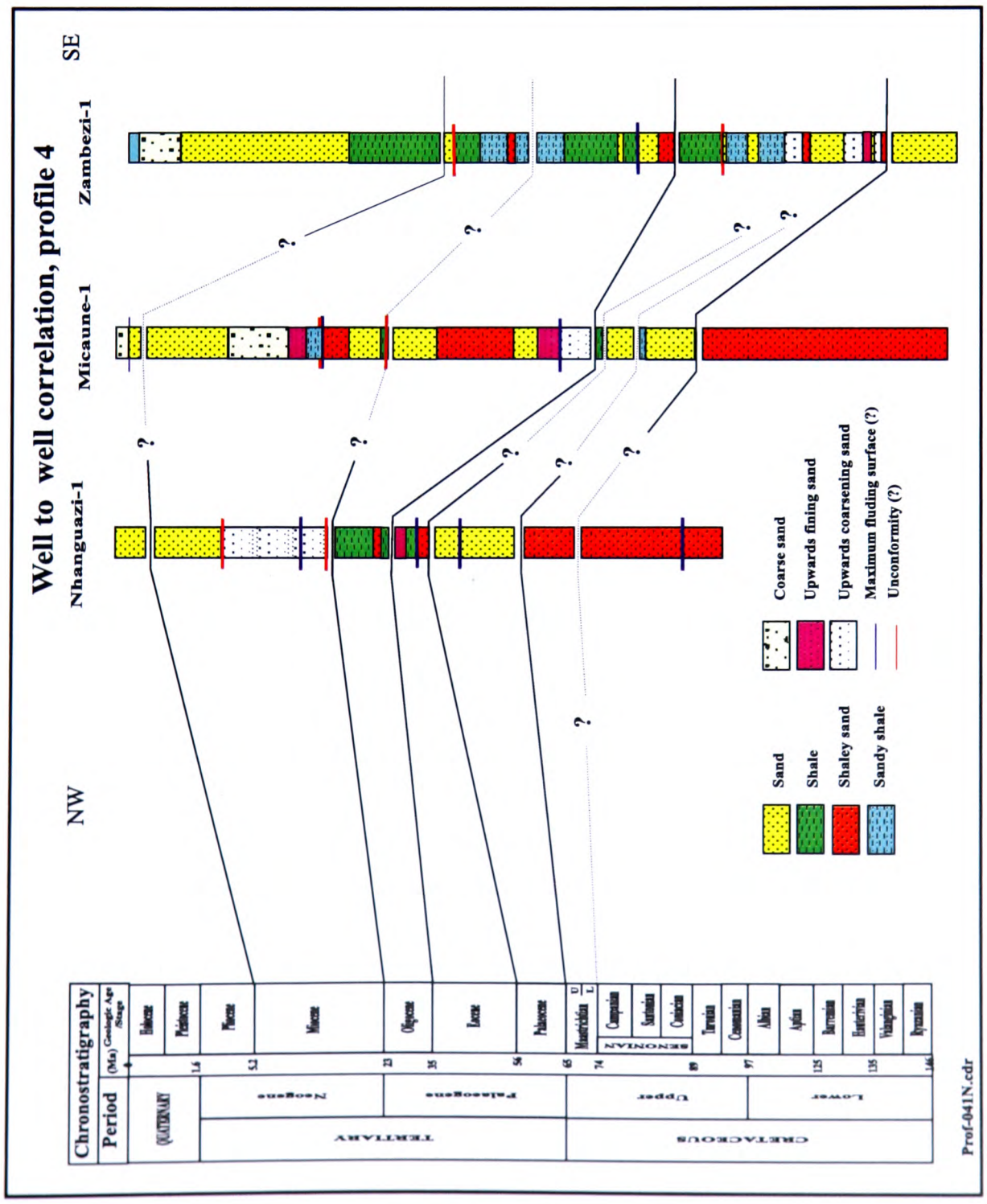

Figure 4.8: Well to well correlation of geologic time boundaries NW-SE in the central part of the Zambezi Delta Basin. Profile location shown by green line on Fig. 4.5.

4.2.3 Well tie to seismic.

Formation tops are used to tie well stratigraphy with seismic sections (see Appendix G). In most cases formation tops coincide with change in rock type, generally signaling a change in the depositional cycle and thus a change in sonic velocity and/or formation density which leads to acoutic impedance contrast. This results in a strong signal in the seismic signature thus producing a seismic reflector on the seismic section. In the processed seismic record, a signal marks the geologic contact of two lithologies of different densities. However, lithostratigraphic formations may in some cases be laterally diachronous, thus, not representing geological time boundaries.

In this work, seismic reflectors are tied to well data by calculating the equivalent depth to the reflector at the well site using the stacking/rms-velocities provided. Usually the derived depth to the seismic reflector coincides with a lithological boundary or with a formation top. The seismic horizons are mapped through the seismic section and tied to all cross-lines and from these to all other lines in closed loops. As several wells are used here to tie well data to seismic the procedure is taken as right when each seismic horizon has the same age at all well sites in the survey.

Ten well tops derived from well reports are used to tie the same number of horizons on seismic sections and all are loop tied through the survey. All ten horizons are interpreted to be depositional unconformities, marked by erosional truncation and onlap, binding nine depositional megasequences (see Appendix H). Formation tops are interpreted from bottom to top as Top Cenomanian, Top Turonian, Top Senonian, Top Upper Palaeocene (Top Palaeocene), Top Middle Eocene, Top Upper Eocene (Top Eocene), Top Oligocene, Top Middle Miocene, Top Upper Miocene (Top Miocene) and Top Pliocene unconformities.

Discrepancies in the geological top dating between wells is overcome by choosing two wells with the most coherent geological information, Sangussi Marin-1 and Sengo Marin-1, to calibrate the other wells in the area. This procedure aided geological dating of the depositional unconformities (time lines) studied here.

4.3 Subsidence history.

4.3.1 Background.

Basin subsidence is the gradual sinking of basins and can be due to tectonic subsidence or to the sediment load generally replacing a column of water of density around $1000 kgm^{-3}$ (in offshore basins) or simply air (in continental basins) by sediments of much higher density. It is known that local Airy isostatic models (Steckler and Watts, 1978) generate 600m of basement subsidence for every 1km of sediments deposited and that sediment accumulation remains limited to $2\frac{1}{2}$ times the water depth. Steckler and Watts (1978) suggest however in their analyses of the Atlantic-type continental margin of New York, that for the sort of shallow water sediment accumulation observed there other causes must have acted other than simply subsidence due to sediment load. They attribute thermal cooling as the additional cause for basin subsidence and they used a flexural model to estimate a 113-139km thickness for the thermal lithosphere. A similar situation may apply for the Zambezi Delta basin, where sedimentation accelerated in Middle Tertiary delivering most of the sediments of the deltaic complex into a basin created by thermal subsidence. However, basin subsidence dating from Middle Jurassic extension would be almost over by Middle Tertiary, therefore delta progradation and sediment loading are the most important components of basin subsidence.

Geohistory analysis, normally using a well database, is conducted to separate out causes of basin subsidence from the analysis of total basin subsidence (Allen and Allen, 1992). Wells studied here are shallow and vary in total depth penetrated (maximum depth penetrated 4.6km) and they do not bottom in the acoustic basement. Sediment thickness in the drilled area of the Zambezi Delta Basin varies from a few kilometres in the northeast to some 12-15km in the Zambezi Delta half graben, most of these sediments being of Cretaceous and Cenozoic age. In extreme cases up to 10km of the lower section is not sampled by the wells and can only be included in geohistory analysis by inference.

The data analysis performed here is based on the procedure discussed by

Steckler and Watts (1978) and Sclater and Christie (1980) and summarized by Allen and Allen (1992). Some simplification however is adopted at stages where adequate information could not be provided.

Well data used in this study is poor in quality and most of the information required to conduct most steps in geohistory analysis is simply not available, or inaccurate. Some well-dated stratigraphic tops are available but most of the lithological boundaries used are not dated; water depths of deposition are unknown and therefore kept constant at sea level throughout the calculations. These factors reduce the relevance of the the results achieved in this study. Therefore, only broad conclusions can be reached.

Curves of total basin subsidence and sedimentation rates are displayed and discussed here and no attempt is made to separate tectonic subsidence for lack of basic information required to objectively carry out the procedure. The observed basin subsidence is interpreted only in terms of sediment load with apparently little or no thermal subsidence component from Middle Jurassic extension, although it is acknowledged that some other causes might have played an important role at times in producing observed stratigraphy. Further assessment is left to future work, recommended here, at the time when more and adequate data is made available.

4.3.2 Interpretation of subsidence history data.

In this section subsidence analyses is carryed out on nine wells based on well log interpretation introduced in section 4.2. Because of lack of accurate water depth information for the well tops, water depth is kept constant through all calculations. Six wells are drilled offshore and three are drilled onshore. Their geographic location allows to study the influence of both tectonic and sedimentation to basin subsidence through the geological period they cover (Late Cretaceous to Recent times).

Aparent accelerated basin subsidence is registered at different well locations between 90 and 85my (Late Cretaceous) and between 40 and 25my (Upper Eocene

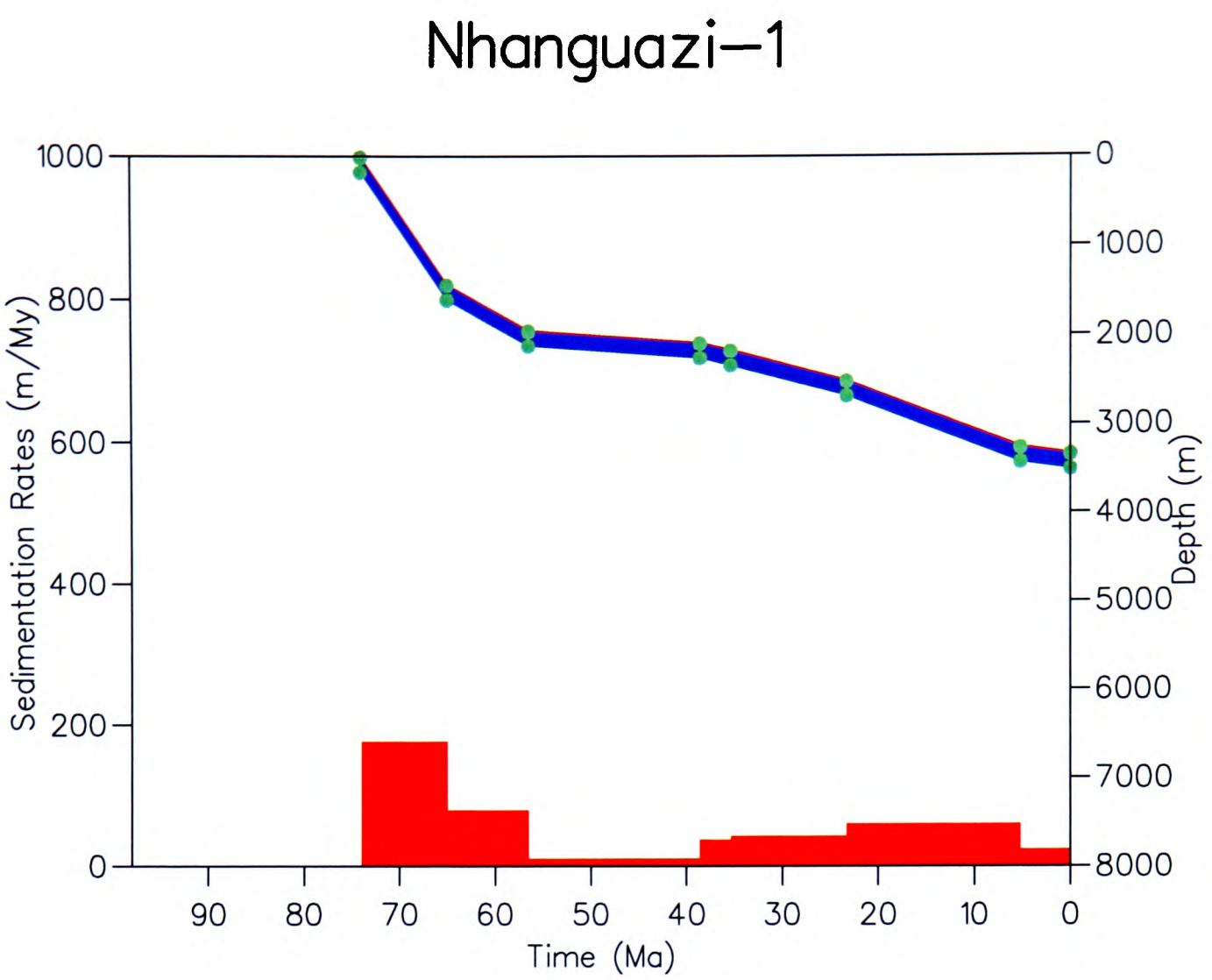

Figure 4.9: Total subsidence (blue) and sedimentation rate (red) curves for the well Nhanguazi-1 (onshore).

and Oligocene). Some exceptions seen in wells Nhanguazi-1 and Zambezi-3 between 75 and 55my (Late Cretaceous to Early Eocene times).

Subsidence analyses of Nhanguazi-1 well begins at about 74my ago (Early Maastrichtian) Maastrichtian) with about 200m/my sedimentation rate signaling a time of relatively high sedimentation in the area (Fig. 4.9). At about 57my (Late Palaeocene times) ago sedimentation rate had decreased to only 20m/my. Low sedimentation persisted until 38my (Late Eocene times) ago when sedimentation gained momentum again but only to reach 30m/my in Early Miocene times for 18my before declining to about 12m/my in Pliocene.

At Nhanguazi-1 well, basin subsidence for the period studied could be only due to sediment load. Any additional causes may only have a very little impact on basin subsidence.

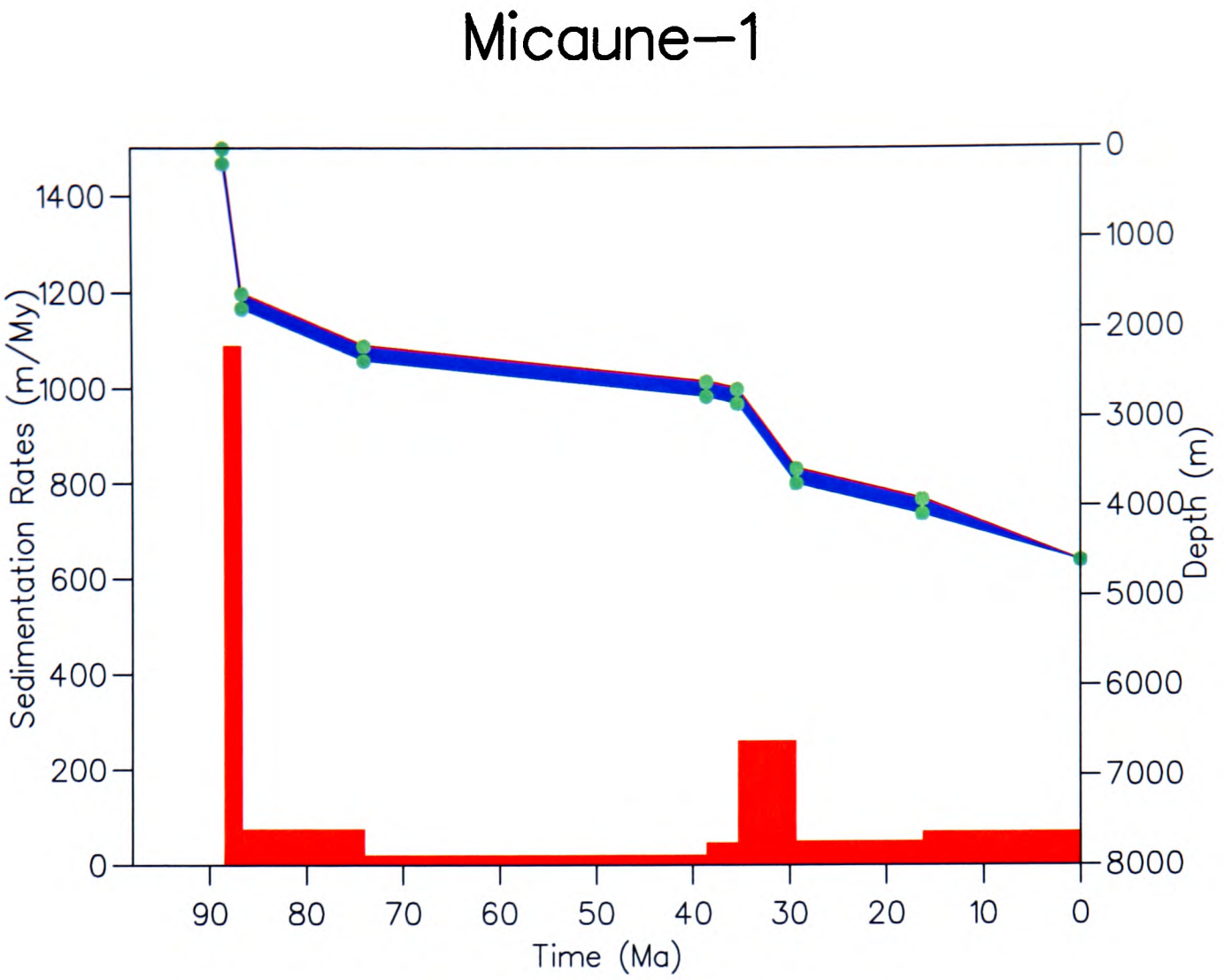

Figure 4.10: Total subsidence (blue) and sedimentation rate (red) curves for the well Micaune-1 (onshore).

The total subsidence curve of Micaune-1 well, drilled just southeast of Nhanguazi-1 well, begins with a sharp gradient due to a very high sedimentation rate of 1040m/my registered at Coniacian times at this well site (Fig. 4.10). Sedimentation however slowed down soon after 88my ago and stayed low at about 30m/my until 40my ago (Middle Eocene times) when sedimentation rate increased, reaching some 220m/my for about 7my duration. After this period of relatively high sedimentation, sediment supply decreased to levels of about 20-30m/my to the present day. Basin subsidence was rapid between 74 and 57my with the basin subsiding about 2.2km followed by a period of very little subsidence possibly due to very low sedimentation between 57 and 38my. After this period, subsidence continued at a pace with sedimentation, reaching 3.5km in total at the present day.

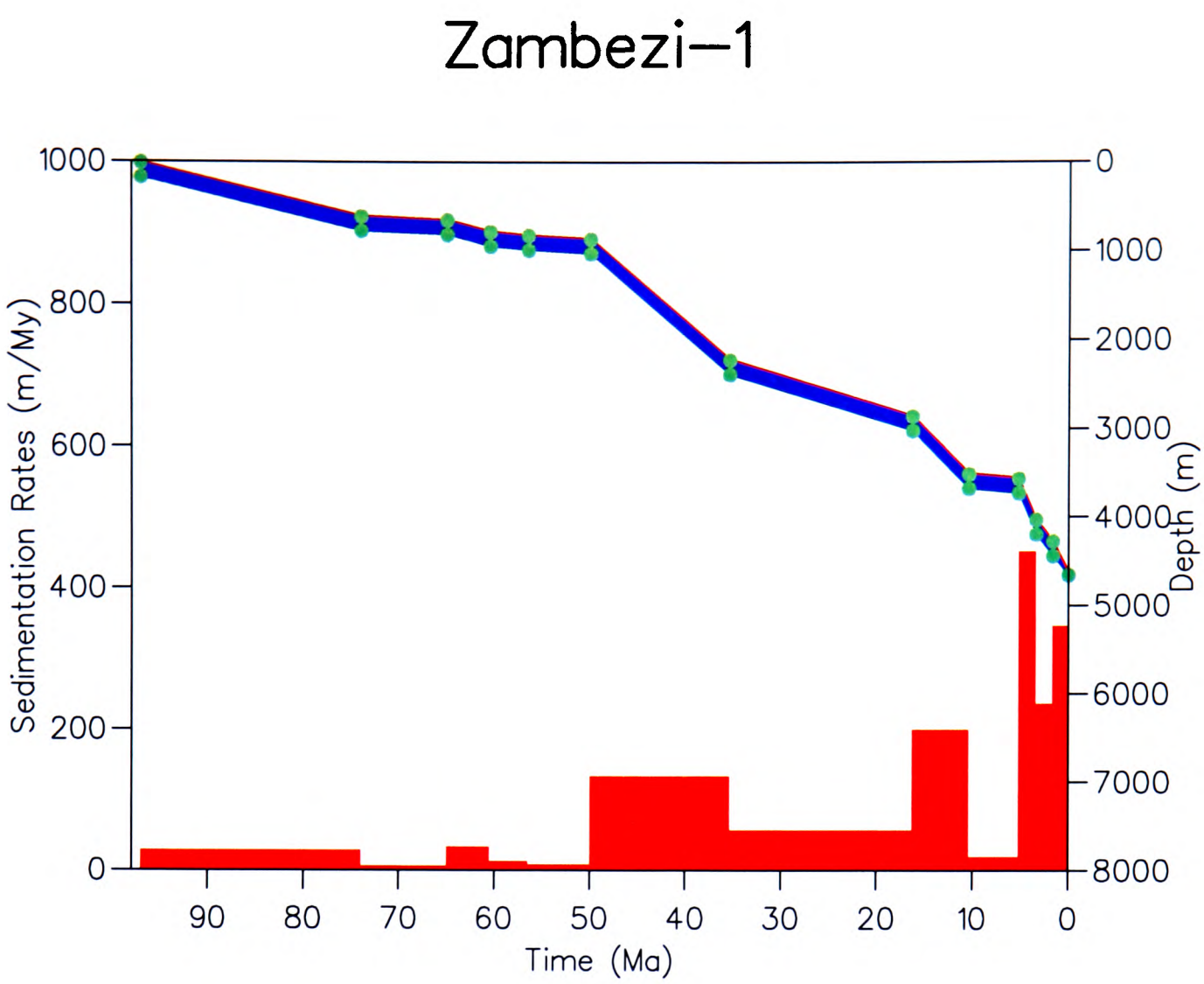

Figure 4.11: Total subsidence (blue) and sedimentation rate (red) curves for the well Zambezi-1 (offshore).

Sedimentation at Micaune-1 well was very low for a long period of geological time (74-38Ma, Maastritchian to Upper Eocene) during which a sedimentation rate of about 7m/my is recorded. A similar but shorter geological time period (57-38Ma, Upper Plaeocene to Upper Eocene) of low sedimentation is recorded at Nhanguazi-1 well. This raises suspicions for both locations possibly being in the same depositional (sediment-starved) environment. The basin subsided about 4.5km during the studied geological time period (88Ma). Circa 2.5km of the total subsidence was realised within the first 15my and about 1.5km were during the last 38Ma with only about 100m during a period of about 35my of very low sedimentation and possibly erosion.

Basin subsidence at Zambezi-1 well site is fairly continuous during the geological time period studied (Fig. 4.11). However, two periods of very little

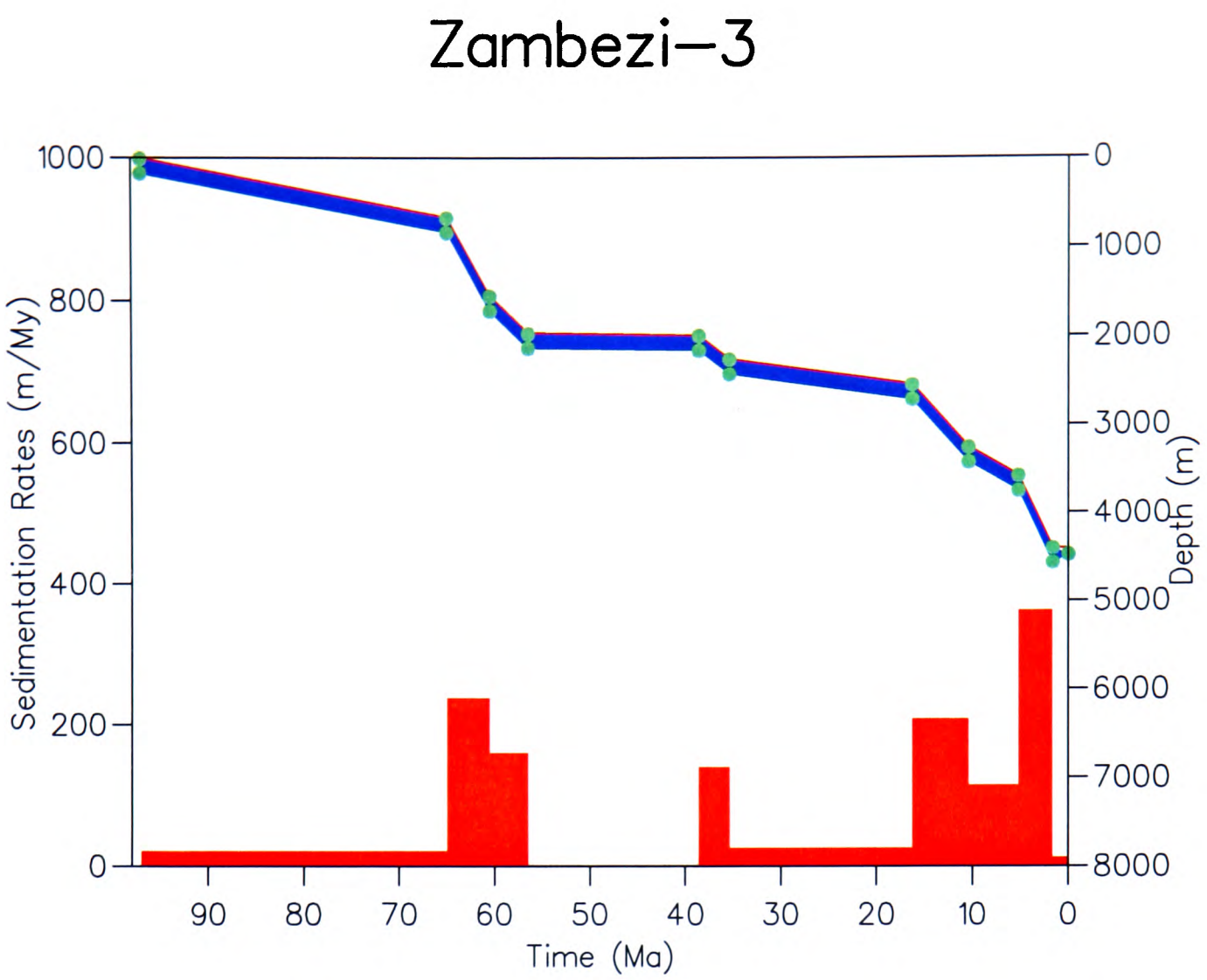

Figure 4.12: Total subsidence (blue) and sedimentation rate (red) curves for the well Zambezi-3 (offshore).

sedimentation are observed during Maastrichtian and Early Palaeocene (74-65Ma) and during Upper Palaeocene and Early Eocene (60-50Ma). For the period between Albian and the end of Senonian sedimentation stayed low at about 10 to 15m/my.

Higher sedimentation rates are recorded for the Middle Eocene and the present day with an average sedimentation rate of over 100m/my. Several peaks of high sedimentation are recorded with the highest sedimentation rates recorded the last 5Ma. The period between Middle Eocene and the present day is the time period of deltaic development in the Zambezi Delta Basin. The basin subsided about 4.5km during the last 100Ma at this well site, with more than 3.3km of basin subsidence within the last 50Ma.

At Zambezi-3 well sedimentation was interrupted for a period of about 18my (Late Palaeocene to Upper Eocene) (Fig. 4.12). This is a period of non-

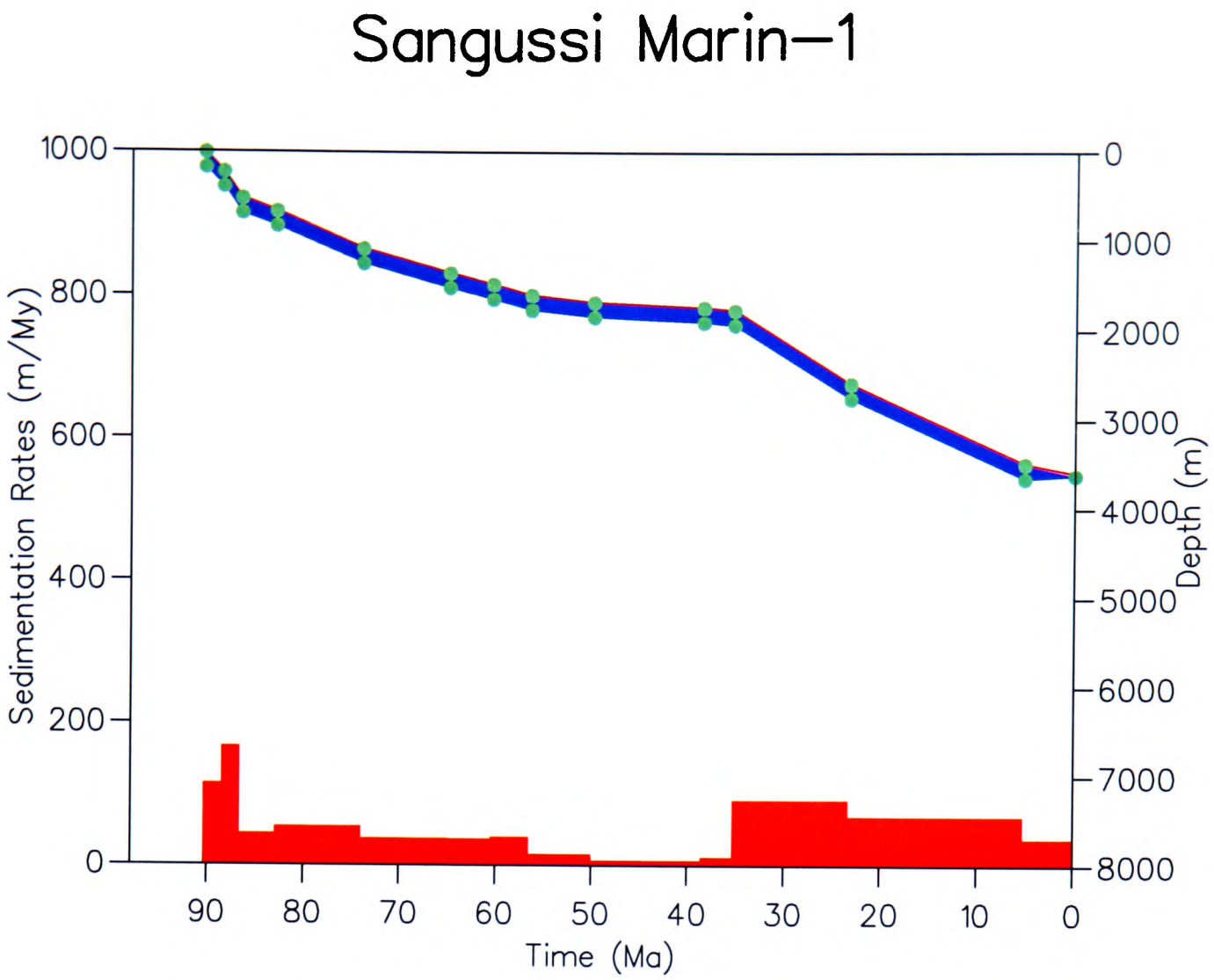

Figure 4.13: Total subsidence (blue) and sedimentation rate (red) curves for the well Sangussi Marine-1 (offshore).

than in the well Zambezi-1 (about 20m/my). Sedimentation is shut off for about 20my until 38Ma ago (Upper Eocene) at the Zambezi-3 while Zambezi-1 registers a sedimention rate of more than 110m/my. After this period sedimentation is steady at different rates to the present day.

Sedimentation at Sangussi-1 well recorded two periods of steady sedimentation separated by a period of very little sedimentation and possibly erosion during Late Palaeocene and Eocene (57-36my) (Fig. 4.13). Sedimentation rates did not reach the 200m/my during the two periods of sedimentation. The second period of sedimentation, however, recorded more sediments than the first, with an average sedimentation rate of about 50m/my against circa 20m/my in the previous period.

Basin subsidence thereafter was smooth between 90 and 50Ma ago and

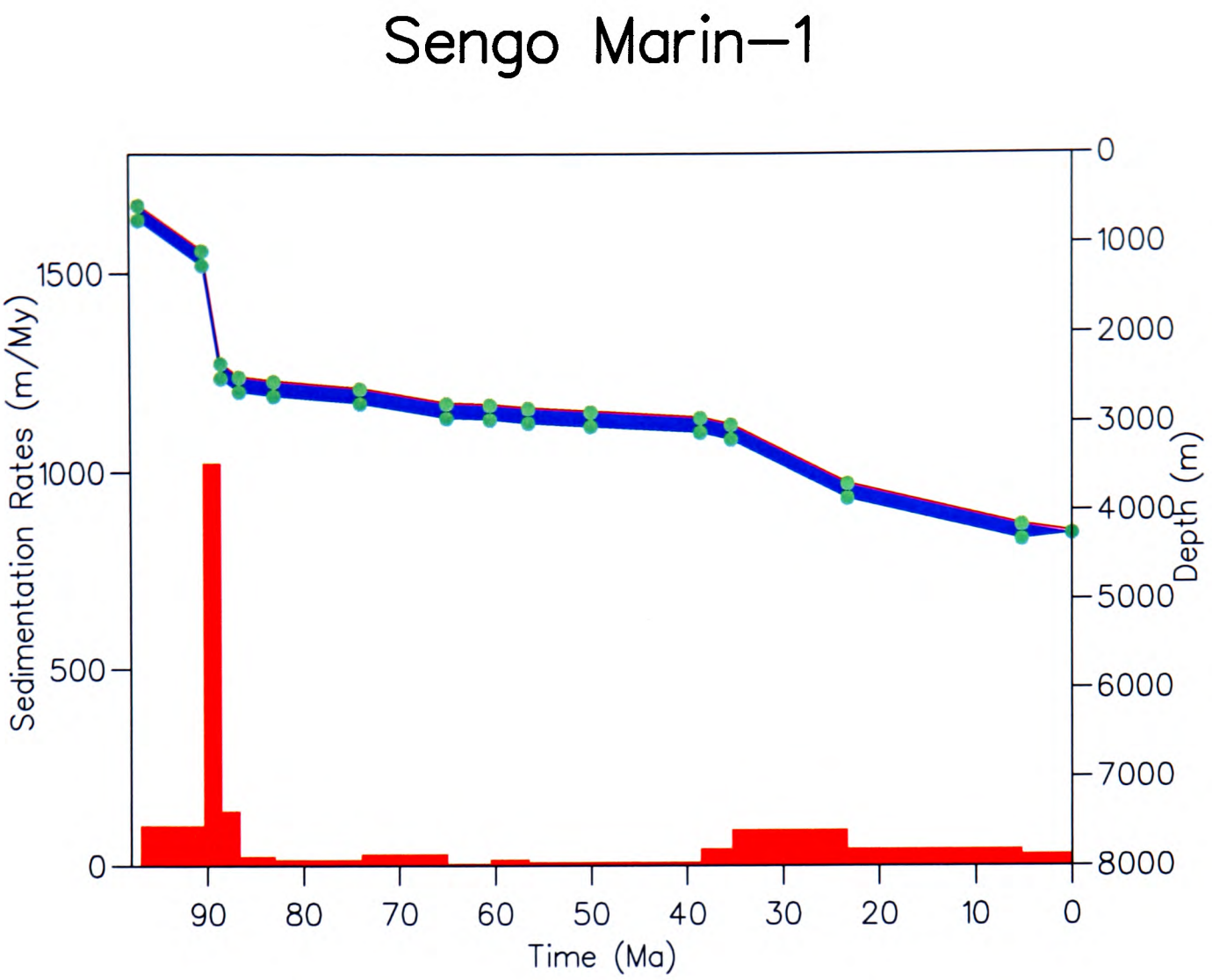

Figure 4.14: Total subsidence (blue) and sedimentation rate (red) curves for the well Sengo Marine-1 (offshore).

steeper in the period between 35Ma and the present day. Total basin subsidence for the studied period is about 3.7km at this well site with about 2.0km realised during the last 35Ma.

The subsidence curve of Sengo Marin-1 well can be subdivided into three distinct segments (Fig. 4.14). The first segment encompasses the period between 98 and 87Ma. During this period sedimentation generally stayed at about 120m/my and recorded a short lived peak of more than 1000m/my for about two million years in Early Maastrichtian. Basin subsidence was more than 2.0km during this very short time period.

The second time period is between 87 and 38Ma during which relatively low sedimentation (0-35m/my) is recorded with some periods of non-sedimentation at times. Basin subsidence stayed below 500m during this period of geological

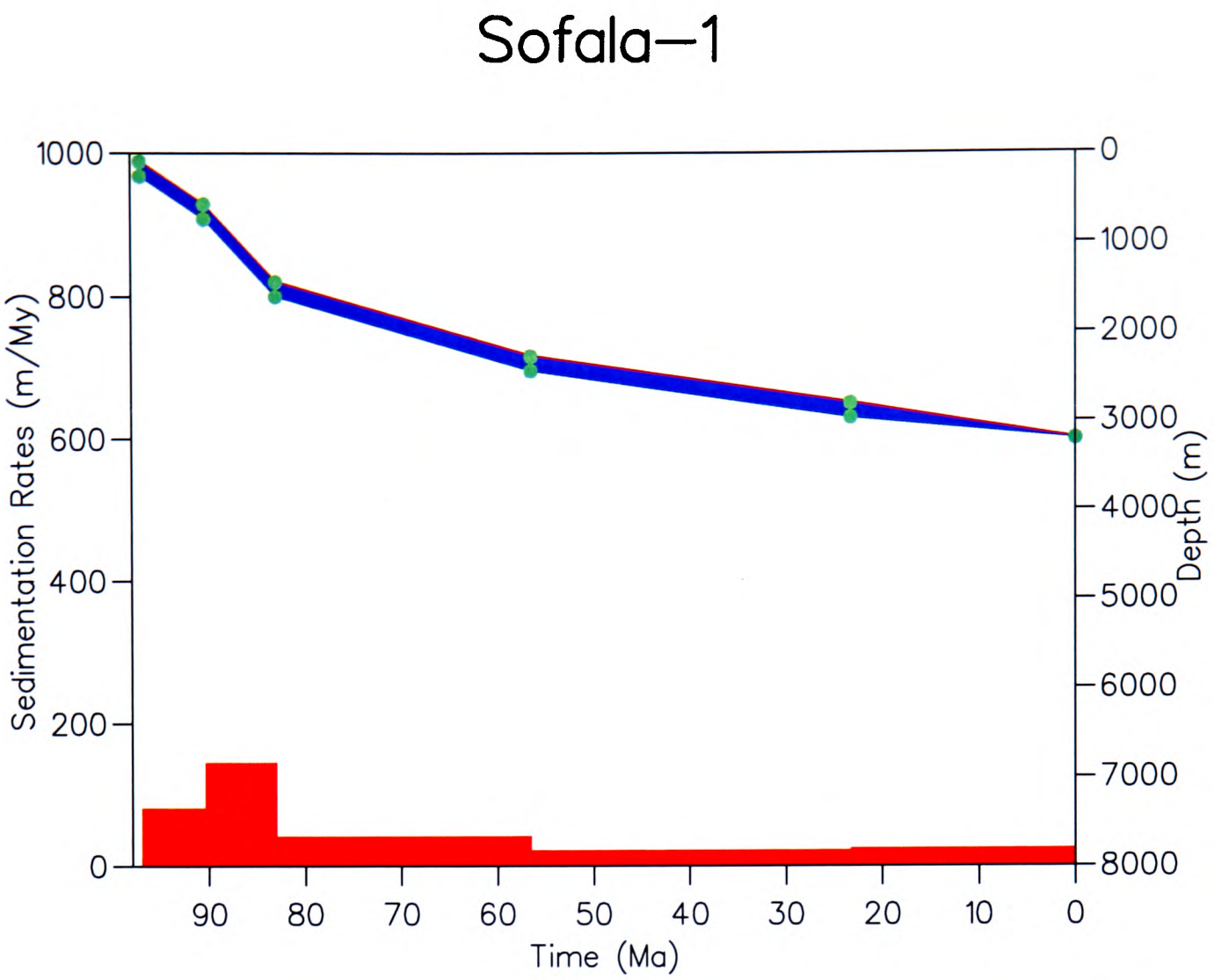

Figure 4.15: Total subsidence (blue) and sedimentation rate (red) curves for the well Sofala-1 (offshore).

time. The third period is from 38Ma to the present day. This period recorded a maximum sedimentation rate of about 200m/my with an average of about 100m/my. Subsidence accelerated after a period of very little subsidence, and realised more than 1.2km of basin subsidence.

Sangussi Marine-1 and Sengo Marine-1 are two adjacent wells (45km apart) offshore northeast of Beira with also a very similar sedimentation and subsidence history at times. The 90Ma sedmentation rate peak is clearly recorded in both wells but showing different sedimentation rates at each location. Sangussi sedimentaton rate is just about 200m/my (Fig. 4.13) while Sengo recorded a 1000m/my sedimentation rate (Fig. 4.14) over a short period of time in Upper Cretaceous (90Ma). After the 90Ma peak sedimentation was steady at both well sites to the present day with only slightly varying sedimentation and subsidence

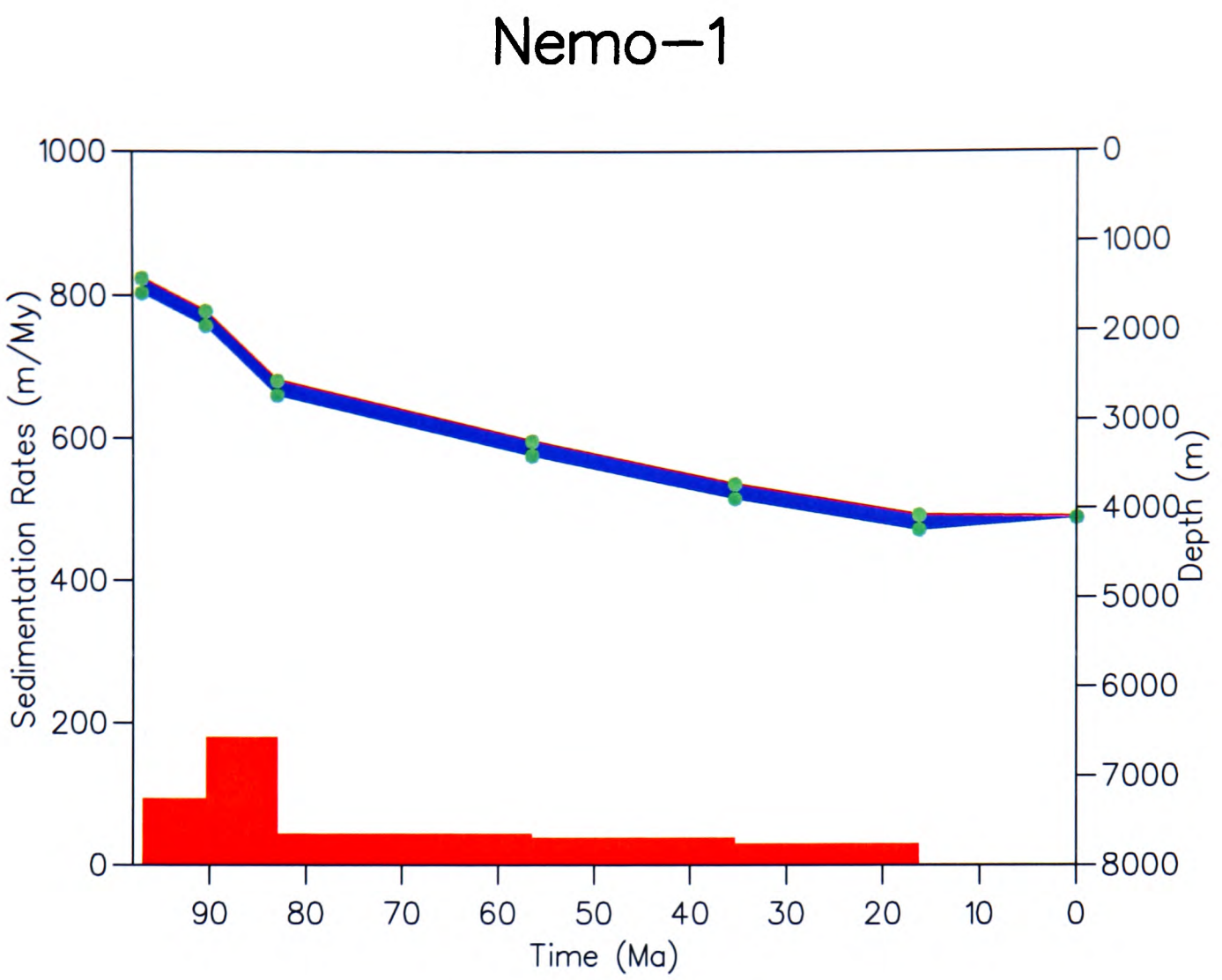

Figure 4.16: Total subsidence (blue) and sedimentation rate (red) curves for the well Nemo-1 (offshore).

patterns.

The subsidence curve of Sofala-1 well is of continuing basin subsidence for the geological time studied (Fig. 4.15). The sedimentary record begins in the upper part of Lower Cretaceous with a sedimentation rate of about 80m/my which rose to about 180m/my 90Ma ago for about 7Ma. This caused subsidence to accelerate and produced about 2.0km of basin subsidence at this location. Sedimentation slowed down with sedimentation rate pluging to some 40m/my 83Ma for a period of 26Ma before reducing to about 20m/my 57Ma ago. It stayed at about this level to the present day. Total basin subsidence thereafter is about 3.0km at the present day.

Sedimentation at Nemo-1 was continuous from Lower Cretaceous until about 17Ma ago (Fig. 4.16). No sedimentation is recorded during the last 17Ma at this

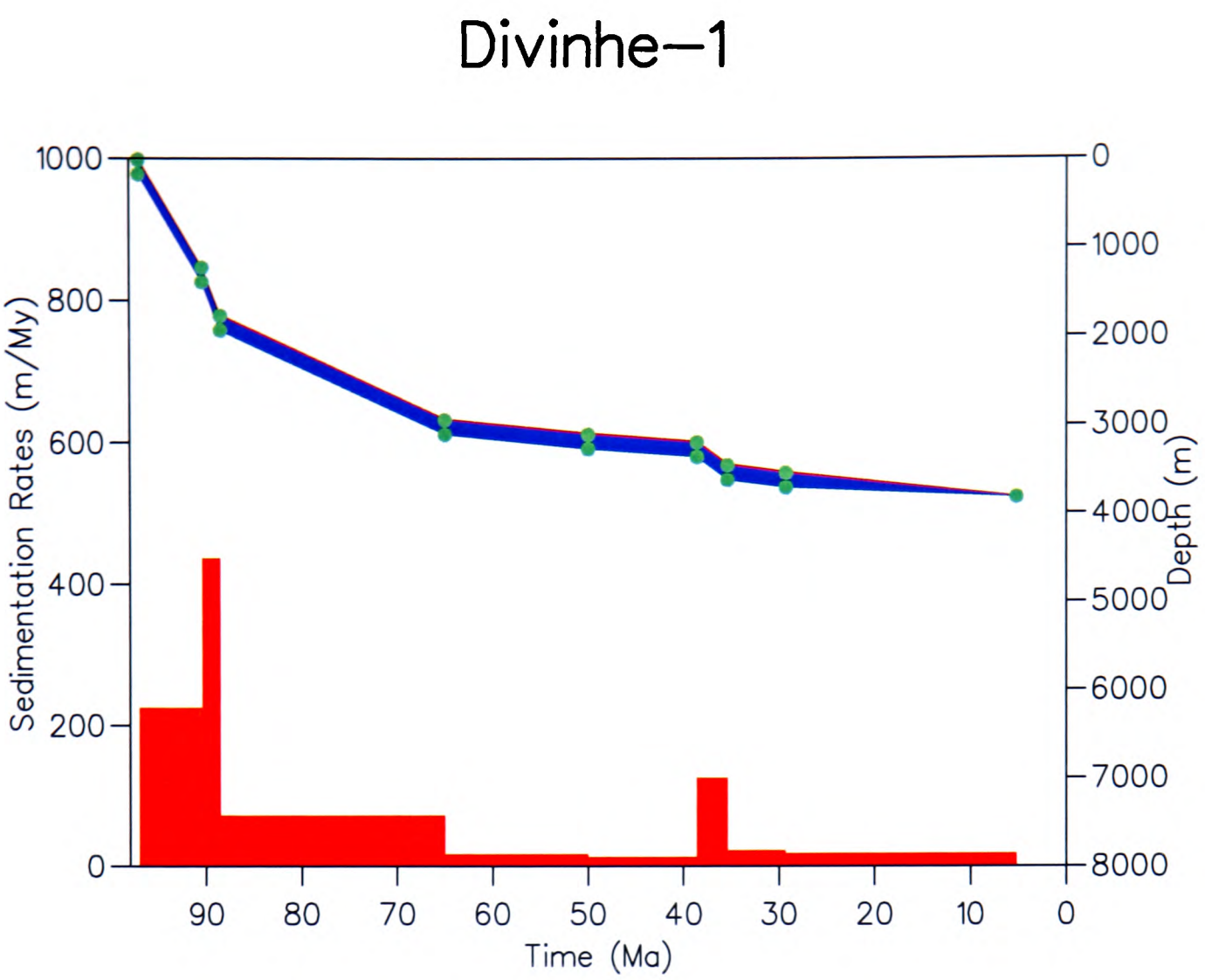

Figure 4.17: Total subsidence (blue) and sedimentation rate (red) curves for the well Divinhe-1 (onshore).

well site. The subsidence curve begins with fast subsidence responding to steady and high sedimentation rates of about 90m/my up to 190m/my between 98 and 83Ma. Sedimentation then slowed down to rates of about 40m/my decreasing twice to about 30m/my at about 36Ma where it stayed until Lower and Middle Miocene. Subsidence was fast between 98 and 83Ma and the basin subsided about 1.2km during this period then subsidence continued at a nearly linear pace following steady sedimentation. Total subsidence at this site is 3.5km.

The wells Sofala-1 and Nemo-1 are drilled 20km apart offshore southeast of Beira. Their sedimention and subsidence curves show very similar patterns. Both wells only registered the 90Ma sedimentation episode with similar sedimentation rate peaks of about 200m/my which then declined to about 20 and 30m/my until Recent times at the Sofala-1 well site (Figs. 4.15; 4.16). Sedimentation stoped 25Ma ago at Nemo-1.

Divine-1 well is the southernmost onshore well studied here. This well also recorded high sedimentation 90my ago with a peak of about 420m/my. As inthe other cases that this peak has been observed, it is a shortlived one (about two million years) followed by a sedimentation slow down (Fig. 4.17). Sedimentation rate was high in Late Cretaceous times at this site (220m/my). Basin subsidence for the first 10Ma of this well (98-88Ma) is about 1.8km. In the following period of about 22Ma a sedimentation rate of 60m/my is reached. The basin continued to subside, reaching more than 3.0km of basin subsidence. Afterwards sedimentation stayed at lower levels of about 20m/my towards the peak in sedimentation at 38Ma. This peak is recorded at this well site with a sedimentation rate of about 120m/my for four million years. Sedimentation returned to lower levels after the 38Ma peak and stayed at about 20-30m/my until five million years ago when no sediment record is kept at this well site. Total subsidence for the time recorded is about 3.8km.

4.3.3 Summary and discussion.

Sedimentation is generally continuous within the basin, but hiatuses of varying duration can be observed at the different well locations throughout the geological period studied. This is the case of wlls Zambezi-3 between 57-38Ma, Nemo-1 between 27-0Ma and Divinhe-1 between 5-0my where no sedimentation is recorded. There is a period of very sparse sedimentation or low sediment preservation preceeding the 38my event which varies in duration at different well locations. This period of low or no sedimentation before the 38my event is recorded in all wells except at Nemo-1 and Sofala-1 about 20km apart in the very western part of the basin.

Total subsidence rates vary at different well locations in the basin. Nemo-1 registered the least subsidence of about 2.0km in 100Ma while the Zambezi-1 has 4.7km of total subsidence in the same time period.

There are three events characteristic at most well locations at 90, 38 and 5Ma before present. Between 90 and 88Ma (Upper Cretaceous) a shortlived (about two to four million years) increase in sediment supply at variable rates can

be observed in almost every well except at Nhanguazi-1, Zambezi-1 and Zambezi-3 wells. Five wells, Divinhe-1, Sangussi Marine-1, Sengo-Marine-1, Zambezi-3, Micaune-1 and Nhanguazi-1 show another sediment supply increase at 38Ma before present (Upper Eocene). This event is probably related to the beginning of tectonic activity in the East African Rift system onshore.

The breach of the Urema graben south of the Lake Malawi during the East African Rift in Middle Tertiary caused uplift in the graben flanks including the Inhaminga High northwest of Beira. This caused sedimentation to slow down in the southwestern part of the Zambezi Delta Basin and sediment supply was cut off in certain areas with Nemo-1 and Divinhe-1 wells recording apparently no sedimention at all during the last 17Ma and 5Ma respectively.

The last characteristic period is at 5Ma (Top Miocene) when an increase in sediment supply was recorded at Zambezi-1 and Zambezi-3, both offshore wells. This is a period of offshore deltaic progradation with sediments building out into the basin. However at the same time sedimentation reduced at wells Nhanguazi-1, Sangussi Marine-1 and Sengo Marine-1 and sedimentation shut off to the present day at Divinha-1 well.

The three events observed at 90, 38 and 5Ma are most likely related to renewed tectonism onshore, with the last event possibly related to the reactivation of the East African Rift active extension in the Zambezi Delta Basin. Sparse sedimentation at the wells to the southwest is probably due to uplift and diversion of sediment conduits during and after the East African Rift propagation and due to lack of accommodation space in this part of the basin. Periods of sparse sedimentation also can be attributed to events controlling sediment source position and availability in onshore areas west and northwest of the basin.

4.4 Structural interpretation of seismic data.

It is known from the literature that the lower Zambezi graben is a product of the Karoo rift phase which was later reactivated during subsequent rift phases, the continental breakup (Middle Jurassic - late Cretaceous) and East African Rift

(Neogene - Recent) (Dingle and Scrutton 1974; Salman *et al.* 1985; Coster and Fortes 1989; Salman and Abdula 1995).

In the offshore part of the Zambezi Delta Basin which is studied here, mapping deep structural features across the Zambezi Delta Basin would require seismic data recording to be extended by two or three seconds in places where the sedimentary succession is thickest. The 6.0s (in shallow waters) to a maximum of 8.0s (in deeper waters) of seismic two-way travel time recording is not long enough to resolve the full sedimentary succession and reach the accoutic basement in some parts of the basin. This is the case in the southwestern and in the northeastern depocentres where the sedimentary section is thickest in the basin.

A denser seismic data grid would certainly prove more helpful in correlating faults mapped in the area. With a 10x10km seismic data grid used in this study, faults are mapped and correlated across the survey with a NE-SW and E-W strike, in line with the main structural trends in the area and supported by the interpretation of gravity and magnetic maps discussed in Chapter 5.

Faults in the offshore part of the basin take two main orientations. One direction is subparallel to the coastline with NE-SW orientation and predominates in the southwest, defining the Zambezi Delta half graben facing northwest. The other direction is E-W and predominates in the northeast, defining the graben system named here the East African Rift active extension (Fig. 6.1). The hanging wall southeast of the Zambezi Delta half graben builds the northwestern limit of the Beira basement high which is the hanging wall to the southern flanks of the graben system to the northwest (Fig. 6.1). The extent of the Beira basement high to the south and southeast is not covered by seismic data used in this study and can be infered from interpretation of gravity and magnetic data in Chapter 5 and from published information.

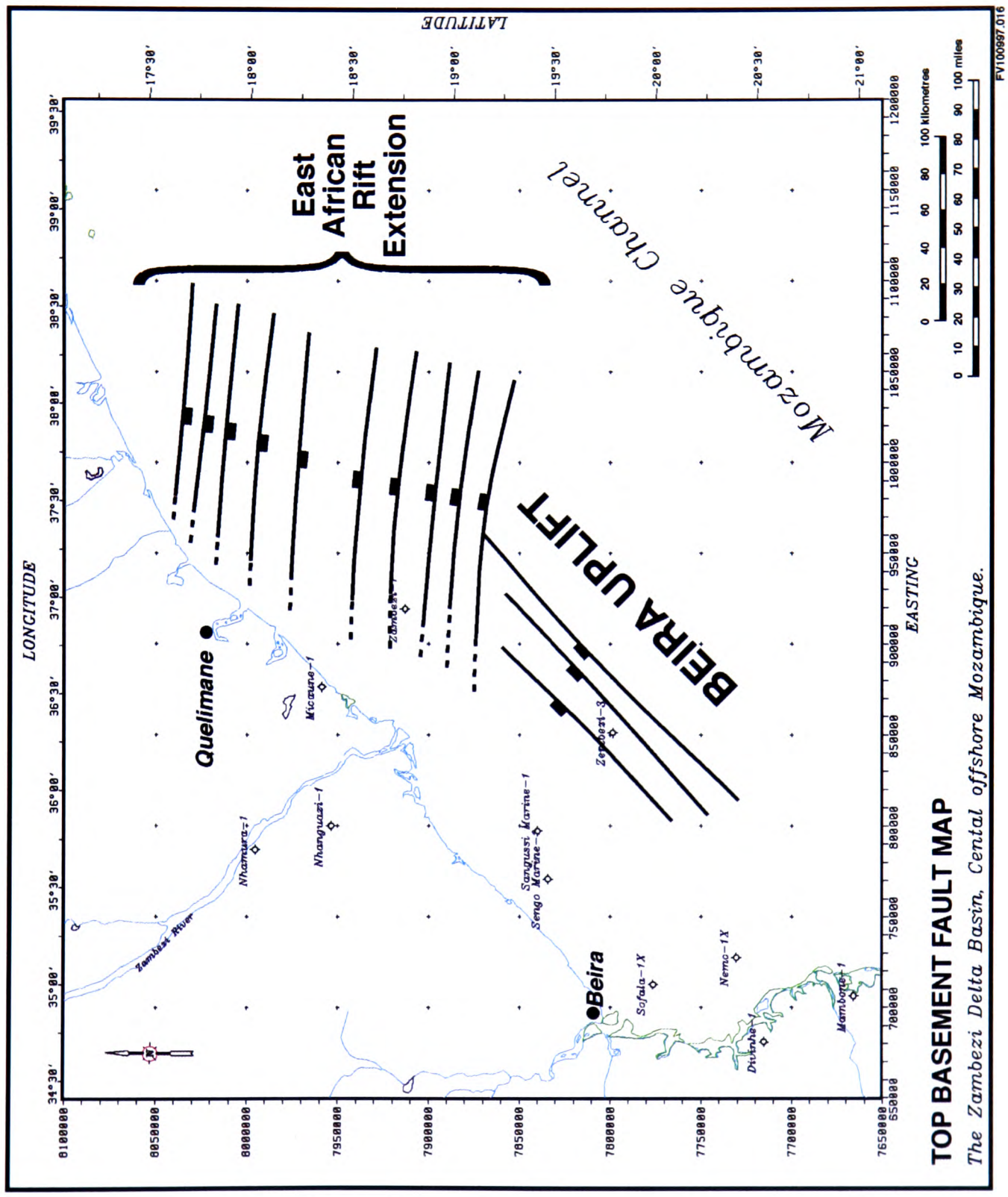

Figure 4.18: Schematic display of the top basement fault map derived from seismic data showing the Beira uplift to the south-west and the East African Rift active extention (active graben structure) as defined in this study.

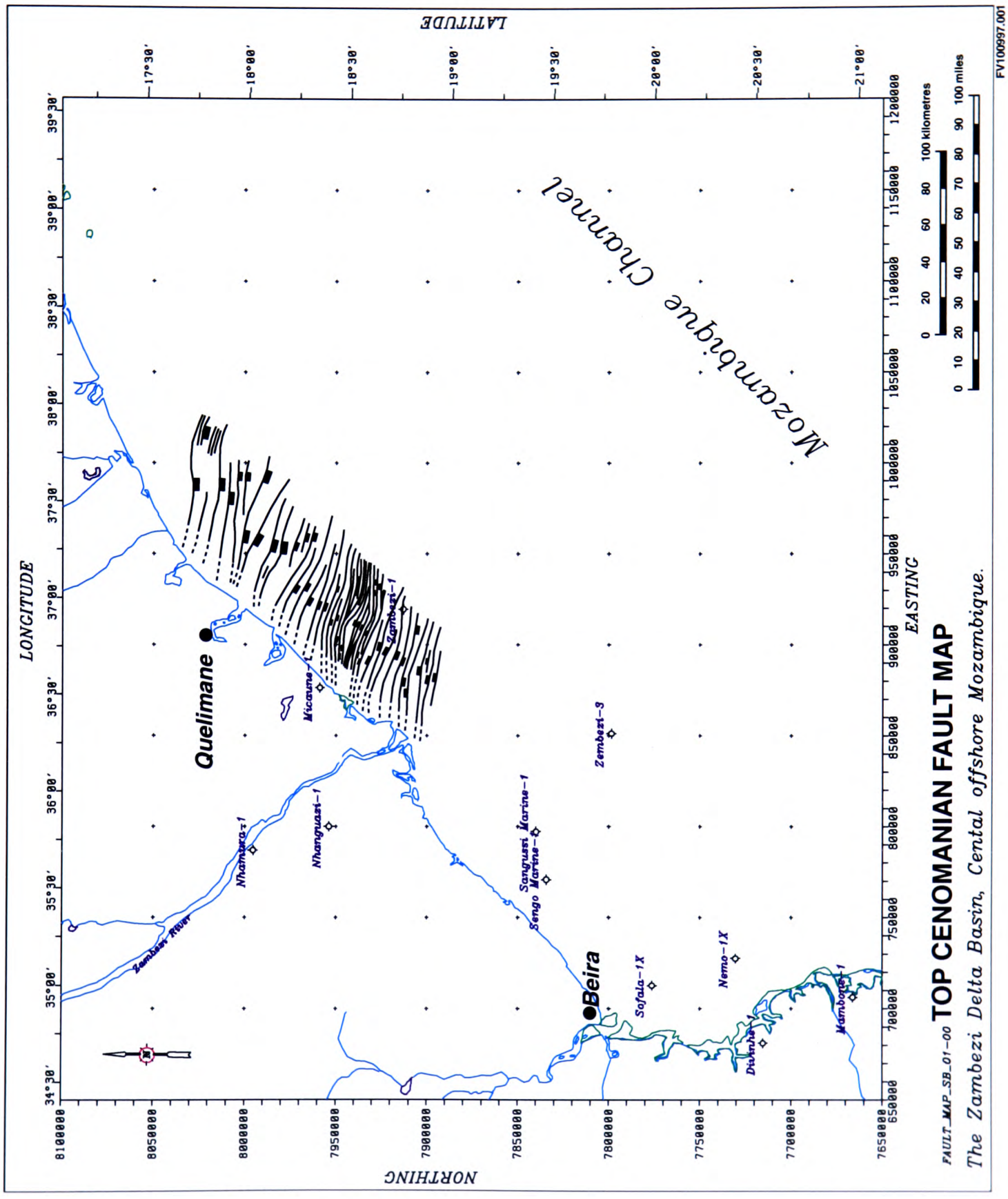

Figure 4.19: Top Cenomanian fault map derived from seismic data.

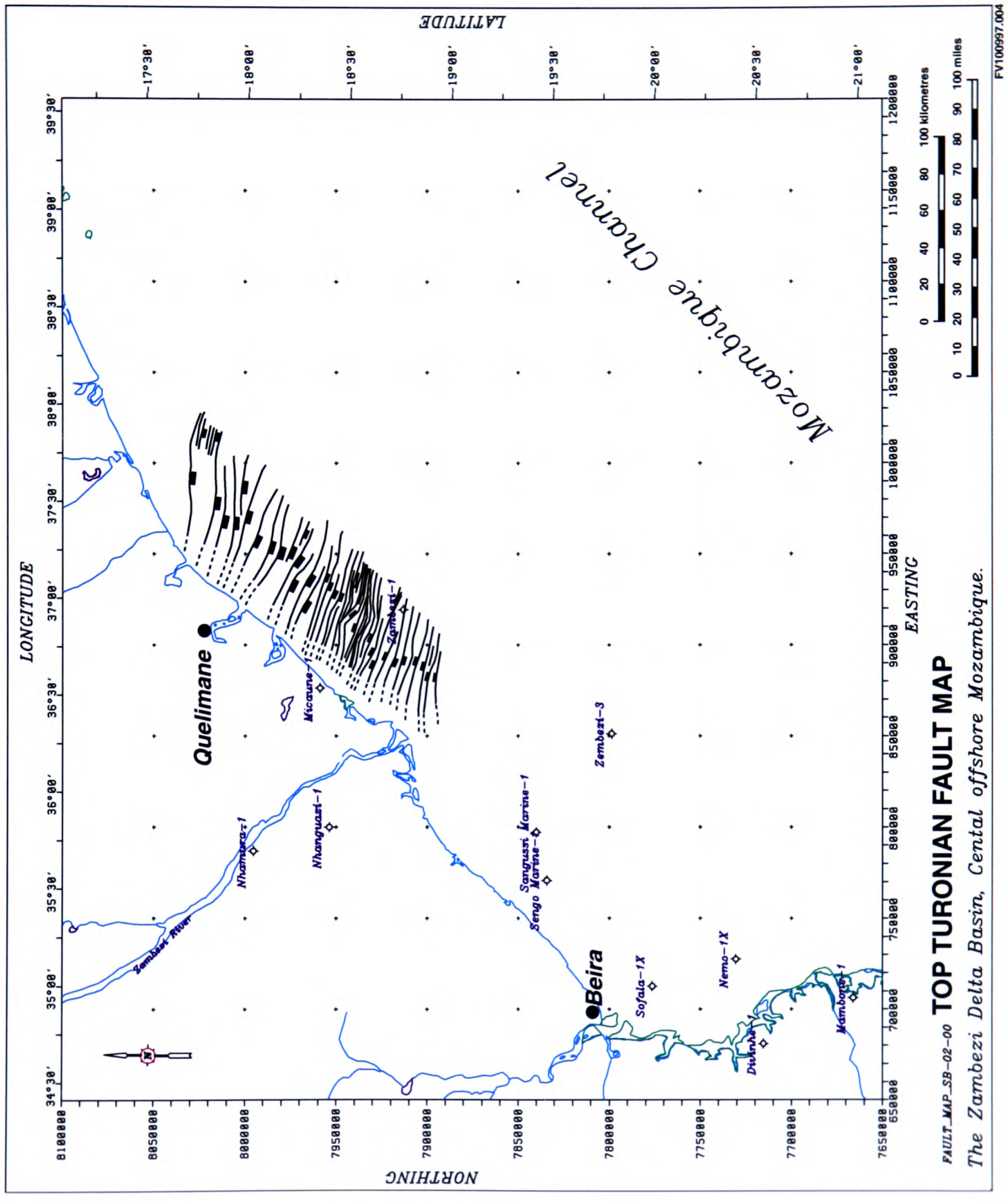

Figure 4.20: Top Turonian fault map derived from seismic data.

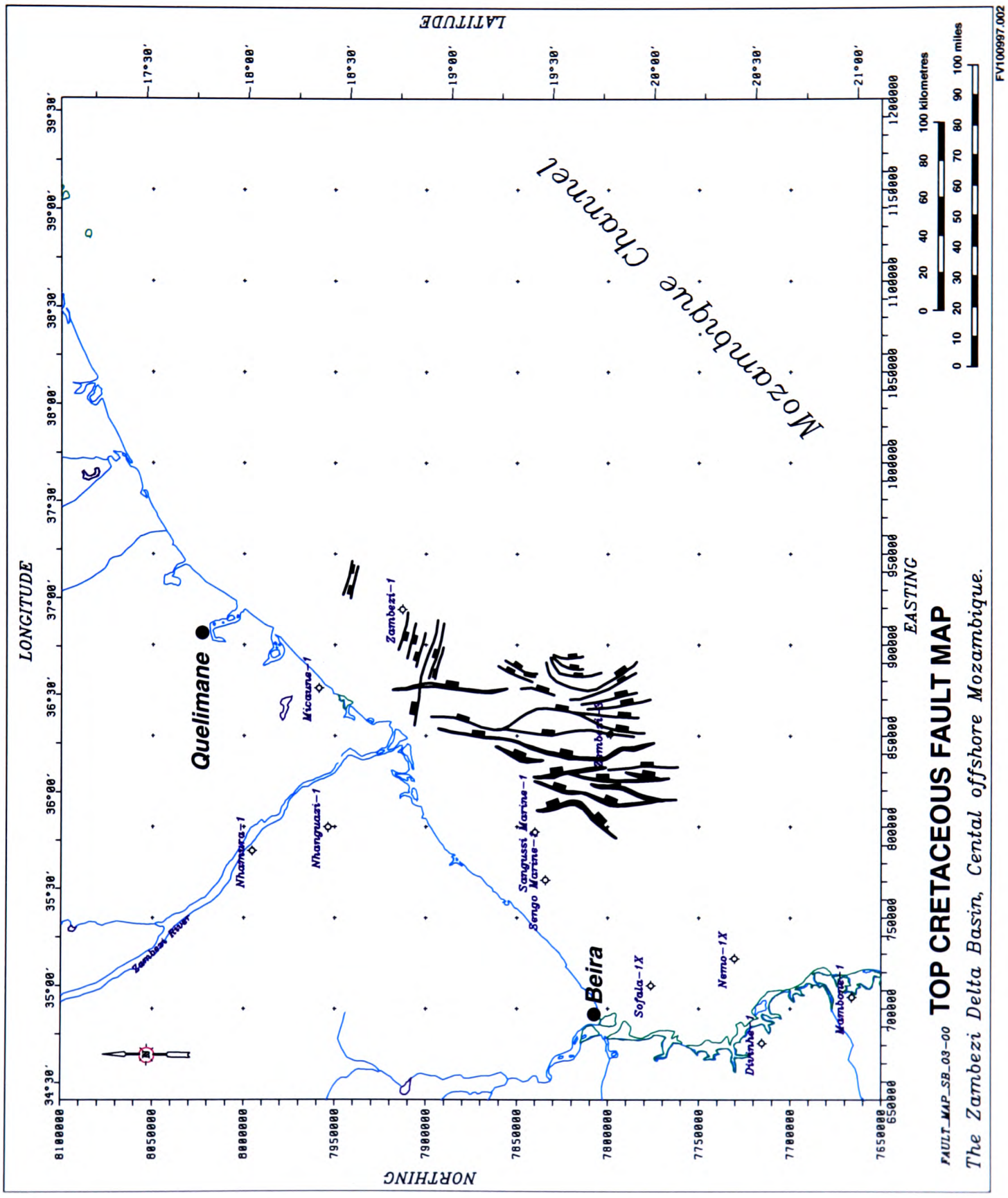

Figure 4.21: Top Cretaceous fault map derived from seismic data.

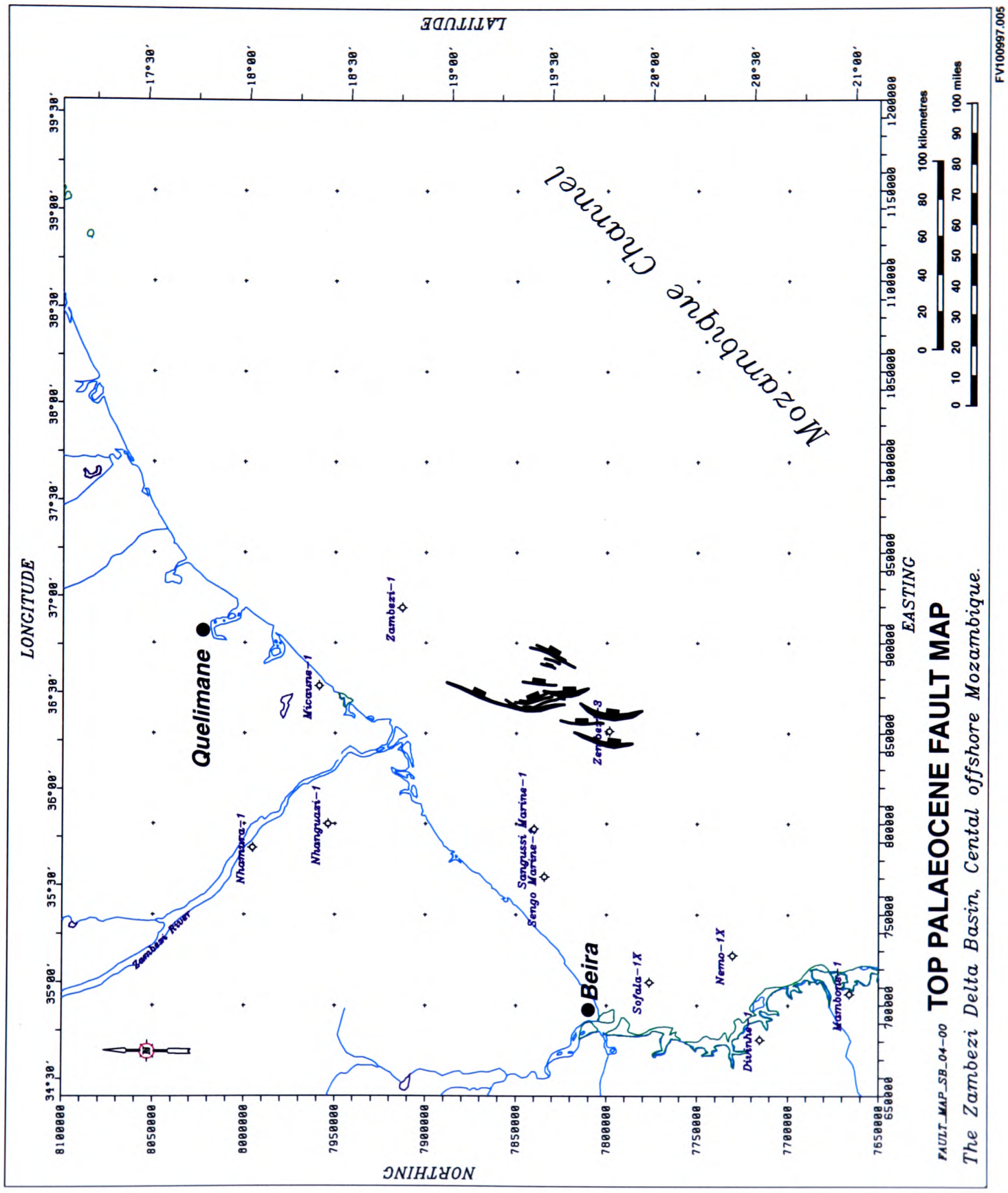

Figure 4.22: Top Palaeocene fault map derived from seismic data.

4.4.1 Fault distribution.

The east African continental margin has undergone three major tectonic episodes which are recorded in the Zambezi Delta Basin sedimentation history. The second was the breakup of the Gondwana continent in Middle Jurassic times, marked the beginning of the development of most of the sedimentary basins in east Africa. This was then followed by the movement of Madagascar from a position close to the east coast of Kenya and Somalia in Late Jurassic to its present position east of Mozambique (Scotese, 1991) in Middle Cretaceous time as discussed earlier in Chapter 1. This event gave way to the opening of the Eastern Somali offshore basin and to the creation of the Mozambique Channel and the Mozambique Basin.

The third major event was the East African Rift System which stretches with an approximately NE-SW trend from northeast Africa inland down to offshore southern Mozambique. This last event is marked by three phases of fault reactivation in various branches of the rift understood as phases of structural adjustment (Chapter 1).

In a broad context, this tectonic history is represented by various fault lineaments: the Karoo rifting in late Carboniferous time, the continental breakup and subsequent plate movements and in the N-S direction of Madagascar movement in late Jurassic, and the mainly NE-SW direction of the East African Rift and rift arms in Middle Tertiary.

The Zambezi Delta Basin is composed of its onshore (much older) part and its present coastal and offshore and most recent (late Cretaceous to Recent times) and deltaic part. The basin owes its position to the Lower Zambezi graben and to the failed arm of the southern most triple junction of the East African Rift which has its centre in the lower Zambezi Basin where old Karoo structures were reactivated. This failed rift arm is a graben structure in a NW-SE direction and sub-parallel to the southern course of the Zambezi River. This graben structure shallows and narrows towards the triple junction to the NW and deepens and widens towards the Indian Ocean (Dingle and Scrutton, 1974; Salman *et al.*, 1985). Because of the sediment thickness, this structure cannot be resolved within

the window of 6.0s to 8.0s of the offshore seismic data base used in this work, but can be inferred from published maps. To the southeast deep basement normal faults can be mapped close to the basement high (the Beira High) responsible for the gravity anomaly known as the Beira High (Salman *et al.*, 1985).

In most parts offshore the basin, tectonic activity can be traced as far back as Late Palaeocene and Early Eocene (Figs. 4.18 to 4.22 and Appendices A.2 to A.5) when listric faulting occurred involving sediments deposited between Top Turonian and Top Palaeocene. The timing of this tectonic event might well be an indication of the reactivation of faults from previous rifting phases prior to the East African Rift. This hypothesis is not examined in this work.

In the northeastern part of the basin, tectonic basin subsidence can be observed at present, suggesting ongoing tectonic activity in the East African Rift active extension possibly triggered by extensive sedimentation during deltaic buildout. The Beira uplift fits within the geotectonics of the second rift phase. Faults mapped from seismic data (this work), cut through sediments of Jurassic, Cretaceous and Early Tertiary (Lower Palaeocene) age.

Faults related to the breakup of the Gondwana supercontinent are not known in the basin although they can be inferred with help of the magnetic anomaly trends (Chapter 4). These are deep, old structures with possibly little or no implications to the petroleum geology of the basin unless it can be proved that they stayed active during early stages of basin sedimentation or they were reactivated during subsequent rift stages.

Fault lineaments related to the movement of Madagascar are generally features with a N-S trend, some of which are still seismically active (the Davie Ridge and the Sea GAP Fracture zone in the Indian Ocean). These lie east and northeast of the Zambezi Delta Basin and have no relevance to the structure of the basin.

The East African Rift phase produced faults with possibly important implications for basin development and basin architecture during deltaic development as they formed within the geologic time period of the Zambezi Delta Basin

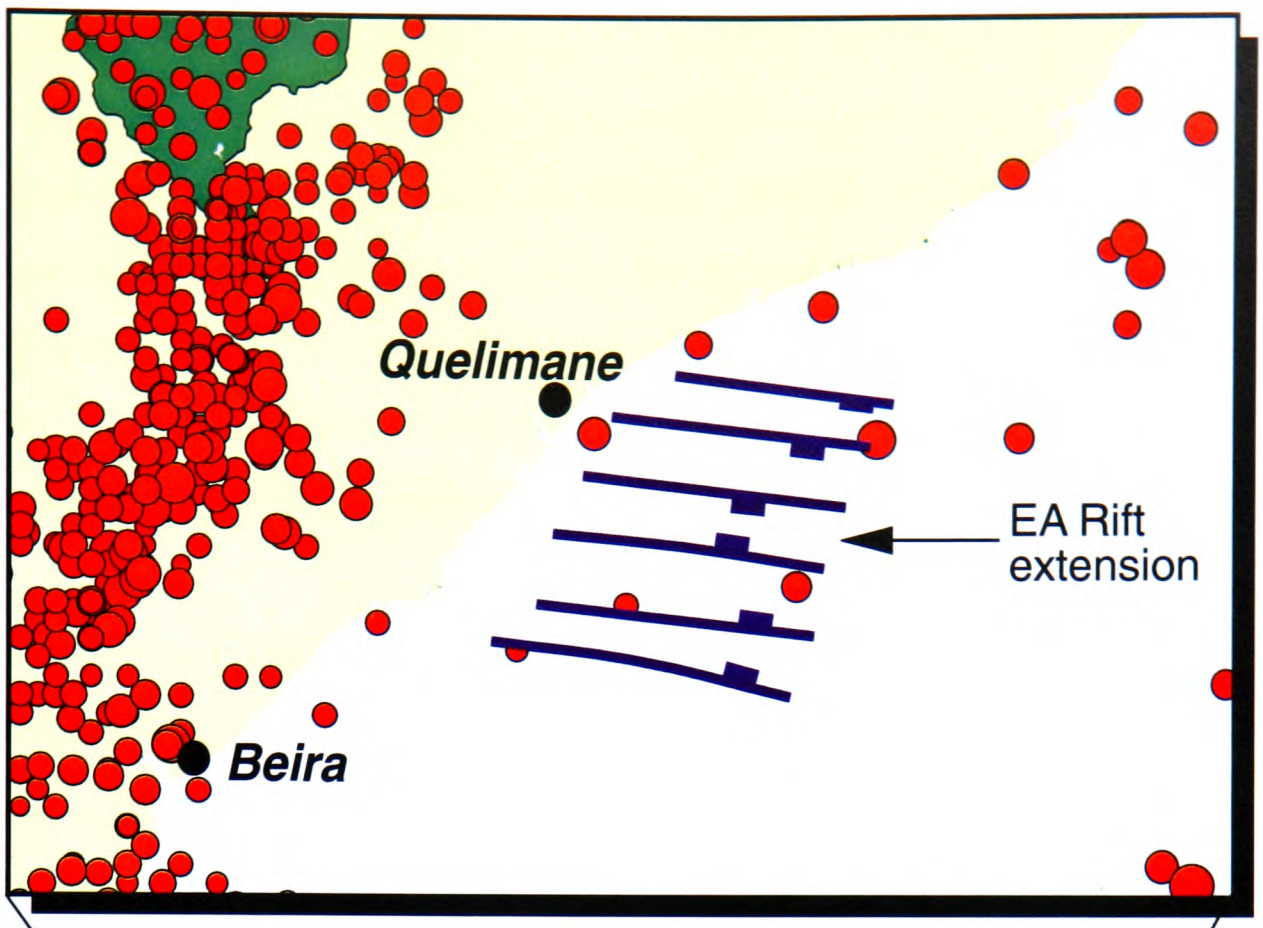

Figure 4.23: Seismicity map of Mozambique and neighbouring regions (1964-1997) highlighting the southern end of the south-western branch of the East African Rift System. Seismic event body wave magnitude (Mb) 2.0 to 6.8. Size of circles in the map is proportional to body wave magnitude. Data source: ISC (International Seismological Centre) catalogue.

buildup. These events have implications for forming the shape of the basin and for basin and provenance source position through Neogene and Quaternary times.

Normal faults are mapped to the northeast, some of which are believed from this work to have been active in early Miocene time (and possibly beyond) of the ancient Zambezi Delta (Miocene to Recent times) development, and might have contributed to the slope failure episode in early Eocene. Some of these faults are as old as early to Middle Cretaceous and might have been reactivated by younger rifting.

The suggestion that the graben structure mapped at the northeastern depocentre of the Zambezi Delta Basin (EAR extention) might still be active today arises from observations made on sediment deformation immediately above the structure, backed by the occurence of strong seismic events in the area around it (east and southeast of Quelimane) (Fig. 4.23). Slope failure occurred along surfaces of failure, generally eroded transgressive surfaces, often coinciding with sequence or parasequence boundaries in Late Palaeocene or Early Eocene times. All surfaces of failure have Top Turonian as a common decollement surface. The slope failure occurs at very shallow angles with a generally N-S strike often with some curvature and with the down fault throw to the east (Figs. 4.21; 4.22).

4.4.2 Folding.

Folds can be observed at the bottom (i.e. late Cretaceous folds) of the seismic record with an average wavelength of a few tens to hundreds of kilometres. These raise the possibility of salt or mud movements during Late Cretaceous time, although there are currently no data to support any salt or salt tectonics in the Mozambique Basin so far. If proved to be true, this could have important implications for hydrocarbons prospectivity in the basin.

4.4.3 Structural controls on sedimentation.

Three rift phases are discussed in Chapter 1 and above. They affected basin creation and development in south and eastern Africa. Their influence on

the Zambezi Delta Basin structural development is variable, as is their influence on basin sedimentation.

The Karoo and the East African rifts effected the structural development of the onshore part of the Zambezi Delta Basin, while the continental breakup phase is responsible for the opening of offshore basins in eastern Africa including the opening of the Indian Ocean and the Mozambique Channel. This includes the begining of marine sedimentation in the Zambezi Delta Basin.

Karoo rifts created, amongst other structures in eastern Africa, the Zambezi grabens which controlled sedimentation, confining it to the graben structures

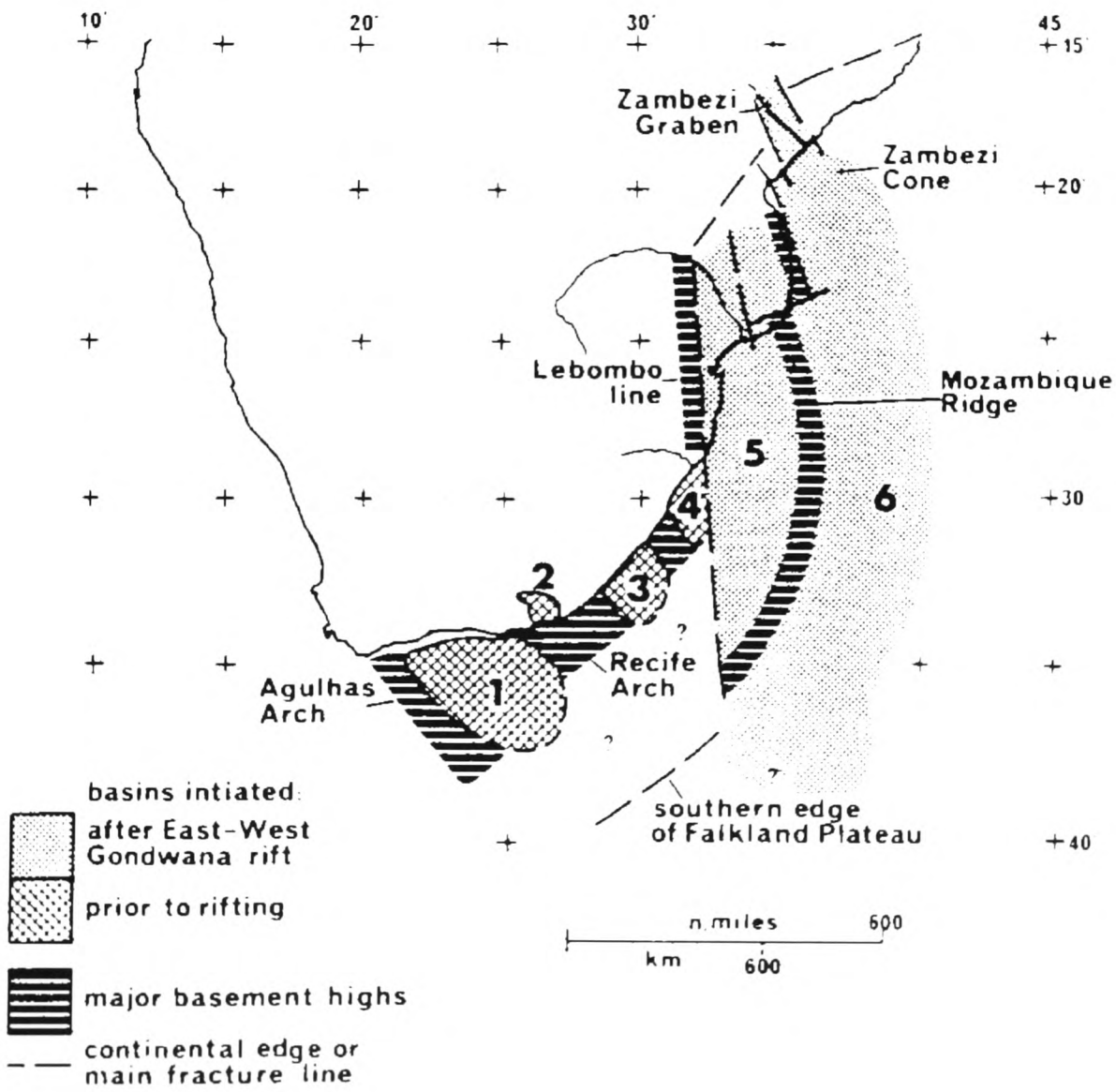

Figure 4.24: Sketch map of main sediment basins, basement highs and fracture lines in existence prior to the breakup of west Gondwana (Late Jurassic), showing the Lower Zambezi graben and the Zambezi Cone, from Dingle and Scrutton (1974). Key: **1,** Outeniqua Basin; **2,** Algoa Basin; **3,** St. Johns Basin; **4,** Durban Basin; **5,** proximal Natal Valley; **6,** western Mozambique Basin.

where accomodation space was available. These structures remained the main sediment conduits to the southeast from the hinterland through the Zambezi Cone (Dingle and Scrutton 1974) (Fig. 4.24). The continental breakup phase did not significantly affect basin development onshore East Africa, but it represents an important period in basin development and was responsible for setting up present day palaeogeography.

The East African Rift system which reactivated some of the old Karoo structures in the Lake Malawi (Lake Malawi rift, Ebinger *et al.* 1984; Ebinger *et al.* 1987) and in the Lower Zambezi graben set up the scenario of source to basin palaeogeography and of the sediment transport pathways which prevailed during deltaic sedimentation in the Zambezi Delta Basin from Middle Tertiary to Recent times.

The palaeodistribution of rivers and their flow patterns during Cenozoic in the northeastern, western and southwestern parts of the basin are important factors in delivering the sedimentation pattern we observe today in both depocentres of the Zambezi deltaic succession. Recent Quaternary tectonics is an additional factor in controlling sedimentation in the northeastern depocentre.

4.5 Seismic stratigraphic interpretation.

4.5.1 Basic principles of seismic and sequence stratigraphy.

Seismic and sequence stratigraphy are two methods which are now routinely used to subdivide and to characterise the sedimentary fill of basins in order to determine their precise tectono-stratigraphic development and evolution through time. It is fundamental that the stratigraphy of a basin can be subdivided into stratigraphic sequences (depositional or genetic stratigraphic sequences) as an aid to understanding the causes involved in generating the stratigraphic sequences.

Amongst the causes involved in generating stratigraphic sequences the most important are tectonic, eustasy, climate, sediment supply and basin subsidence.

The relative importance of each of these factors may differ for each particular basin setting.

4.5.2 Definition of boundaries.

Seismic reflectors are generally believed to approximate to bedding planes, especially so for low frequency seismic data like that used in this study, which represent brief periods of non-deposition, and are isochronous surfaces. However, the process is generally thought to be so brief that seismic reflectors may be effectively drawn as horizontal lines on a chronostratigraphic diagram.

The depositional sequence is a stratigraphic unit of relatively conformable succession of geneticaly related strata bounded at its top and base by unconformities or their correlative conformities (Mitchum and Vail 1977b; c). Boundaries to sequences are thereafter determined by only one objective criterion, the physical relation of the strata themselves. This and the systematic patterns of deposition of the geneticaly related strata within the sequence, makes the depositional sequence concept a fundamental and practical basis for the interpretation

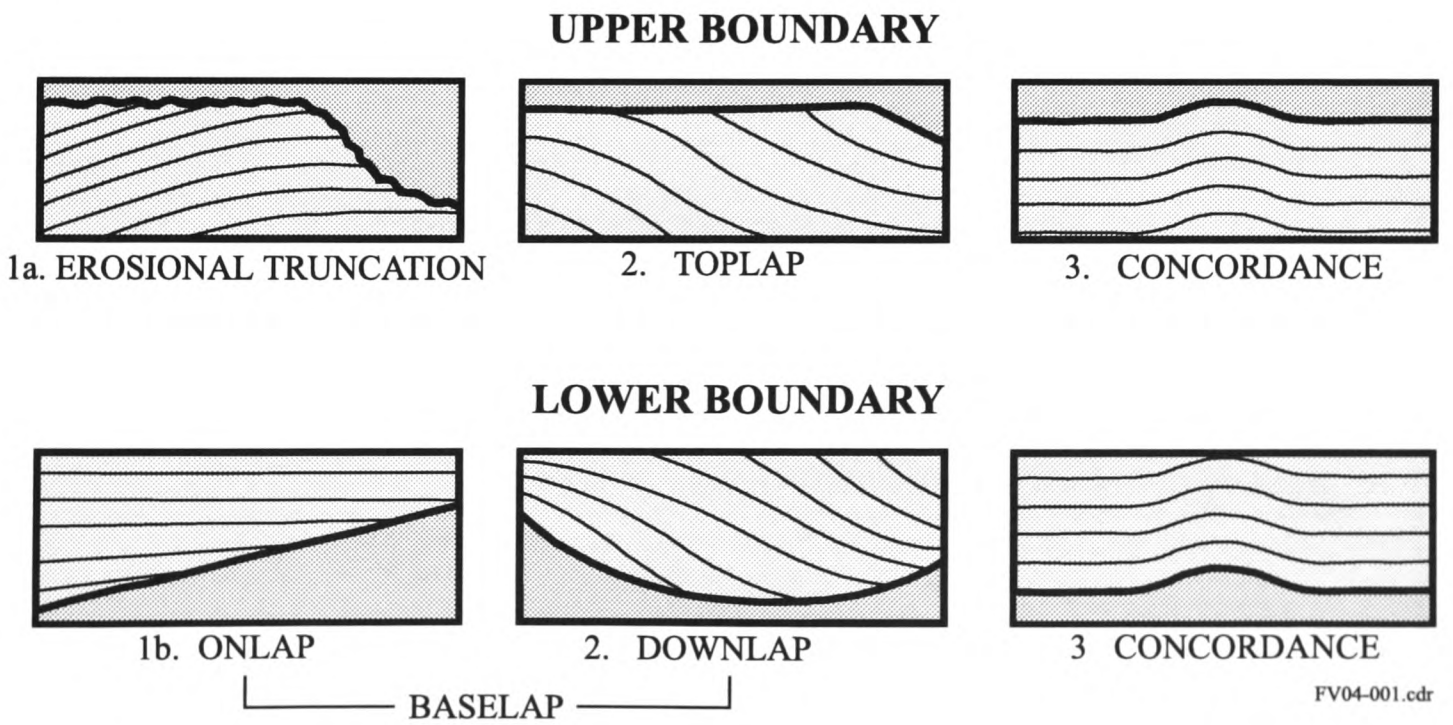

Figure 4.25: Relationship of strata to boundaries of depositional sequences, redrawn and modified from Mitchum, *et al.* (1977a).

of stratigraphy and depositional facies.

Depositional sequences are defined and correlated by defining and tracing sequence boundaries. These are defined at unconformities and traced to their correlative conformities using discordance of strata as the main criterion in the determination of sequence boundaries. The type of discordant relationship is the best indicator of whether an unconformity results from erosion or non-deposition or both. Stratal terminations indicating non-deposition hiatuses are onlap, downlap and toplap, (Fig. 4.25 1b and 2.) while erosional hiatuses are indicated by erosional truncation (Fig. 4.25 1a.) unless the latter is caused by structural disruption. Stratigraphic sequences defined in this way are generally believed to be chronostratigraphically significant because they are deposited during given interval of geological time limited by the ages of the sequence boundaries where these are conformities. However the age range of the strata within the sequence may vary from place to place where the boundaries are unconformities.

The identification and mapping of widespread unconformities is the first and fundamental step in defining depositional sequences of genetically related strata (Fig. 4.26). The depositional sequence is the basic stratigraphic unit in sequence stratigraphic analyses (Sloss, 1963; Vail, 1987; Miall, 1997). Important

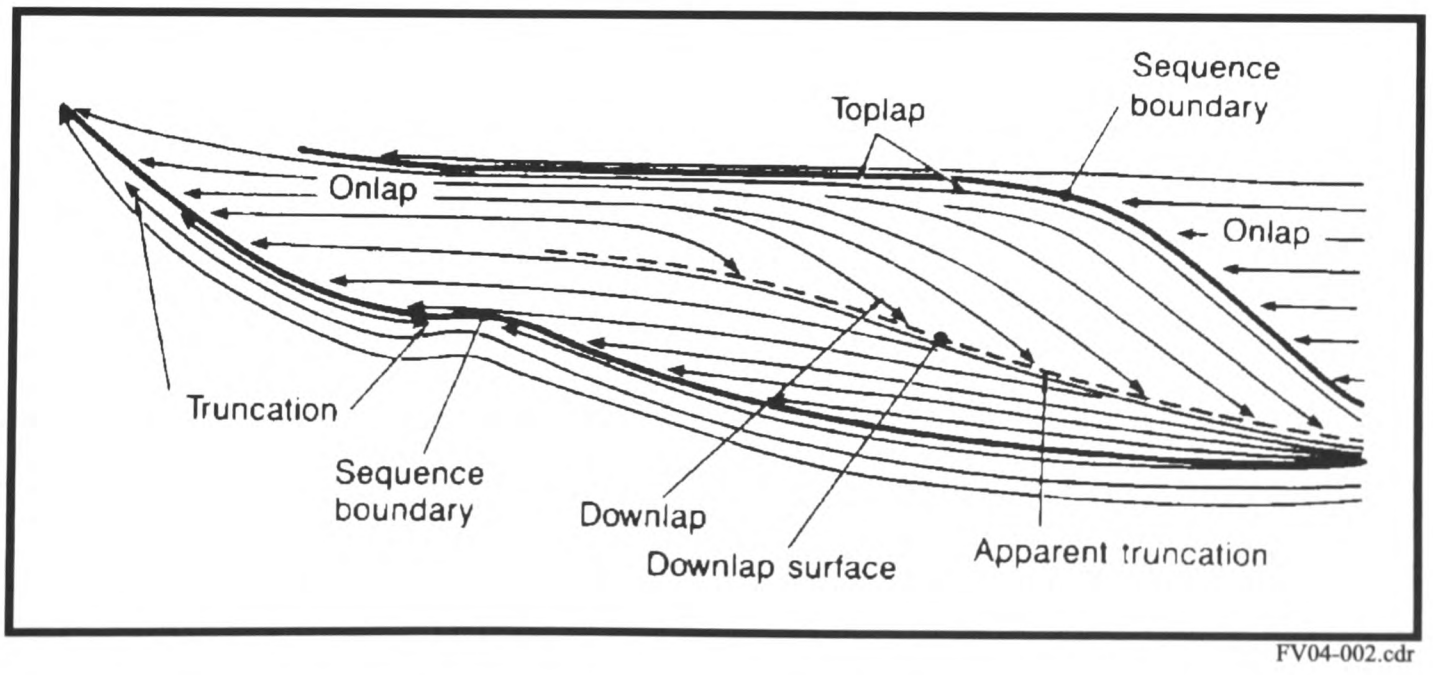

Figure 4.26: Seismic patterns that are used in seismic and sequence stratigraphic interpretation to indicate eustatic sea level changes. Types of reflection terminations from Vail (1987).

for a sequence stratigraphic study is the appropriate assessment of regional structural features and of their relevance to large-scale configuration of depositional sequences.

Internal and external reflector terminations of depositional sequences are mapped and can provide more helpful information in determining the depositional environments and the vertical and lateral facies changes within the sequences and for the complete stratigraphic section.

For Mitchum *et al.* (1977a; b) the distribution of most depositional sequences and facies is controlled by eustatic sea level and therefore comprehensive global stratigraphic frameworks can be established from them. This view however, has been consistently chalenged over the years (Hubbard *et al.*, 1986a, b; Underhill, 1991; Miall, 1997) as it became clear that some sequence geometries can be produced by the interplay of tectonics and sediment supply alone.

4.5.3 Sequence boundary types.

In defining depositional sequences two types of unconformities (sequence boundaries) can be distinguished (Vail *et al.*, 1984), a type 1 (SB1) and a type 2 (SB2) unconformity, each developing in different circumstances (Fig. 4.27). Type 1 unconformities develop when a sharp fall in sea level occurs and the rate of subsidence at the shelf edge is slower than the rate of sea level fall. Type 2 unconformities on the other hand develop as the result of a slowly falling sea level, with base level not falling below the shelf edge, thus causing no significant erosion to exposed sedimentary strata. In this case the rate of basin subsidence at the shelf edge is higher than the rate of sea level fall. A condensed section, however is deposited on top of the maximum flooding surface which develops at times when sea level rises rapidly followed by stillstand and slow sea level fall. It is known that a condensed section is developed during the rapid rise and stillstand. If sea level continues to rise the highstand systems tract is deposited (see below). Following the deposition of the HST, if a slow sea level fall is observed the result is the basinward deposition of a stratigraphic unit known as the forced regression.

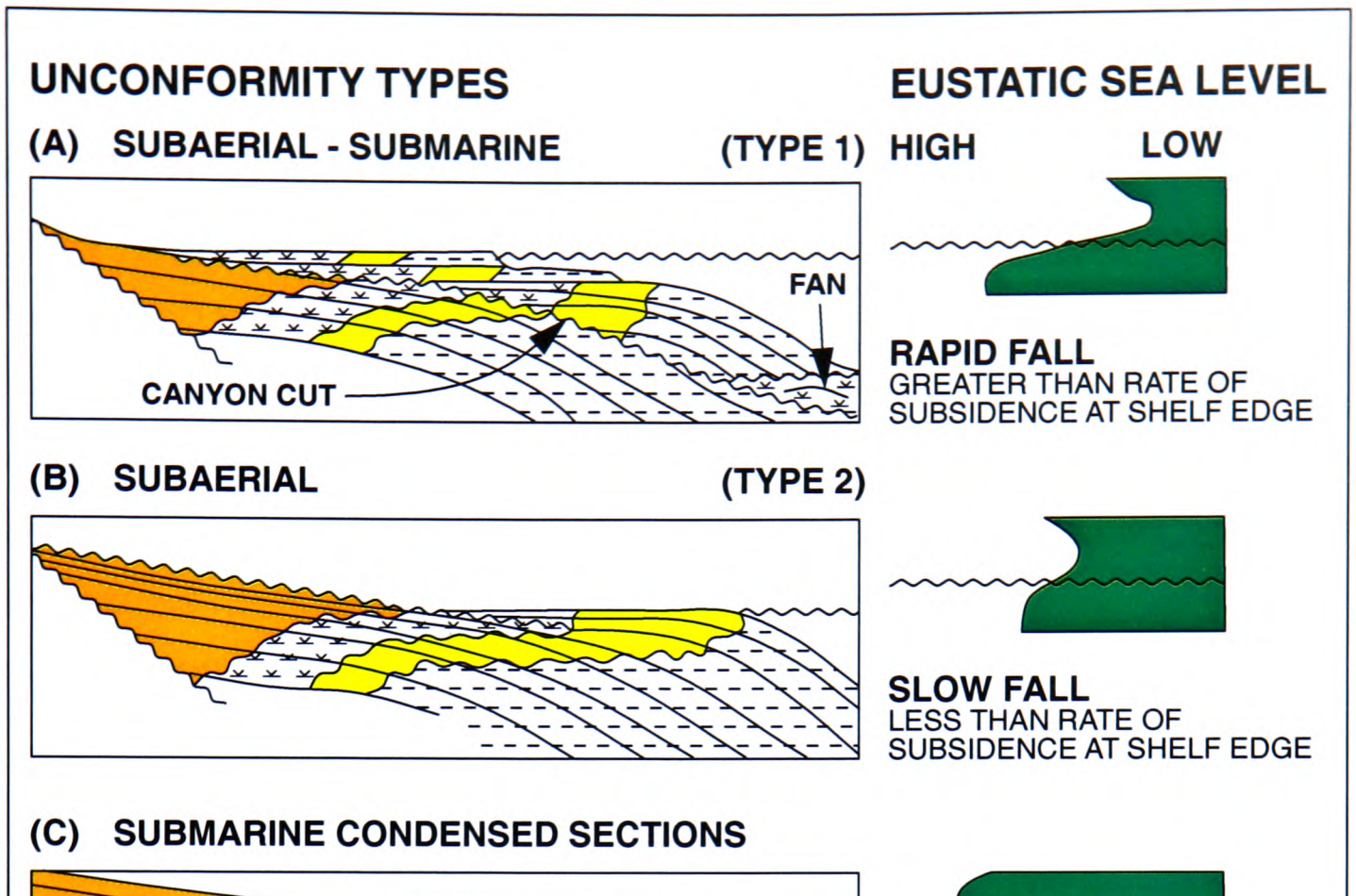

Figure 4.27: Type 1 and type 2 unconformities and the condensed section as defined by Vail *et al.* (1984).

The above definition of type 1 and type 2 unconformities only considers sea level fall and basin subsidence as causes for their development but it should be noted that tectonism alone could cause the same sort of unconformities to develop.

During the rapid sea level fall, a type 1 sequence boundary (SB1) is developed at the exposed shelf edge. Sedimentation is shifted from the highstand systems tract and takes place in the prodelta, deep in the basin. Sediments supplied during the fall and lowstand, including those eroded at the shelf edge and elsewhere in the basin, get deposited as basin fan, slope fan and lowstand wedge. When sea level comes to rise again a transgressive surface is produced onto which

sediments of the transgressive systems tract (TST) downlap into the basin.

At the end of the deposition of the TST generally a rapid sea level rise and stillstand produces the maximum flooding surface (Fig. 4.28), discussed by Vail (1987) and Van Wagoner *et al.* (1987), and the condensed section before the highstand systems tract (HST) is deposited. If at the end of deposition of the HST, a slow sea level fall occurs which keeps pace with the rate of sediment supply and generally does not fall below the shelf edge, a type 2 sequence boundary (SB2) is then developed. When sea level stays above the shelf break, the first unit to be deposited is the shelf margin systems tract (SMST) which onlaps and downlaps onto the type 2 sequence boundary.

The recognition of regional and smaller scale reflections or reflection discontinuities is a fundamental step in subdividing the basin fill in stratigraphic units of genetically related strata and in producing a basin stratigraphic framework. This must be done before seismic data is integrated with well data and other relevant geological and geophysical information, correlation of palaeontologic data with regional and local reflections to develop basic chronostratigraphic framework in the basin. Isopach maps of regional and local seismic stratigraphic units, velocity analysis data correlated with well data aid in developing summary maps of facies distribution and depositional models for each seismic stratigraphic unit.

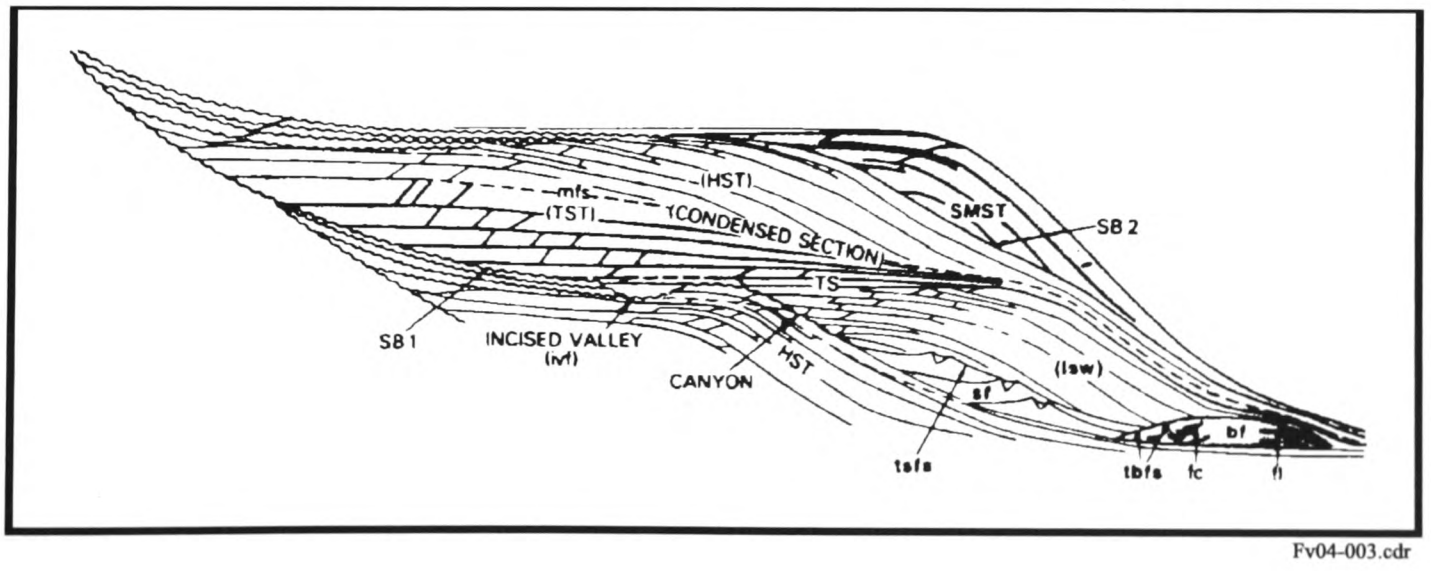

Figure 4.28: Schematic diagram illustrating the definition of systems tracts, from Vail (1987). Key: HST - highstand tract, TST - transgressive tract, SMST - shelf margin tract, SB1 - type 1 sequence boundary, SB2 - type 2 sequence boundary, bf - basin fan, sf - slope fan, lsw - lowstand wedge and mfs - maximum flooding surface.

This methodology was applied successfully by Brown and Fisher (1977) in a study of Brazilian basins, including some important deltaic basins. With this methodology the spatial arrangement and chronological order of facies within each depositional system can be estimated and sequencial events during deposition can be distinguished, opening way for predicting potential traps and reservoirs within the seismic stratigraphic unit. The depositional mode interpreted for each successive stratigraphic unit provides the basis for infering the overall tectonic and depositional evolution during basin fill and leads toward potential prospects giving types, stratigraphic position, geographic location and trend, structural situation and reservoir character (Brown and Fisher 1977).

The maximum flooding surface is the third important surface in sequence stratigraphy and is related to the condensed section which is deposited in a relatively short period of geological time along this surface, containing important fossiliferous content used in biostratigraphic age dating. It separates the transgressive from the highstand systems tracts and is the downlap surface during deposition of the highstand systems tract, an important reference in relative sea level changes.

The mapping of depositional environments and facies changes enable a further subdivision of the stratigraphic succession into its depositional sequence components and depositional systems tracts (Fig 4.28) which provide an indication of relative change of sea level.

Galloway (1989a; b) used the maximum flooding surface to introduce the concept of the genetic stratigraphic sequence bounded at its top and base by maximum flooding surfaces, suggesting that the maximum flooding surface offered more objectivity in defining stratigraphic sequences than the type 1 and type 2 sequence boundaries defined by Vail *et al.* (1984). However, and as alluded to before the recognition of the maximum flooding surface requires biostratigraphic indicators from the condensed section which only are available if wells exist in the area which bottomed through that section. This and other practicalities discussed by Walker (1992a) renders Galloway's type sequence less practical in seismic and sequence stratigraphic interpretation in areas with no/or

poor well control. Nonetheless, the importance of the maximum flooding surface is widely acknowledged for its link to the condensed section which contains valuable biostratigraphic information used for geological age dating and in identifying sepecific palaeoenvironments which might have prevailed during limited time in geological history. Furthemore, Galloway's use of the mfs has been found to be more convenient for sequence mapping as it may produce a prominent gamma-ray spike in wireline logs in the Jurassic succession of the North Sea (Underhill and Partington, 1993), or it may correspond to widespread and distinctive goniatite bands in the Carboniferrous succession of the Clare Basin in Ireland (Martinsen, 1993) in areas with good well control. The condensed section deposited on top of the mfs is an important stratigraphic unit because of its abundant, diverse and

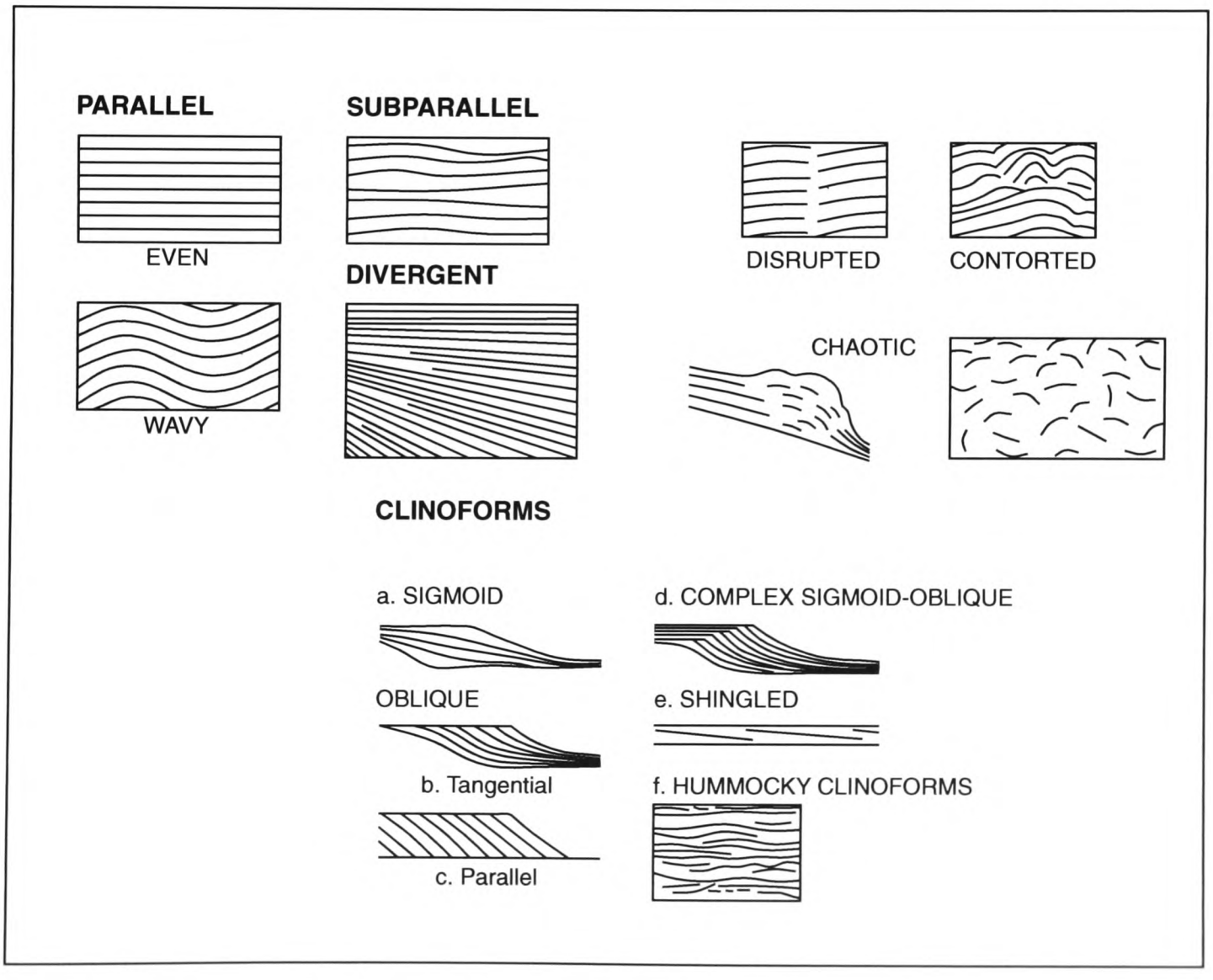

Figure 4.29: Schematic illustration of the concept of seismic facies using typical seismic reflection patterns often observed in seismic sections. Redrawn from Mitchum *et al.* (1977b).

distinctive faunal and floral assamblages (e.g. Partington et al. 1993) which makes it suitable for geological age dating thus providing a better correlation.

For a sequence stratigraphic study to be fully accomplished one requirement is that depositional sequences be precisely dated and correlated with adjacent basins and in tectonically unrelated regions. Here, biostratigraphic data is essential. Following from this, a detailed chronostratigraphic framework is possible, the basis for testing any correlations with known regional and global events, of which tectonic activity and eustasy are the most important.

Once depositional sequences of genetically related strata are mapped, depositional environments and facies anlyses can be carried out.

Well information and other geological and geophysical data, including velocity data, can be used. Mitchum *et al.* (1977b) introduced the concept of seismic facies and facies analyses with a set of typical seismic reflection pattern (Fig. 4.29) which can be successfully used in deriving seismic facies from seismic data.

The Exxon sequence model (Mitchum *et al.,* 1977a) has been applied to most sedimentary basin studies but its universal validity has been several times challenged by various authors (Hubbard *et al.,* 1986a, b; Underhill, 1991; Miall, 1997) because of its dependency on eustatic (global) sea level changes and the global sea level chart by Vail *et al.* (1977a; b) and modified by Haq *et al.,* (1987) and Haq *et al.* (1988).

The genetic stratigraphic sequence model introduced by Galloway (1989a) is not as dissimilar from the one proposed by EXXON 1977 as might be supposed. One important difference between the models lies in the definition of the boundaries to the sequence. Furthermore sequence boundaries develop by removing stratigraphy and can not be used to obtain the time duration of the deposition of the stratigraphic sequence they define unless their correlative conformities can be traced. The genetic sequence is deposited during the time difference given by the difference in geological age of the bounding maximum flooding surfaces. However the improvement suggested by BP (Hubbard *et al.,* 1986a, b) with the introduction of tectonics as an important control over the stratigraphic sequence

geometry gave the sequence model a much wider and more acceptable form mainly for basin settings with synrift tectonics effecting sedimentation. The eustatic sea level curve as known to date, lacks a permanent reference point and uniform data distribution over the earth. The chart by Vail *et al.,* (1977a) and the subsequent modifications by Haq *et al.,* (1987) and Haq *et al.,* (1988) are based on data predominatly from the northern hemisphare and thus less representative and unsuitable for use in some parts of the southern hemisphare and in tectonicaly complex areas.

Unfortunately, the term "sequence boundary" has been used widely in the literature to describe other surfaces used in the definition of "depositional sequences". For example, throughgoing reflectors which show no evidence for truncation have been described as such and used to define "seismic sequences". Many of these throughgoing surfaces have transpired to be condensed intervals which reflect times of maximum transgresion with a genesis completely oppsite to the sequence boundaries (sensu strito) formed during relative sea level fall and minima events.

4.5.4 Methodology used in this work.

As alluded to above, the quality of data available to this study is not good enough to support a strictly sequence stratigraphic study. However the interpretation technique outlined by Michum and Vail (1977c) and applied with some improvements by Hubbard *et al.* (1986a, b) provide the basis for the seismic stratigraphic study carried out here. This technique requires: seismic sequences to be identified, correlated throughout the basin and age dated; recognition, mapping and interpretation of seismic facies and depositional environments; and regional analyses of relative changes of sea level (regional eustasy).

Depositional sequences are defined objectively using terminations of reflections along surfaces of discontinuity (sequence boundaries) interpreted as stratal boundaries (time lines). Sequence boundaries are diachronous because they are developed during periods of erosion and non-deposition at some parts of the basin (delta top and delta front).

The deposition of major sequences is related to some extent to relative changes of sea level which allows some degree of predictability of age and depositional characteristics within a depositional sequence based on comparison of depositional processes with sea level changes.

This approach to seismic stratigraphy includes the subdivision of the seismic section into depositional sequences which are stratigraphic units of relatively conformable and genetically related strata bounded to top and bottom by unconformities. Depositional sequences defined in this way are chronostratigraphically significant because they represent sedimentary strata deposited during a given interval of geological time limited by the ages of the sequence boundaries where these are conformities, although the age range of the enclosed strata may differ from place to place where sequence boundaries are unconformities (Vail et al., 1977c and Mitchum and Vail, 1977c). This procedure is contrary to the conventional interpretation methods in which seismic reflectors are picked with reference to geological age or formation tops in wells and then tied to seismic. Seismic reflectors defined in this way may have little or no relation to sequence boundaries.

In this study surfaces of discontinuity are recognised by systematicaly interpreting reflection terminations (onlap, downlap, toplap and truncation) along the reflector. Reflectors of this type are sequence boundaries (depositional unconformities) and can be extended into areas of the basin where their surfaces are concordant (correlative conformities). In this way depositional sequences of geneticaly related sedimentary strata are defined and correlated in the basin. This state of seismic stratigraphic analysis is reached with no reference to any information other than seismic sections.

Age determination of the depositional sequences is based on well information which allows the physically defined seismic sequences to be tied into the standard chronostratigraphic framework of the study area.

A detailed interpretation is carried out within the three uppermost depositional sequences of the seismic section. This allows a better understanding of

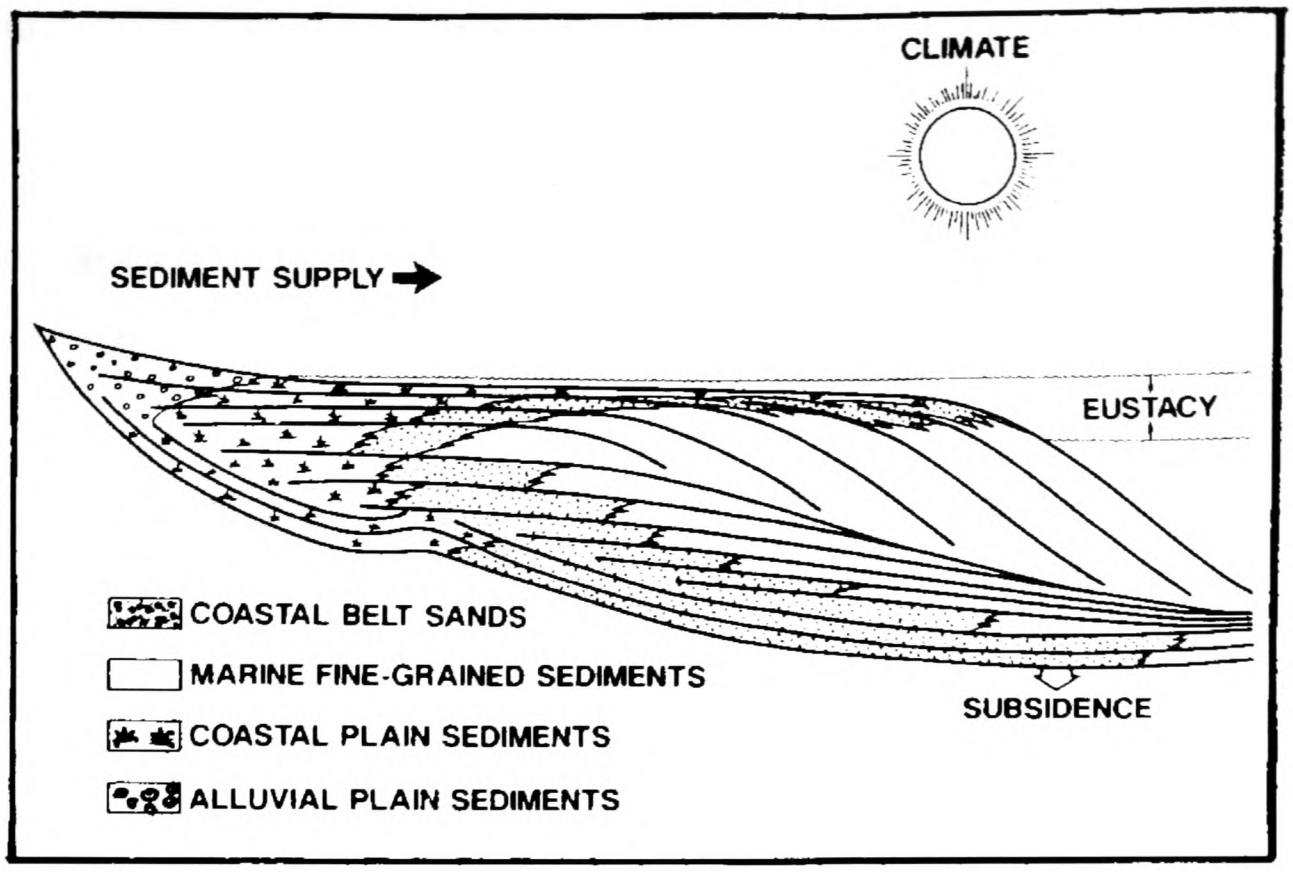

Figure 4.30: Schematic depositional sequence displaying relationships between seismic architecture and depositional environments and showing the three major controls on stratigraphic architecture (Vail, 1987).

the depositional processes within these depositional sequences as discussed later in this Chapter.

The following step is the analysis of seismic facies and depositional environments as illustrated in Fig. 4.30, aimed at grossly determining lateral lithological changes, facies stratification and depositional features of the sediments generating the sedimentation cycles. This, plus the study of the upper portion of the seismic section, leads to a detailed basin development model with the assessment of the roll and importance of depositional channel switching, sediment supply, sediment bypass and erosion, tectonic basin subsidence and eustasy through geological time.

Time isochron maps are constructed for all unconformities mapped and displayed alongside the time isopachs maps defined by two superadjacent unconformities expressing the thickness variation of the strata throughout the basin. The time isopach maps of the megasequences, depositional units and depositional unit sets are interpreted in terms of depositional environments.

Rms-velocities from seismic data proved unreliable for use in depth conver-

sion and qualitative depositional environments and facies analyses, see section 4.7.

A cumulative dip section is constructed based on the seismic stratigraphic interpretation from which a broad qualitative assessment of regional eustatic sea level changes (coastal onlap curve) is made.

4.6 Results.

4.6.1 Introduction.

The sedimentary succession in the offshore part of the Zambezi Delta Basin is subdivided into 10 unconformity defined mega-sequences in this study. The unconformities can be correlated regionally and generally they coincide with geologic time boundaries and with lithological boundaries derived, for the wells. They are from bottom to top: the Top Cenomanian, Top Turonian, Top Cretaceous, Top Upper Palaeocene, Top Middle Eocene, Top Upper Eocene, Top Oligocene, Top Middle Miocene, Top Upper Miocene and Top Tertiary unconformities (Figs. H.1; H.2; H.3). Each unconformity is identified on seismic as a regional seismic horizon (a time line).

These time lines are tied to well stratigraphy and dated according to well information provided. All unconformities and relative conformities are mapped and correlated in closed loops throughout the seismic survey. The top of the basement surface is mapped at sites where it is resolved by the seismics to constrain the lowermost megasequence (Top of Basement to Top Cenomanian).

Two chronostratigraphic diagrams are produced in dip and strike directions (Figs. 4.31; 4.32), illustrating in summary basin sedimentation and stratigraphy in the offshore Zambezi Delta Basin, with some insights into stratigraphic patterns onshore. Fig. 4.31 shows the stacking patterns and basinward extent of stratigraphic sequences and parasequences as interpreted in this study. It is clear from both diagrams that at times sedimentation is restricted to some areas of the basin with lowstand fans being deposited as a sign of eustatic sea

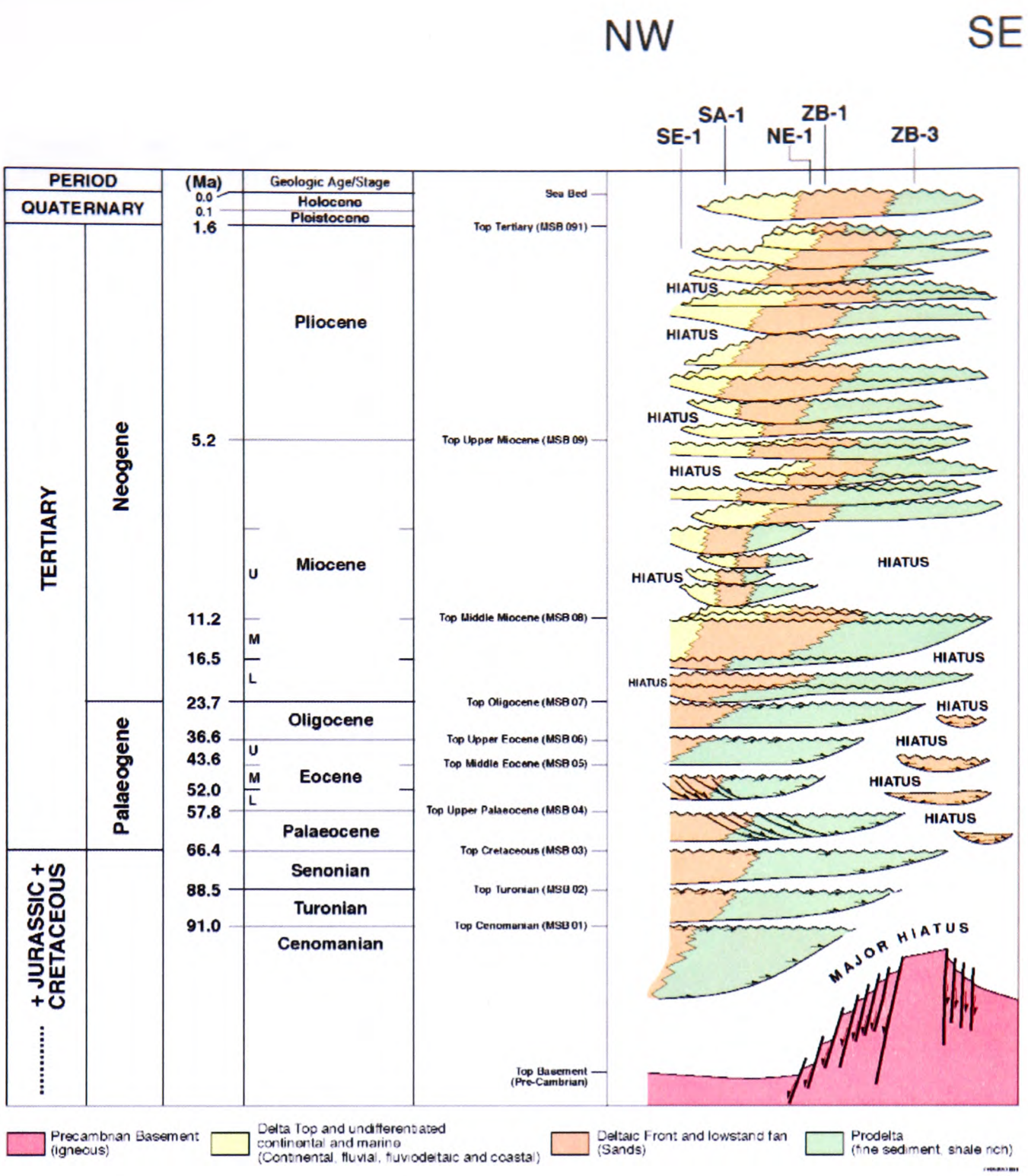

Figure 4.31: Chronostratigraphic diagram along dip offshore the Zambezi Delta basin, summarized from seismic interpretation. For colours in this diagram see legend at the bottom of figure. Key for projected wells: SE-1 - Sengo Marin-1, SA-1 -Sangussi Marin-1, NE-1 - Nemo-1, ZB-1 - Zambezi-1 and ZB-3 - Zambezi-3.

level fall and some channel-confined sedimentation characterizing other times (Middle Miocene). Several channel base and tops are mapped across the basin, as illustrated in Figs. H.1, H.2 and H.3, along with some minor event horizons, which enabled detailed chronostratigraphic diagrams for Neogene to Recent deltaic development to be produced.

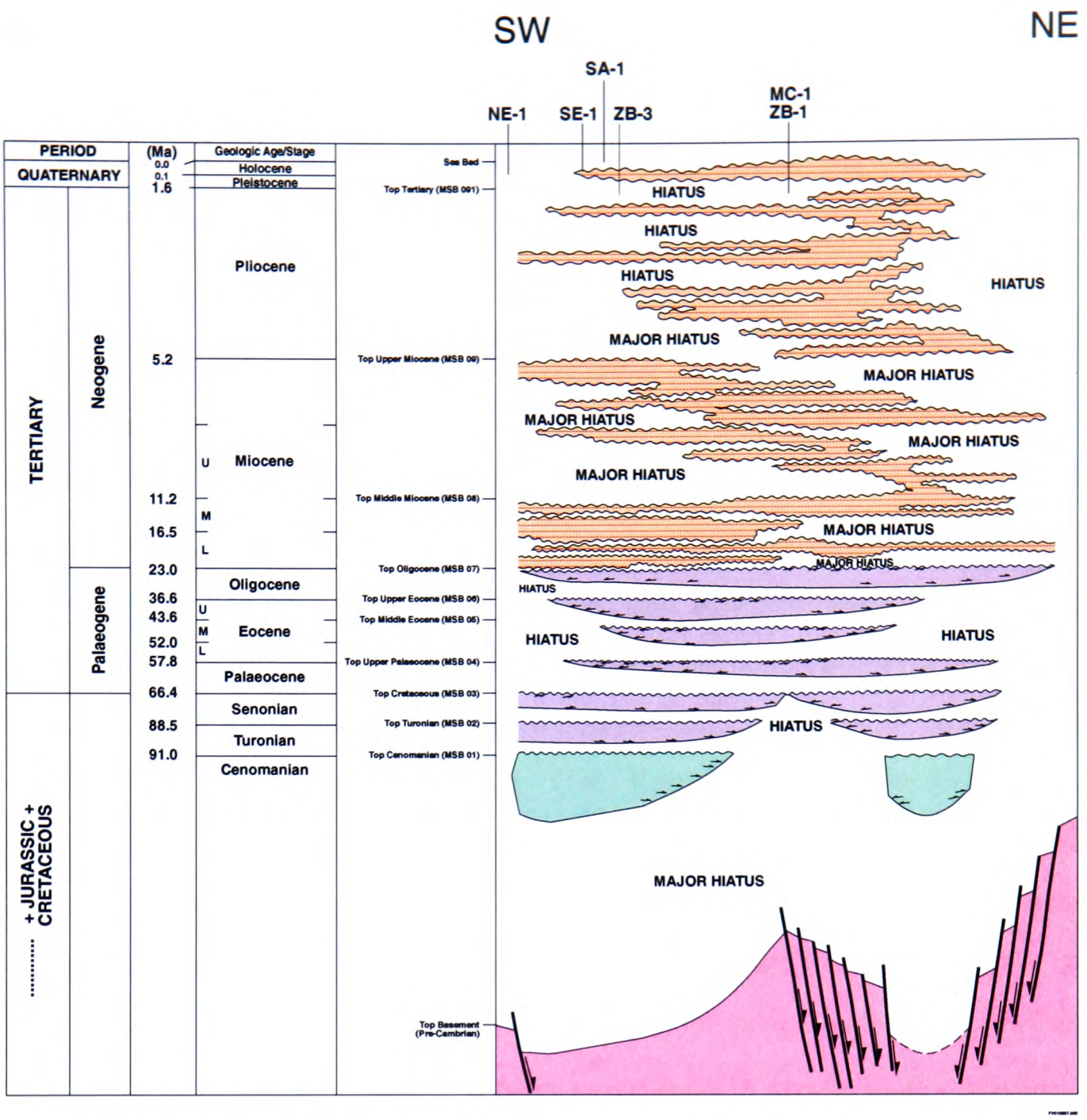

Figure 4.32: Chronostratigraphic diagram in the strike direction offshore the Zambezi Delta basin, summarized from seismic interpretation. Colours in this diagram have no geological meaning. In orange are the four uppermost megasequences interpreted in some detail; purple are the six lowermost megasequences; green is the succession between the basement rock (light purple) and Top Cenomanian. Key for Projected wells: NE-1 - Nemo-1, SE-1 - Sengo Marin-1, SA-1 -Sangussi Marin-1, ZB-3 - Zambezi-3, MC-1 - Micaune-1 and ZB-1 - Zambezi-1.

21 depositional hiatuses of varying amplitude are mapped and displayed in this study and are displayed in both chronostratigraphic diagrams. Their duration varies in the two main depocentres of the basin (Fig. 4.32) and they alternate with sideways switching sedimentation. The mapping of these hiatuses is very important as they might answer questions about the places where supply from hinterland and reworked sediments through erosion in the basin at these time intervals where redeposited downdip in the basin. However, sedimentation during the duration of the hiatuses took place in deeper parts of the basin, which

correspond to the deep waters of the Mozambique Channel today.

The chronostratigraphic diagrams as they are the summary of the stratigraphy in the basin are used to derive the coastal onlap curve which is displayd and discussed later in this chapter.

4.6.2 The Top Basement to Top Cenomanian succession.

The basement structure beneath this succession is highly faulted and steep along the flanks of the Beira basement uplift, and at the gently shallowing basement surface in the northeast. Fault throws are generally small and face to the northwest in the Zambezi Delta half graben, and face northeast and southwest in the EAR active extension. Fig. 4.18 is a simplified schematic fault map of the faulted basement designed to highlight basement structural trends in the basin.

From this point Figs. A.x; B.x; C.x; E.x; G.x; H.x refer to figures in the Appendix, thesis Volume II. x is the figure number in the Appendix. F.x is a table displayed as Appendix F. Also important is the definition used here for ***"depositional unit"*** and ***"depositional unit set"***. A depositional unit is defined as a relatively conformable succession of progradational, genetically related beds bounded by laterally traceable surfaces of discontinuity marked by an abrupt change in the seimic reflexion signal on the processed seismic section. A depositional unit set is thereafter, an assemblage of well identified and mapped gentically related depositional units representing a major depositional event.

Figure A.1 displays the Top Basement isochron in two patches where the basement is resolved by seismic data (basement faults not displaed). To the northeast the basement shallows to the northeast and then onshore where it is outcropping (the Mozambique Metamorphic Belt). In the south the isochrons define the Beira basement high. The steep gradients on both isochrons express the steep flanks of the East African Rift active extension and the Zambezi Delta half graben as displayed on Fig. 4.18.

The sediment isopach between the basement and the Top Cenomanian unconformity (Fig. A.2) displays thinning strata to the northeast and southeast where the strata onlap and downlap onto basement rock. Sediment thickens from

the Beira high northwestward before thinning again onto basement rock in the onshore area. In the EAR active graben area (Fig. 6.3) it is thickest in the graben centre where it remains unresolved by seismic data available to this study (Fig. 6.1).

During deposition of this succession the sediment supply main conduits could have been from the west and northwest (Save and Zambezi rivers) and from possible old north- and northeasterly sediment sources or tributaries. This is suggested by stratal terminations (onlap and downlap) onto major stratal surfaces resolved by seimic data in some areas in the offshore part of the basin.

4.6.3 The Turonian megasequence.

Structural trends mapped on top of the Cenomanian unconformity (Fig. A.3) cut through the Turonian megasequence and display the same E-W strike. They are the expression of basement faults reactivated in Palaeocene (Fig. 4.19).

Turonian deposition began at a time when one main depocentre was situated in the northeastern part of the basin. Two progradational fronts can be seen advancing basinwards in the northeast and southwest and interacting with each other near present day Zambezi River mouth and a third front from further southwest, probably fed by the Save River (Fig. A.4). Sediments from this front also interfinger with sediments to the north. Onlap is to the northeast and northwest while downlap is basinwards.

4.6.4 The Senonian and Maastrichtian megasequence.

This megasequence is structurally disturbed by the reactivation of basement faults during Palaeocene in the EAR active extension. Some of these faults cut through the sedimentary succession and reach Palaeocene sediments while most faults die within the succession. Fig. 4.20 is a schematic summary of the faults cutting through the Top Turonian unconformity (Fig. A.5).

The deposition of this megasequence is widespread in the basin (Fig. A.6) with a NE-SW strike. It thickens basinwards and to the northeast suggesting

a stronger sediment input from the northeast. Downlap is basinwards to the east and onlap is landwards and northeastwards. This megasequence is generally progradational while aggradation is more apparent in the northeast where sedimentation was more active.

4.6.5 The Palaeocene megasequence.

A few normal faults are mapped on top of the Top Cretaceous unconformity (Fig. 4.21 and Fig. A.7) which die out within the Palaeocene megasequence. At this time listric faulting through slope failure is observed southwest of the basin in the Zambezi Delta half graben (Fig. 4.21). These are shallow angle faults with basinward throws to the east, the direction in which slope failure occured. These faults run through stratal surface which often are former surface of minor erosion and all faults flatten onto the same decollement surface, the Turonian unconformity.

This megasequence was deposited in two depocentres (Fig. A.8), northeast and southwest of the basin. Deposition in the northeast is a widespread area with sediments thickening basinwards into the deeper parts of the basin. In the southwest sedimentation produced a sediment wedge in the deeper part of the half graben with some sediments bypassing down into the basin. Onlap is generally landwards and northeast- and southwestwards with downlap patterns to the east (basinwards).

4.6.6 The Lower and Middle Eocene megasequence.

The timing of the tectonic fault reactivation of basement faults in the northeast is thought to have been during the early stages of deposition of this megasequence. Listric faults mapped on the Top Palaeocene unconformity (Fig. 4.22 and Fig. A.9) cut right through to the Top Turonian unconformity (the common decollement surface) and they die out upwards within the Lower and Middle Eocene megasequence.

If significant deposition was registered during this time period, the following

time of non deposition and erosion (depositional hiatus) will have reworked most of its strata and redeposited it further down in the basin (see Figs. 4.32; 4.31). Sediment preservation for this time period was very low and restricted to the central part of the basin (Fig. A.10). Erosional truncation of this and the previous megasequence is apparent all over the basin.

4.6.7 The Upper Eocene megasequence.

The Upper Eocene unconformity (Fig. A.11) represents a major depositional hiatus and thus a time of sediment reworking in parts of the Zambezi Delta Basin and adjacent areas with sediment redeposition in deeper parts of the basin. Erosion is more accentuated in the northeastern part of the basin where the period of non-deposition persisted well into Oligocene times.

Sedimentation was restricted to the central and southern parts of the basin (Fig. A.12). Sediment preservation is somewhat better in the Upper Eocene than it was in the previous megasequence. Two sediment wedges are mapped advancing southeast- and eastwards in the northeast and southwest respectively.

Erosional truncation is apparent in the southwest, south and northeast. Onlap is to the northwest (landwards) and downlap is basinwards. The southwesterly deposited sediment wedge is part of delatic buildup to the west.

4.6.8 The Oligocene megasequence.

At the end of the Eocene time period a double slope system of subparallel strikes had developed in the southwest with a double slope system advancing eastwards. In the northeast another double slope system is apparent with both slope systems converging in the northeast (Fig. A.13). This might be the sign of the advancing deltaic system from the onshore sector (not covered by seismic data studied here).

The Oligocene megasequence is the first phase of widespread sedimentation in the Zambezi Delta Basin since the deposition of the Palaeocene megasequence (Fig. A.14). Erosion declined in the northeast to allow the deposition of a

sediment wedge lying unconformably onto Palaeocene sediments.

In the southwest, deltaic progradation accelerated and advanced from the west and southwest with a NNE-SSW striking through. Some sdimentation also occurred in the deeper parts of the basin. Downlap is to the east and southeast with onlap to the west and southwest. The deposition of this megasequence is followed by a widespread depositional break, the Top Oligocene unconformity.

4.6.9 The Lower and Middle Miocene megasequence.

This megasequence is the first studied in detail and five parasequence sets are identified as genetically related strata. These five parasequence sets, each one has up to four cycles of deposition, with some degree of depositional break between them. Deposition during this time was widespread through the Zambezi Delta Basin with sediments being laid on top of the Top Oligocene unconformity (Fig. B.1).

During deposition of this megasequence, delta development stabilised in the southwest, where possibly two main sediment sources were active at the same time (Fig. B.2). Deltaic deposition in the northeast was provided by at least two sediment sources, one major in the centre of the basin and another relatively small further northeast.

Sediments from these two sources bypassed the shelf break and were deposited in the deeper part of the basin in the east and northeast. This style of deltaic sedimentation allowed a three slope deltaic system to develop from the time of the deposition of the Oligocene megasequence to the present day. Onlap is generally landwards and to the southwest and northeast with downlap almost basinwards to the southeast.

Depositional unit set B.2 of two depositional units is the first to be deposited on top of the Top Oligocene unconformity (SB07 - Sequence Boundary 07) southwest of the basin. It spreads from the Zambezi River mouth south and eastwards about 200km and striking NE-SW. Onlap patterns are to the northeast with basinwards downlap. Three basinward prograding fronts are mapped during this depositional cycle, one at the Zambezi River mouth and two to the southwest

(Figs. B.). Deposition at this time was restricted to the southwestern part of the basin (the Zambezi Delta half graben).

This set of depositional units comprise an on- and offshore section and it reaches the Save Delta in the southwest. The upper part of B.2 is progradational basinwards and stratal thickness is greater along strike and possibly in the onshore for the two southeasterly delta fans.

The three depositional units of B.3 are all deposited in the northeast (Fig. B.8) suggesting a depositional switch from the southwestern depocentre to the north and northeast. The first unit clearly thickening to the northeast and also prograding northeastwards had sediment sources from the northeast and is a channel valley fill into a channel curved during the last period of non-deposition in this part of the basin.

The following depositional unit (Fig. B.10) is more widespread to the the northeast and southwest along strike and prograding basinwards. Onlap is to the northeast, northwest (landward) and southwest with basinward downlap patterns. The last unit to this parasequence set is deposited in a deltaic fan just north of the Zambezi river mouth (Fig. B.12).

B.4, a set of four depositional units represents a period of steady deltaic development in the Zambezi Delta half graben (southwestern depocentre) while the northeastern depocentre was undergoing a period of non-deposition and errosion (Figs. B.14; B.16; B.18; B.20).

The delta front advanced basinwards about 30-40km in a delta progradational fashion to the southeast. Onlap is landwards to the northwest and southwest and northeast with downlap basinwards.

Depositional unit set B.5 (Appendix B.5) is made of two distinct depositional units, one deposited to the northeast and the second widespread in the east and southwest of the basin (Figs. B.22; 24, respectively). First deposition was in the northern depocentre and migrated with time to the southern depocentre, allowing erosion to take place in the northern depocentre. Erosional truncation is evident during the time of non-deposition in both depositional units. Onlap is landwards and downlap is basinwards to the southeast, the direction of stratal

progradation.

At the end of deposition of megasequence MSEQ-07, B.6, a set of one depositional units was deposited in the northeastern depocentre. This is a channel fill and sediment bypass into the basin and was deposited in fan deltas (Fig. B.26). Onlap is to the northwest and south with downlap basinwards to the east. The deposition of this unit is followed by a depositional hiatus, the Top Middle Miocene unconformity.

During deposition of the Lower and Middle Miocene megasequence three widespread hiatuses are mapped in the Zambezi Delta basin. Sedimentation is recorded in the southwestern depocentre in between the hiatuses while in the northeastern depocentre no sedimentation is recorded between the second and third depositional hiatuses, thus signaling a much longer period of non-deposition at this time in this part of the basin.

Channel deposition at this time is scarse in the area covered by seismic data, but some suggetion can be made for possible deep water fan deposition from the northeastern channel as sediment bypass might have been active during the deposition of this megasequence.

4.6.10 The Upper Miocene megasequence.

The isochron of the Top Middle Miocene unconformity (Fig. C.1) shows basin position at the time prior to the deposition of the Upper Miocene megasequence. The picture of double slope basin is still present but the upermost northeast and southwesterly slopes are now linked forming a concave delta front advancing to the basin offshore. This picture also shows sites of possible sediment source location at the present day Zambezi delta river mouth and two more locations to the north.

The isopach for this megasequence (Fig. C.2) confirms the three locations above as the main sediment suply conduits during deposition of the Upper Miocene megasequence. It is a deltaic depositional unit set of progradational strata towards the basin in several depositional cycles. Twenty four depositional units are mapped and grouped according to their genetic relationships in 10 sets

of depositional units described below.

The Top Middle Miocene unconformity is followed by a period of restricted deposition in the northeast in form of distributary channel and channel valley fill for quite some time. This episode allowed the deposition of depositional unit sets C.2, C.3 and C.4 while sedimentation was shutt of in the southern depocentre. This period of deposition in the northeastern depocentre itself did not produce significant strata in the depocentre but might have been an important period for sediment bypass into deeper parts of the basin (submarine fan deltaic deposition), to be tested in the future by deep water exploration work.

The deposition of C4, a depositional unit set of one depositional unit (C4:1), marked the return to activity of a sediment source north of the Zambezi River mouth (Fig. C.18) which was active before during deposition of the Lower and Middle Miocene megasequence. This depositional unit is a fan delta deposited in the northeastern depocentre after a possibly shortlived period of non-deposition in the Zambezi Delta Basin (Fig. 4.31).

The depositional unit set C5 of four depositional units (C5:4), is deposited from a channel in the northeast in four depositional cycles each migrating southwestwards. By the end of the deposition of this depositional unit set the channel had migrated about 80 km to the southwest with sedimentation spread over a distance of about 220 km in the same direction (Figs. C.20; C.22; C.24; C26). Downlap is east- and southeastwards with west- and southwestwards onlap. The deposition of depositional unit C5 is followed by a period of non-deposition in the basin, a depositional hiatus (see Fig.4.32).

Following the hiatus at the end of deposition of depositional unit set C5, sedimentation switched back to the northeastern depocentre where unit C6 was deposited in three depositional cycles.

The first depositional cycle only produced a small patch NE-SW elongated (Fig. C.28) followed by two widespread depositional units of delta fan deposition advancing basinwards more than 100km in some places (Figs. C.30; C.32, respectively). Onlap is landwards and southwestwards with basinwards downlap in direction of delta progradation. This perod of deposition cincided with

non-deposition in the southwestern depocentre.

The next depositional period begins with the deposition in the central part of the basin where deposition of the previous depositional units set had stopped. At this time, two depositional cycles are registered with sediments supplied from two locations, one in the northern depocentre and the other in the southern depocentre (Figs. C.34; C.36, respectively). This produced two delta fans prograding into the depocentres and interfering in the central part of the basin. Downlap is basinwards with onlap to the northeast and southwest.

The depositional unit set C8 of one depositional unit is a channel fill in the northeast possibly feeding deeper parts of the basin (Fig. C.38) not covered by seismic data studied in this work.

After some hiatus in the southeastern depocentre, sedimentation returned, with depositional unit set C9 of three depositional units. The sediment source for this depositional unit set is close to the present day Zambezi River mouth. Earliest sedimentation was in the central and deeper parts of the basin and then migrated southwards in the late stages (Figs. C.40; C.42; C.44, respectively). Onlap is to the northwest (landwards) and northeast and southwest with basinwards downlap. Most of this depositional unit set is deposited in a deep water delta fan in the central and southern parts of the basin.

Sedimentation continued in the southern depocentre with the depositon of the last depositional unit set C10 of three depositional units. Deposition recommenced where it had stopped during deposition of depositional unit set C9 and prograded basinwards with the shelf break striking NE-SW during deposition of depositional unit C10:3-1 (the first depositional unit of depositional unit set C10) (Fig. C.46).

The following depositional unit is more widespread and retrogadational with possible sediment sources from the northwest and southeast (Fig. C.48). sedimentation ends with the deposition of a southerly spreading delta fan striking NE-SW (Fig. C.50) which is followed by the Upper Miocene unconformity. Onlap is to the northwest (landwards) and downlap is basinwards to the southeast for all depositional units in this depositional unit set.

Within the Upper Miocene megasequence three depositional hiatuses are identified and mapped across the whole Zambezi Delata Basin. These are important switches in sedimentation from one depocentre to the other, with marked erosional patterns at sites where non-sedimentation occurs. Most of the channel structures during this depositional period are in the northeastern depocentre.

4.6.11 The Pliocene megasequence.

Upper Miocene strata were exposed during a period of non-deposition and erosion which caused the Top Miocene (Top upper Miocene) unconformity to develop (Fig. 4.32). The isochron map of the Top Miocene (Fig. D.1) shows basin position and architecture at the time prior to the deposition of the Pliocene megasequence. The two slope system is still apparent with the upper slope almost consolidated (Fig. D.1).

Sediment input during deposition of the Pliocene megasequence (Fig. D.2) is mainly through the source located close to the Zambezi River mouth with some point sources in times in the northeast. Sediment progradation basinwards is apparent with a NE-SW strike. This megasequence is made of twenty nine depositional units mapped here most of which are deposited in the northeastern part of the zambezi Delta basin. The Pliocene isopach shows little sedimentation in the southwestern part of the basin for this period.

The depositiona units set D1 of two depositional units (Fig. D.4) is the first sediment set deposited after the Upper Miocene unconformity. The first unit (Fig. D.4) is a delta fan deposited northeast of the Zambezi mouth feed by a point source. The second unit is deposited in the same area and it extends northeastwards (Fig. D.6). Sediments for the second depositional unit are from two sources, all in the northeastern part of the basin. Onlap is to the northwest with downlap basinwards to the southeast.

The deposition of depositional unit set D2 started in the northeast moving down to the southwest through a point source located in the north. This depositional unit comprise four depositional units. The first two are both fans deposited in the northeast, southwards (Figs. D.8; D.10) with onlap to the north

and northwest and downlap to the south and southeast.

Depositional unit three is also deposited in the northeast by the same sediment source and spreads southwards (Fig. D.12). A second source is active in the southern part just north of the Zambezi mouth at this time. It is the most significant unit of this depositional unit set and sets the strike of the shelf break to the usual NE-SW as observed before. Onlap is to the northwest and downlap is to the east and southeast.

The closing depositional unit is a small delta fan deposited in the northern part covered by this depositional unit set (Fig. D.14).

The depositional unit set D3 of two depositional units is a delta fan deposited in the central part of the basin by a single sediment source. It represents a southwards migration of the sediment source through geologic time. Sediments of this depositional unit set bypassed older strata through a channel and are deposited further down in the basin. Onlap is northwest (landwards) and northeast and southwest with basinward downlap pattern to the southeast.

Sedimentation switched back to the northeast for the deposition of depositional unit set D4 in two depositional cycles. Southeastwards progradation produced a sediment wedge extending into the deeper basin. The sediment source migrated south to deposit the second depositional unit (Fig. D.22) in the central part of the Zambezi Delta Basin. Onlap is to the north, northwest and west with downlap to the east and southeast.

Following the deposition of D4, is depositional unit set D5, also deposited in the northern depocentre and spreading some 250 km to the southwest. It is deposited in two cycles, the first one covering a small area in the northeast with the second cycle over-running the first one several 200 km (Figs. D.24; D.26). The source for both depositional units is from the northeast resulting in the onlap being north northwest and the downlap pattern to the east and southeast.

The depositional unit set D6 is also deposited in the northeastern depocentre in four depositional cycles. Depositional unit one (Fig. D.28) of this depositional unit is deposited southwards and south of the area where the subsequent three units lie southeastwards, successively on top of each other (Figs. D.30; D.32;

D.34). Onlap is to the southeast and northwest and downlap to the southwest for the first depositional unit. For the three following depositional units onlap is to the west and southwest while downlap points to the southeast.

Deposition continued in the northeastern depocentre and depositional units set D7 of two depositional units, riching the southwestern depocentre during the deposition of the second unit. The deposition of this depositional unit set marked the begining of the switch to the southwestern depocentre which has been starved for some time, since depositional unit set D5 was deposited.

The first depositional unit is a delta fan lies in the northeastern depocentre (Fig. D.36). Onlap is to the northwest, southwest and northeast with downlap to the southeast (basinward). The second depositional unit is layd southwestwards with sediments coming from various sources and includes sediments from the Save River system (Fig. D.38). For the second depositional unit onlap is to the northwest and downlap is to the southeast (basinwards).

Progradation initiated during deposition of the second depositional unit of depositional unit set D7, continued during deposition of depositional unit set D8 in three depositional cycles accross the two depocentres. Sediments at this time are from a source in the northeast. Onlap is to the northwest and downlap to the southeast for the first and second depositional units (Figs. D.40; D.42). The third cycle switched sedimentation back to the northeast where a prograding delta fan is produced. Onlap is to the northeast and northwest with downlap to the southeast.

The depositional unit set D9 deposited after D8 in the northeast is made of three depositional units. They are all delta fans deposited from the same sediment source and lie on top of each other and prograde to the southeast (Figs. D.46; D.48; D.50). Onlap is to the east and west with downlap to the southeast.

Sedimentation continued in the northern depocentre during deposition of depositional unit set D10 in three depositional cycles of deltaic prograding units. A deltaic fan is first deposited in the northern depocentre extending basinwards to the southeast where it downlaps onto older strata with onlap to the northwest, northeast and southeast (Fig. D.52).

Two sources are active at this time. After a depositional break, sedimentation restarted in the northeastern depocentre with two active sediment sources which produced a delta fan in the northeastern depocentre and a basinwards prograding sediment wedge in the southwestern depocentre, thus marking the return of sedimentation to the Zambezi Delta half graben after a considerable time of depositional cessation (Fig. D.52). Onlap is to the northwest (landwards) with downlap to the southeast (basinwards).

The closing stages of deposition of the Pliocene megasequence is characterised by a slow down in sedimentation (see section below on subsidence history). Depositional unit set D11 lies in the northeastern depocentre, in two subsequent depositional cycles. The first cycle produced a deltaic fan in the northeastern depocentre followed by a second smaller delta fan deposited regressively on top of the first one. These two events formed the last depositional unit set of the Pliocene megasequence. Following this event is the Top Tertiary unconformity.

Pliocene sedimentation is characterized by deltaic fan deposition in the northeastern depocentre and widespread periods of non-deposition (depositional hiatus) in the central and southwestern parts of the Zambezi Delta Basin, with only ocasional widespread sedimentation in both depocentres. Three depositional hiatuses are mapped during deposition of the Pliocene megasequence in the whole basin. Periods of deltaic progradation are often distinct in the two depocentres during this depositional period.

4.6.12 The Quaternary succession.

The time isochron map for the Top Tertiary unconformity (Fig. E.1) displays a well established single shelf break for the first time in the depositional history of the Zambezi Delta Basin. It strikes NE-SW and two channel valleys are the most notable topographic features in the northeast.

Quaternary sedimentation in the offshore part of the Zambezi Delta Basin is marked by continued delta progradation after a possibly short period of non-sedimentation (Top Tertiary unconformity). Two depocentres are active during deposition of the Quaternary succession (Fig. E.2), the southwestern depocentre

and the northeastern depocentre, both prograding basinwards. Onlap is landwards, northeast and southeast with basinwards downlap.

Synrift sedimentation and sediment bypass through the channel valleys (Figs. E.1; E.2; E.3) occurred in the northeastern depocentre with accelerated basin subsidence facilitating the opening of sediment bypass channels down into the deeper sector of the basin.

Faults in this part of the basin, the northeastern sector of the EAR active graben system, were reactivated after the Quaternary unconformity and are still causing the basin to subside at the present time. Two major channel valleys are mapped on some strike lines and they are clearly the result of basin subsidence. This interpretation is supported by seismological data which report some strong seismic events of up to 5.5 body wave magnitude in the same area (Fig. 4.23).

4.7 Rms-velocity and depth conversion.

Seismic velocity in clastic sediments is a function of depth due to increasing sediment compaction caused by increasing pressure with depth. It also varies laterally, although perhaps more subtley, with changing facies. The best-documented velocity variation is the variation with depth but several attempts have been made to date with the aim of improving the vertical and lateral velocity functions used in depth conversion of seismic data and in seismic facies analysis (Al-Chalabi, 1974; 1979; Davies, 1990, Schneider *et al.,* 1994).

Davis (1990) classified the various velocity fields used in depth conversionof seismic time section as: the constant average velocity, the constant interval velocity, the average time-depth velocity curve, the average velocity functions and the velocity functions with varying parameters. All these velocity types were defined to account for different aspects influencing seismic velocity in rocks and all pursuing the same goal of providing better velocity functions for describing vertical and lateral lithology variations.

Velocities commonly available for depth conversion are the rms-velocities

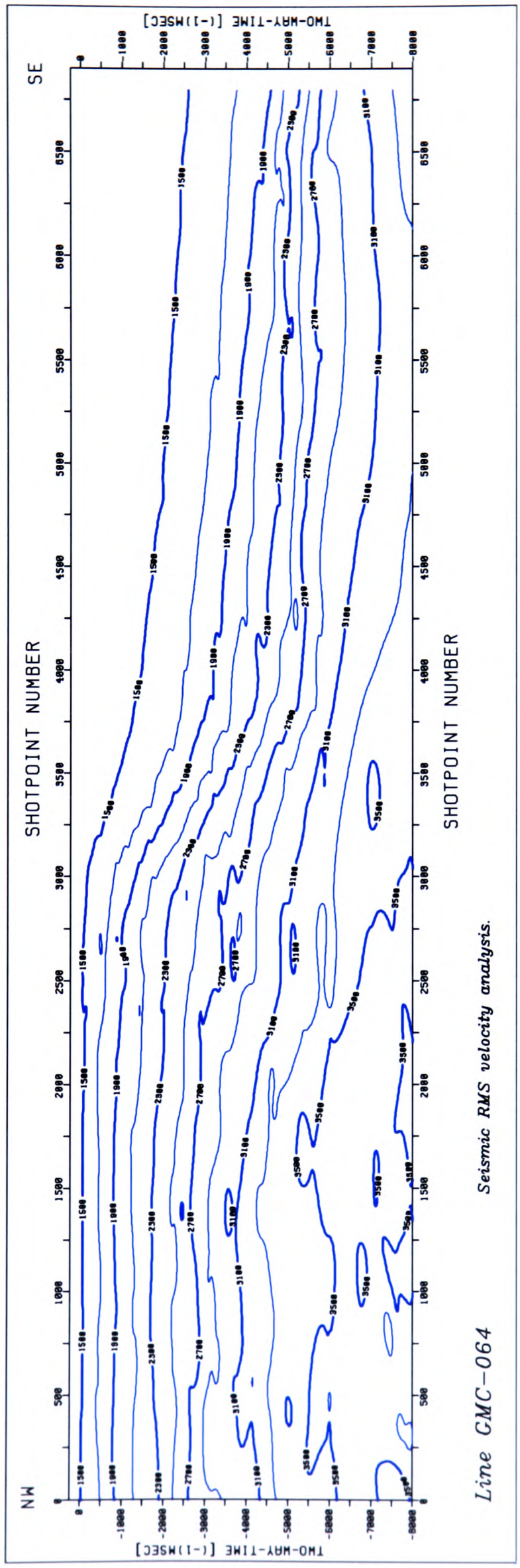

Figure 4.33: Rms velocity contour map of line GMC-064. Contour interval 200 m/sec from 1500 m/s at the sea floor.

(stacking velocities), CDP (common depth point) velocities, the check shot velocities and the sonic velocities. Each of these velocity types represents a different degree of accuracy in velocity determination and have different physical meaning.

In seismic data processing the gross velocity distribution in the ground from CDP reflexion data depends primarily on the determination of the velocity producing maximum coherency in the stacked seismic data. While interval and average velocities describe meaningful physical parameters and are related to the maximum coherency stacking velocity through the rms-velocity, the stacking velocity itself is a mathematical quantity with no physical significance (Al-Chalabi, 1974; 1979; Davies, 1990). Generally the velocities derived with this method can be used only for qualitative seismic data evaluation, but they would generally result in wrong depth estimates if applied in depth conversion with no further corrections. Rms-velocities are a first approximation to the maximum coherency stacking (MCS) velocities and can be up to 12 or even 15% smaller than the actual formation velocity (Al-Chalabi, 1974; 1979). They are also sensitive to the direction in which profiles are shot.

Observations made in this study on rms-velocity anisotropy generally show higher velocities in the dip direction at track crossovers, actual values perhaps depending on lithology. Observed velocity differences between dip and strike are between 1.3 and 14.2%. These velocity differences between dip and strike would require calibration with more reliable velocity data (i.e. check shot velocity data not available to this study) and some processing to remove velocity at crossover points. CDP derived velocities, for example, are subject to numerous errors, some of which are generated during the acquisition and processing stages and during the wave propagation in the ground, while others arise from geological complexities in ground. In poorly explored areas however, very often the only source of velocity information is the stacking velocity, sometimes aided by sonic velocity if any wells exist in the area.

The only velocity available to this study is the rms-velocity displayed on top of the seismic sections which varies both laterally and as a function of depth.

Table 4.1: Summary of calculated rms-interval velocity values and of velocity derived geologic interval average densities for the Zambezi Delta Basin.

Velocity and density data summary

Geologic interval	Parameter	Along dip	Along strike	Difference [%]	Average
Quaternary	Velocity [m/s]	1854.8	1712.7	8.30	1783.8
	Density [kg/cm^3]	**2026**	**1994**	**1.60**	**2010**
Pliocene	Velocity [m/s]	2409.2	2147.0	12.21	2278.1
	Density [kg/cm^3]	**2163**	**2109**	**2.56**	**2136**
Upper Miocene	Velocity [m/s]	2828.9	2484.0	13.88	2656.5
	Density [kg/cm^3]	**2249**	**2184**	**2.97**	**2216.5**
Lower and Middle Miocene	Velocity [m/s]	3139.7	2880.9	8.98	3010.3
	Density [kg/cm^3]	**2309**	**2267**	**1.85**	**2288**
Oligocene	Velocity [m/s]	3689.8	3317.4	11.23	3503.6
	Density [kg/cm^3]	**2396**	**2342**	**2.31**	**2369**
Upper Eocene	Velocity [m/s]	3923.6	3602.3	8.92	3763.0
	Density [kg/cm^3]	**2430**	**2387**	**1.80**	**2408**
Lower and Middle Eocene	Velocity [m/s]	4325.8	3787.2	14.22	4056.5
	Density [kg/cm^3]	**2478**	**2417**	**2.52**	**2447**
Palaeocene	Velocity [m/s]	4059.4	3805.6	6.67	3932.5
	Density [kg/cm^3]	**2454**	**2422**	**1.32**	**2438**
Senonian	Velocity [m/s]	4320.9	3959.1	9.14	4140.0
	Density [kg/cm^3]	**2496**	**2454**	**1.71**	**2475**
Turonian	Velocity [m/s]	4882.4	4324.6	12.90	4603.5
	Density [kg/cm^3]	**2554**	**2506**	**1.92**	**2530**
Karoo - Cenomanian	Velocity [m/s]	4266.9	-	-	4266.9
	Density [kg/cm^3]	**2494**	-	-	**2494**

The rms-velocity function generally shows a steady increase with depth but its quality worsens as depth increases (Fig. 4.33). Fig. 4.33 is a typical rms-velocity profile of the study area in the dip direction. No check shot velocities were available to the study and the sonic log is only available for a few wells and is very often not continuously recorded.

Some corrections would have to be applied to bring the velocity values closer to the actual velocity values of the stratal units involved. The latter could be

achieved by using the check shot velocity functions from wells within the study area (not available here) or from wells in adjacent areas to calibrate the stacking velocities. No time was left in this study to proceed with this extra step in velocity processing and instead all interpretation is carryed out in time domain.

However, the density for the stratal units (megasequences) studied are calculated from the rms-average velocities calculated for each unit using the empirical equation known as the Gardner's equation (Gardner *et al.* 1974) as follow;

$$\rho = av^{\frac{1}{4}}, \tag{4.1}$$

where ρ is the density in g/cm^3, v the rms-average velocity in m/s and a the empirical factor set to $a = 0.23$ for porous rocks (Dobrin *et al.*, 1988). The densities calculated in this way using rms-interval velocities are smaller than the actual stratal densities for the same reasons discussed before. The density values calculated with above equation for the geological intervals studied here are summarized in Tab. 4.1. These density values are used in Chap. 4 in gravity modelling of a Free-Air profile across the Zambezi Delta Basin.

4.8 Relative sea level changes in the southeastern African region.

Two cross-sections in dip and strike are produced showing sediment distribution throughout basin history (Figs. 4.34; 4.35). A curve of relative change of coastal onlap is also produced and displayed on Fig. 4.34 for the time period from Late Carboniferous to Recent times. This curve, which shows more detail for the last 23.7my (from Top Oligocene) before present is characterized by various periods of transgression and regression which shifted sedimentation landward and basinward, respectively. However, most notable in this curve is a period of sea level lowstand starting in late Middle Miocene and lasting well into Upper Miocene with sedimentation confined at some tributaries in the northeastern part

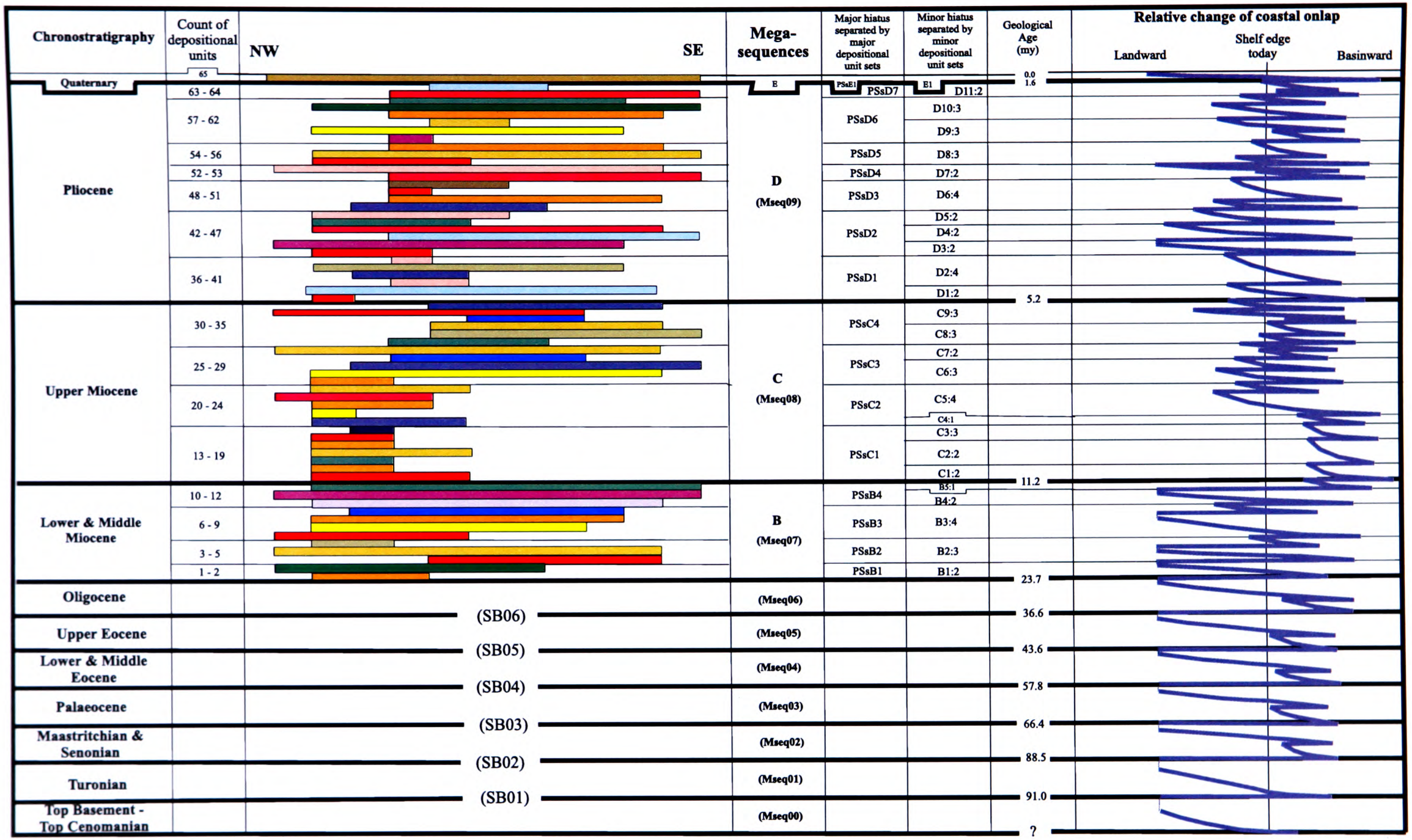

Figure 4.34: Chronostratigraphic diagram in the dip direction offshore the Zambezi Delta basin, summarizing depositional units derived from seismic interpretation. Colour bars express relative lateral extent of depositional units along the NW-SE direction where the colour fill does not bear any geological meaning.

of the basin with possible deposition of lowstand fans in the deeper parts of the basin (not covered by data used in this study) during this time period.

Sea level remains generally high throughout the time period of deltaic deposition in the basin with some high order cyclicity recorded in the upper part of the stratigraphic section.

The global sea level chart produced by Vail *et al.*, (1977a) and later modified by Haq *et al.*, (1988) is not adequate for use in all sedimentary basins bearing marine sediments in the various settings on earth's continental margins (Miall, 1997). Sea level changes are one of the main controls on sedimentation but its interplay with other factors like climate, tectonic movements, sediment supply and accommodation space is another important factor to be observed in the study of marginal basins. On the other hand, tectonic movements alone can under certain circunstances produce sedimentation styles which previously were atributed only to sea level variations.

Any comparison to the global sea level chart from Vail *et al.* (1977a), Haq *et al.* (1988) and others versions should be attempted only for first order cycles which are more likely to be of global extent while in any comparison to second or third order cycles more care should be taken and regional and local tectonics should be accounted for in the analyses.

The chronostratigrahic diagram on Fig. 4.35 emphasizes the gaps in the stratigraphic record and displays along-strike variability recorded in the basin during the time period from Miocene to the present time. This period of progradational and aggradational deposition is clearly characterized by channel sedimentation and channel switch from northeast to the southwest and vice versa.

Channel deposition is generally observed during sea level lowstand, and the early stages of sea level rise lead to filling the channel valleys produced on the exposed delta top and delta front. These periods of sedimentation in the basin are very important as they might hold clues to sediment reworking on the exposed delta areas and redeposition in fan systems in the deeper parts of the basin. They are also important as they hold clues about sediment bypass during lowstand

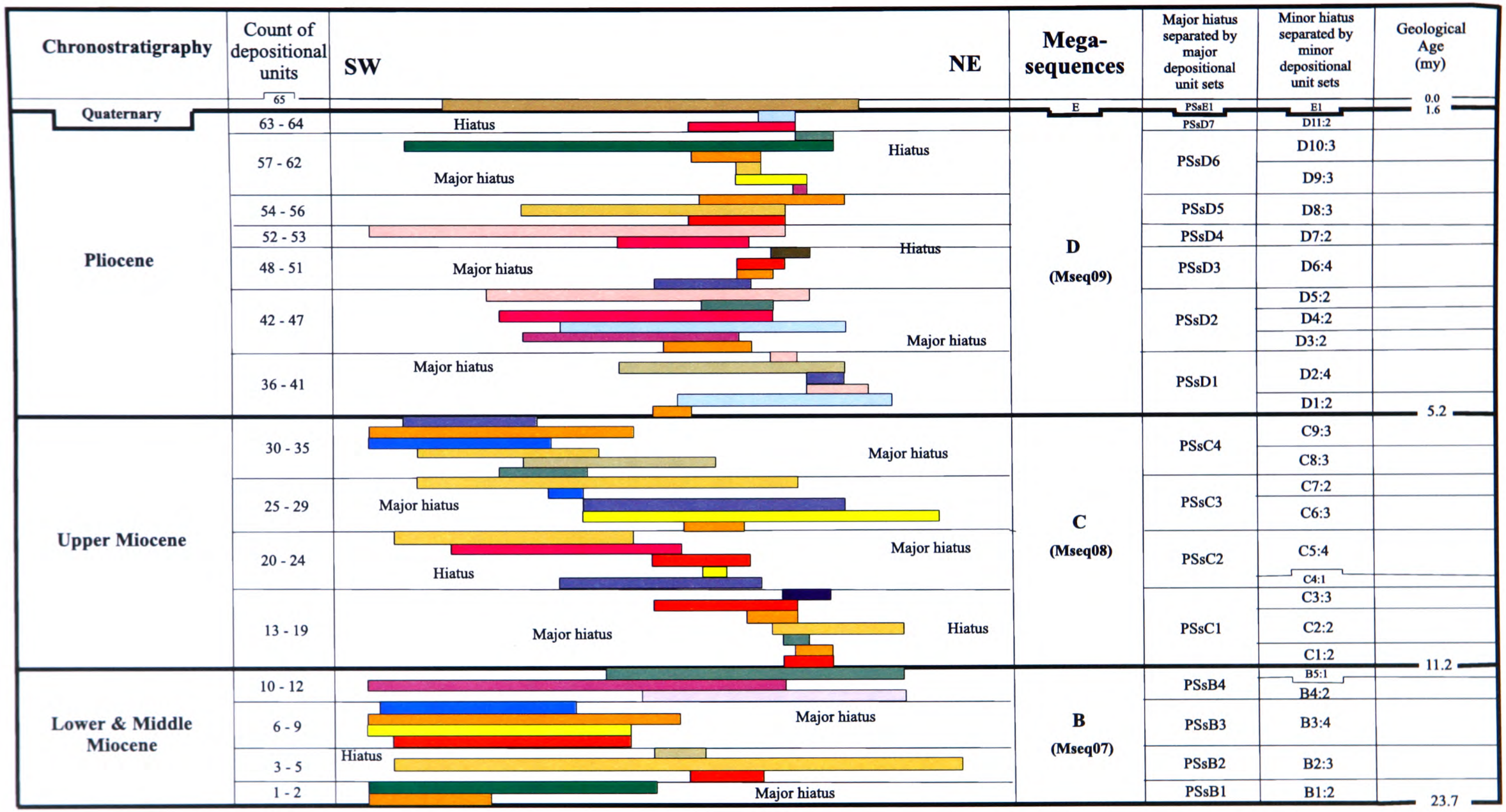

Figure 4.35: Chronostratigraphic diagram in the strike direction offshore the Zambezi Delta basin, drawn in a way to emphasize the depositional hiatuses and the along-strike vaiability during Neogene times. Colour bars express relative lateral extent of depositional units along the SW-NE direction where the colour fill does not bear any geological meaning.

into deeper areas where lowstand fans might have been deposited and therefore stratigraphic traps created.

4.9 Summary and discussion of results.

Analyses of seismic and well log data, has enabled an improved seismic stratigraphic model of late Cretaceous and Tertiary evolution of the Zambezi Delta Basin to be made, which allows for a better understanding of the depositional setting of the basin. The results demonstrate that the Zambezi Delta Basin is one of a number of major sedimentary depocentres situated along the southeastern African continental margin. It is situated in central Mozambique at the present day Zambezi River mouth and it extends from onshore to the offshore in a WNW-ESE direction into the waters of the Mozambique Channel over an estimated area of about 290,000 square kilometres both on- and offshore extending to the 500m isobath.

Approximately 21,700km of seismic data and logs from nine wells are used to re-evaluate the sedimentary and geotectonic history of the Zambezi Delta Basin, offshore sector. Seismic stratigraphic methods applied to the seismic data, allow a detailed basin seismic stratigraphy and a basin development model to be constructed. Sedimentation during Tertiary and Quaternary deltaic buildout in the Zambezi Delta Basin is interpreted here as alternating between two main depocentres both of which are structurally controlled.

Sedimentation switched along a NE-SW strike from one depocentre to the other with times of widespread basin sedimentation. The Zambezi Delta half graben to the southwest and striking NE-SW is bounded to the southeast by the Beira basement uplift, and the East African Rift active extension to the northeast, which is an active graben structure striking E-W, is also bounded to the south by the northeastern flank of the Beira basement high. Interpretation of seismic data in this work shows that there is strong evidence for marked along-strike variability throughout Cenozoic time. Deltaic sedimentation across the basin switched from one depocentre to the other via distributary channel switch.

However major depositional switches may be related to sediment supply switches caused and controlled by tectonics and climat affecting the source rock area in the hinterland (upper and middle Zambezi hydrographic basin) throughout geologic time.

Of particular importance is along-strike variability during deltaic buildout indicating the role of the interplay between sediment supply, sediment source location and the evolution of accommodation space (basin subsidence) in controlling palaeo-geography in the basin at various stages of basin development.

Strike variability as mapped in the Zambezi Delta Basin in this work has a potential not only to impact upon existing sequence stratigraphic models for deltaic settings but also on the existing interpretation methods, for example the interpretation of depositional sequences and "system tracts".

It is shown that several periods of non-deposition and erosion (hiatus) are recorded across the basin, some of which are restricted to parts of the basin while others are widespread in the basin (regional unconformities). Generally periods of sedimentation in one depocentre mean a period of non-deposition and erosion in the other depocentre with sediment bypass and reworking and redeposition in deeper parts of the basin (not covered by seismic data used in this study). Moreover, sedimentation is controlled by onshore tectonics influencing sediment sources with tectonics, eustatic sea level variations, and sediment load controlling basin subsidence and accommodation space in the basin offshore.

At the beginning of major depositional cycles, sedimentation generally starts in channels and then becomes widespread in the depocentres and at times reaching the whole basin. Depositional unit sets PSsB2 and PSsB4 (see Fig. 4.35) deposited in Lower and Middle Miocene, PSsC3 deposited in Upper Miocene, PSsD2 and PSsD4 and PSsD6 deposited during Pliocene times are examples of this this type of deltaic sedimentation. Depositional unit sets PSsB2, PSsB4, PSsD2 and PSsD4 area deposited during major transgressive cycles characterized by landward onlap onto older strata caused by sea level rise (Fig. 4.34). However, depositional unit sets PSsC3 and PSsD6 are basinward regressive characterized by basinward prograding wedges with some significant stratal aggrada-

tion. These two depositional styles show the variation through geological time of the rate of rate of basin subsidence and sea level change to sediment supply to the basin. A relative balance is achieved when stratal aggradation is more apparent, whilst rapid . Lithofacies relationships are very complex in the basin due to the sedimentary architecture produced by the interplay between sea level variation, tectonic and sediment supply. This complexity rendered the attempt to produce a lithofacies correlation through the well connecting profiles an inconclusive task.

Subsidence analyses confirm observations made on seismic data on the interference of sediments from the Save River Delta with those from the Zambezi Delta. Subsidence curves reveal a common character for the wells Sangussi Marine-1, Sengo Marine-1, Zambezi-1, Zambezi-3, Micaune and Nhanguazi-1 during Tertiary deltaic development in the Zambezi Delta Basin. However the amount of basin subsidence observed is variable for each well. This might be explained by the wells geographic position in relation to the main tectonic events onshore which determined source position relative to the basin. This also will have determined the sediment supply routes, the amount of sediments supplied to those location as well as the amount of time these locations were exposed to erosion during depositional hiatuses. For the wells Sofala-1, Nemo-1 and Divinhe-1 to the southwest, a different picture emerges from the subsidence analyses, probably suggesting a different dominant deltaic setting for the stratigraphy of these wells.

Chapter 5

Interpretation of gravity and magnetic data.

This chapter is to assist in investigating and modelling deep geologic structures and in estimating the depth to geologic basement at depths not penetrated by seismic and well data discussed in chapter 4. The results achieved in this chapter aid development of a basin model and allow a better appreciation of basin dynamics as suggested by subsidence data. Several magnetic profiles are used to estimate depth to magnetic basement at different sites in the basin. In addition, a gravity profile running accross the basin is modelled.

5.1 Introduction.

Gravity and magnetic surveying in oil prospecting are generally employed as reconnaissance methods for locating major geologic features and structural boundaries in geologically less well-known areas, before more detailed studies are undertaken using more powerful and accurate surveying methods like seismic methods and well drilling, sampling and logging. The latter methods are now very well developed in both data acquisition and processing and allow very detailed and accurate mapping and structural definition, but they are the most expensive

of all methods in exploration. Generally only sources of gravity and magnetic anomalies within the upper crust of the earth are of interest when it comes to mineral and hydrocarbons exploration. But more recently there has been an appreciation of what gravity can reveal about basin dynamics that may explain stratigraphic patterns (Allen and Allen, 1992).

Gravity and magnetics are two potential methods which exploit the earth's gravitational field and the earth's magnetic field respectively. Commonly used gravity anomalies are the Bouguer anomaly, the Free-Air anomaly and the Isostatic anomaly. These anomalies relate to three different aspects of gravity and they are important for studying crustal behaviour in response to tectonics and sediment load (Free-Air anomaly and the Isostatic anomaly) as well as for mapping and studying the influence on the gravity field of mass inhomogeneities within the earth crust caused by density differences (the Bouguer anomaly). While the Free-Air anomaly is more used in structural modelling, the Bouguer anomaly is more widely applied in the mapping of major geological features and in mineral exploration and engineering geophysical exploration (Militzer and Weber, 1984; Militzer *et al.*, 1986). Important, however, for gravity anomalies to be observed, is a reasonable density difference between adjacent geologic structures, the structures size and relative depth of burial.

In this study three anomaly maps of the study area were used, the Free-Air and the Bouguer anomaly maps and the total field magnetic anomaly map. An attempt was made to calculate and map gravity and magnetic derivatives in order to exploit their anomalous characteristics at structural boundaries but they were found unusable due to the poor quality of the anomaly data used to derive them. The Free-Air and the Bouguer anomaly maps and the magnetic map were interpreted and two-dimensional anomalies were modelled (sections 5.4, 5.5 and 5.6).

Generally the main objective of gravity and magnetic surveys is to determine the spatial distribution of density and susceptibility within the upper portion of the earth crust. This task cannot be accomplished by the use of gravity or magnetic surveying techniques above. It requires the use of additional geological

and/or geophysical information to overcome what is widely known as the non-uniqueness of gravity and magnetic interpretations (Militzer and Weber, 1984; Dobrin and Savit, 1988; Telford Geldart and Sheriff, 1990).

Non-uniqueness follows from the very basics of the potential field theory much discussed in the literature (Skeels, 1947 and Militzer and Weber, 1984) which means that a single gravity or magnetic anomaly can be modelled for a large number of geologic bodies of varying geometries and density or susceptibility contrast to the host rock at different depth of burial. This makes it impossible to determine the exact shape and depth of burial of the geologic structure causing the anomaly for chosen density or susceptibility contrast without the use of additional geological and geophysical information. Both the size and the depth of burial of the geologic structure are parameters of prime interest in exploration.

The aim of this chapter is to study gravity and magnetic anomalies in and around the Zambezi Delta Basin and derive their relevance to the structural development of the basin. Profiles derived from gravity and magnetic maps are used to performe depth estimates to structural features and a Free-Air gravity profile is modeled constrained by some results from chapter 3.

5.2 Methodology.

Gravity and magnetic data were supplied by GETECH at Leeds University in ASCII file format containing regular grids of 5x5' for gravity and 1x1km for magnetic data. These data were gridded and contoured at suitable contour intervals (20 mGal for gravity anomaly maps and 50 nT for the magnetic anomaly map) for the purpose of this work. Subsequently, second derivative maps were constructed so as to exploit their potential in highlighting geologic boundaries. The results of second derivative maps of both gravity and magnetic data were found to be of very poor quality and are not discussed further in this work. Profiles across the Zambezi Delta Basin were derived from gravity and magnetic anomaly maps and are discussed later in this chapter.

Six Airy isostatic models were also calculated to compare with each other

and with published work assuming a constant crustal thickness for isostatic equilibrium at the coast line and by maintaining the local isostatic equilibrium conditions for both on- and offshore. This was achieved by using the concept of continental, transitional or standard crust and oceanic crust as outlined by Worzel and Shurbet (1955) and Worzel (1974). This concept allowed the definition of three different geological models for the study area each with two special cases concerning the density of the geology above sea level. These models were however found to physically represent only two distinctive cases (see section 5.5.1). These models gave a first approximation to crustal thickness variation throughout the study area under the assumption that the area is in local Airy isostatic equilibrium. In turn, this also provided the first estimate of the depth to the Moho which is used in section 5.6.3 to constrain the gravity model.

The gravity anomalies are used to study large-scale crustal structure and a gravity profile across the Zambezi Delta Basin is modelled in section 5.6.3. Results from Chapter 4 are used to constrain estimates of depth to geological boundaries in a 2D gravity model of the profile in section 5.6.3. The modelled profile runs NW-SE through the well Nhamura-1 across the Zambezi Delta depression (Zambezi Delta half graben) and over the Beira basement uplift in the south-east. In addition, depth to magnetic basement estimates were made on several 2D magnetic profiles across chosen magnetic anomalies using the empirical slope and half slope rules.

5.3 Controls on models.

As a first approximation to crustal thickness variations along the 2D profile across the Zambezi Delta Basin (for location see Fig. 1.1) an Airy isostatic model was constructed. A crustal thickness at the coastline of 27.5km was assumed, based on information published in the literature (Worzel, 1974; Stuart and Zengeni 1987; Qiu *et al.,* 1996). The densities used for water, crust and upper mantle were 1.03, 2.85 and 3.33 g/cm^3 respectively. These were based on density values published in the literature (Worzel, 1974). Initially no account was

taken of the presence of sedimentary layers at the top of the crust that would affect isostatic balance. Subsequently, sediment load and associated compensation at the Moho were introduced.

Evidence from the deeper part of the GECO seismic data (Chap. 3) suggest small vertical displacement at basement fault-blocks. Therefore in the models the main constrain on intra basin prism boundaries is basin subsidence and crustal stretching at the time of Gondwana breakup. The multi-phase tectonic history (section 1.1) certainly caused crustal thinning at the present location of the Zambezi Delta depression, continuing until Late Cretaceous times, which is represented by the deepest reflectors on the seismic profiles.

The depth of the basement surface along the modelled profile was defined in the northwest by using the depth to basement obtained from the Nhamura-1 well, which bottomed in the crystalline basement of Precambrian age. At the southeast end, the depth to the basement obtained from seismic data offshore in the area of the Beira uplift was used. The surface of the sediment layers of the model were derived from seismic interpretation undertaken in this study and discussed in Chap. 4 and from published information (Mascle *et al.*, 1987). The layer of volcanics was inferred from the literature (Salman *et al.*, 1985) and represents the assumed time line (Late Cretaceous) equivalent to the end of the phase of crustal stretching.

The density values for the two upper sediment layers of the model were derived from seismic velocities (rms-velocities) of the GECO seismic survey using the velocity-density relationship of Gardner *et al.*, (1974), while the density for the Karoo sediments layer was derived using the density-depth relationship often discussed in the literature (Dobrin and Savit, 1988). The densities for post-rift volcanics was also derived from the literature (Worzel, 1974; Stuart and Zengeni, 1987; Qiu *et al.*, 1996).

5.4 Interpretation of gravity anomaly maps.

In this study, maps of the Free-Air and the Bouguer anomalies were used.

These anomalies represent different aspects of gravity and differ in their use in exploration. The Free-Air gravity anomaly is the most-used anomaly in offshore exploration because it allows the use of fewest assumptions in data processing and is convenient because it reflects isostatic state. The Bouguer gravity anomaly is the most used gravity anomaly in onshore exploration because it is necessary to reduce to a datum and it reflects density variations in the upper crust.

Usually gravity maps can be found with Bouguer gravity anomaly (onshore) and the Free-Air gravity anomaly (offshore) merged at the coast line, where both anomalies will have the same gravity value. This is the case of the Free-Air gravity map used in this study.

5.4.1 The Free-Air anomaly map.

The Free-Air anomaly map displays the double gravity edge effect across the Zambezi Delta Basin east and north-east of Beira (Fig 5.1) (Watts *et al.*, 1995). The double gravity edge effect at the Zambezi Delta Basin consists of two negative anomalies, a relatively small anomaly onshore separated from the second negative anomaly offshore by a positive anomaly accross the Zambezi Delta platform.

Offshore Free-Air gravity anomalies vary between -90 and +50 mGal in the Zambezi Delta Basin area (Fig. 5.1) and gravity values are negative seawards from the shelf edge as expected. The negative anomaly offshore is about double the size of the onshore anomaly in amplitude and is due to the abrupt deepening of the sea bed topography. The small negative anomaly is caused by the landward basement deepening caused by increased sediment load of the basinward prograding Zambezi Delta (Watts and Marr 1995).

The shelf edge is marked by the zero gravity contour line on this map. To the east and north-east the Free-Air anomaly becomes poorer in resolution as data coverage is more sparse in this part of the basin. Gravity anomalies in this part of the basin display the gravity effect caused by the topographic expression of the southern end of the Davie Ridge offshore northern Mozambique.

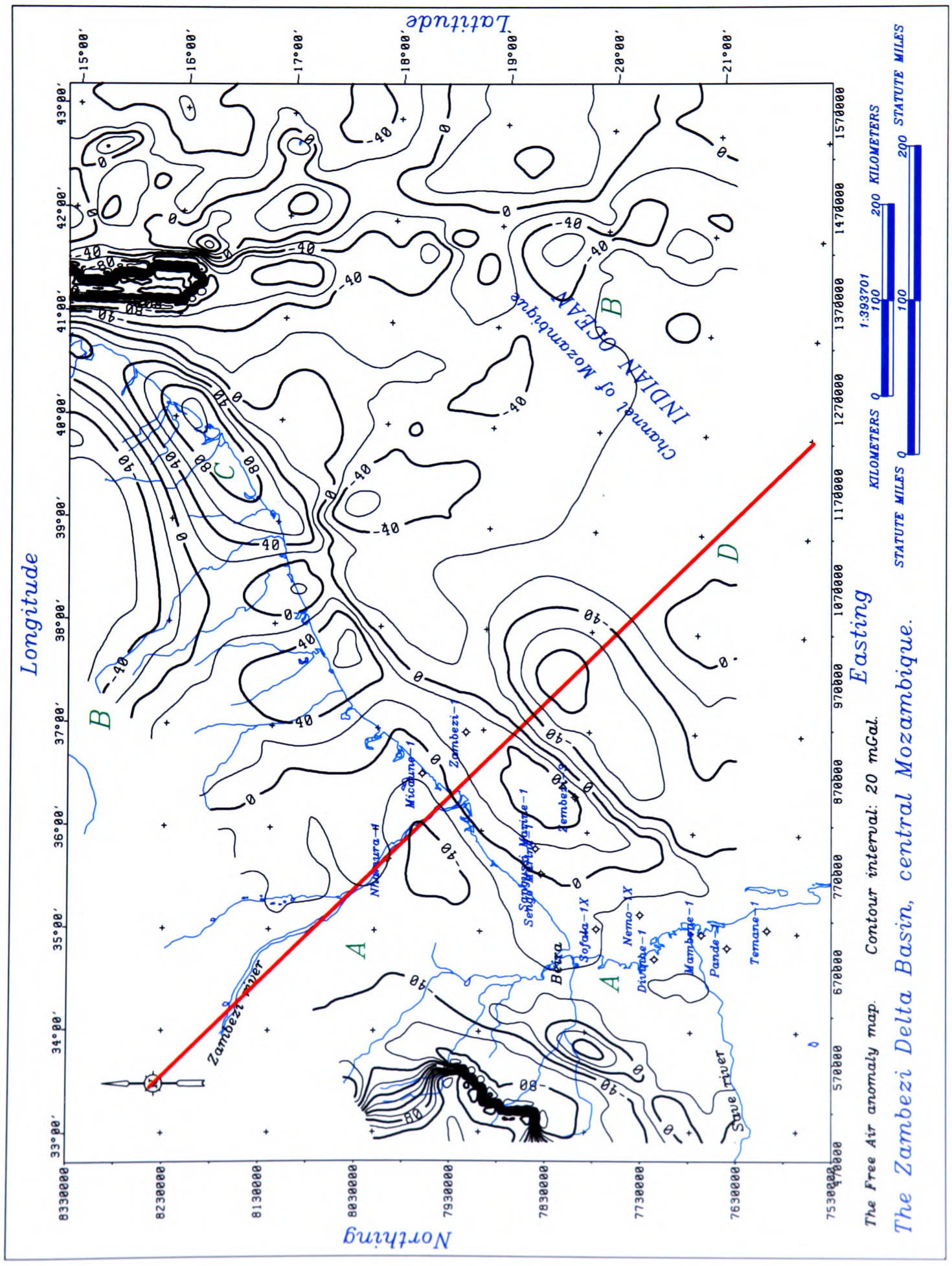

Figure 5.1: The Free-Air anomaly map (offshore) of the study area joined with the Bouguer anomaly (onshore) at the coast line. Red line is the modelled gravity profile. A-A and B-B are trends in the gravity field and C and D are positive gravity anomalies

To the west and northwest an area, A-A, of low amplitude anomalies reflects the gravity effect of the (mainly Karoo and Mesozoic) sediment fill of the Lower Zambezi graben. This is bounded further west by anomalies over the igneous Gorongosa Mountain range and by the western flank of the Urema graben.

To the northeast poorer coverage makes maps less reliable. A gravity gradient lies just offshore, over the continental shelf break. The high landward appears segmented along strike; the low seaward is also variable in character. It is possible that NW-SE as NNW-SSE basement structural trends are influencing gravity. One such trend, B-B, extends from onshore to offshore and may point to continental crust, albeit thinned and subsided, extending some 300km offshore, although data coverage and quality should be checked for the validity of the observed anomalies.

A continental margin sediment prism is not well developed here. The landward high culminates at +100 mGal at C where Precambrian basement is at the coastline. East of this area the strong North-South trend belongs to the Davie Ridge with the Davie Fracture Zone on its eastern side.

The southern limit of the map lies about 50km from the northernmost M sequence magnetic anomaly of Patriat *et al.,* (1985), Martin, (1987) and Patriat and Segoufin (1987), are proof that oceanic crust with an E-W spreading fabric and N-S fracture zones is not far away (Fig. 1.4). In fact, the change in character of the gravity anomalies from west to east at the southern limit, D, may be at the location of the northern tip of one of Segoufin's fracture zones (Segoufin, 1981).

5.4.2 The Bouguer anomaly map.

In contrast to the Free-Air anomaly map, the Bouguer gravity map (Fig. 5.2) offshore is poor in resolving the Zambezi Delta Basin as a well-defined geologic feature, suggesting a gradual landward density change from the offshore part of the basin. The Bouguer gravity generally finds more applications onshore were it correlates better with geologic structures with some reasonable density difference to produce observable anomalies. Consequently, the gravity low

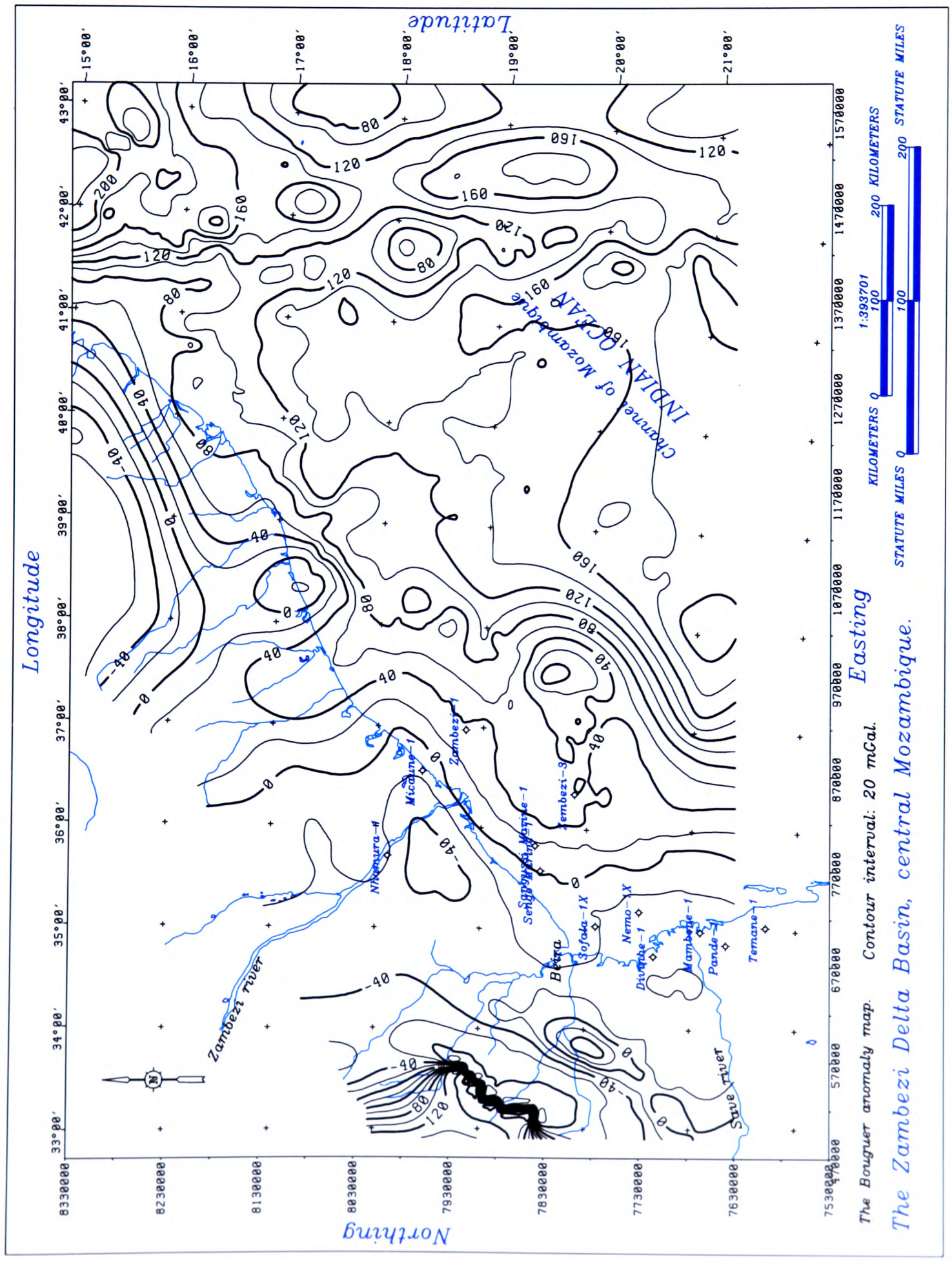

Figure 5.2: The Bouguer anomaly map, on- and offshore the study area.

associated with the Precambrian metamorphic basement in eastern Mozambique can now be seen to extend to the Davie Fracture Zone.

Over and above what can be interpreted from the Free-Air anomaly map it is worth observing that the Zambezi Delta area is marked by a smooth positive gravity anomaly with a sharp gradient south-east of the basin. This feature possibly denotes the rise of the mantle due to the thinning of the crust or flexure towards oceanic crust to the south and, possibly, to the east (sect. 5.6).

5.5 Interpretation of the magnetic anomaly map.

5.5.1 Regional magnetic anomalies.

The magnetic anomaly map of the study area (Fig. 5.3) is dominated by an area to the north and northwest with very intense magnetic anomalies, caused by the out-cropping Mozambique Metamorphic Belt, and its contrast with the remainder of the map where basement is at greater depth. An exception to this is the zone of intense anomalies at 20°-21°S, 39°E over a distance of about 100km striking NE-SW. This feature on the map is clearly an artifact resulting from the gridding process just as the long and curvelinear feature to the west, because both features lie at areas of data gaps and they are not supported by any other data available.

The Zambezi Delta basin is characterized by a low (A) with surrounding highs. All these strike SW-NE or WSW-ENE. The high (and associated low) to the south coincide with the Beira High (BH), a basement feature described by Salman *et al.* (1985) as of the same geological composition as the geological basement in the area. The anomalies to the northeast of this, also a positive-negative pair but WSW-ENE striking, may represent a Beira High extension (BHE?) as far as 38°E with a small change in trend and reactivating it as it has developed.

The magnetic trend B is the same orientation as the Beira High extension,

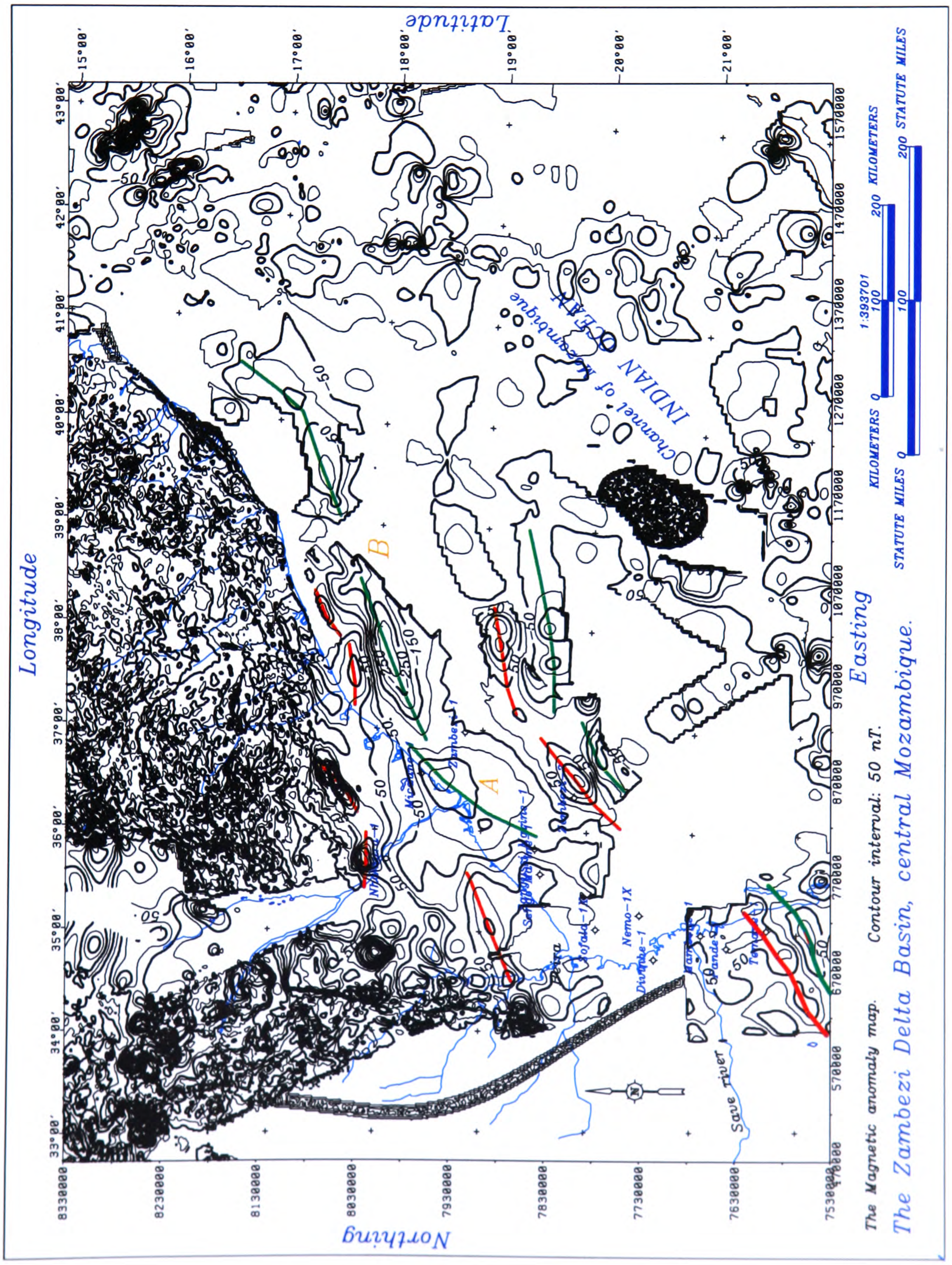

Figure 5.3: The magnetic anomaly map of the study area highlighting the main magnetic anomaly trends in the study area. Red line for positive anomaly trends and green line for negative anomaly trends.

the edge of outcropping metamorphic basement to the north and the continental slope and clearly reflects a major structural trend in this area. Later in Chap. 4 it is demonstrated how the Beira High extension on the magnetic map and the magnetic trend B, both have the same orientation as the East African rift active extension mapped on seismic data and thus they build the flanks of the late graben structure. The presence of a similar anomaly trend west of the Zambezi Delta Basin points to the possiblity of the basin being built on top of this WSW-ENE trend.

In the Zambezi Delta Basin area, the total magnetic anomaly varies between +400 and -400 nT in amplitude on- and offshore. Patchy anomalies in the east and south of the map reflect poor data coverage, although the trend of the Davie Ridge is clear.

5.5.2 Integration of gravity and magnetic.

Despite the poor quality of the magnetic anomaly map (Fig. 5.3), the magnetic anomaly trends reveal the main structural features of the study area. The quality of gravity maps is good and data coverage of the area is better than for magnetics. Fig. 5.4 summarises major trends and features mapped on the gravity and magnetic maps. From Fig. 5.4 it is clear that gravity and magnetic derived structural trends resemble features known from the literature related to the Middle Jurassic continental breakup and the East African Rift phases in this area (Scrutton *et al.,* 1981; Segoufin, 1981; Al-Kasim *et al.,* 1985; Mascle *et al.,* 1987; Coster *et al.,* 1989; Scotese, 1991). Three areas can be recognised, each with distinct gravity and magnetic characteristics. They are separated by longitudes ca. 35.0°E, 38.0°E and 41.5°E.

The region east of longitude 41.5°E is bordered by the Davie Fracture Zone and, at these latitudes, it is composed of the continental crust of Madagascar. Madagascar drifted south to this position in Mid to Late Jurassic times.

Between 38.5°E and 41.5°E is a deep water area of weak gravity and magnetic anomalies, reflecting an absence of major structures. However, about 300km to the south, the E-W linear magnetic anomalies M0 to M22 of the Mozambique

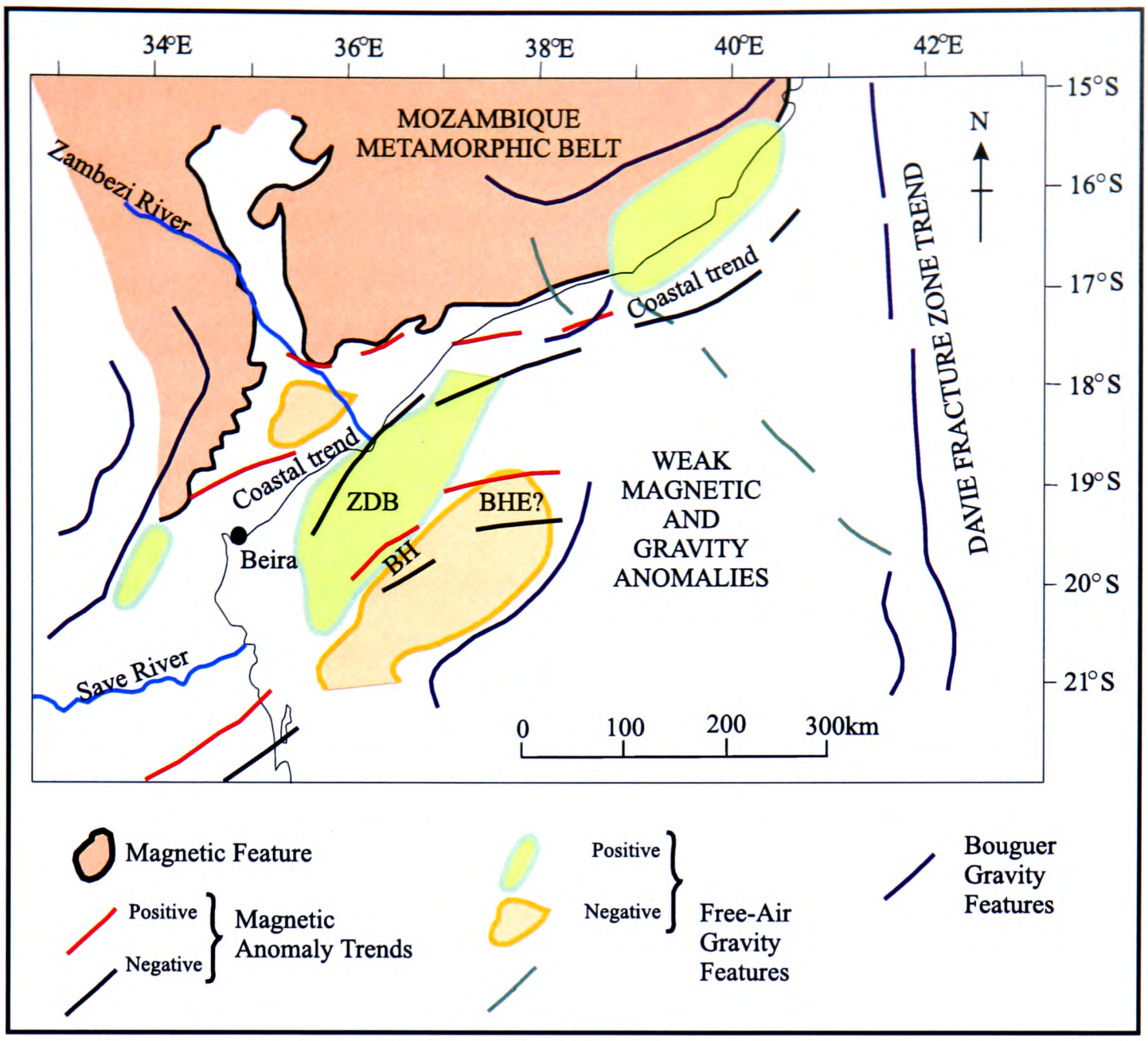

Figure 5.4: Sketch map summarizing the main structural features mapped from gravity and magnetic data of the study area. *Key: ZDB - Zambezi Delta Basin; BH - Beira High; BHE? - Beira High Extension.*

Basin are found (Mascle *et al.*, 1987). The quiet potential fields would be consistent with this area being a wide zone of stretched continental crust bordered to the south by Jurassic oceanic crust. The 38.5°E boundary aligns southwards with the Segoufin Fracture Zone and may also be a structural boundary within the continental crust.

The area between 35.5°E and 38.5°E contains some strong anomalies. The Free-Air gravity over the Zambezi Delta Basin is represented by a pair of negative anomalies separated by a positive, in part reflecting the thick sediment load but also representing the continental edge effect. It is demostrated later that the basin probably sits on thinned continental crust. The strong northeast

trends in the magnetic anomaly map labelled BH and BHE indicate the presence of the Beira structural high, which may be in part volcanic and probably a product of the Jurassic rifting process. Their confinenment to the 35.5°E to 38.5°E area would support some compartmentalisation by north-south structures as mentioned above. The Beira High extension is also terminated to the east by a positive gradient in the Bouguer anomaly field, which probably indicates the shallowing of the Moho to the southeast, towards oceanic crust. At the southwest end of this feature it turns southwards to align with the Mozambique Fracture Zone.

West of 35.5°E, northeast trends are again seen in the magnetic field, but offset southwards from the line of the Beira High. The 35.5°E boundary separates the Zambezi Delta Basin from the "Sul do Save" region of north-south graben structures.

To the north of all these areas lies a series of subparallel positive and negative magnetic anomalies representing a coastal magnetic trend which may be caused by the outcropping Mozambique Metamorphic Belt (Fig. 5.4). This magnetic trend is interpreted as the expression of basement shallowing, often referred to in the literature as a basement hinge line trending in the same direction (Al-Kasim *et al.*, 1985; Salman *et al.*, 1985).

5.5.3 2D interpretation of magnetic anomalies.

This section aims at using 2D magnetic profiles across geologic features in the study area to estimate the depth to the anomalous magnetic structures which here are interpreted as expressions of either the highly magnetic metamorphic or volcanic basement.

Smith (1959; 1961) demonstrated that an estimate of the maximum depth to a magnetic body causing a certain magnetic anomaly could be made regardless of the geometric shape of the body. This was a significant step in magnetic anomaly interpretation since the depth to the anomalous structure is a very important parameter in exploration.

Smith's rules for maximum depth determination, however, require the knowl-

edge of the maximum amplitudes of the first and of the second horizontal gradients of the vertical flux density and of the magnitude of the magnetisation vector (Parasnis, 1979). They also assume the magnetic body magnetisation to be parallel everywhere. They make the even more restrictive assumption that the magnetic body magnetisation is everywhere vertical if the maximum amplitudes of the first and second derivatives of the vertical magnetic anomaly are to be used instead of the maximum amplitudes of the first and second horizontal gradients of the vertical magnetic flux density (Parasnis, 1979; Telford *et al.*, 1990).

As the direction and magnitude of the magnetisation vector are not known for the anomalies studied here, the Smith's rules would become even more speculative and more inaccurate in this case.

Some empirical depth estimate rules were developed in the last fifty years and summarised by Telford, Geldart and Sheriff (1990). They represent a less speculative option than the Smith's rules for depth estimates of magnetic structures. Most of these rules of thumb relate to profile shapes, where horizontal widths and horizontal distances are used for symmetric and asymmetric magnetic profile anomaly curves.

Peters (1949) related the horizontal distances of sloping flanks to the maximum depth of magnetic structures and Rao and Ram Babu (1984) used the maximum slope method for depth estimates from magnetic anomalies to derive further relationships between the horizontal distance and the maximum depth of magnetic structures. Rao and Ram Babu (1984) accounted for the angle of dip of the magnetic structure and for the symmetry of the magnetic anomaly curve. This approach allowed them to deduce various proportionality factors to be applied for depth estimates for several structural body shapes, given the angle of dip and the structural shape are known. Barongo (1985) used a variation of the same rules for vertical magnetic gradient for the same purpose of depth estimate.

Despite the availability of various depth estimate rules, the slope and half slope methods remain some of the most popular methods in use thanks to their simplicity and due to few assumption being necessary as prerequisites for their use. Figure 5.5 is a graphic illustration of how the geometric parameters S and

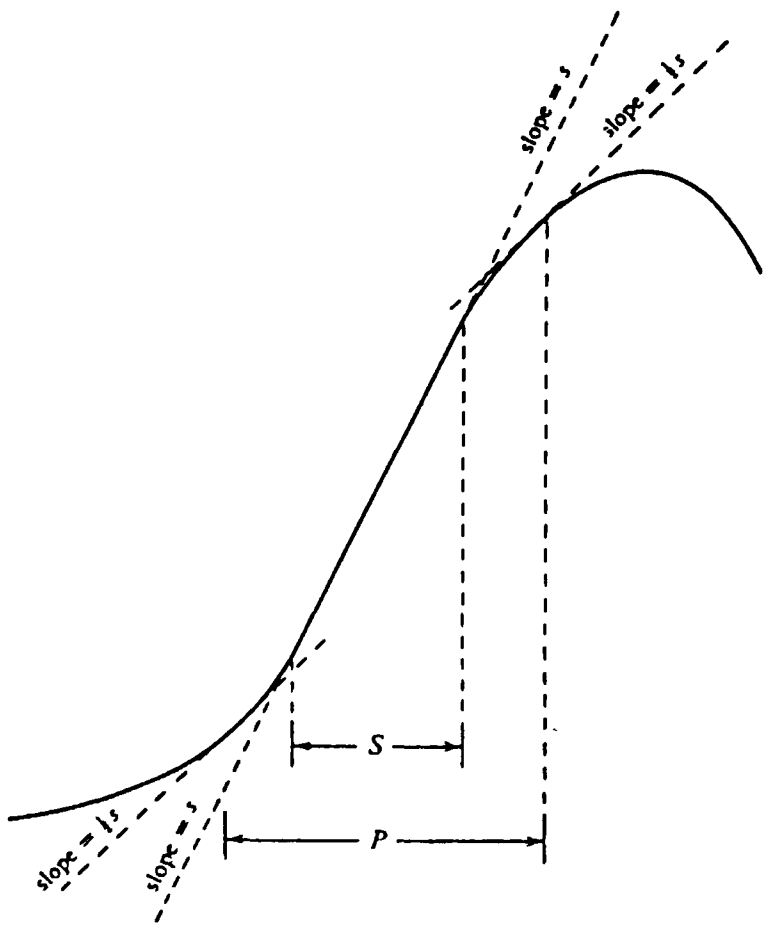

Figure 5.5: Graphic illustration of the parameters used in the slope and half slope methods for depth estimates from a magnetic anomaly curve, after Telford, Geldart and Sheriff (1990).

P can be estimated from a magnetic anomaly curve for the maximum slope and half slope methods respectively.

The slope and half slope methods, both relate the maximum depth z_S and z_P to the horizontal distances S and P (Fig. 5.5). S is defined by the horizontal extent of the portion of the magnetic anomaly curve that is nearly linear at the maximum slope of the curve (slope method). P is the horizontal distance between the points of tangency of two line segments drawn parallel to the half slope of the maximum slope. They are mathematically related to depth using the proportionality factors k_S and k_P:

$$z_S = k_S S \tag{5.1}$$

for the slope method and

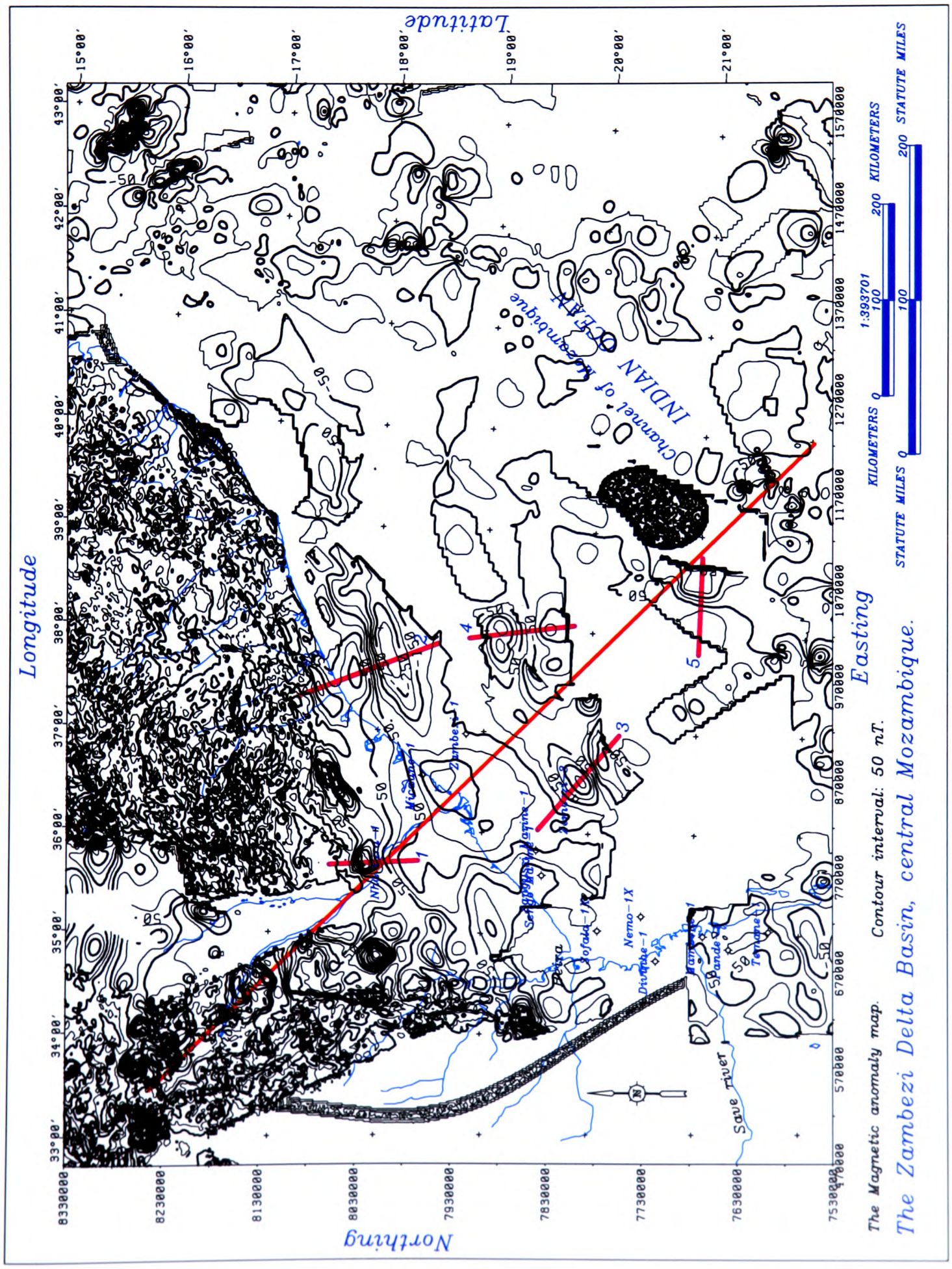

Figure 5.6: The magnetic anomaly map of the study area showing a regional gravity profile (red line) and five magnetic profiles (purple lines) numbered 1 to 5.

$$z_P = k_P P \tag{5.2}$$

for the half slope method. For the depth estimates made here the proportionality factors were kept constant with the values $k_S = 1.82$ and $k_P = 0.63$, after Telford, Geldart and Sheriff (1990).

After consideration of the slope and half slope methods employed and the results of maximum depth estimates achieved on five magnetic profiles (Fig. 5.6) using both the slope and the half slope methods, it was felt that due to uncertainties in determining the parameter S for less symmetric curves the slope method is more likely to result in erroneous depth values. On the other hand, less uncertainty is associated with the half slope method where the determination of the parameter P is relatively simple and more exact, thus allowing a better estimate of the maximum depth. This conclusion was reached in part after comparing the results achieved by both methods with the depth to basement values obtained using seismic methods where available in Chap. 4. Table 5.1 summarises maximum depth values calculated for five magnetic profiles (Fig. 5.6) of the Zambezi

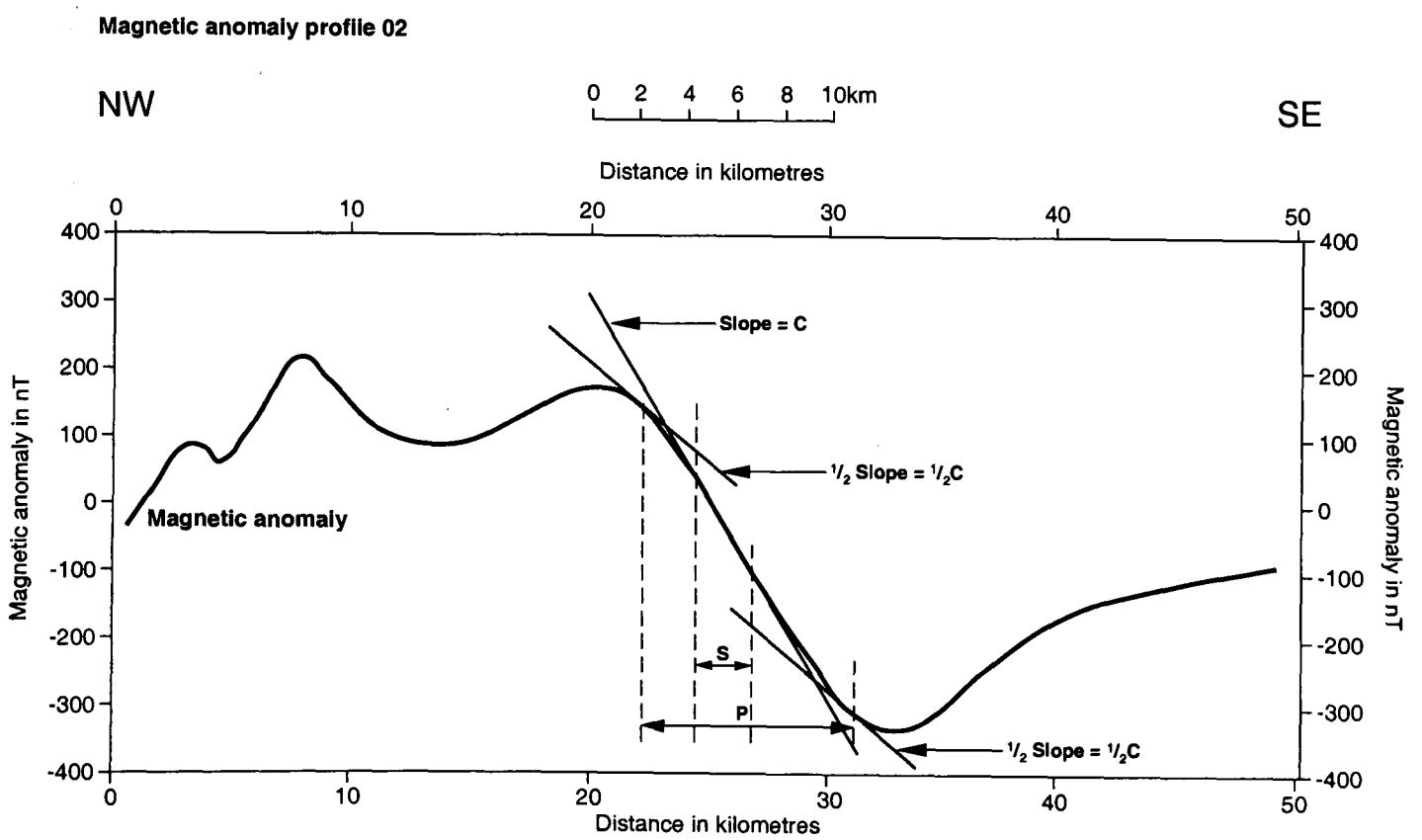

Figure 5.7: Magnetic profile number 2 across the northern part of the East African Rift active extension, interpreted after the empirical maximum slope and half slope methods.

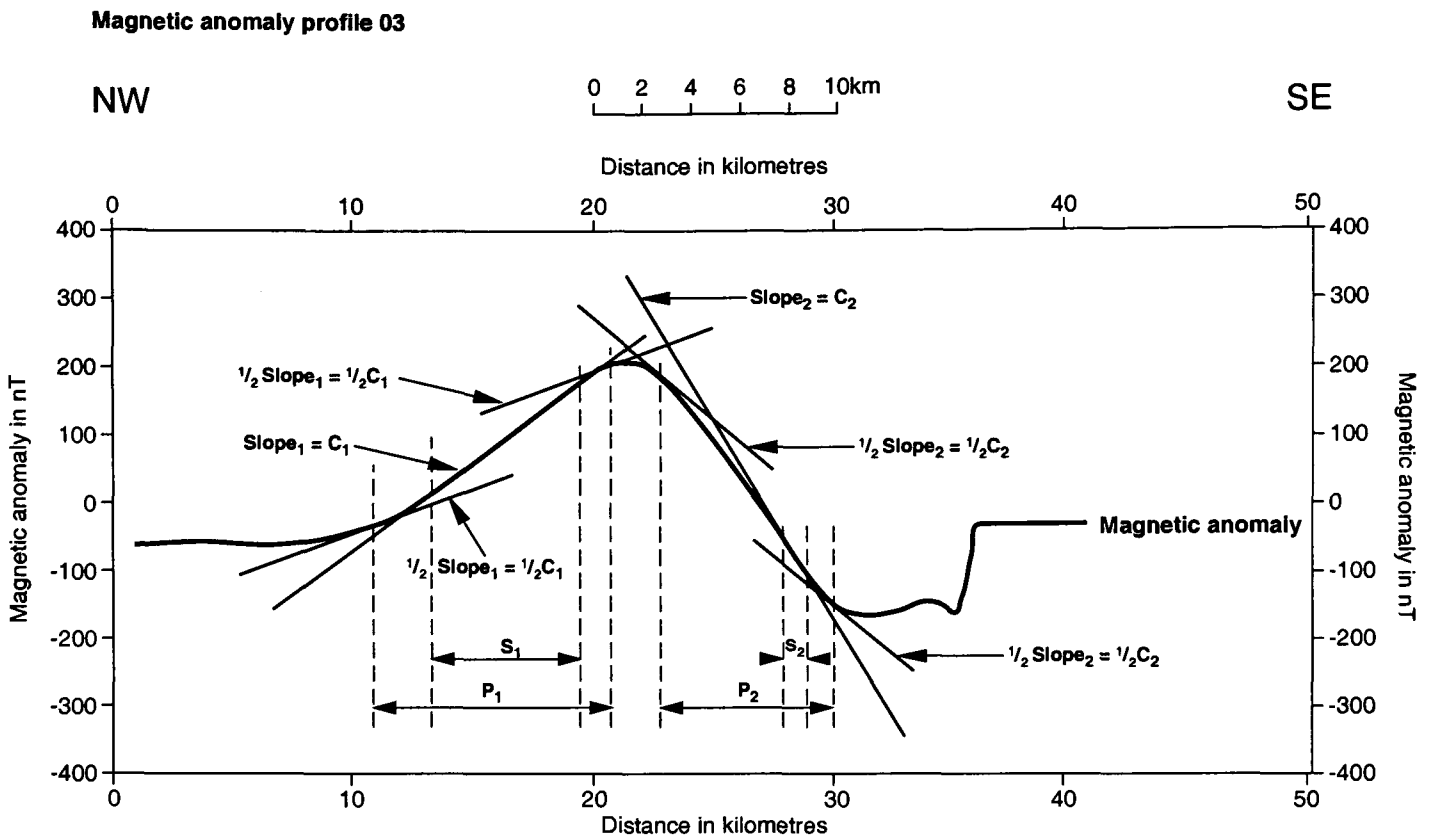

Figure 5.8: Magnetic profile number 3 across the Beira basement uplift, interpreted after the empirical maximum slope and half slope methods.

Delta Basin for both the slope and half slope methods.

Figure 5.7 shows the graphic interpretation of magnetic profile number 2 using the slope and half slope methods. This profile runs across the northeastern part of the Zambezi Delta Basin across the East African rift active extension (see Chap. 4 and 6). The values calculated for the estimate of the maximum depth to the magnetic basement at the above profile by both methods differ by 25% (see Tab. 5.1) and both are close to the depth values obtained from seismic data for the same geological structure. Slopes at northwestern end of the profile suggest the existence of a possibly shallower structure of small lateral extent (about 10km width).

Fig. 5.8 shows the graphic interpretation of magnetic profile number 3 using the slope and half slope methods. This profile runs across the Beira basement uplift, a well known geological structure (Salman *et al.*, 1985). The shape of the magnetic anomaly along this profile suggests a structure of about 10km width. The values obtained here for both methods suggest a deeper structure to the north-west and shallower to the south-east which again supports the seismic

Table 5.1: Summary of measured and of calculated parameters for five 2D magnetic profiles across the Zambezi Delta Basin.

Summary of 2D magnetic profile interpretation.

Profile number	Method	Slope and $\frac{1}{2}$slope values	Geometric parameters (S and P) [km]	Maximum depth [km]	Depth difference between methods [km]
01					
NW side	Slope	0.20	0.9	1.6	0.1
	$\frac{1}{2}$Slope	0.10	2.7	**1.7**	
SE side	Slope	0.50	1.1	2.0	1.2
	$\frac{1}{2}$ Slope	0.25	5.0	**3.2**	
02					
	Slope	0.60	2.3	4.2	1.4
	$\frac{1}{2}$Slope	0.30	8.9	**5.6**	
03					
NW side	Slope	1.30	6.4	11.6	-5.3
	$\frac{1}{2}$Slope	0.65	10.0	**6.3**	
SE side	Slope	0.60	1.1	2.0	2.4
	$\frac{1}{2}$Slope	0.30	7.0	**4.4**	
04					
	Slope	1.10	10.0	18.2	-10.9
	$\frac{1}{2}$Slope	0.55	13.2	**8.3**	
05					
	Slope	1.00	3.0	5.5	-0.3
	$\frac{1}{2}$Slope	0.50	8.2	**5.2**	

derived depth trends across the structure. The depth values themselves should in this case and in that of the other profiles studied here, be interpreted only qualitatively if one accounts for the already discussed poor quality of the magnetic anomaly contour maps (Chap. 3) used in this study. Therefore the results obtained here should be used as an additional aid for determining broad structural trends in the study area as has been attempted in Fig. 5.3 but not recommended for any quantitative evaluation of the anomalies displayed.

The maximum depth estimate values obtained for both the slope and the half slope methods do not qualitatively contradict expectations from studying

other geological and geophysical data, as well as from published and unpublished work studied here. However better magnetic anomaly maps for the area could certainly help reach more conclusive results.

5.6 Gravity data modelling.

This section summarises the work done using the topographic (onshore) and bathymetric (offshore) data to produce various structural models of the earth crust in the study area and also summarises the results of a 2D gravity modelling undertaken on a Free-Air gravity profile striking NW-SE across the cental part of the Zambezi Delta Basin.

5.6.1 The standard earth crust model.

The earth's crust generally thins from the coast line seawards into the deep waters of the ocean and thickens landwards from the coast line with increasing topography. The average crustal thickness beneath the continents is 35km and is greater at mountain ranges. It reaches a lower value of about 6km in the deep ocean waters. The continent-ocean boundary is commonly offshore between thinned continental crust and (Airy isostasy) ocean crust. Apart from the differences in thickness, the continental crust is made of material of relative higher density than that of the oceanic crust mainly of basaltic rock. Strictly oceanic crust can be found underneath ocean waters around 5km deep and deeper. At such depths generally a sediment thickness of 1km is asumed on top of a basltic substrate.

A further subdivision of the crust is sometimes introduced into models, a transitional section separating the continental from the oceanic crust. In the past, the transitional crust (Worzel, 1974) has been defined as the section of the earth crust underneath the area of basin sedimentation generally between 300m topography from the shore line and the 200m isobath. The density value of this section of the earth crust lies in-between the densities of the continetal and

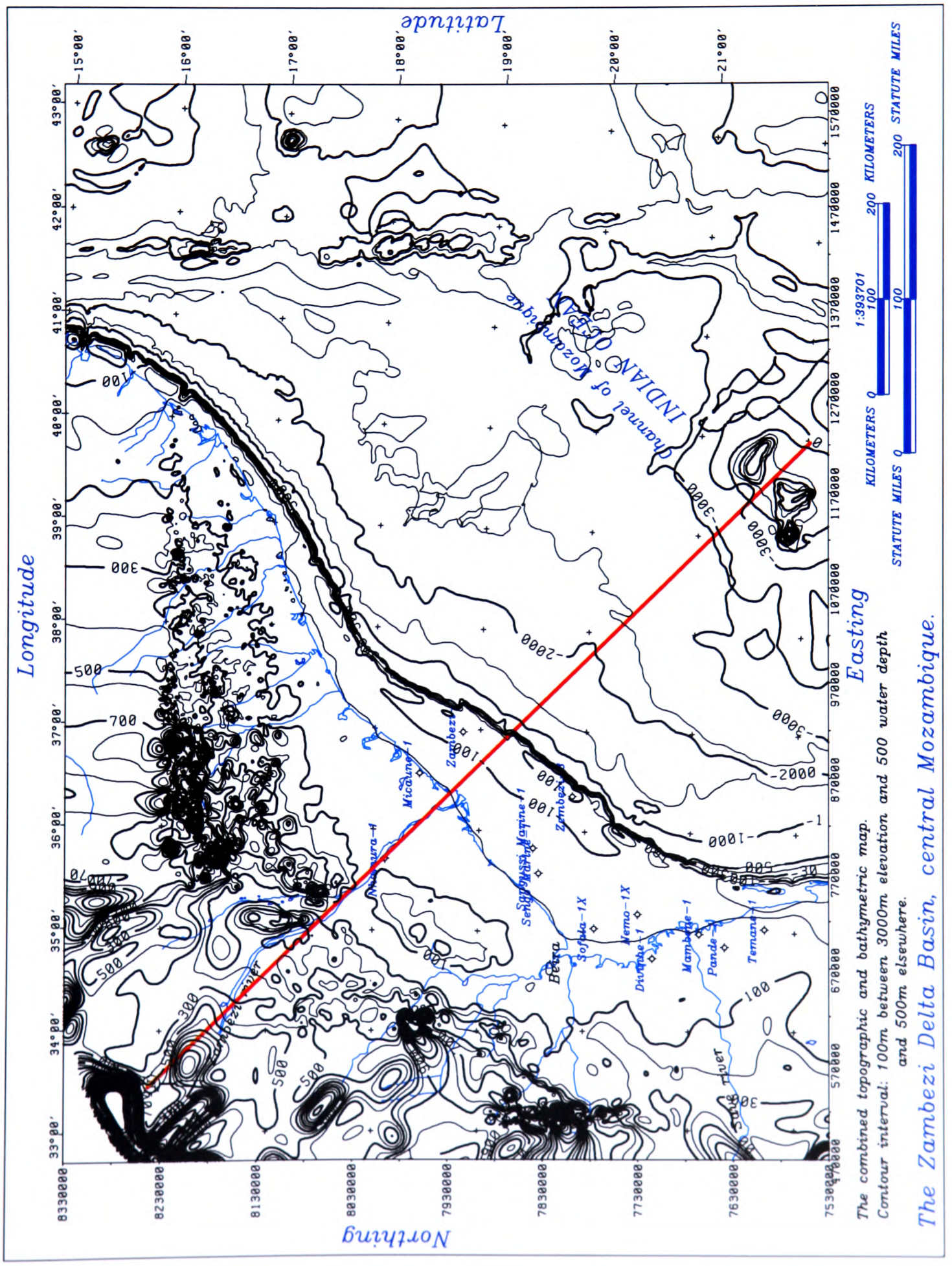

Figure 5.9: The combined topographic and bathymetric map joined at the coast line. Red line is the gravity profile.

oceanic crust density values. More recently it refers to a section of crust that is neither purely continental nor oceanic but stretched continental crust with a significant volume of basic intrusive and extrusive material related to rifting (Kearey and Vine, 1990).

The concept of a standard earth crust (Worzel, 1974) generally comes into use when the crust is being treated as a homogeneous uniform layer of the earth structure, generally for the sake of simplification. This concept is exploited here and allows the production of a simplified crustal structural model over the study area using the topographic data (onshore) and the bathymetric data (offshore) merged at the coastline, which are displayed in contour form on Fig. 5.9.

The crustal thickness of the study area was derived for three basic models: (1) a model with a continental and a oceanic crust meeting at the 200m isobath; (2) a model with all three sections of the earth crust, continental, transitional and oceanic crust and (3) a model with the standard crust. For each of the three models a second model was calculated where the geology above sea level was assumed to be of less denser material than the rest of the crustal section. This allowed six different models to be derived.

The crustal thickness of 27.5km at the coastline was derived from crustal thickness values published in the literature for the African continent and assumed to be in Airy isostaic equilibrium (Worzel, 1974; Stuart *et al.*, 1987; Qiu *et al.*, 1996). A column mass balance between the earth crust and the upper mantle is achieved by introducing an arbitrary surface within the upper mantle.

The crustal thickness offshore $\Delta z_{c_{off}}$ is calculated by

$$\Delta z_{c_{off}} = 27500 - \Delta z_{wd} \frac{(\rho_m - \rho_{sw})}{(\rho_m - \rho_c)}, \tag{5.3}$$

onshore the crustal thickness $\Delta z_{c_{on}}$ is calculated by

$$\Delta z_{c_{on}} = 27500 + \Delta z_{top} \frac{(\rho_m - \rho_{sg})}{(\rho_m - \rho_c)} \tag{5.4}$$

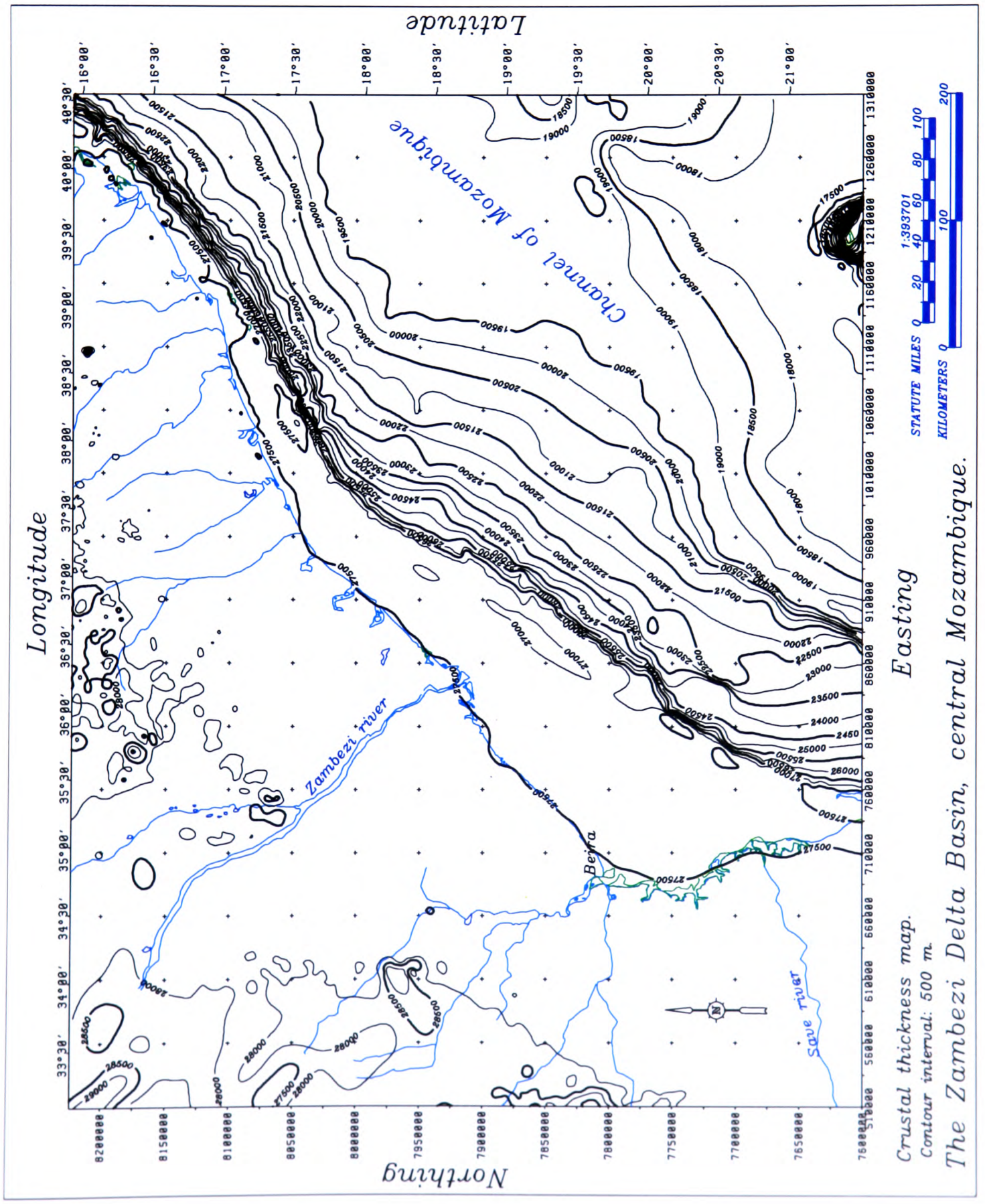

Figure 5.10: The standard crust thickness of the study area derived from topography and bathymetry.

where Δz_{wd} is the water depth, Δz_{top} is the the topography above sea level, ρ_m is the density of the upper mantle, ρ_{sw} is the density of the sea water, ρ_c is the density of the earth crust and ρ_{sg} is the density of the geology above sea level.

The densities used in the calculations are obtained from the literature. They were as follows for the three main models:

- Model (1) - continental crust density, 2.84 gcm^-3, continental mantle density, 3.35 gcm^-3, oceanic crust density, 2.68 gcm^-3 and oceanic upper mantle density, 3.30 gcm^-3;

- Model (2) - continental crust density, 2.84 gcm^-3, continental mantle density, 3.35 gcm^-3, transitional crust density, 2.79 gcm^-3, transitional mantle density, 3.33 gcm^-3, oceanic crust density, 2.68 gcm^-3 and oceanic upper mantle density, 3.30 gcm^-3;

- Model (3) - standard crust density, 2.79 gcm^-3 and standard mantle density, 3.33 gcm^-3. The density for the geology above sea level is kept constant for all models calculations at a value of 2.65 gcm^-3 and water density used is 1.03 gcm^-3.

The crustal thickness calculated for the six models is very similar onshore with some variations in the range of a few hundreds of metres at moutain ranges due to the effect of the assumed lighter geology above sea level. The average crustal thickness differences between models is less than 1km in the offshore section of the crust. Figure 5.10 displays the crustal structure for the standard crustal thickness which is viewed here as the most simplified crustal model which is used to give a first approximation to the crustal structure of the study area.

5.6.2 Gravmag program features.

Gravmag (a commercial software by the BGS) was used because it allows a simple model of the crustal thickeness to be produced from a broad knowledge of regional geology of a continental margin. It is an interactive software program for either inverse modelling both gravity and magnetic field data or to calculate theoretical gravity or magnetic curves out of supplied geologic models (Pedley *et al.*, 1993). The program can read field data, gravity or magnetic data or both

for a given equally or unequally spaced profile and then interactively build the geologic model and it can read a model file and then interactively calculate the theoretical gravity or magnetic curve or both. Model parameters for gravity or magnetics can also easily and interactively be edited into the program for different polygonal bodies via the menu. The program allows one to zoom in and out parts of the model and includes a facility to produce high quality hardcopy plots in both black and white and colour.

Gravmag also allows the separate assignment of a half strike value for each polygonal body to express its lateral extent normal to the profile and thus allowing the $2\frac{1}{2}$D gravity modelling to be performed but this facility was not used here.

5.6.3 2D gravity modelling.

The geological model for gravity calculations is first constrained by the topography and bathymetry profiles merged at the coast line and by the Moho boundary. It includes the sea water column in the offshore part of the gravity profile. The initial Moho boundary for the modelled profile is calculated on the basis of the topographic and bathymetric dataset (sect. 5.6.1). The initial geological model for forward gravity modelling is a simplified one which consists only of three polygons representing the water layer (offshore), the solid crust layer (as a homogeneous solid body, standard crust) and the mantle layer. This simple model allows the assessment of the gravity profile on a regional basis.

The sedimentary section of the geological model for the gravity profile modelled below is obtained from seismic and well data interpretation (this study) reconciled with previous results (Salman *et al.*, 1985; Stuart *et al.*, 1987; Qiu *et al.*, 1996) and with the results from sect. 5.5.3. Three distinct sediment layers are introduced to represent sediments deposited during the three main stages of basin development. The upper sediment layer is of post-East African rift-onset sediments (Neogene and Quaternary), the middle layer is of sediments deposited between the early stages of Gondwana break-up until the beginning of the East African rift (Early Jurassic - Palaeogene) and the lower layer is of Karoo sediments representing the Karoo rift phase (Carboniferous - Early Jurassic) with a

thin layer of Post-Karoo volcanics (about 1km thick) of high density between the Karoo layer and the post break-up sediment layer.

The end of the main phase of crustal extention and hence continental crustal thinning is assumed to be sometime during Gondwana break-up. It is also assumed that only thermal subsidence and sediment loading has occured since breakup and the thermal anomaly has completely decayed. The crustal structure is then derived in three steps. The first step consists of removing the two upper sediment layers and calculating the water depth in the absence of sediment loading, ie. due only to crustal thinning, (Fig. 5.11 A) by

$$z_w = z_{w0} + \Delta z_{s0} \frac{(\rho_m - \rho_s)}{(\rho_m - \rho_w)}, \tag{5.5}$$

where z_w is the water depth at the time of break-up, z_{w0} is the water depth today, Δz_{s0} is the sediment thickness of all post break-up sediments, ρ_m is the density of the upper mantle, ρ_s is the average density of the two upper layers calculated from the density values of the two layers given in Tab. 4.1 and ρ_w is the density of the sea water. The densities for the deep structure are obtained from published information (Worzel, 1974; Stuart and Zengeni 1987; Qiu *et al.*, 1996). The second step is to calculate the crustal thickness along the profile by assuming isostatic equilibrium at the coast line. This is achieved by

$$z_c = z_{c0} - \Delta z_w \frac{(\rho_m - \rho_w)}{(\rho_m - \rho_c)}, \tag{5.6}$$

where z_c is the crustal thickness at a point on the profile, z_{c0} is the crustal thickness at the point where the profile crosses the coastline and Δz_w is the water depth (Fig. 5.11 A). Here the crustal thickness is calculated with no account of sediment layer 1 of Karoo sediments and the volcanics layer (Fig. 5.11 B), both of which are assumed to be of the same density as the crust for simplification. Step three consists of re-loading with the two upper sediment layers removed in step one and thus recontructing the geological section along the profile (Fig. 5.11 C.

The Moho boundary in Fig. 5.11 C is shallower than the one obtained in

sect. 5.6.1 beneath the Zambezi Delta Basin (Fig. 5.11 D), because a thicker

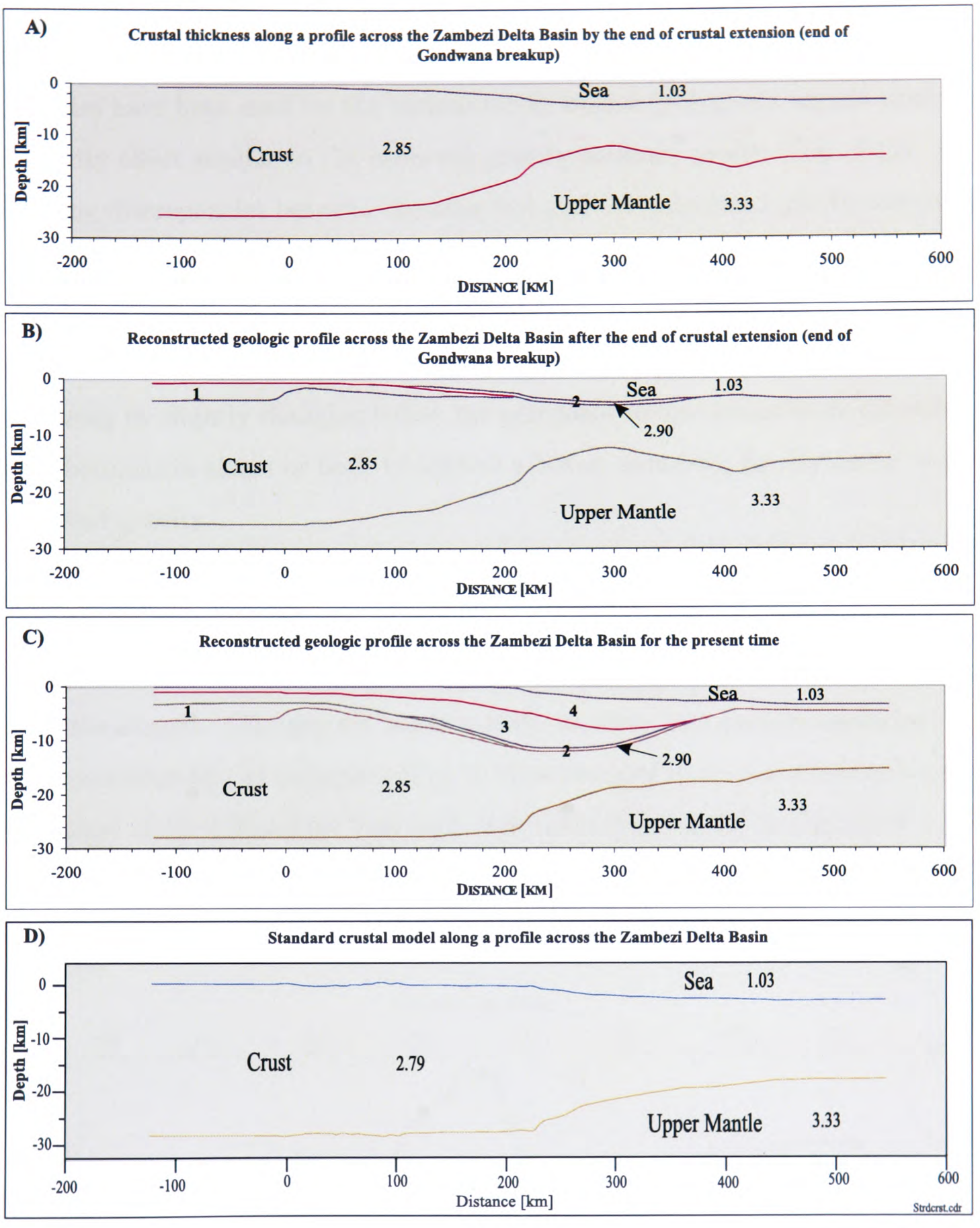

Figure 5.11: A three step crustal reconstruction of the geological profile modelled with Gravmag. Key: A - Crustal thickness at the end of the extensional period; B - Post extension earth crust along the gravity profile with the Karoo sediment layer (1) and the end of extension volcanics layer (2) inserted in the upper crust; C - The complete profile reconstructed for the present day. (3) - Late Cretaceous to Early Tertiary sediments and (4) - Post East African rift-onset sediments; D - is the standard crustal model along the same profile derived from Fig. 5.10. 1.03 - density value in kg/cm^3.

column of dense mantle material is required to compensate for the light sediment load of the basin fill. The model in Fig. 5.11 C, provided all relevant aspects of the geology along the gravity profile have been accounted for and the right densities have been used for the various model bodies (polygons), should produce a gravity effect similar to the observed gravity anomaly profile (Fig. 5.12). Remaining discrepancies between the observed and the calculated gravity anomaly curves can be attributed to wrongfully derived densities or to wrongfully derived structural boundaries for the geological model polygons where there is no independent control on the model. These discrepancies are resolved interactively with Gravmag by slightly changing either the polygonal bodies densities or the polygonal boundaries shape or both to achieve a better matching gravity curve to the observed gravity.

Fig. 5.11 C is the initial model for the gravity profile (Fig. 5.12). The final model (Fig. 5.13) is achieved by introducing alterations to the boundaries of the polygonal bodies based on Fig. 5.11 C. Density values of the polygons here are kept unchanged. Changes are made mainly to three polygonal boundaries: (1) the lower boundary of polygon 5 (Fig. 5.13) is changed to accomodate a sub-basin southeast of the Inhaminga basement high (see Chap. 4); (2) polygon 6 is

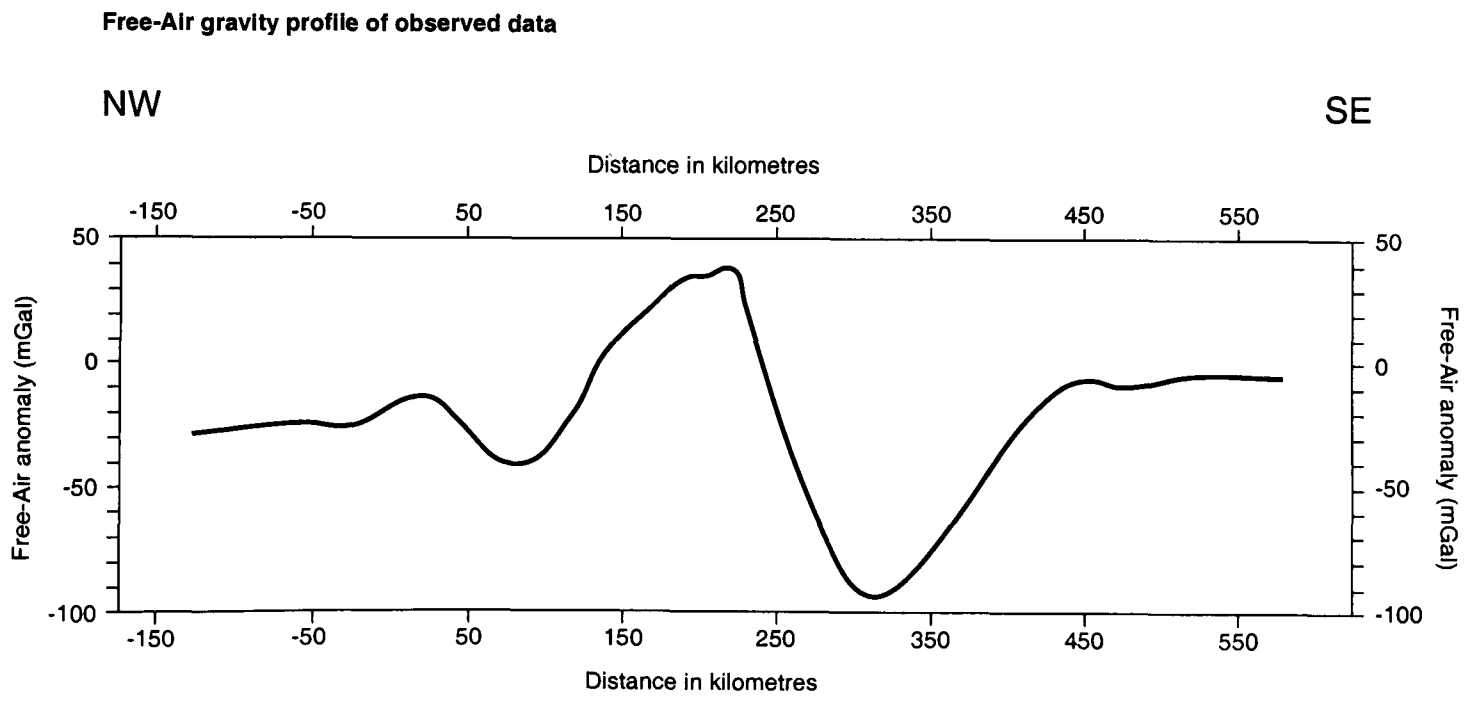

Figure 5.12: A Free-Air anomaly profile across the Zambezi Delta Basin, southwestern depocentre.

changed to a slightly thicker polygon of volcanic material and (3) the Moho boundary is changed underneath the thickest part of the basin to compensate for the light sediment layer above. The last change results in a further thinning of the crustal structure underneath the basin to a crust of about 6km thickness.

The final model produces a good match between the observed and the calculated gravity along the modelled profile. This model corresponds to the best match for the density values employd for the polygonal bodies of the initial model.

The thinner crust underneath the prograding delta basin can be attributed to the relatively low densities derived for polygons 2 and 7 (Fig. 5.13) combined with the shelf edge effect compensated at the crust-mantle boundary. These low density values for polygon 2 and 7 are derived from rms-interval velocities from

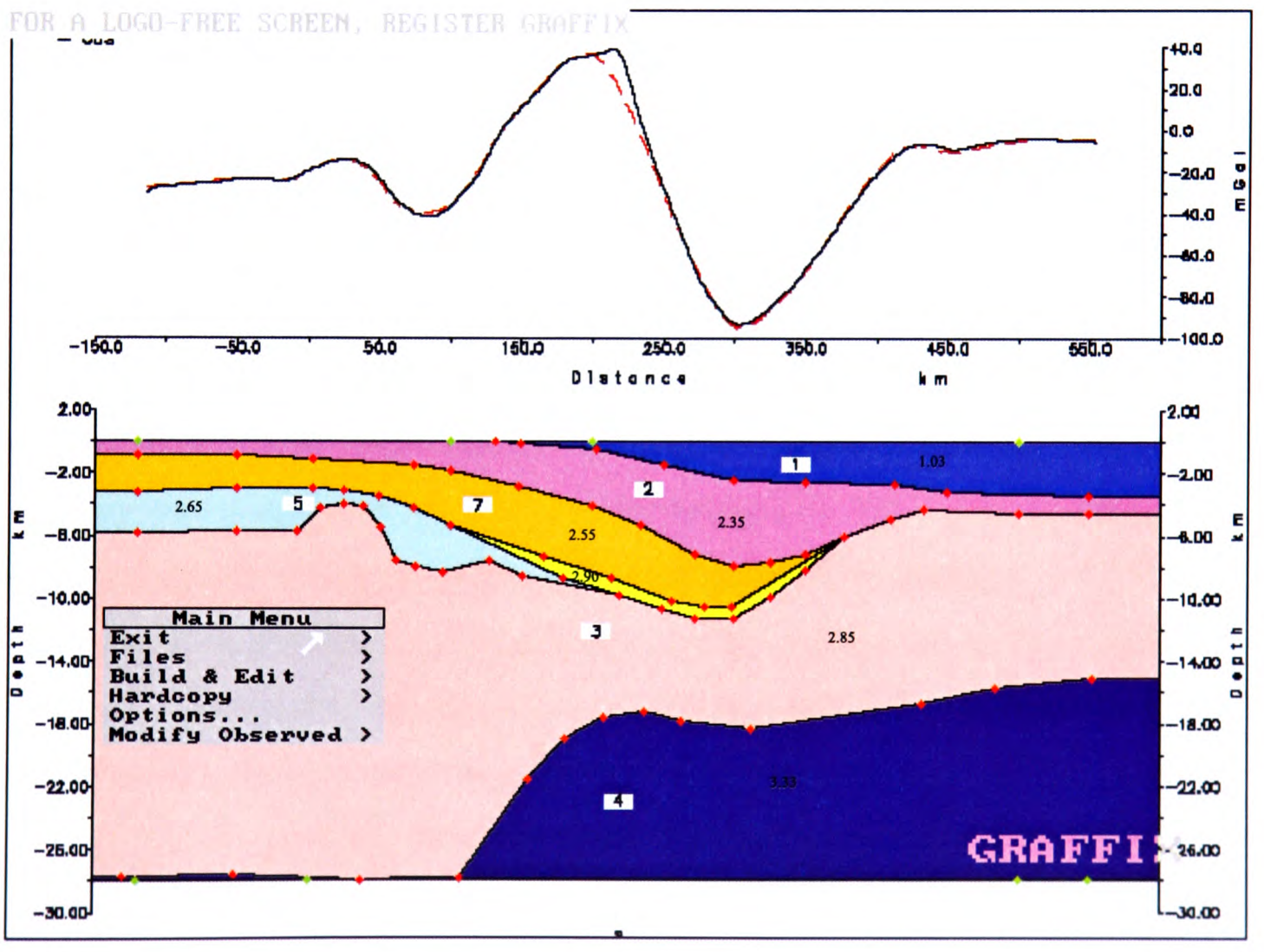

Figure 5.13: 2D gravity model, generated with Gravmag for a Free-Air profile across the Zambezi Delta Basin. *Key: Red dashed line is the calculated gravity curve, black continuous line is the observed gravity curve, 1 - sea water, 2 - Neogene to Recent sediments, 3 - earth crust, 4 - upper mantle, 5 - Karoo sediments, 6 - end-of-Karoo volcanics, 7 - Late Jurassic to Palaeogene sediments. 1.03 - density value.*

seismic data which are considered low for both sediment layers. More discussion on the velocity derived densities is in Chap. 4.

5.7 Summary and discussion of results.

The integrated study of gravity and magnetic contour maps enabled the identification of the main structural trends of the Mozambique Basin (Mozambique Channel area) summarised on Fig. 5.4. The structures identified here are in line with structures and structural trends mapped more locally on seismic data and discussed in Chap. 4 or mapped and discussed by other workers in the literature both regionally and locally. It can be suggested that the NW-SE stress field which characterized the Karoo Rift system (Castaing, 1991) in east Africa was initiated with the late separation of Antarctica during continental breakup, from a position close to the central and southern coast of Mozambique. The separation of Antarctica to the south in Middle/late Jurassic times will have opened the Mozambique Basin on which the Zambezi Delta Basin later developed.

Results from 2D depth to magnetic basement on five profiles across choosen locations showed some correlation with results achieved with seismic data. Due to poor data quality these results can only be used qualitatively. Nevertheles, they are agreement with results reflecting regional tectonic developments in the eastern continental margin achieved previously by other workers.

The Free-Air gravity model achieved here is a variant of the usual model achieved when crustal thinning and accumulated sediments only extend seaward from the coastal area at a rifted passive continental margin. In the context of the pull-apart model, the thin crust beneath the Zambezi Delta basin sediments would be continental in origin and stretched immediately prior to breakup in mid Jurassic times. One interpretation of the gravity modelling is that a double positive-negative anomaly pair can be loosely related to the Watts and Marr (1995) idea of a "weak margin". However, the modification to Moho depth in the final model away from local isostatic equilibrium poses questions about the accuracy of the deep structure of the model. Since the shallow structure cannot

be significantly in error it raises the possibility of the existence of undetermined deep density variations. One option would be to introduce a significant thickness of crustal underplating instead of increased crustal thinning in Fig.5.13 in order to achieve a better compromise between the final gravity model and isostatic equilibrium model (Fig. 5.11 C). Alternatively, the significant Neogene-Recent layer of 5-6km thickness may be receiving some isostatic compensation flexurally because of the increasing stretch of the lithosphere as the margin has aged. This would allow explanation of part of the shelf-edge gravity high without recourse to extra crustal thinning or underplating. In this case the gravity profile would reflect a "strong margin" as described by Watts and Marr (1995). My preference, however is for this latter interpretation, because this is consistent with basin evolution.

Chapter 6

Controls on Late Mesozoic and Cenozoic basin development.

This chapter discusses the controls on basin evolution and sedimentary architecture based on the seismic stratigraphic and well interpretation and gravity and magnetic modelling of chapters 4 and 5. Results from literature review, seismic, borehole logs, magnetic and gravity data interpretation are discussed in an integrated way and basin tectono-stratigraphic evolution is assessed. A short discussion and comparison of the present results to previous work on the Zambezi Delta Basin including a comparison of the latter to other well studied deltas around the world is provided.

6.1 Introduction.

The Zambezi Delta Basin represents one of the most important sediment accumulations in eastern Africa extending on- and offshore. However it remains an underexplored basin with only a few exploration wells and only regional seismic grids in some of its onshore areas and in the offshore shallow waters.

The stratigraphic relationships observed in the Zambezi Delta Basin depocentres are in places very complex in detail due to channel activity (channel

valley incision and channel switch) during deltaic build out.

In this study attention has focussed upon the Late Cretaceous and Cenozoic deltaic development using 2D-seismic data and wire line well log data. This is the time period believed here to include all stages of Zambezi Delta evolution on- and offshore. Isochron and isopach maps (produced and discussed in Chap. 3) show a typical deltaic prograding basin fill in several alternating transgressive and regressive depositional cycles of variable duration and areal extent.

The basin seems to have developed on two main fronts in the early stages of deltaic deposition. One front is dominantly from the northwest, the Zambezi River Delta front, probably supplied with sediments by the Lower Zambezi Graben, and the other from the southwest, the Save River Delta front supplied by the Save River. In the northeast, a series of apparently small rivers seem to have been active for some time during Tertiary deposition with some noticeable impact at times. This type of deltaic development lead to the development of a "three-slope" basin. Two of the three slopes (upper slopes) represented the two main delta fronts advancing eastward and southeastward with a common lower slope generally lying in the deep waters of the Mozambique Channel. The three slopes were united in late Tertiary times when the Zambezi River became the dominant sediment supply pathway.

The most important structural control over sediment supply in the early stages was the Lower Zambezi Graben, which acted as the main sediment conduit for sediments drained from uplifted areas of the hinterland during previous rifting episodes. Later graben structures of the Middle Tertiary East African Rift system will have modified drainage pattern in the west and northwest affecting sediment supply to areas of the Zambezi Delta Basin, thus being partly responsible for the modified sedimentation pattern observed in Neogene units of the deltaic build out.

Depth to magnetic basement and gravity interpretation clearly defines a thin crust beneath the basin. Regional tectonic models imply that there is thin continental crust which will have subsided to generate accommodation space for Tertiary deltaic sedimentation.

6.2 Late Cretaceous and Cenozoic basin development.

The Mozambique Basin, of which the Zambezi Delta Basin is part, is a product of continental breakup in Middle Jurassic times. While the Western Somali and the Rovuma Basins to the north were affected by marine incursion of the Tethys Ocean from the north in the early stages of rifting in late Carboniferous to Middle Jurassic time, the Mozambique Basin in general and the Zambezi Delta Basin in particular did not exist as marine basins.

Only in Jurassic times marine incursions reached today's onshore parts of southeast Africa after the south and southeasterly drift of Antarctica and Australia and the southward movement of Madagascar to its present position gave rise to the opening of the Mozambique Channel. Marine transgression is known to have reached 300 km inland from the present day coastline in some areas of the basin (Salman *et al.*, 1985; Coster *et al.*, 1989; Salman and Abdula 1995). Three major rivers are known to have played a significant role in delivering sediments drained from uplifted inland areas by the rifting episodes to the various places in the Mozambique Basin. These are the Limpopo in the south and the Save and the Zambezi rivers in the northern part of the basin. At times in the past geologic history the three above mentioned rivers may have shared or even solely benefited from sediments drained from the upper and middle Zambezi hydrographic basins as rifting prevented comunication between the middle and the lower Zambezi hydrographic basins (see Chapter 3).

It is likely that the geological and sedimentary history of western Madagascan basins prior to continental breakup will be genetically related to that of the Western Somali, the Mombasa and the Rovuma basins. Any sedimentary strata on- and offshore the Mozambique Basin of pre-breakup age will be of continental, lacustrine and fluviatile type.

It is believed here that marine conditions prevailed for the first time in the Zambezi Delta Basin in the Late Jurassic when continental drift was underway (Scotese, 1991). It was only then that the sea entered the newly open Mozambique

Basin from the north before the Mozambique Channel was completely open in Early Cretaceous (Forster, 1975; Al-Kasim *et al.*, 1985; Coffin and Rabinowitz 1987).

Jurassic diapir type structures are known from seismic data in the Rovuma and salt layers and diapirs have been mapped in the Western Somali basins of the northeast coast of Africa and also in the Majunga and Morondava basins of western Madagascar (Rona, 1982; Coffin and Rabinowitz 1987). It is unclear why salt is apparently absent in the Mozambique Basin. However, long wavelength and low amplitude folding observed in the lower part of the dip seismic sections studied here give rise to questions about what may be causing it. There is a strong belief (Rona, 1982 and this study) that a Jurassic salt layer equivalent to that mapped in the Rovuma (southern Tanzania and northern Mozambique), Kenya and the Western Somali Basins may lie deep underneath post-Jurassic sediments in the Zambezi Delta Basin and possibly in other areas of the Mozambique basin. The observed folding in the Zambezi Delta Basin may be the salt layer response to continued sediment accumulation in the basin.

Results from seismic data studied here suggest that marine sedimentation in the Mozambique Basin might have started sometime between Late Jurassic and Early Cretaceous. The sediment strata is characterized by sequences of conformable and regularly layered sediments generally thinning basinward where they downlap onto progressively younger strata (Fig. 6.1). These sequences of generally conformable strata are separated by erosional surfaces caused by periods of relative sea level fall and subsequent exposure of the shoreface.

Several transgressive and regressive cycles of variable duration are recorded within the Upper Cretaceous to Recent sedimentary succession of the basin. Transgression through sea level rise produced flooding surfaces while sedimentation in areas deep in the basin shifted landward. The sedimentary strata laid down in each cycle during deltaic deposition is observed to be of variable extent laterally, often only covering some areas of the basin, while leaving the remainder

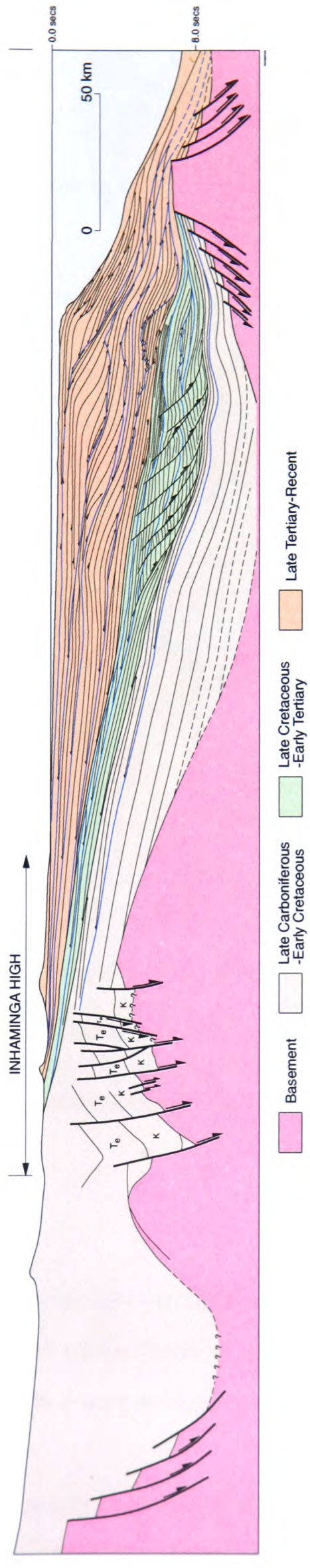

Figure 6.1: A schematic geological cross-section across the Zambezi Delta Basin along dip, summarizing the main geological features of the basin, highlighting the stratigraphic subdivision introduced in this study. Offshore part derived from seismic (this study) and onshore part of the section from Salman (Pers. comm. 1997; BP unpublished inhause data). For location see Fig. 6.2.

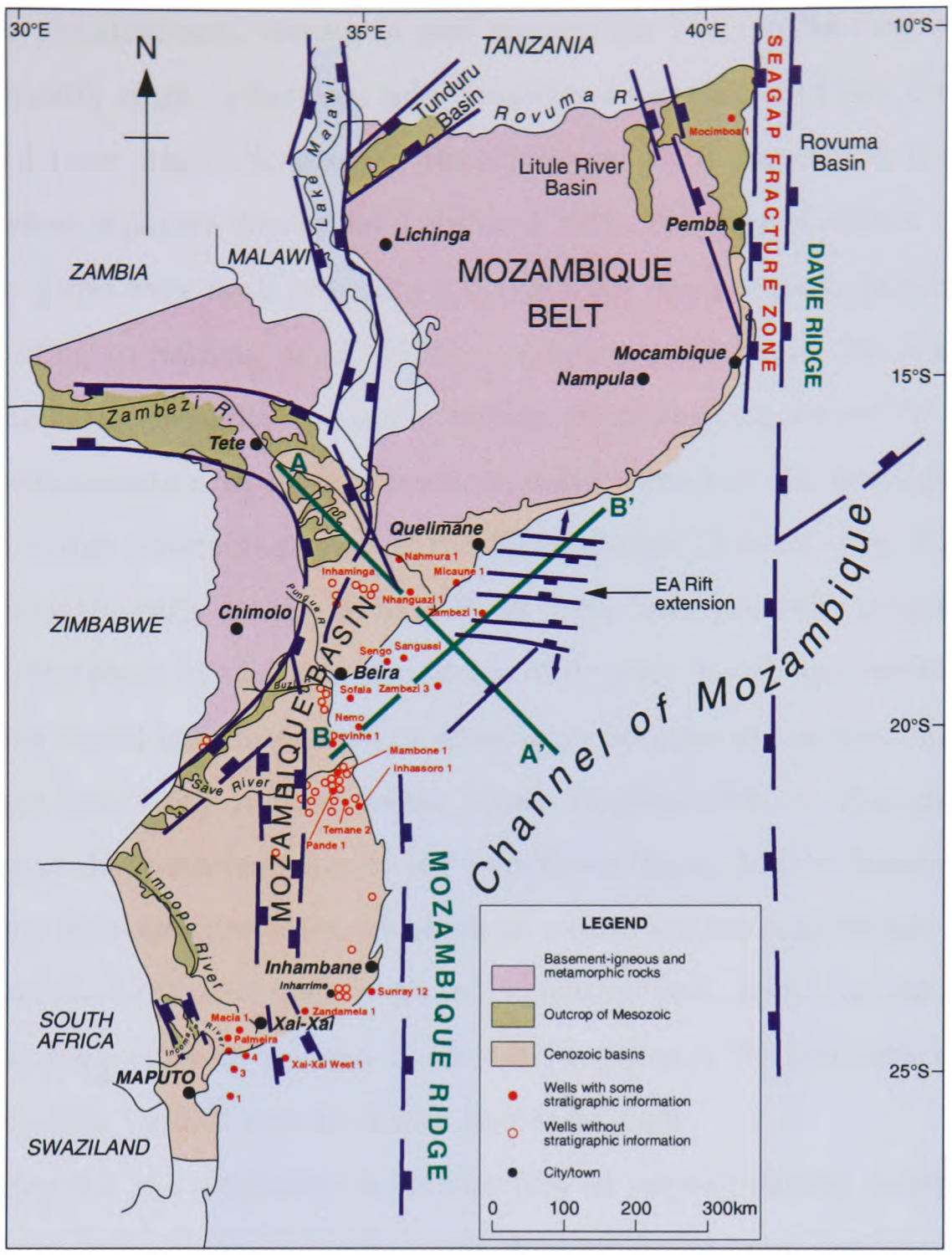

Figure 6.2: Schematic top basement fault map derived from seismic data shown on a map summarizing the regional geology of Mozambique and regional fault trends on- and offshore Mozambique. Sections A-A' and B-B' refer to Figs. 6.3; 6.1, respectively.

exposed to erosion and sediment reworking. However, the general mode of sedimentation in the Zambezi Delta Basin is basinward progradation, a clear sign of sedimentation keeping pace and at times exceeding basin subsidence in a fluvial dominated delta style.

According to this study it is important to define two stages in basin development characterised by different styles in sedimentation and by different roles

played by the structural setting in and around the basin. The first stage, also called the early stage, is between mid Creatceous (Aptian) and late Eocene, and the second (late stage) Neogene to Recent times. This distinction is suggested here to reflect separate depositional styles. Firstly, the time of deltaic deposition when two rivers were both prograding towards the southwestern depocentre and and according to Salman *et al.* (1985), turbidite sands were deposited in this part of the basin; secondly, the upper section which is characterised by a gradual shift in sedimentation to the northeastern depocentre and the development of a sediment wedge prograding towards the Mozambique Channel (Fig. 6.3).

During the early stage, the Save River delta front generally prograded eastward into the basin at the present position of its river mouth and sediments from both deltas would have interacted at some stage because at the time the Zambezi River must have been confined to the Lower Zambezi Graben, thus draining all sediments to the southwest close to the Save River Delta. This is demosntrated by the seismic data interpretation which show sedimentation only to the southwest of the Zambezi Delta and least or no sedimentation and erosion to the northeast. The main depocentre is believed to have been between the southern end of the Lower Zambezi Graben and the Beira Basement high.

Figure 6.1 is a schematic representation of the generalised stratigraphy of the Zambezi Delta Basin in dip direction displaying the most important regional depositional and structural features mapped in this study and known from the literature. This figure also illustrates folding at the bottom of the section northwest of the Beira basement high. The folding observed here may be related to basement structural features not resolved by seismic data studied here or may be related to not jet proved Jurassic salt and or shale movement at the bottom of the sediment succession. Above it is the Lower Eocene turbidite slumping involving Late Cretaceous to lower Eocene sediments. Important in the above figure as well as in Fig. 6.3 is the difference in style between Late Cretaceous - early Tertiary sediment succession and the Neogene - Recent succession, which is an almost structurally undisturbed basinward prograding sediment set. During

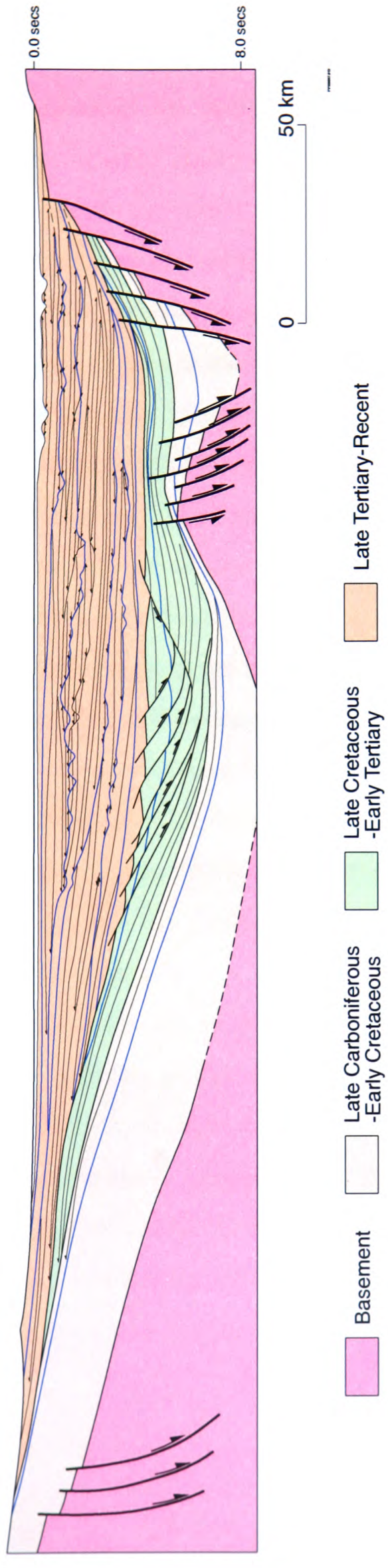

Figure 6.3: A schematic geological cross-section across the Zambezi Delta Basin along strike, summarizing the main geological features of the basin, highlighting the stratigraphic subdivision introduced in this study. For location see Fig. 6.2.

deposition of the upper deltaic succession, the shelf break advancement to the sea is thought to have exceeded 100 km.

Tertiary sedimentation in the Zambezi Delta Basin is characterized by deltaic development which started earlier in Late Cretaceous in the onshore part of the basin. Sediment supply increased considerably during the Tertiary after the Top Eocene unconformity and added to the main factors controlling sedimentation in the basin. The increase in sediment supply may have been caused by tectonics in the drainage basin inland. Basin subsidence accelerated in the Eocene when sedimentation rates of about 200m/my and more are recorded at some locations in the Zambezi Delta Basin.

Subsidence data (Chapter 3) show that wells Divinhe-1, Sofala-1 and Nemo-1 recorded a different sedimentation and basin subsidence history from the remainder of the wells studied here (Figs. 6.4; 6.5). The subsidence curves for these three wells are convex, differing from the remainder, which are concave. The convex shape seems to be in line with declining sedimentation rates observed in the three well locations for the period from late Cretaceous to Recent times. From the geographic position of these wells it can be suggested that the declining sedimentation rates with time may be related to the position of sediment source and with the changing flow path of the Zambezi River during this period caused by East African Rift tectonics onshore.

East African rift tectonics will have affected sedimentation and deltaic development in the basin between 55 and 38Ma with variable periods of relative sediment starvation at different location in the basin (Fig. 6.4). This is probably the time when the Zambezi River changed its flow path from a position along the Lower Zambezi graben eastwards to its present position (Fig. 1.1), possibly due to tectonic fault reactivation in the area. Higher sedimentation rates are recorded in the northeastern part of the basin, wells Sengo, Sangussi, Zambezi-1 and Zambezi-3.

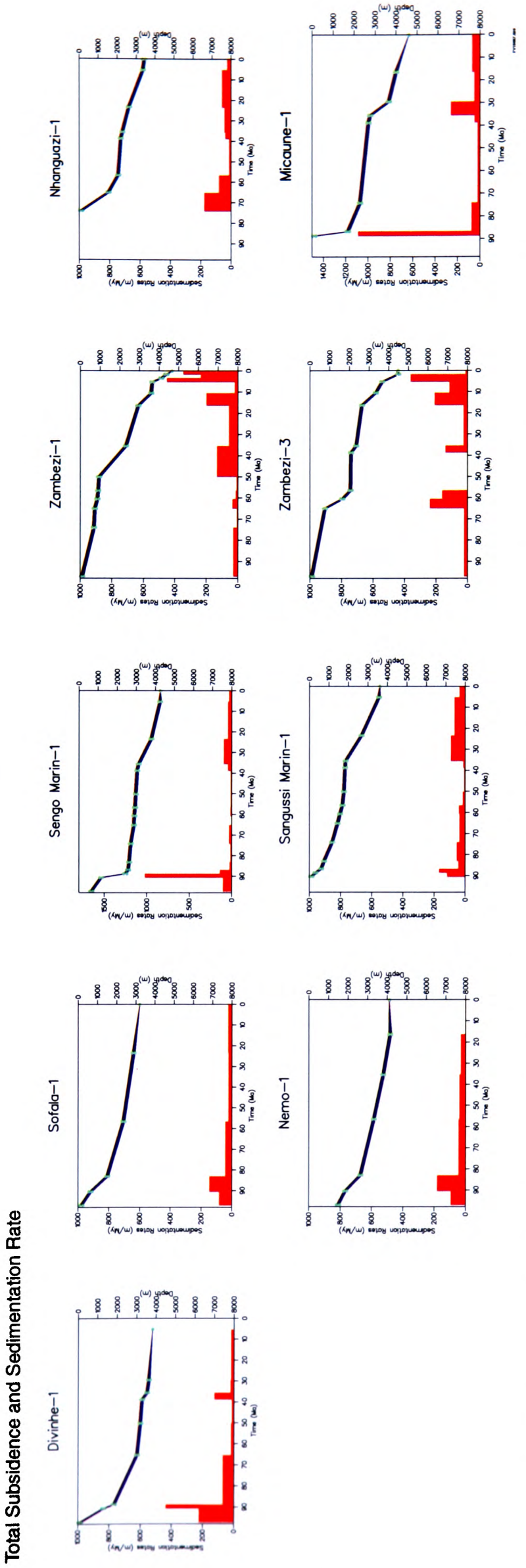

Figure 6.4: Total subsidence and sedimentation rate curves derived from well data for nine wells used in this study.

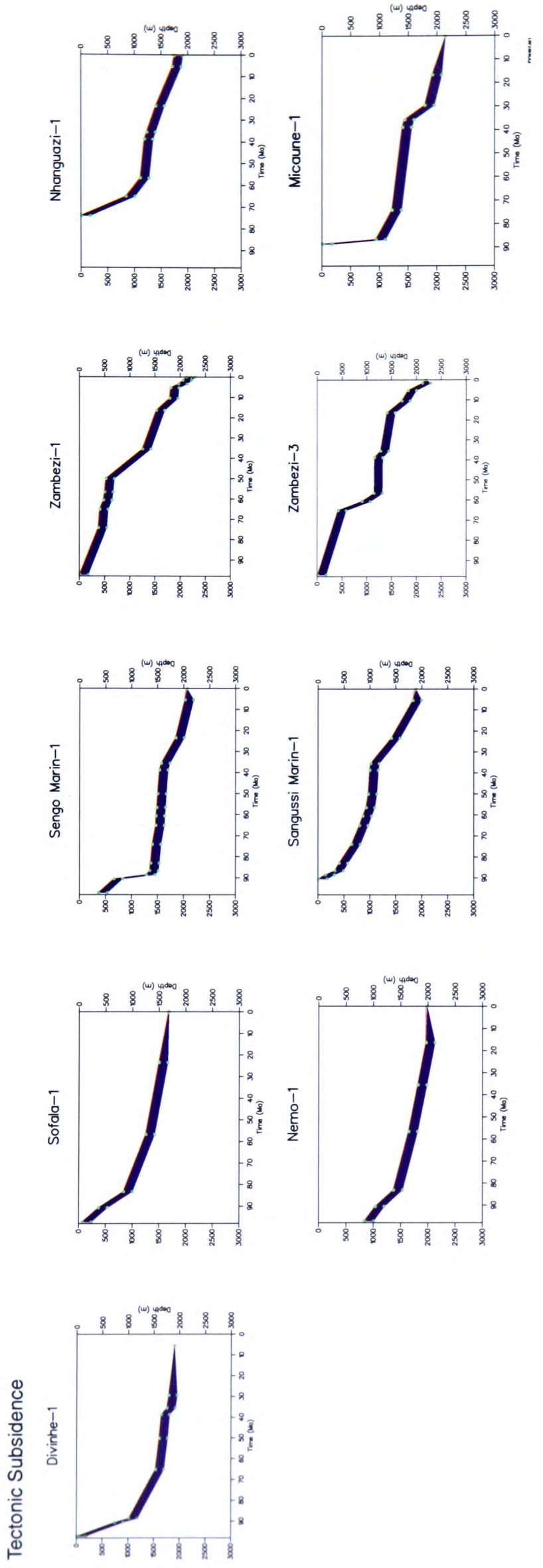

Figure 6.5: Tectonic subsidence curves derived from well data for nine wells used in this study.

6.2.1 The Beira basement high and the East African Rift active extension.

The thin crust beneath the Zambezi Delta Basin determined from gravity modeling (Chapter 4), seen in the context of regional tectonics (Chapter 2) suggests that a kinematic model similar to the one presented in Fig. 2.27 might be applicable to the east African continental margin. "3" in that figure would be the site of the Zambezi Delta Basin, with the rift setting and continental breakup being established in Middle Jurassic times. The Beira high and a structural low to the north (the Zambezi Delta active graben) may have been established at this time. Subsequently the Beira High may have subsided to its present depth during thermal coolling in Cretaceous times. The graben structure to the north at the centre of the northestern depocentre of the Zambezi Delta Basin was reactivated during the East African Rift in Neogene times and remains active at present.

In this study, three distinct styles in sedimentation are identified and are ilustrated in Figs. 6.1 and 6.3. They represent different phases of basin development and are separated by major depositional hiatuses of regional extent.

The Beira High is a structural high of Jurassic age. It is probable that it was produced during continental breakup and is therefore related to the departure of Antarctica and Australia south and southeastwards respectively.

The graben structure mapped on seismic data to the northeast and named here the East African rift active extension may also be a by-product of continental breakup, which was reactivated during the East African Rift in Middle Tertiary times and is still subsiding at present. These are the two main depocentres of the Zambezi Delta Basin, which are both structurally controlled.

6.2.2 Basin depositional architecture.

From the the early stages of the opening of the Mozambique Basin in Middle - Late Jurassic, sedimentation will have been dominated by various factors within the Zambezi Delta Basin. It seems that during the early stages, accommodation

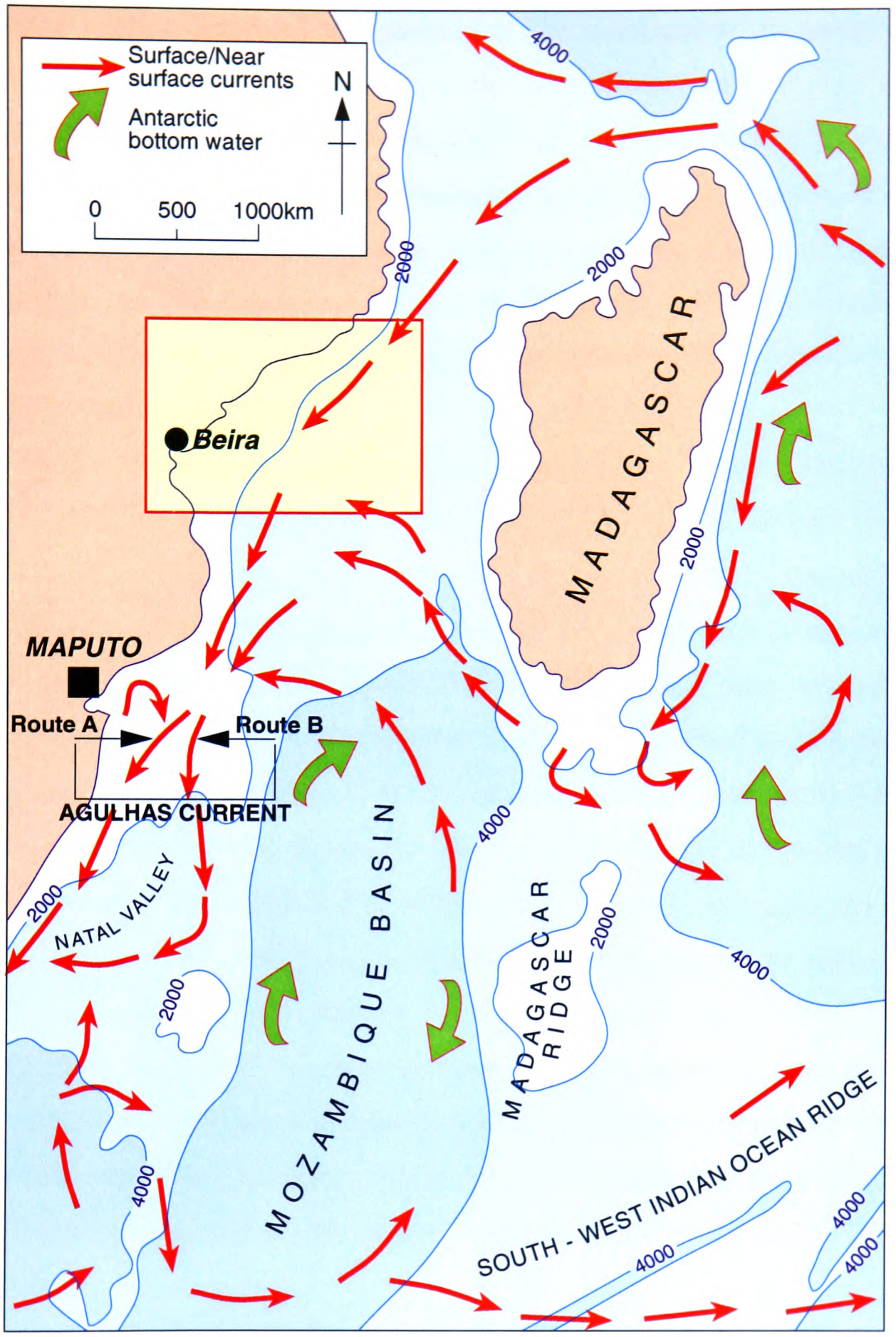

Figure 6.6: Map of ocean water circulation in the Mozambique Channel and south-western Indian ocean, redrawn and modified after Martin, 1984.

space created by the departure of Antarctica from southeast Africa was available within a large scale "pull-apart" setting southeast of the Lower Zambezi Graben which will have acted as the main sediment conduit to the basin from the west and northwest. The seismic data suggest that at the same time a relatively small

depocentre became active at the position of the northeastern depocentre (i.e. the EAR active extension). Sediments to this depocentre may have been from a different source in the northeast. Gradually these two depocentres will have been linked with sedimentary processes developing in both sector at the same time. Different subsidence rates during the deltaic development in Tertiary times will have allowed the two depocentres to behave differently, causing sedimentation to switch between depocentres producing along-strike variability observed in the Neogene to Recent succession.

Oceanic circulation in the Mozambique Channel (Fig. 6.6), established after the opening of the Channel during Late Cretaceous to Middle Tertiary (Martin, 1984) is an important factor to consider while seeking a better understanding of sediment dispersal and redistribution during the various sedimentation cycles in the Mozambique Basin in general and in the Zambezi Delta Basin in particular. Since the establishment of the Mozambique Channel, the surface and near surface currents and the Antarctic bottom water circulation will have influenced sediment dispersal and redistribition within the Mozambique Channel and in the Indian ocean in general. The erosional and sedimentation pattern we might observe in the sedimentary record today may shed light upon activities of the above water currents throughout geologic history. As currents are common to all oceans, some understanding of the interplay between them and other factors controlling sedimentation and sediment dispersal in Zambezi Delta Basin might hold the key for a better understanding of the geologic history. However, sedimentation in the Zambezi Delta Basin remain dominated by sedimets delivered by the Zambezi River system.

6.2.3 Distributary Channels.

Distributary channels played an important role during Tertiary deltaic sedimentation in the Zambezi Delta Basin. The regressive and transgressive cycles recorded in the basin separate depositional units very often characterized by incised channels and channel valleys in different parts of the basin. During Tertiary times these features generally started earlier in the northeastern depocentre

and diachronously migrated southwestward, along strike, to the southwestern depocentre. This southwestward migration in deltaic sedimentation generally follows the migration of sedimentation to previously sediment starved areas of the basin where non-deposition and erosion (depositional hiatus) and sediments laid down during the previous depositional cycle were removed.

In this study and in respect to channel and channel valley-related erosion observed in the Zambezi Delta Basin, deltaic development is believed to have started in late Cretaceous times and, two distinct periods are identified. The First period includes late Cretaceous to Upper Eocene successions, and the second is composed of all post-Eocene deposits. However, Coster *et al.* (1989) (Fig. 2.26) suggests Early to Middle Tertiary times for the beginning of the Zambezi deltaic development. This difference in geological time may be due to various factors, of which the differences within the various well data interpretations produced by Salman *et al.* (1985), Droz and Mougenot (1987) and others, and the way geological age data from wells is tied to seismic sections may be the main cause. This study is based on its own revised well log and well top determinations.

The first period of delta development is characterized by deposition of fan deltas from two main delta fronts, one advancing northeast (presumably from the Save River) and another advancing southeast (from the Zambezi River), which lasted until Upper Eocene times. This period has no significant channel activity recorded in the offshore area of the basin studied here. However, sedimentation was dominated by sediment inputs from the Save River, with sediment wedges showing a strong progradational component from the southwest into the southwestern depocentre of the Zambezi Delta Basin. Erosion during this period was widespread, at times with relatively little sediment preservation during Palaeocene and Eocene times across the basin.

The second period covers the post-Eocene period, with channel and channel valley dominated sedimentation. Rapid sedimentation returned to the basin during Oligocene times when the Zambezi River is thought to dominate over the Save River delivering lots sediment into the basin. The relevance of the Save sediments is thought to have decreased to a minimum at late Middle Miocene

before the most recent late Tertiary to Recent times sediment increase into the basin. Channel activity on the slope and upper slope area was more evident in the early Upper Miocene, when several stacked channel valleys were developed are observed in the northeastern depocentre. This was a time of erosion in the sediment-starved southwestern depocentre (Figs. 4.34; 4.35). Several cycles of channel switching, most of which started in the northeastern depocentre and migrated to the southwest, are recorded in Neogene times. The amount of sediment preserved in each cycle is variable, and is at times dependent on the erosional activity in the slope and upper slope areas.

However, there were significant river drainage changes in the northeastern part of the basin, presumably by distributaries of the Zambezi River or other short-lived rivers. This was particularly prominent during late Palaeogene and Neogene times when wide drainage channel valleys were incised into older sediment. Droz *et al.* (1987) suggested this to have been a very important sediment bypass area during a sea level lowstand in Neogene, which fed the Zambezi Canyon and the Mozambique Upper Fan. This area migrated with time soutwestwards along the main depositional strike to the present position of the Zambezi delta active graben in the northeastern basin depocentre, preserving a considerable seaward (southward) prograding sediment wedge.

At the present time, erosional channels are minor in the southwest while in the northeastern depocentre several deep cutting, incised channel valleys can be observed just above the subsiding graben strcture. The location of the four channels is believed not to be a coincidence but is thought to be triggered by the underlying fault activity which is driving this part of the basin to subside at present and sediment deformation is observed in the upper deltaic succession. Relatively strong seismic episodes recorded in the area between 1977 and 1995 support the idea of active faults in the graben structure. However, faults can not confidently be traced to the sea bed because of the data quality, but sediment disruption and deformation features right across the structure go beyond features which could be caused by velocity attenuation caused by the water collumn above.

The size of the channel and channel valleys observed in the basin is variable,

but generally the widest features are observed in the northeastern depocentre during Middle and Upper Tertiary times.

6.2.4 Upper slope instability.

The upper slope failure involving sediments of Palaeocene to Middle Eocene age could be due to various factors among which tectonic reactivation of old faults beneath the sediment pile or upper slope, instability caused by sediment dewatering after shoreface exposure at sea level lowstand could be the main reasons.

In the Zambezi Delta Basin, slope failure occurs along major and minor erosion surfaces which share a common decollement surface, the Top Turonian unconformity. Sediments involved in mass movements down slope consist

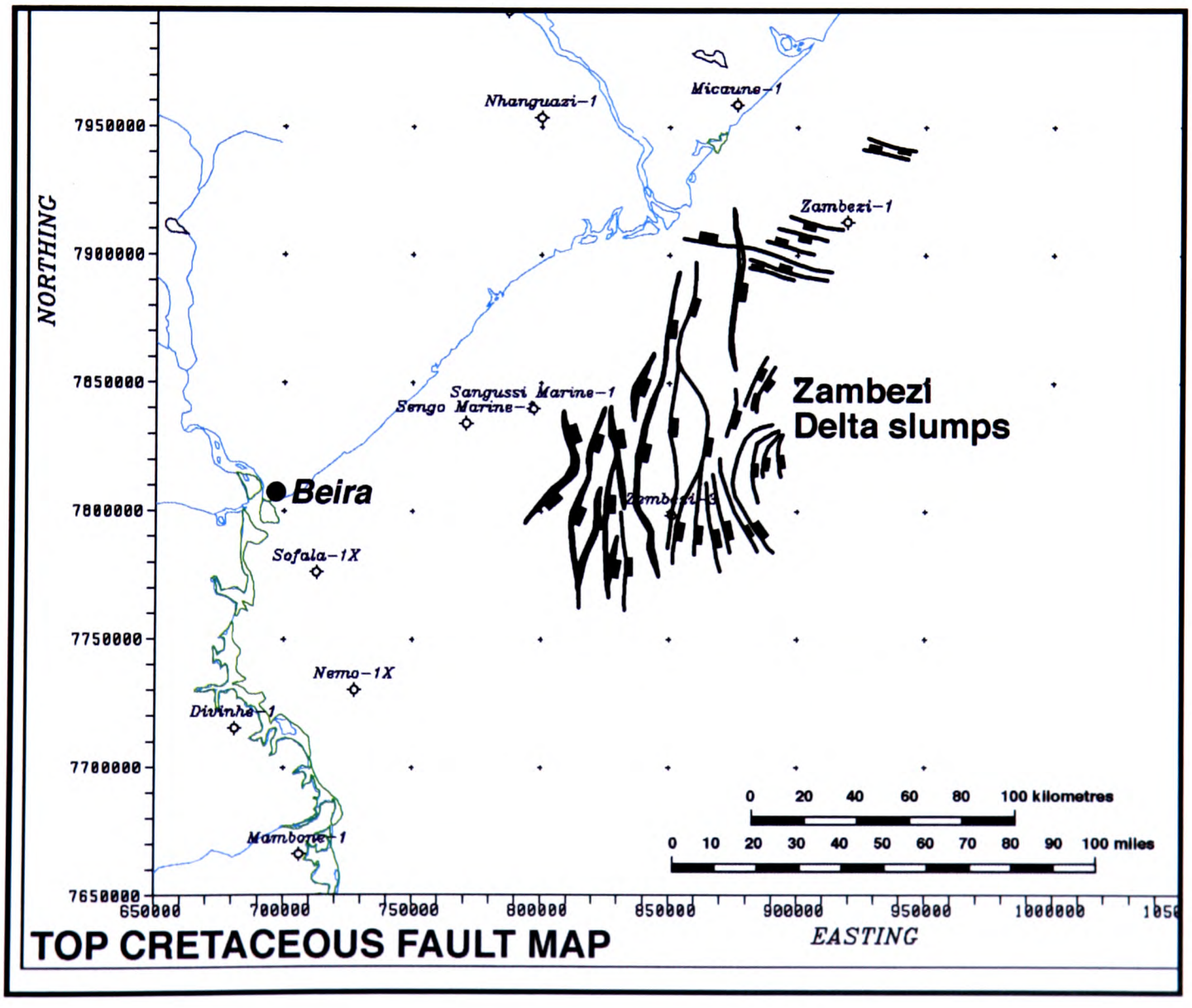

Figure 6.7: Fault map of top Cretaceous unconformity, displaying the Zambezi Delta slope slumps involving turbidity deposits. Figure zoomed from Fig. 4.21.

largely of these turbidity deposits from the northwest which preceeded slope failure. This unique slumping event is only observed in the southwestern depocentre where turbidity deposition occurred may represent the most important hydrocarbons related structural feature in this delta basin. Slumps are well known in other delta systems for providing with important reservoir traping mechanisms.

The slumps in the Zambezi Delta Basin have been identified as such for the first time in this work and should be examined for their future exploration potential and drilling activities in the basin. Unfortunaltely no wells penetrate the slumps; the Zambezi-3 well drilled in the seventies, fell a few hundreds of metres short of the slumps. Future wells in the area should target areas of the hanging wall of the slumps and possibly the strata underneath to probe the possibility of Jurassic salt occurrence in the basin.

In some well studied deltas (Gulf Coast, Niger and Beauforth-Mackenzie) rollover anticlines are often related to salt and/or shale diapiris, which does not seem to be the case in the Zambezi Delta Basin, where the timing of the slumping event is nearly coincident with the onset of the East African Rift in Neogene times. However, it can be also sugested that a long wavelength and low amplitude fold observed underneath the slumps could be related to unknown Jurassic salt movements which could have triggered the slumping of turbidites in Neogene times. This latter hypothesis remains to be tested by future drilling activities in the basin.

6.3 Strike variability of depositional units.

6.3.1 General characteristics.

Strike variability in clastic depositional systems is caused by varying sediment supply to the depositional system. Although it is well known that both sediment supply rates and accommodation space are temporally and spatiatially variable parameters, they have not always been accounted for in seismic and sequence stratigraphic evaluations that often consider systems tracts to have chronostratigraphic significance. Variations in sediment supply have a number of important

implications for seismic and sequence stratigraphic interpretations. One of the most important implications is the spatial variability in sediment supply, which may produce a wide range of coeval stacking patterns. Different and more complex stratal architecture might be expected to be the norm in different areas of deltaic basins like the Zambezi. Fig. 6.8 shows diagrammatically the possible behaviour of a stack of delta lobes that successively step obliquely sideways along a coast. In the case of a basin with variable along strike suply may lead, the overall progradational depositional units deposited during highstand conditions in one locality (Fig. 6.8A), and an overall retogradational depositional unit deposited during transgression (Fig. 6.8B) typical of a transgressive depositional unit in the seismic and sequence stratigraphic methodology (Martinsen and Helland-Hansen 1995; Church and Gawthorpe 1997) in another location. Consequently,stacked depositional units will appear to step in opposite directions in cross sections at different locations in the basin.

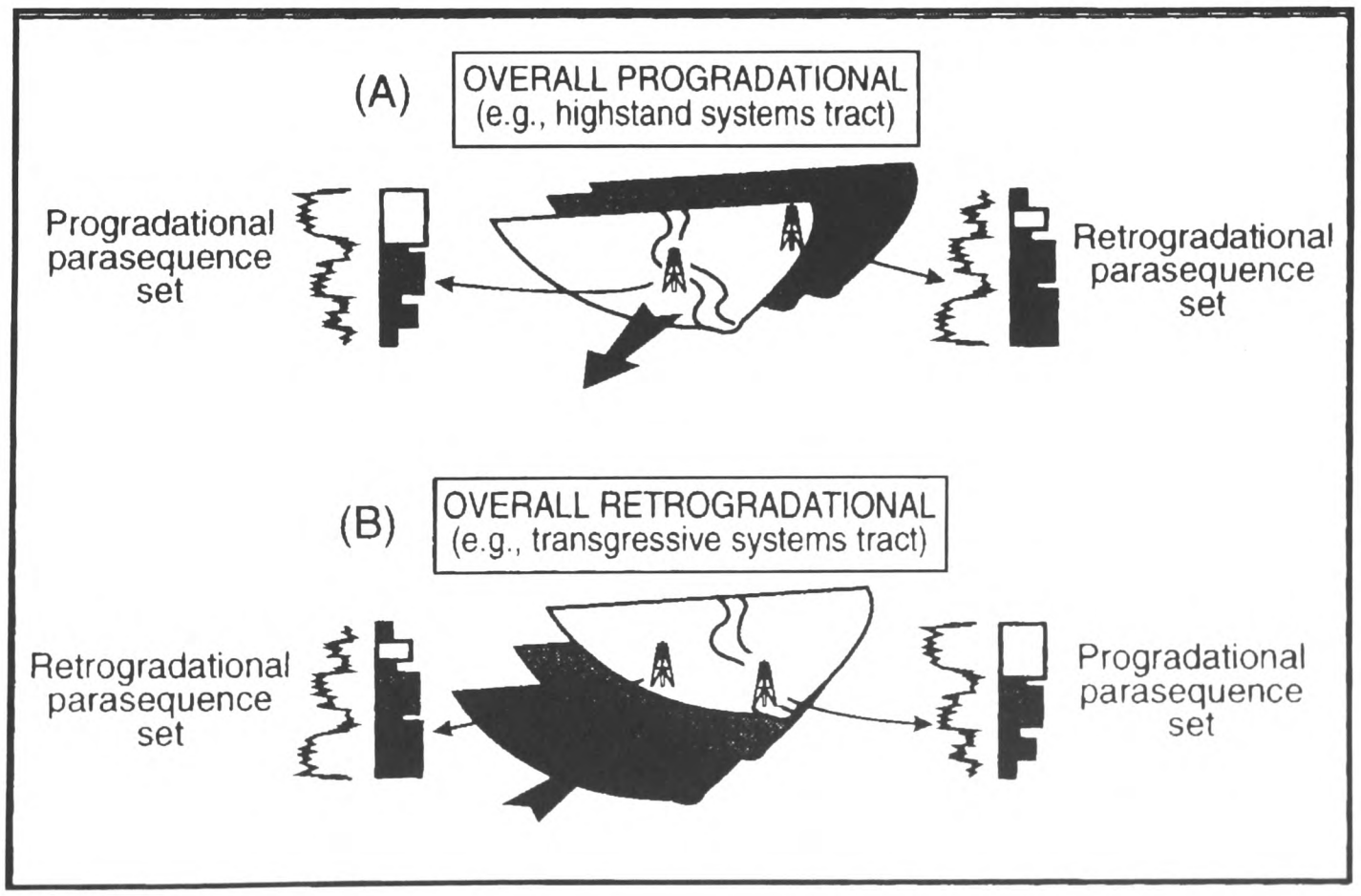

Figure 6.8: Conceptual diagram of delta lobes that creates oppositely arranged stacking patterns depending on location within the depositional system, after Martinsen and Helland-Hansen (1995).

Examples of coeval patterns caused by the spatial variability in sediment supply in clastic depositional systems are known from the Late Namurian of northern England (Church and Gawthorpe 1997), Montana and Wyoming in the United States (Gill and Cobban, 1973; Martinsen and Helland-Hansen 1995) and now in the Zambezi Delta Basin (this work).

The identification and recognition of these contrasting stacking patterns is very important because seismic and sequence stratigraphic models in use are commonly two-dimensional and use as a basic premise the fact that particular stacking patterns are tied to specific sections of the sea-level curve. This is commonly thought to be a good method for predicting variability in depositional-dip sections (Martinsen and Helland-Hansen 1995). However, the spatial and temporal variability of sediment supply and accommodation space must be considered. Consequently seismic and sequence stratigraphic methods are often less reliable in predicting strike variability.

Sediment supply and its spacial and temporal variability is very important controls in producing regional and local progradational and retrogradational stratal stacking patterns in clastic depositional systems. The way the incoming sediments enter the basin (point or line source), sediment volume and the interplay between river outflow processes and basinal energy and the geometry of the receiving basin are amongst the most significance factors on which dip and strike sequence variability depends in, for example, foreland basins and deltaic settings. Line sources are characteristic of high energy wave dominated depositional systems with sediments generally supplied along strike. However, point sources are characteristic for most deltaic depositional systems and sediment source switch is very common.

6.3.2 Zambezi Delta along-strike variability.

It has been observed in this study that the Zambezi Delta Basin developed in various stages characterized by spatially and temporally variable sediment supply rates causing significant along-strike variability (Fig. 6.9). Sedimentation in the basin at the end of Turonian was dominated by two line sources, one in

the southwest and another in the northeast of the basin, as derived from seismic interpretation (see Volume II, this work). During this time basinal energy was relatively high and part of the sediments reaching the basin from both sources was reworked and redeposited along strandlines in the coastal area. Progradation continued on both fronts during Senonian times apparently with diminished basin energy and low sediment supply in the southwest. The decreasing sediment supply during Senonian transgression caused the shoreline to retreat in the central part of the basin.

High wave energy returned to the basin during Palaeocene times when high sedimentation rates are recorded in the northeastern part of the basin. However, relatively low sediment preservation in the southwest might be linked to

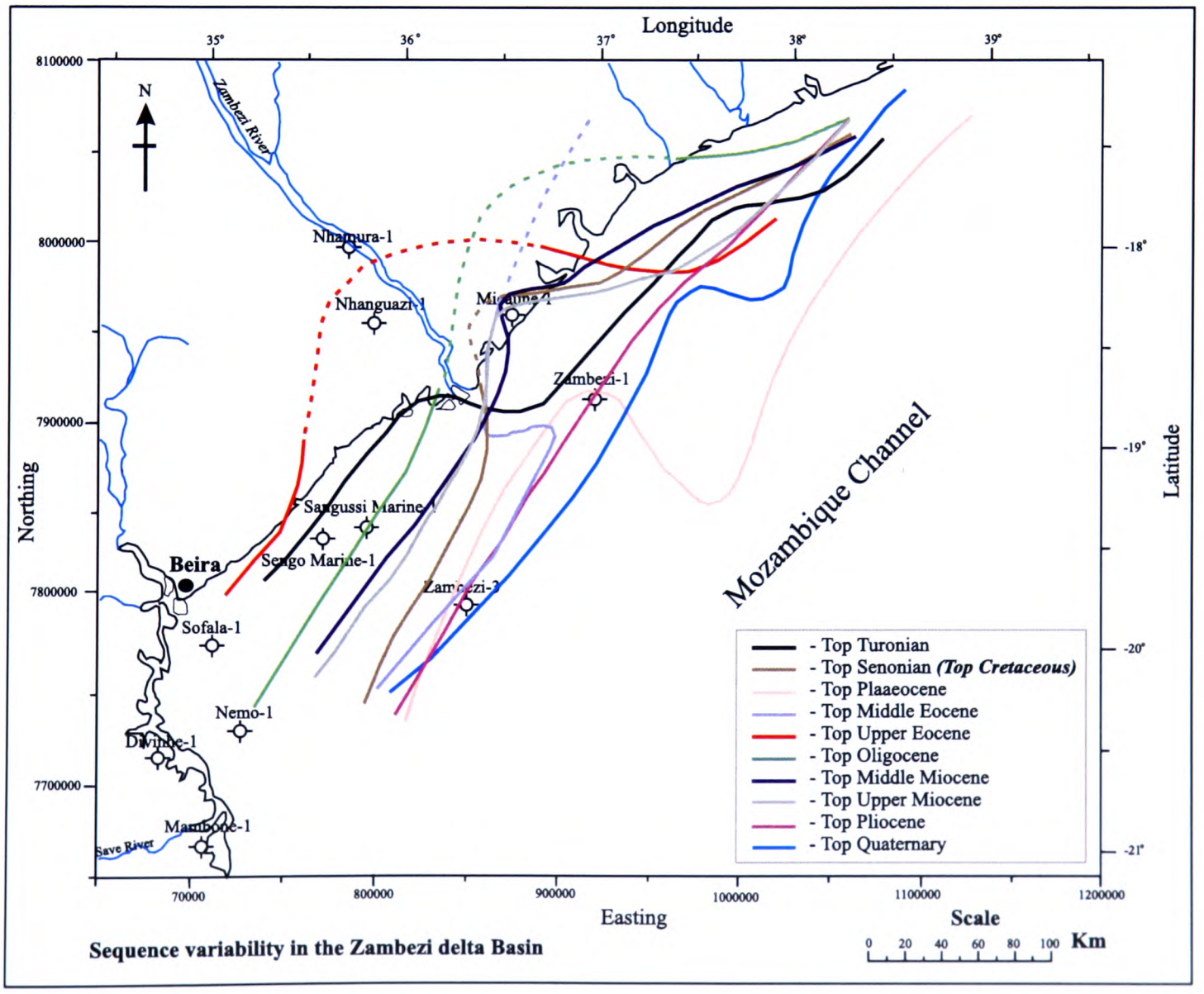

Figure 6.9: Approximate position of shoreline for various stages of deposition between Turonian and the present day.

decreasing sediment supply to this particular part of the basin during Palaeocene (Fig. 6.9). Shoreline advance to the sea was minimal in the southwest, while it reached its overall maximum advance in the northeastern depocentre (Appendix A, Fig. A.8).

Sediment preservation is very poor for the Lower and Middle Eocene megasequence. Widespread exposure and erosion of the shoreface left very litle evidence of Lower and Middle Eocene sedimentation in the basin (Appendix A, Fig. A.10). It is possible that during this time the line source to the north in the previous depositional periods was cut off, possibly signaling the onset of the East African rift system in the onshore sediment source area. The top Middle Eocene unconformity is of regional extent and is more noticeable in the northeastern part of the basin where complete sections of Lower and Middle Eocene stratigraphy have been removed. These sediments will have been redeposited in areas down dip in the basin, which are in the deep water environment at the present time, and they may constitute important prospects. It is suggested here that ocean currents circulation may have been important during periods of high basinal energy and during periods of shoreface exposure and erosion. However, evidence for the above suggestion from seismic data is not clear and deep water seismic data (not available in this study) may show some evidence of ocean circulation and its role in sediment reworking and redeposition.

Sediments reached the basin through two point sources in Late Eocene, one in the southwest and another in the northeast. Again basinal processes during deposition of the Upper Eocene megasequence were less important than fluvial processes (Fig. 6.9). The two point sediment sources continued active during deposition of the Oligocene megasequence. The source to the southwest was more charged with sediments than the one to the northeast where apparent transgression is recorded during this time period caused by reduced sediment supply. This is thought to be the time when basin (wave energy) based processes regained control of the Zambezi Delta depositional processes.

In Early and Middle Miocene times two line sources reached the basin from the northeast and the southwest with a relatively small point source active just

northeast of the present day Zambezi River mouth (Appendix B, Fig. B.2). The latter source possibly signals the beginning of the activity of the Zambezi River in this particular part of the basin, which stabilized delta slope formation. The shoreline advanced from both fronts east- and basinward. This type of development continued during deposition of the Upper Miocene megasequence. After the top Middle Miocene unconformity, deposition continued in the basin, starting in incised valleys and channels in the northeast (Fig. 4.35).

A one-line source system was in place during deposition of the Pliocene

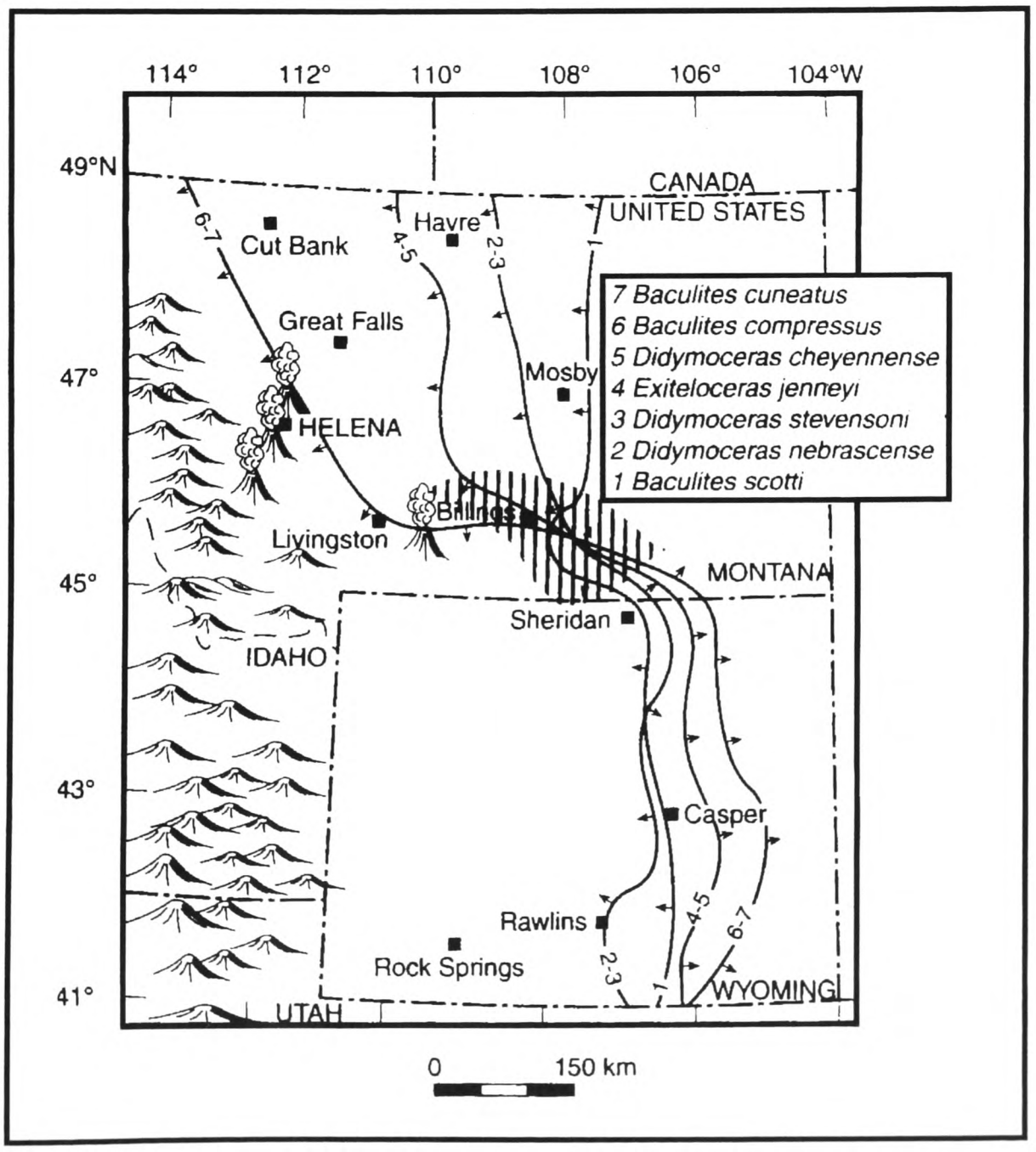

Figure 6.10: Approximate position of strandlines during transgression (Beaupaw transgression) in Montana, northwest United States, after Gill and Cobban (1973). Arrows showing the direction of strandline movement. Shaded area is the complex strandline cross-over zone.

megasequence, with most sediments reaching the basin from the Zambezi River in the central part of the basin (Fig. 6.9). Basinal processes are clearly the most dominant during this phase of basin development (Appendix D, Fig. D.2).

The deposition of the Quaternary megasequence was predominantly through a two point sources with the Zambezi River possibly acting as the main source in the southwest, while another source reached the basin from the northeast. This caused progradation to progress faster in the northeast, while the southwestern front was left behind with very little basinward advance of the shoreline.

It is clear from the above picture that the Zambezi deltaic complex can be

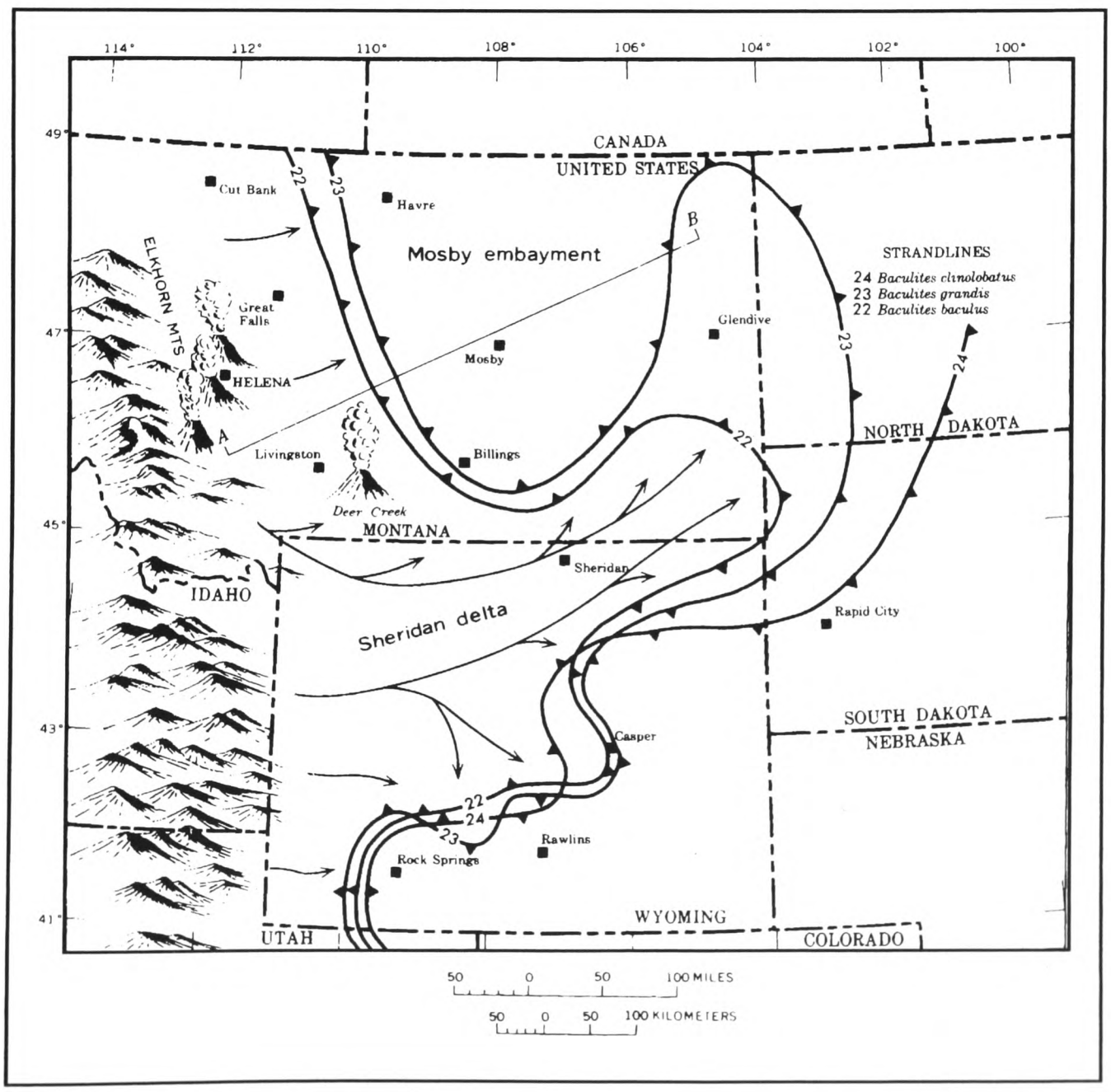

Figure 6.11: Approximate position of strandlines during the initial phase of regression (Fox Hills regression), after Gill and Cobban (1973).Barbs show the direction of strandline movement. Cross-section AB not shown here.

subdivided into two main depocentres and that the basin evolved from an intially wave-dominated depositional system to a fluvial-dominated system in Late Eocene and Oligocene and back to a wave-dominated system from Early/Middle Miocene until recent times. During deltaic build out, coeval stacking patterns developed in the Zambezi Delta. Coeval transgressive and regressive depositional systems (transgressive and either highstand or forced regressive) systems tracts respectively developed particularly at times when point sources were active in different parts of the basin with different sediment charge causing progradation at one location whilst retrogradation was recorded at other locations in the basin.

The relationships displayed by the shoreface position through geological time confirm the very complex stratigraphic relationships highlighted in Figs. 4.34 and 4.35 in Chapter 3. The cross over areas displayed on Fig. 6.9 represent the areas of most complex stratigraphic relationships between the strata of the various depositional units resulting from distinct sediment supply rates varying in time and space. Similar stratal relationships displaying strike as well as dip sequence variability have been discussed by Gill and Cobban (1973) (Fig. 6.10), Martinsen and Helland-Hansen (1995) (Fig. 6.11) and Church and Gawthorpe (1997) (Fig. 6.12). Figs. 6.10, 6.11 and 6.12 are examples of coeval transgressive and regressive sequences in Montana, northwest United States respectively, where preferential progradation or regression is coeval with regression during time of overall sea-level rise (Figs. 6.10 and 6.11).

The results of this work are a test of the validity of the traditional seismic and stratigraphic methodologies which rely on the basic premise that strata are always related to a specific section of the sea-level curve (Posamentier 1988; Van Wagoner 1990). As discussed before, this method fails to take account of the spatial and temporal variability in rates of sediment supply and the evolution of accomodation space in order to address successfully the stratigraphic complexities characteristic of clastic depositional systems.

Current results on the Zambezi Delta depositional system emphasize the need for a careful account of current seismic and sequence stratigraphic methodologies in order to achieve appropriate stratigraphic interpretation, because

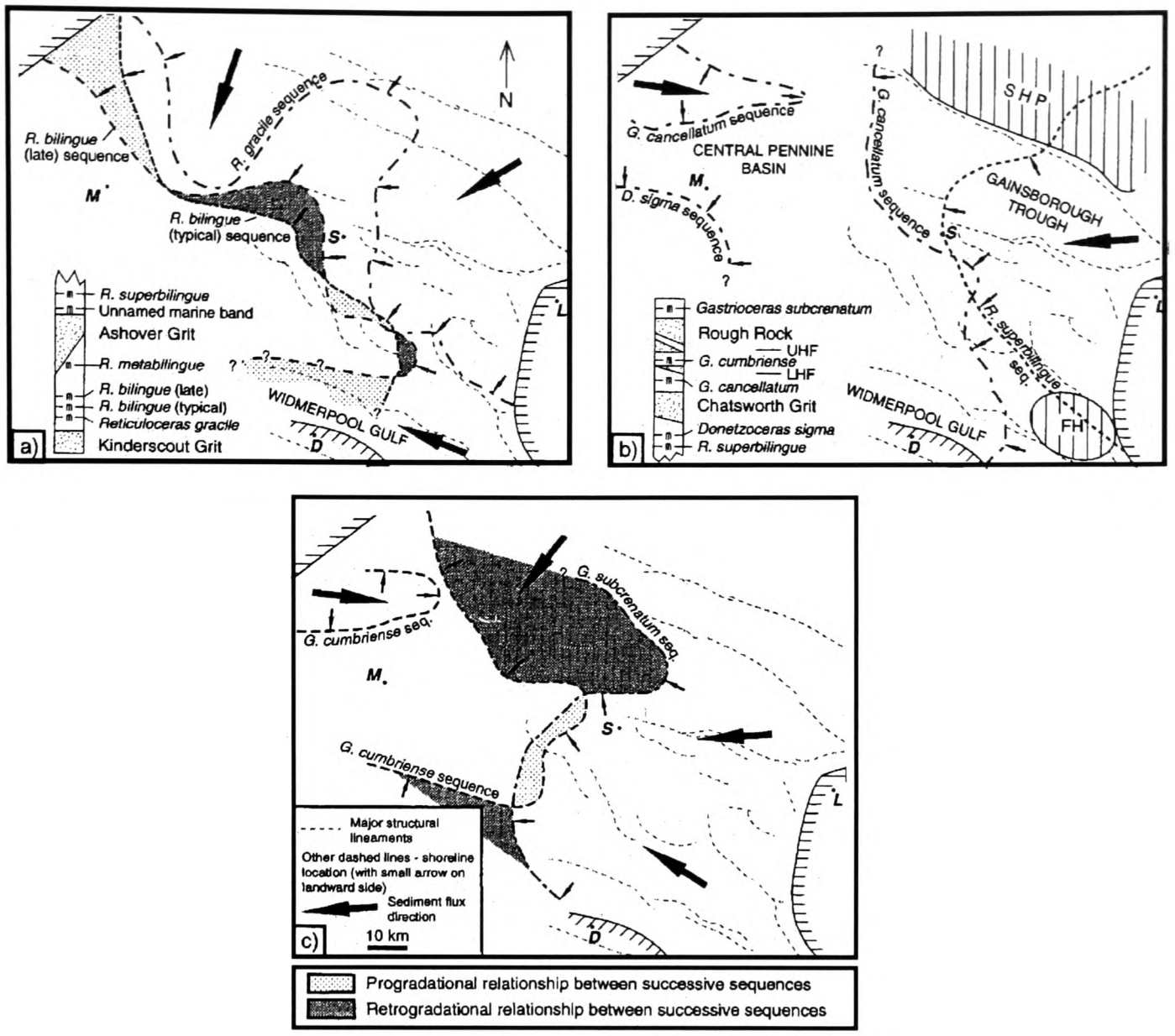

Figure 6.12: The maximum basinward shoreline progradation during highstand of ten sequences recognized in the Marsdenian/Yeadonian, redrawn from Church and Gawthorpe (1997). Key: **(a)** R. gracile to R. bilingue (late) sequence highstand shorelines, **b** R. superbilingue to G.cancellatum sequence highstand shorelines and **c** G. cumbriense and G. subcrenatum sequence highstand shorelines. Vertically hatched areas indicate non-deposition of highstand.Horizontal dashes in the far northwest and southeast represent the limits of Marsdenian/Yeadonian outcrop and deposition respectively. Diagonal dashes to the north and east of Derby represent the top Namurian subcrop to Permian. FH, Foston High; SHP, South Humberside Platform; D, Derby; L, Lincoln; M, Manchester; S, sheffield.

current perception that systems tracts are isochronous is not always consistent. Therefore the results achieved and discussed in the present work make an important contribution to the debate on the validity of currently used systems tracts models, because the present results clearly demonstrate that the current perception does not apply to the Zambezi Delta system, where transgressive systems tract are often coeval with highstand systems tract for example. Therefore, care needs to be applied in distinguishing between interpreting transgressive versus

highstand systems tract and the description of retrogradation versus progradation.

6.4 Implications for basin stratigraphy, reservoir facies distribution and quality.

It is evident that sedimentation is influenced not only by onshore tectonics, which largely controlled sediment sources, but also by thermal subsidence, eustasy and sediment load controlling basin subsidence offshore. The high frequency cyclicity characteristic of the upper section of the delta in combination with sedimentation switch between the two main depocentres produced a sediment fill which is complex in detail.

The relationship between facies from different depositional units building depositional unit sets represents at times isolated relatively small formation units (compared to basin scale). As schematically displayed in Fig. 6.13 basinward progradation is dominant during deltaic development. However this is the general trend in dip direction, (Figs. 4.34 and 4.35 in Chapter 3) shows a more complex relationship between depositional units and depositional unit sets than the along-strike section.

Formation units resulting from this style of sedimentation are basinward and generally NE-SW diachronous. This can be demonstrated by dip and sub-dip crossections drawn in the basin (Fig. 4.35). Stratigraphic trap formation is greatly dependent on the strata deposited during flooding events to produce a seal and their stratal relationships with potential reservoir sand formations. Most-favoured plays may well be in the deep water environment, where reworked prodelta sands have been deposited during periods of sea level lowstand as low-stand sand fans on top of probable source rock deep in the basin.

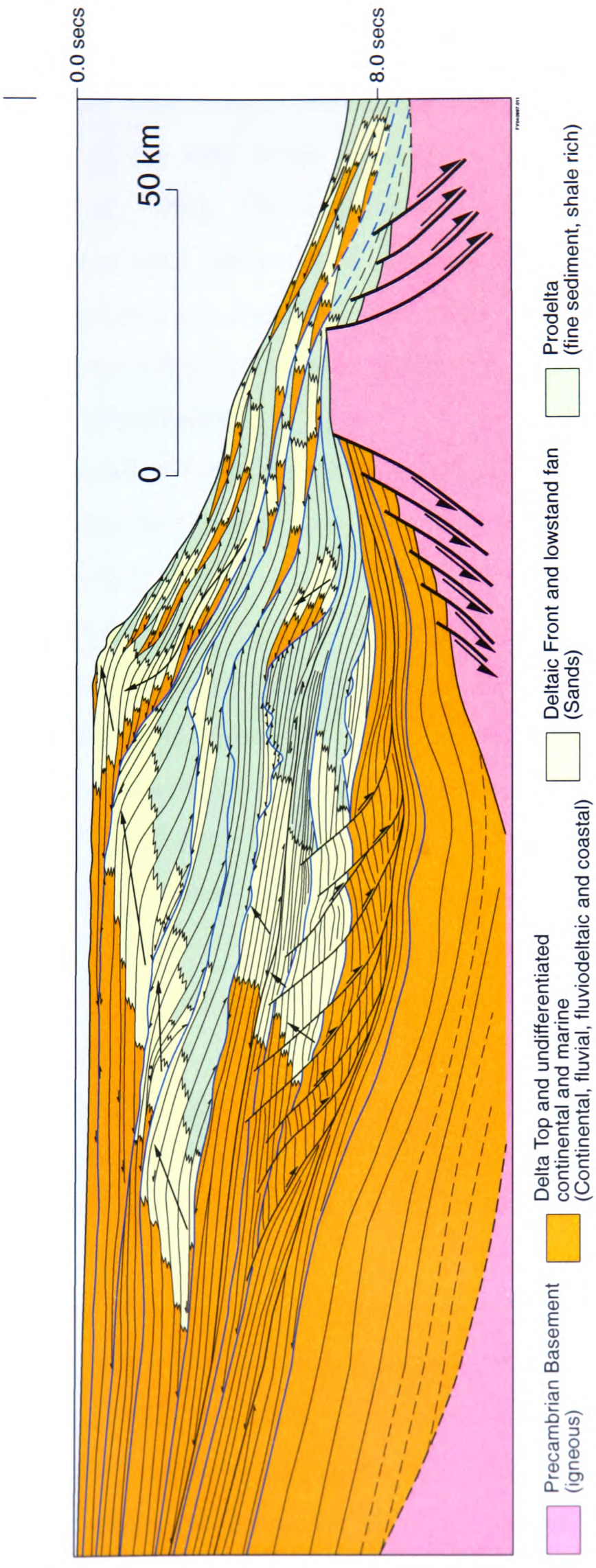

Figure 6.13: Schematic cross-section in dip direction summarizing offshore stratigraphy of the Zambezi Delta Basin. *Arrows represent estimated average summation of aggradation and progradation for distinctive sediment sets.*

6.5 Hydrocarbon prospectivity.

Generally, with only a few exceptions of deltaic basins, post-Middle Jurassic sedimentation in the East African continental margin, is low and in the well oxygenated waters of the shelf where organic carbon preservation is generally poor (Al-Kasim *et al.*, 1985). This might explain why no significant quantities of oil appear to have been generated at the East African continental margin. However, basin configuration during the rift phase (generally in pre-Callovian times) in certain areas could have created moderately anoxic conditions, suitable for organic carbon preservation.

Sediments deposited during the early phases of rifting (mainly of continental nature) would be expected to bear some terrestrial organic matter which would form coal deposits releasing dry gas, as is the case in most Karoo basins (i.e. the Karoo Basin of South Africa and the Middle Zambezi Karoo Basin of Mozambique). In turn, proto-oceanic gulfs, gulfs in "failed rift arms" and subsidiary near meridional rifts, would be expected to contain marine organic matter as well as terrestrial derived cutins and surface waxes, which is more oil-prone. The subsequent deposition of this more oil-prone organic matter, would have taken place in relatively anoxic conditions, which would help preservation prior to burial. However, in areas with relatively high heat flow during the syn-rift gulf stage of basin evolution there would be a possibility of over-maturation and destructive transformation of oil to gas. This is not the case in the Zambezi Delta Basin. In areas with relatively lower heat flow, a thermal history suitable for oil generation and preservation should be expected. Oil generated in these areas could be found in intercalated sand reservoirs, often characteristic of the stratigraphic record in eastern Africa.

According to Al-Kasim *et al.* (1985) the stratigraphic record of "Persian Gulf basins" shows active faults at the basin margins during deposition suggesting that intercalations of reservoir sands within the source shale section should be expected. This is similar to observations made by Al-Kasim *et al.* (1985) in the Ngerengere deltaic sands and the marine Lower Jurassic to Bajocian shales of the Selous-Ruvu rift of Tanzania and in the Isalo sands and Lower Jurassic shales of

Madagascar with similar geohistory.

The open ocean circulation attained after the opening of the western Indian Ocean will have provided the marine depositional environments with well oxygenated conditions, thus leaving very little organic matter preserved for burial. This fact would explain the absence of large oil accummulations in the East African region. The mouths of major rivers, which existed for long periods of time in the region, (i.e. the Rufiji in Tanzania, the Rovuma, the Zambezi and the Limpopo Rivers in Mozambique) may be the only exceptions, where high rates of sedimentation may have prevented degradation of oil-prone organic matter by oxidation.

6.6 Comparison of the Zambezi Delta Basin to other delta basins around the world.

6.6.1 Introduction.

Deltas on passive continental margins are important important hydrocarbon habitats because of their orderly and predictable stratigraphy and the obvious interrelationship between stratigraphy and structure. In this section a brief summary of the geological, tectonic and stratigraphic setting of three Tertiary and one Carboniferous deltaic basins is presented. These are the Mississippi (Gulf Coast), Niger (Western Africa), the Beaufort-Mackenzie (Alaska-Canada) and the Western Irish Namurian deltas (Fig. 6.14A, B, C and D). This summary aims at establishing common characteristic features and major geological and tectonic differences of continental margin deltaic basins with which to compare and contrast the interpretation from the Zambezi Delta Basin.

The Tertiary deltas are examples of geologically well studied deltaic basins in a state of oil production, although they represent different stages of exploration and production. The onshore Tertiary deltaic depositional system of the Gulf of

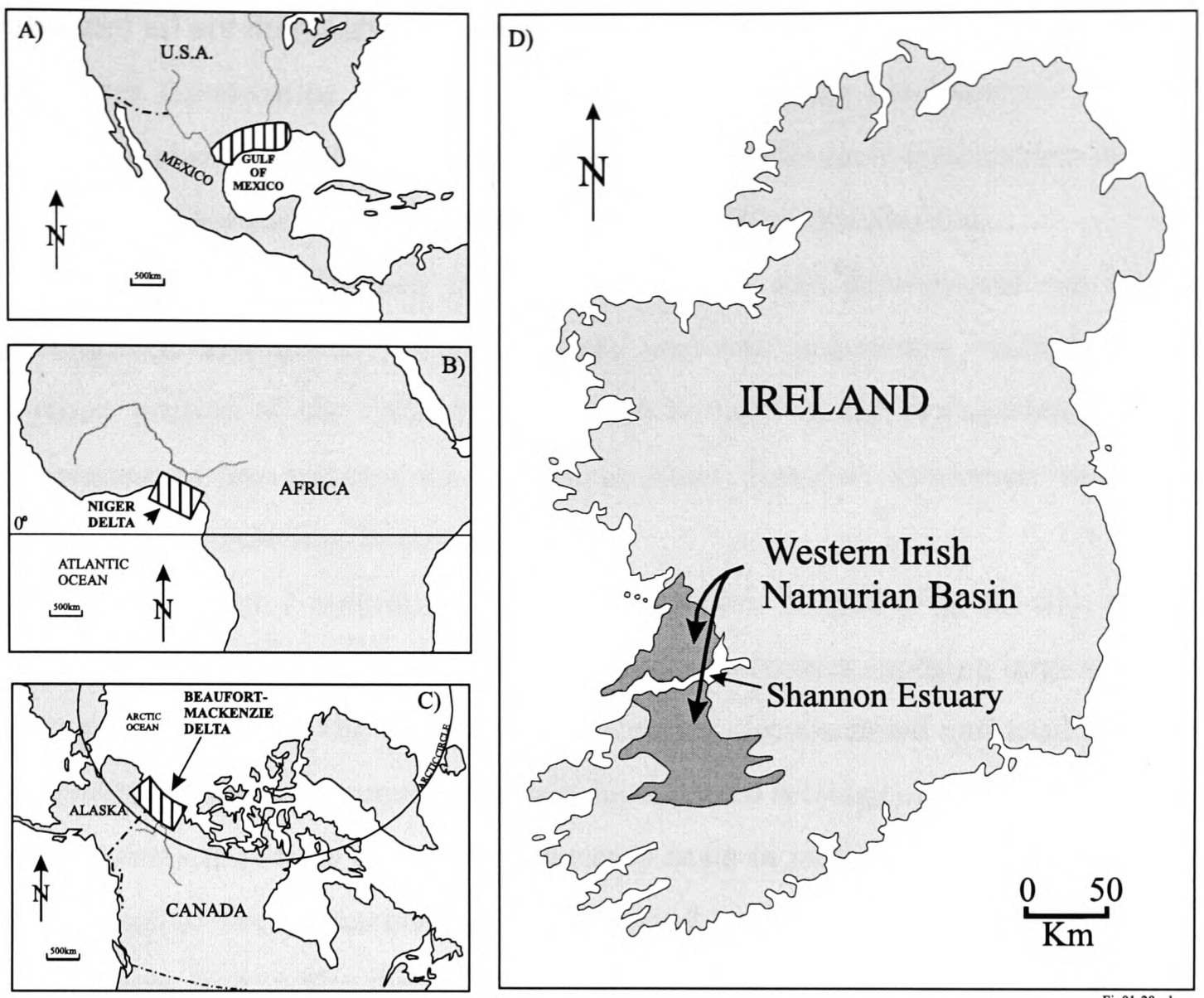

Figure 6.14: Location maps of the Mississippi (Gulf coast), Niger, Beaufort-Mackenzie and the Western Irish Namurian Basin. Key: **A** - Gulf Coast (USA); **B** - Niger Delta (Africa); **C** - Beaufort-Mackenzie Delta (Canada-Alaska) and **D** - Western Irish Namurian Basin (Ireland).

Mexico basin is mature, being highly explored and developed while the Niger Delta Tertiary sedimentary section is relatively less well known and the Beaufort-Mackenzie delta is still a frontier area. The Western Irish Namurian Delta of the Clare Basin is a good example of a well-exposed deltaic succession which is useful in demonstrating that initial depositional structures and sedimentation patterns in deltaic settings reflect basin geometry and the interaction of the main processes involved in deltaic sedimentation. This last example, as will be demostrated, offers *in situ* observation and study of some of the most important depositional features typical of deltaic deposition such as soft-sediment syn-sedimentary deformation, growth and listric faulting, mud slumps and shale diapirism.

Broadly, the three Tertiary deltas are characterized by similar geological fea-

tures and all are dominated by gravity tectonics and by salt and/or shale diapiric structures constituting the main hydrocarbon trapping mechanisms. Deltaic basins are also characterized by an orderly, predictable inter-relationship in time and space of tectonics, stratigraphy and hydrocarbon distribution.

The differences in their stages in exploration and development can be exploited such that the very well-developed and well-understood concepts of the Tertiary portion of the Gulf of Mexico can be used in the exploration and develepement of less matured basins like the Niger, Beaufort-Mackenzie and other similar deltaic systems around the world.

The Western Namurian basin of southwestern Ireland (Fig. 6.14D), a Carboniferous delta basin which underwent Tertiary tectonics exposing large sections of its stratigraphy off the west coast of Ireland is also discussed and used to highlight certain aspects common in deltaic depositional settings observed at outcrop. The depositional styles observed on outcrop scale in this delta basin show many similarities to the sedimentary styles observed on seismic data in the Zambezi Delta Basin, and in the three Tertiary deltas discussed here, as can be found in other delta settings aound the would.

6.6.2 The Mississippi Delta *(U.S Gulf Coast).*

The Mesozoic and Cenozoic of the Gulf of Mexico, of which the Mississippi delta sediments (Tertiary) are part, build the coastal plain and continental shelf that rims the Gulf and is surounded by Palaeozoic and Precambrian basement rocks with prominent older structural features (Fig. 6.15). The tectonic structure of the sedimentary section of the Gulf Coast is dominated by gravity tectonics and is reflected in the interrelation of stratigraphy and structure. Arcuate listric faults are subparallel to depositional strike and are contemporaneous with deposition (syndepositional faults) and are intimately related in time and space with the changing depocentres (Fig. 6.15). Most of these faults were active during deposition, and offset the surface of deposition down to the Gulf. The syn-depositional

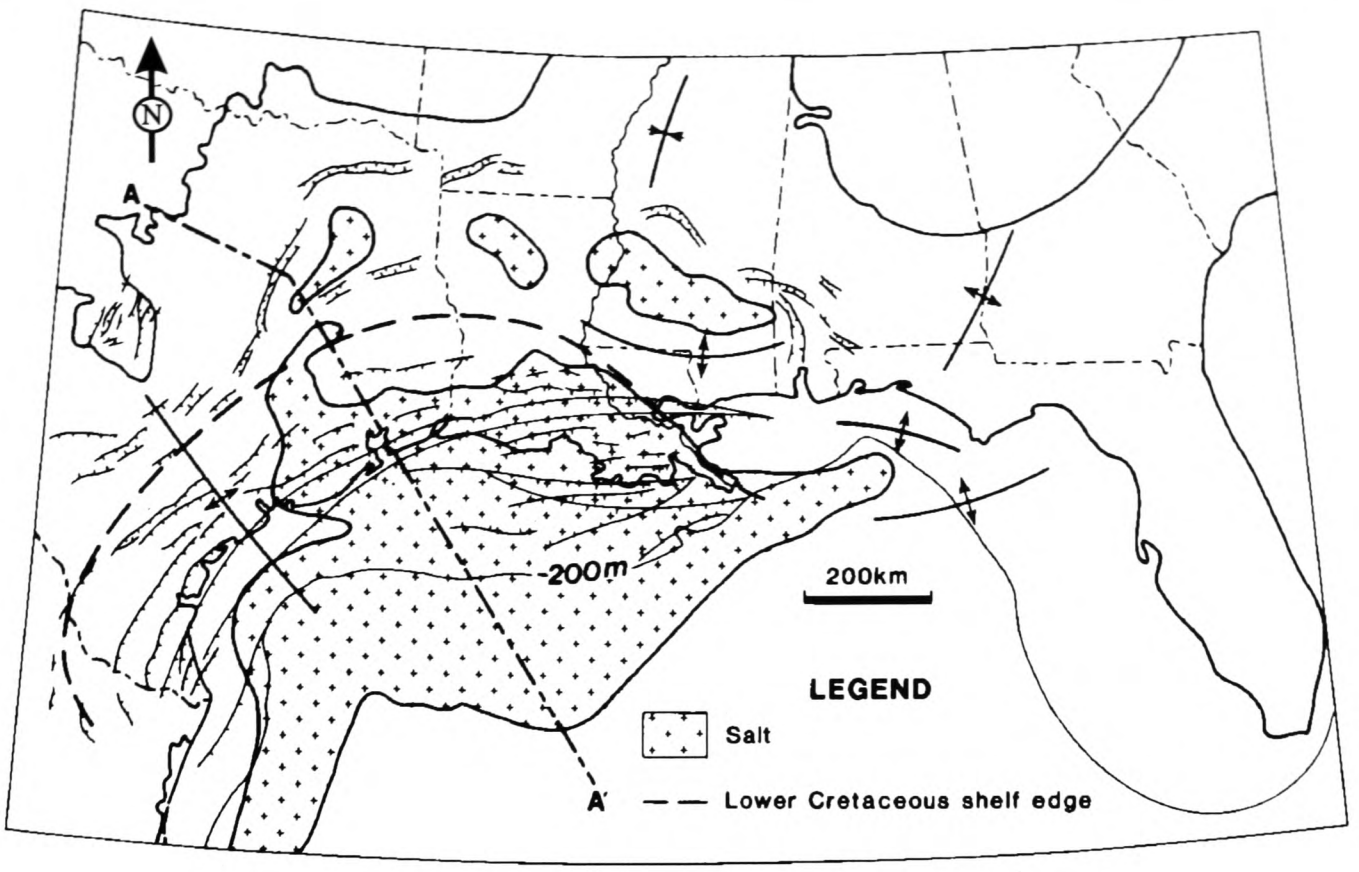

Figure 6.15: Schematic tectonic map of the Gulf Coast area, displaying major structural features, salt basins and the Lower Cretaceous shelf edge, and major growth-fault trends (after Curtis, 1986). The cross-section along AA' is displayed on Fig. 6.30.

listric faults are responsible for the thickening of the sediment accumulates on the downthrow side of each fault. Curtis (1970; 1986) observed that in the Gulf Coast basin several families of growth faults can be identified in each major depocentre and are related to each of the many basinward regressive (progradational) cycles (Fig. 6.16). These sets of regional faults originate in places where regressive sands prograde beyond older marine shales across a older shelf edge and they are a direct indicator of how the delta system prograded through geological history. Because of the regressive (basinward progradation) nature of the Mississippi deltaic sediment fill, major growth observed in each listric fault or fault family is progressively younging gulfward.

This type of sedimentation-structure relationship results in two kinds of structure being developed, rollover into the fault in the downthrown block and the broad uplift or upwarp at the toe of the fault. The rollover is important as it is later buried and preserved as a rollover anticline which commonly

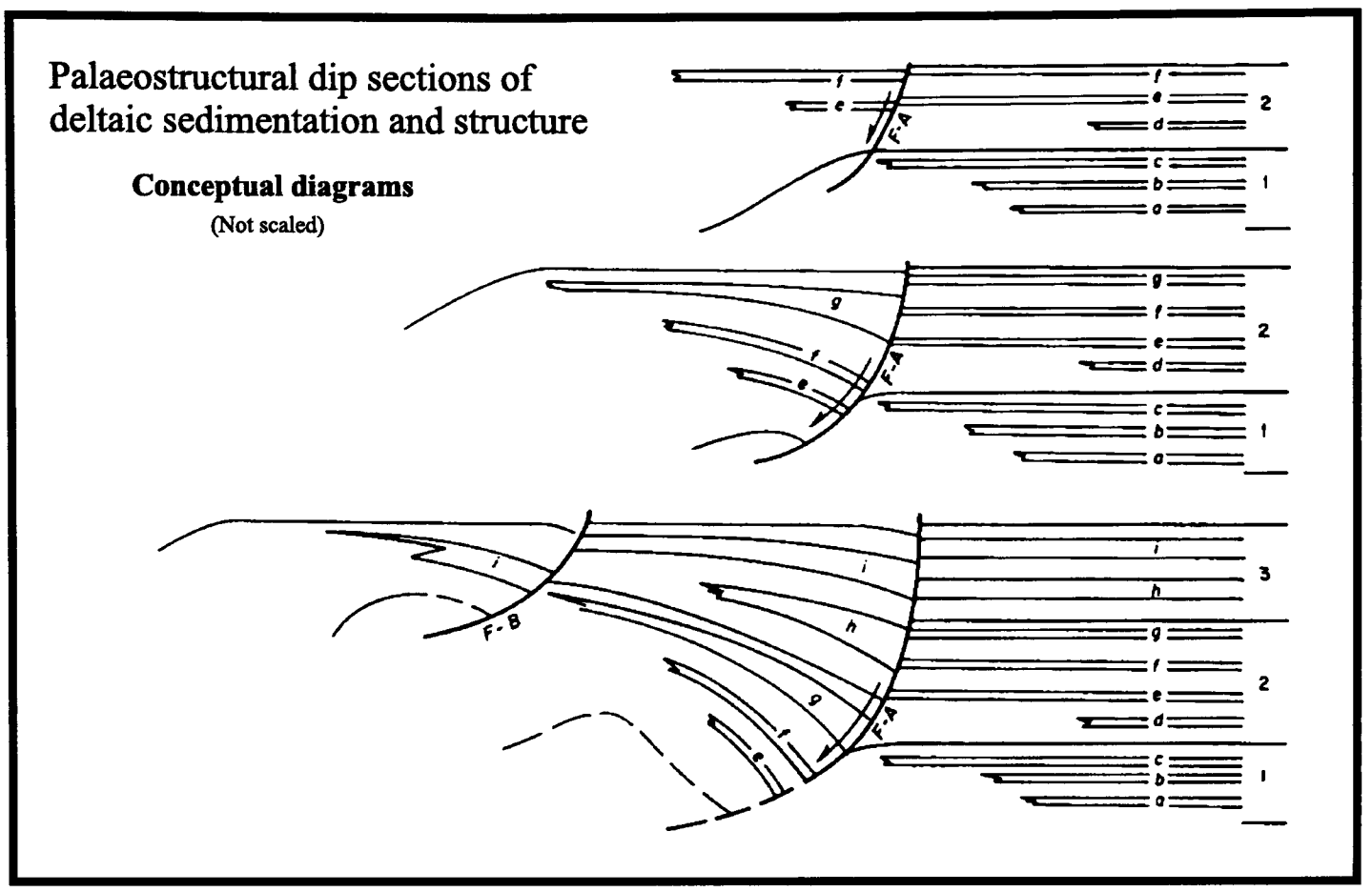

Figure 6.16: Schematic conceptual diagrams showing successive stages in development of counter-regional dip and shale uplift during syndepositional faulting, redrawn and modified from Curtis (1970).

associate with antithetic faults. The broad uplift is subsequently buried and becomes a low relief domal structure which may facilitate shale diapirs to form.

In addition to the synsedimentary structures discussed, above the intrusion of Jurassic salt into Tertiary deposits has produced diapiric structures (salt domes and salt ridges) which are some of the most prominent and distinctive structures of the Gulf Coast. Salt movement is known to be caused by gravitational instability resulting from the density contrast between the underlying Jurassic salt and the overlying terrigenous sediment buildup.

The coastal plain is a buildout of massive volumes of progradational terrigenous sediment derived from the extensive continental interior drainage basin which began to develop during the Laramide orogeny in Early Tertiary times. Tertiary deposition generally developed from southwest to northeast in a succession of younging depocentres in a generally prograding, basin-regressive fashion into the Gulf of Mexico (Curtis, 1986). They were laid on top of older sandstones, shales, limestones and evaporates which were deposited on thinned continental

crust.

The stratigraphy of the deltaic succession of the Gulf of Mexico represents a generally regressive, offlaping and prograding fill of a basin in the late stage of basin evolution on a passive continental margin of Atlantic-type. Tectonic subsidence at this late stage is very small (Curtis, 1986).

The Mississippi delta sediments, estimated to be more than 15 km of sandstones and shale, fill a bowl-shaped basin defined by a Lower Tertiary carbonate shelf edge (Curtis, 1986). The stratigraphy is distinctive vertically and laterally with each successive depocentre representing various sequences of regressive-trangressive cycles. Regressive sequences generally represent seaward prograda-

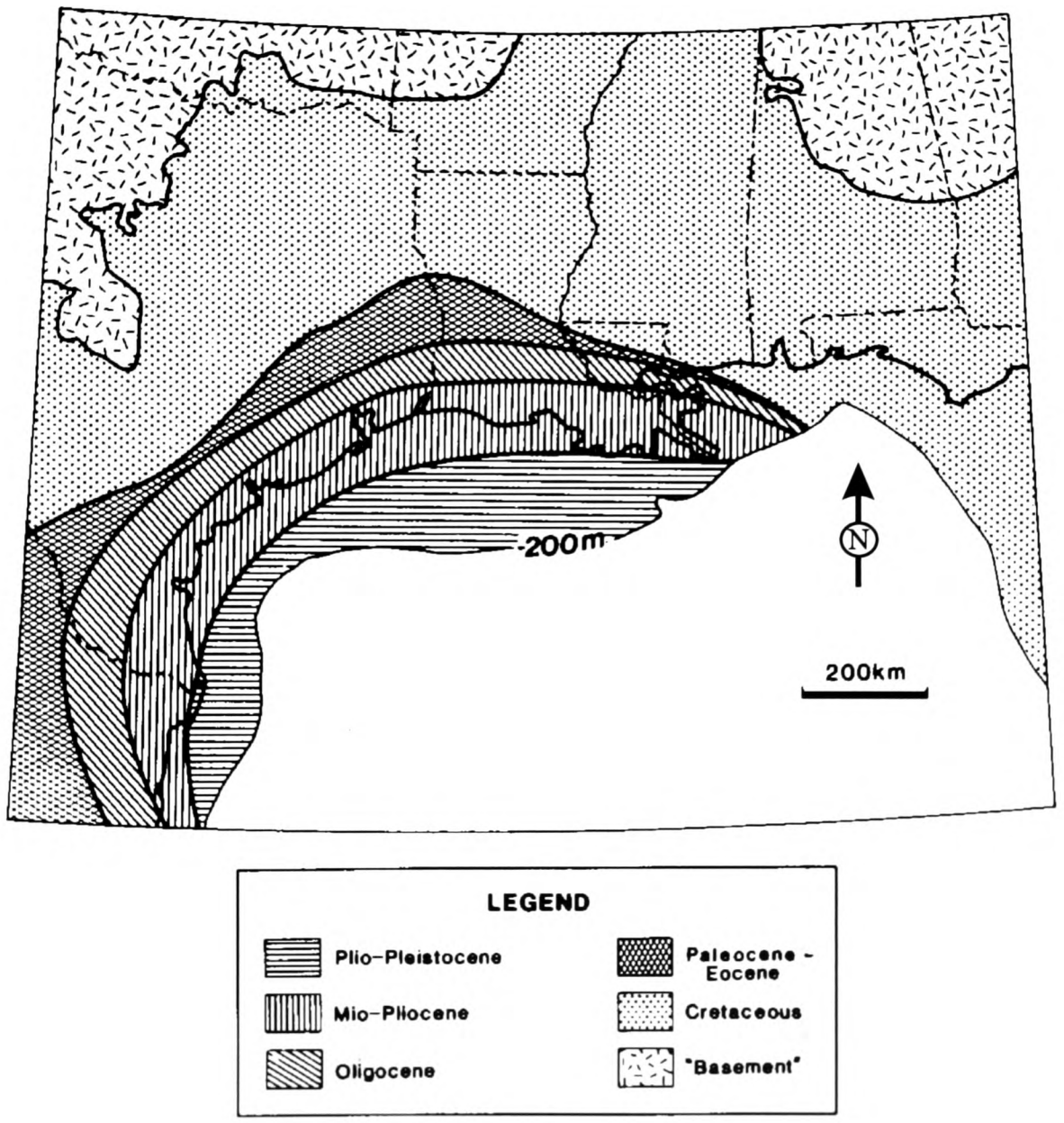

Figure 6.17: Generalized stratigraphic map of the Gulf Coast (from Curtis 1986).

tion (offlap) beyond earlier sequences, establishing new shelf edges while the transgressive sequences represent landward advance (onlap) of the sea beyond older shorelines.

As Tertiary sedimentation progressed, initially with sediments apparently supplied from minor river streams from the west, and later, beginning in Miocene time, by the Mississippi river drainage, depocentres of deltaic sedimentation shifted eastward and gulfward. The most important depocentres of Neogene times, and related to the integrated Mississippi River drainage system , were in the Louisiana portion of the Gulf (Fig. 6.17). The observed lateral shift in depocenter in the Mississippi Delta may have been the response to shift in accommodation space or to changes incurred in the drainage basin throughout geological time.

The transgressive cycle is of relatively little importance in sediment deposition with thin marine shale and basal transgressive sand.

The regressive cycle is the most important in Tertary sediment deposition, with landward non-marine and nearshore thick sand facies of alluvial and upper delta plain deposits, mixed near-shore deltaic and shallow marine sand-shale facies of lower delta plain to delta front deposits, marine-shaley facies of prodelta and open marine deposits and bathyal marine shales. In the Gulf of Mexico the vertical stratigraphic sequence resulting from repeated cycles of gulfward offlapping regressive deposition combines similar facies of different ages into diachronous lithological units (formations) which range in age from Tertiary through to Quaternary. The regressive cycles are intercalated by brief transgressive cycles which allow deposition of a marine shale formation which forms the bottom of the next stratigraphic sequence. These marine shales are generally undercompacted, overpressured and of lower density and are very likely to engage in the formation of shale diapiric structures.

The Mississippi Delta is a birdfoot delta system with deposits in its major depocentres revealing a river dominated delta type throughout Tertiary time (Curtis, 1986). However throughout the Gulf Coast Tertiary deltaic succession, each of the delta development variations discussed above can be observed, al-

though the dominant mode is seaward progradation taking place over a slowly subsiding continental crust.

6.6.3 The Niger Delta *(West Africa).*

The Tertiary Niger Delta is a major delta on the River Niger mouth at the Gulf of Guinea in West Africa (Fig. 6.18). Several years of exploration work carried out by several multinational oil companies in the area have proved the Niger Delta to be a hydrocarbon rich area. The Benue Valley, behind the delta, originated from rifting (Cratchley and Jones 1965) in Early Cretaceous times as a NE-SW trending depression sited above and dissected by NE-SW and NW-SE trends (Fig. 6.19), that correspond to basement complex shear zones of the African shield (Short and Staeuble 1967).

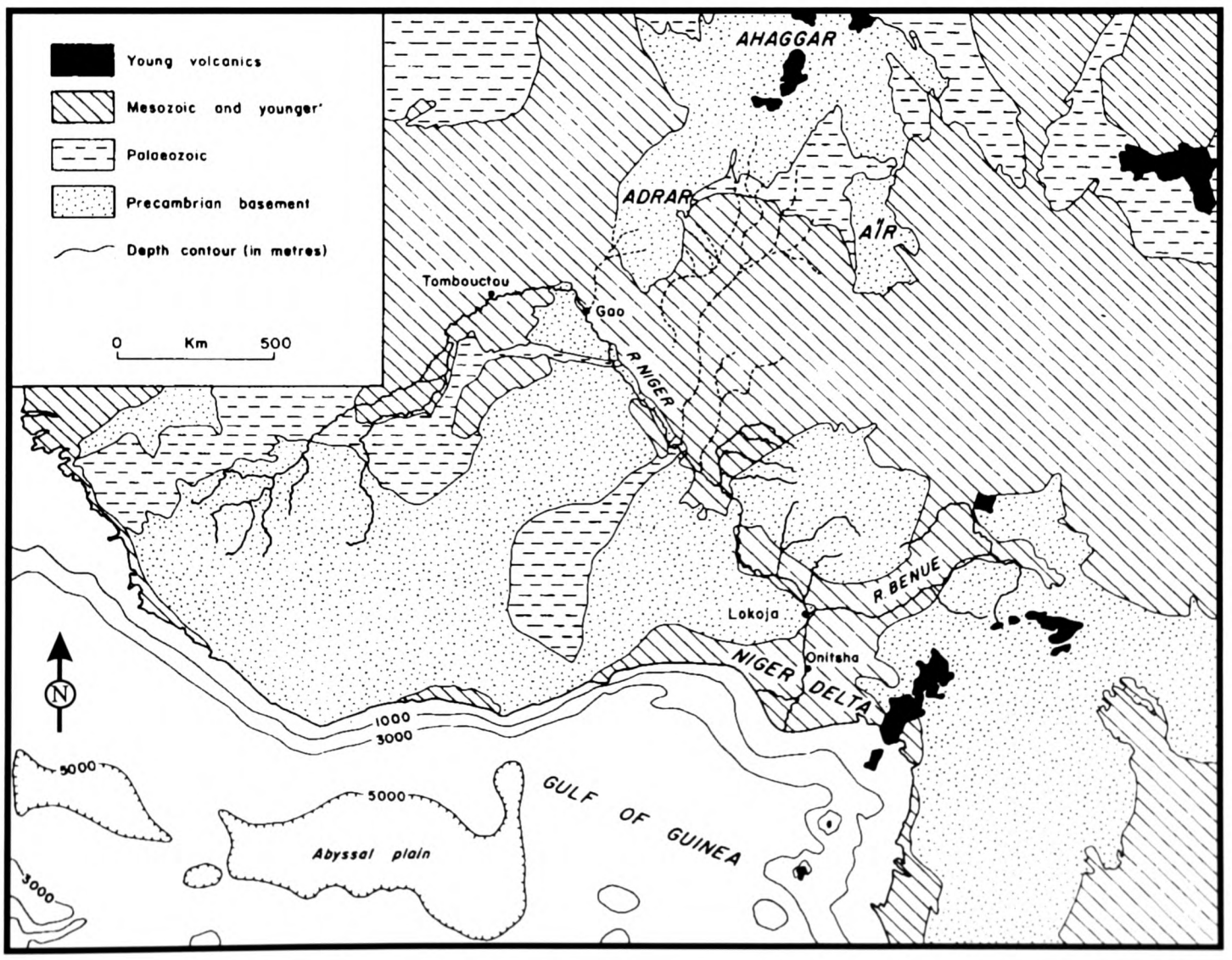

Figure 6.18: Generalized geological map of the west African Coast, including the Niger Delta (after Allen, 1970).

Tectonic movements in the Benue trough were initiated in Coniacian time and culminated during Santonian times when sediments of the trough, mainly supplied via the Niger and the Benue rivers, were folded in long gentle anticlines and synclines parallel with the trough margins in a NE-SW direction (Fig. 6.19).

The pre-Tertiary structural framework responsible for generating a depression in the area of the Gulf of Guinea controlled the direction of progradation of deltaic deposition across a narrow continental shelf. Pre-existing structural controls in the area seem to be of no influence to Tertiary deposition and delta evolution, however. Dominant structures in the deltaic succession are those developed during Tertiary deposition (syn-sedimentary tectonics). These are complex arcuate normal growth fault structures (Fig. 6.19) generally dipping into the basin and subparallel to the strike. For simplicity Fig. 6.19 displays only a few

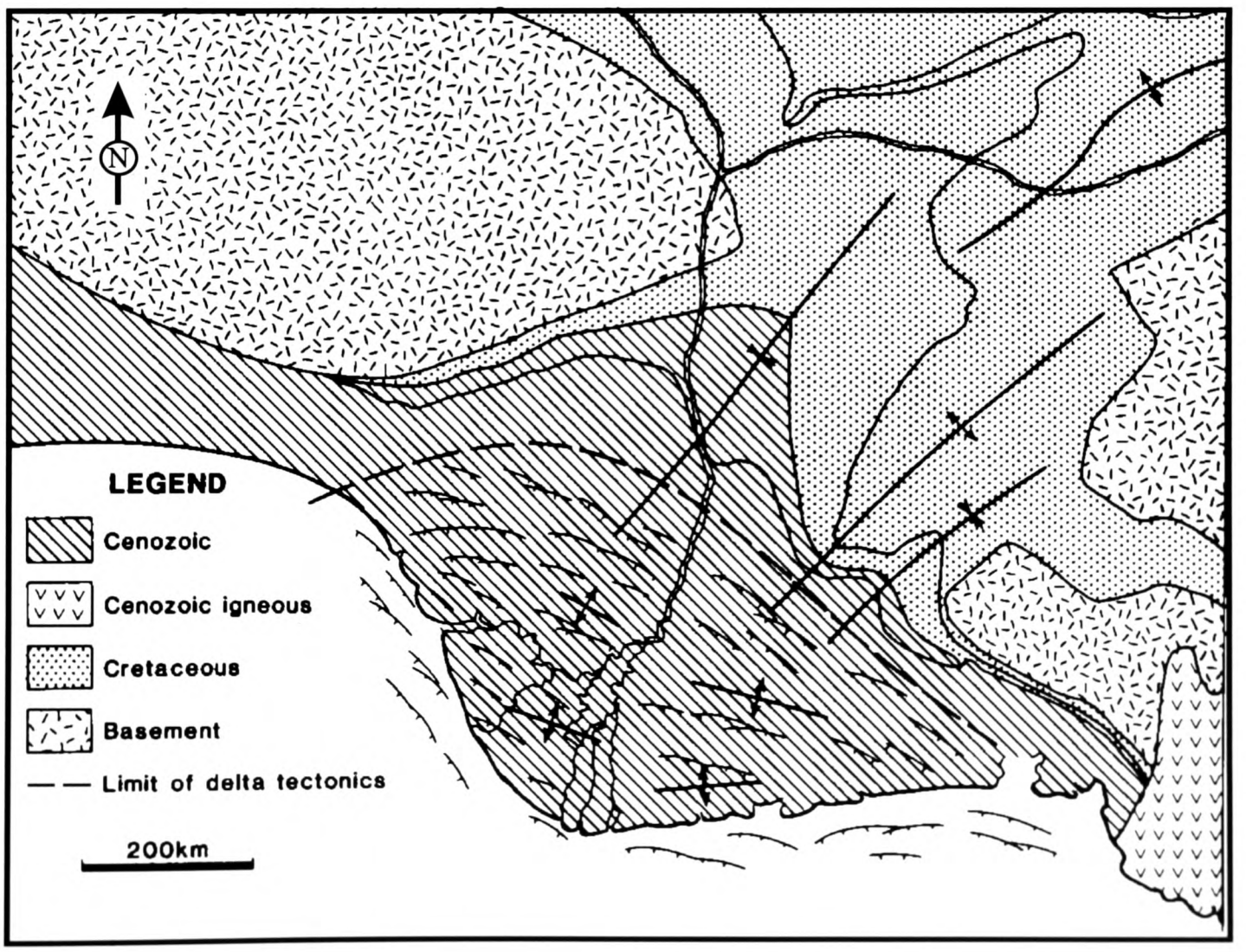

Figure 6.19: Schematic geological map of the Niger Delta area (after Curtis, 1986).

of these faults. The Gulf of Guinea area, contrary to the Gulf Coast, was not an evaporite basin in the early rifting stages during the opening of the South Atlantic Ocean in Early Cretaceous time. The absence of Mesozoic salt below the Tertiary sediments represents a major difference between the Niger Delta and the Gulf Coast of the USA and means that no salt domes and ridges characteristic of the Gulf Coast are expected in the overall structure of the Niger Delta. For the same reason, no such structural features can be expected in the Zambezi Delta Basin. Instead, the complex system of arcuate subparallel listric normal growth faults with antithetic faults and associated rollover anticlines, shale diapirs and ridges are the most common structural features of the Tertiary Niger Delta. These

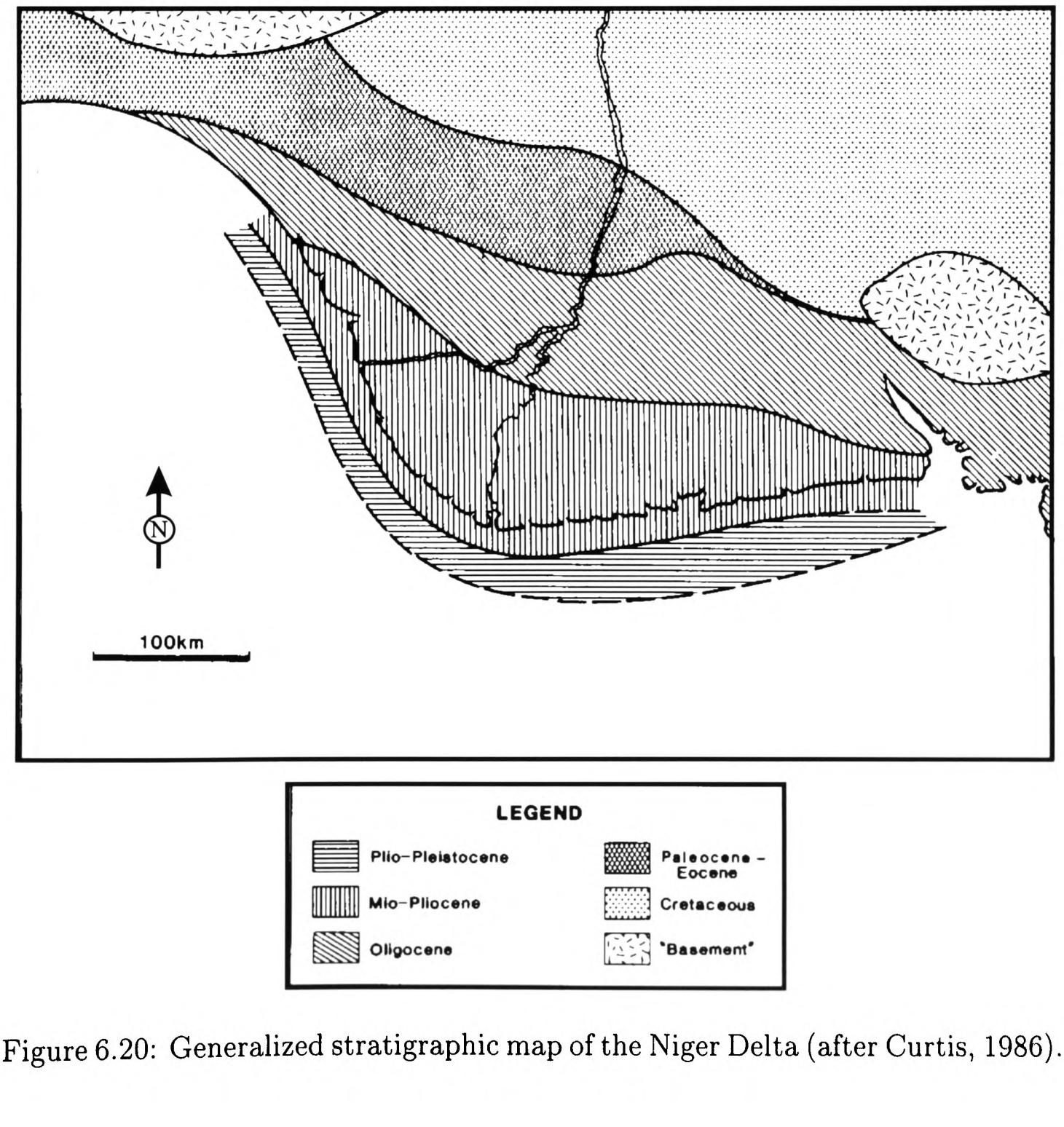

Figure 6.20: Generalized stratigraphic map of the Niger Delta (after Curtis, 1986).

characteristic structural features of the Niger Delta are progressively younger seaward as the delta progrades into the South Atlantic Ocean.

The Tertiary Niger Delta developed from a relative narrow shelf across the continental slope in the Benue trough and prograded over a relatively rapidly subsiding basin on ocean crust. It prograded in a NE-SW direction as depocentres shifted and migrated seaward out over oceanic crust into the Gulf of Guinea (Curtis, 1986) (Fig. 6.20). Tectonic events in the source area during Tertiary times may be the main reason for increased sediment supply to the Niger Delta during Tertiary as is the case in the Zambezi Delta Basin.

The sediments deposited in the Niger delta are provided by the large Niger and Benue River systems and are modified by basinal processes generated in a high energy depositional system in the Gulf of Guinea (Allen, 1970). The resulting

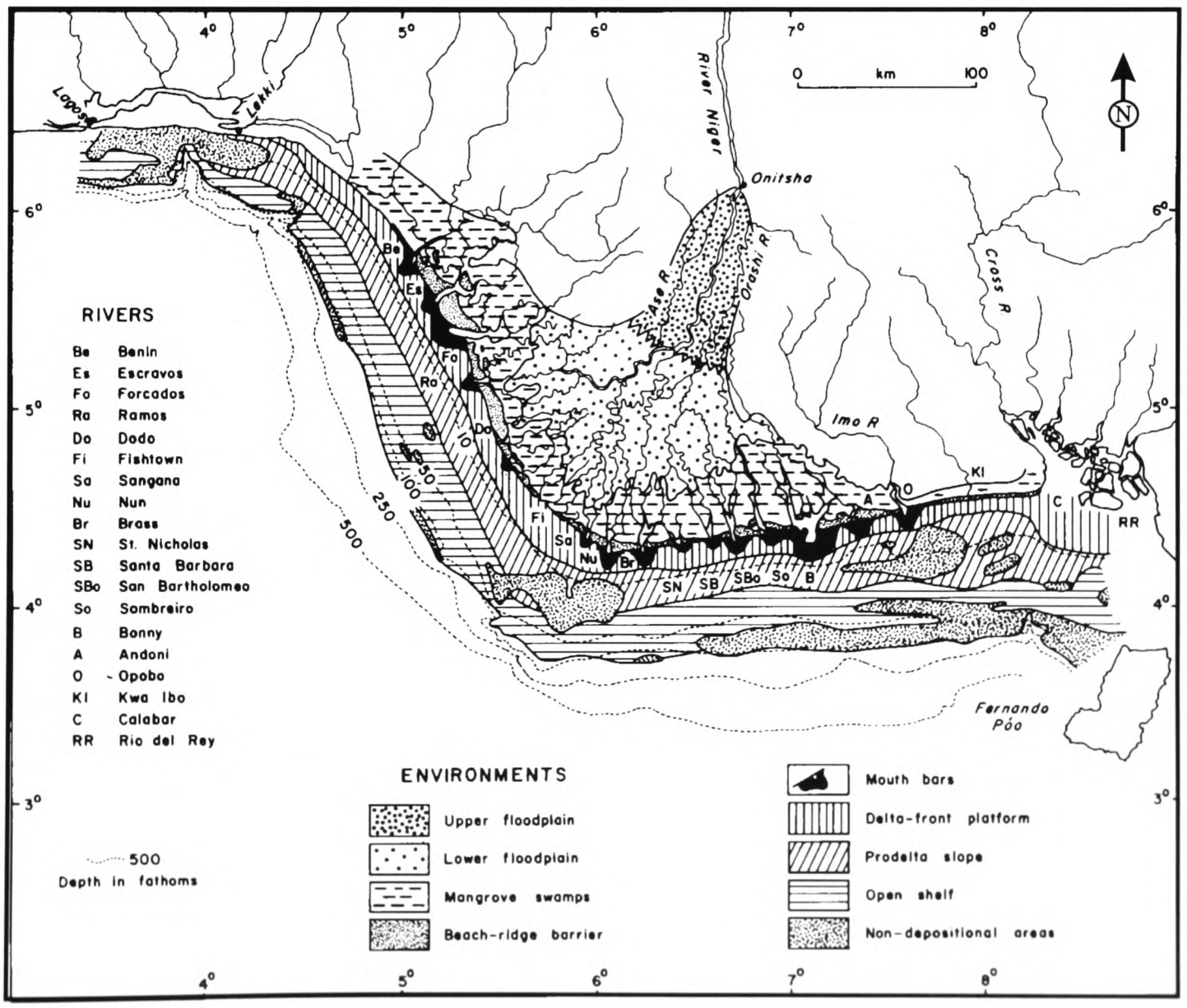

Figure 6.21: Map of the main sedimentary environments of the Niger Delta (after Allen, 1970).

vertical and lateral stratigraphy of the sediment prism, is typical of an offlapping delta sequence (progradational fill), but aggradation is more prominent, revealing the balance maintained between basin subsidence and sediment supply during deltaic sedimentation (Curtis, 1986). Prevalent strike-orientated, wave and current dominated sand bodies are typical of a wave and current dominated delta setting.

Sedimentologically, these delta deposits decrease in grain size laterally from the floodplain to the open shelf and vertically they reproduce a coarsening upward sediment profile beginning with the silty clays of the open shelf to the predominantly fine to medium-grained sands of the floodplain (Allen, 1970).

The scenario portrayed above for the Niger Delta development produced lateral stratigraphy similar to that observed in the Gulf of Mexico, where each depositional unit grades from sandstone facies landward to marine shale downdip. Vertical stratigraphy grades from marine shale at the base up through fluvial and aluvial sands at the top. These lithofacies (three main lithofacies) are generally diachronous and their boundaries tend to express a strong vertical component caused by the balance maintained between basin subsidence and sediment supply during sedimentation (Short and Staeuble 1967; Curtis, 1986).

Similarly in the Gulf Coast, the marine shale facies of low density in the Niger Delta Tertiary succession is undercompacted, overpressured, is highly mobile and responsible for generating listric growth faults and diapiric shale structures. Antithetic faults observed by Curtis (1986) in the Niger Delta tend to develop in connection with aggradational sequences and are characteristic of the Niger Delta structure. Figure 6.21 displays the main sedimentary environments of the Niger Delta where NE-SW regressive delta sediments progressed into the high energy waters of the Gulf of Guinea.

6.6.4 The Beaufort-Mackenzie delta *(Alaska-Canada)*.

The Beaufort-Mackenzie Delta basin in western Canada and northeast Alaska (USA) is a hydrocarbon rich basin (Fig. 6.14C). This basin contains Upper Cre-

taceous to Recent siliciclastic sediments deposited as a series of northward prograding deltaic sequences with a total net thickness of 12-16 km. Hydrocarbon discoveries have been made in recent years (Dixon *et al.*, 1992) rendering the basin an oil and gas exploration province.

The older structural features of the Beaufort basin are of Jurassic and Early Cretaceous ages and are mapped across the Tuktoyaktuk Peninsula in the eastern Beaufort Sea (Dixon *et al.*, 1992). These features can be grouped into fault zones or hinge lines with faults penetrating deep into the upper crust (Hawkings and Hatfield 1975; Dietrich *et al.*, 1985); Cook *et al.*, 1987. These structures are part of continental breakup and the formation of the Canada Basin and subsequent basin subsidence with later minor fault reactivation affecting post-rift sedimentation in the basin.

Dixon *et al.* (1992) grouped the structures within the Upper Cretaceous to Tertiary succession of the Canada basin in three key areas, namely: the west and north-central Canadian Beaufort Sea, the Mackenzie delta and the adjacent offshore area and the continental rise of the Canada basin. Under the above grouping the Upper Cretaceous to Miocene succession underneath the west and north-central Canadian Beaufort Sea is folded into an arcuate fold belt, the Beaufort fold belt (Fig. 6.22A,B), while listric faults and associated tilted fault blocks are characteristic in the area underneath the Beaufort-Mackenzie delta area and the same strata are undeformed or mildly deformed underneath the continental rise of the Canada basin (Dixon *et al.*, 1992).

Gravitational instability and gravity inversion caused by overpressured, undercompacted, low density shales as discussed before for the Gulf of Mexico and the Niger delta are also observed in the Beaufort-Mackenzie delta of the western Canada basin. Synsedimentary growth faults and reverse drag into the growth faults are related in time and space to the northward growth of the Tertiary Beaufort-Mackenzie delta (Curtis,1986; Dixon *et al.*, 1992). They formed broad rollover anticlines in the downthrown blocks in the sand-shale facies. These Tertiary syn-sedimentary faults cross older Mesozoic faults that are subparallel with the older northward structural trend (Dixon *et al.*, 1992).

The deltaic succession of the Beaufort-Mackenzie basin consists of eleven alternating transgressive and regressive sequences of regional extent (Dixon *et al.*, 1992). These sequence were deposited within a stratigraphic framework of four major tectonostratigraphic phases which characterise the basin. Each of these

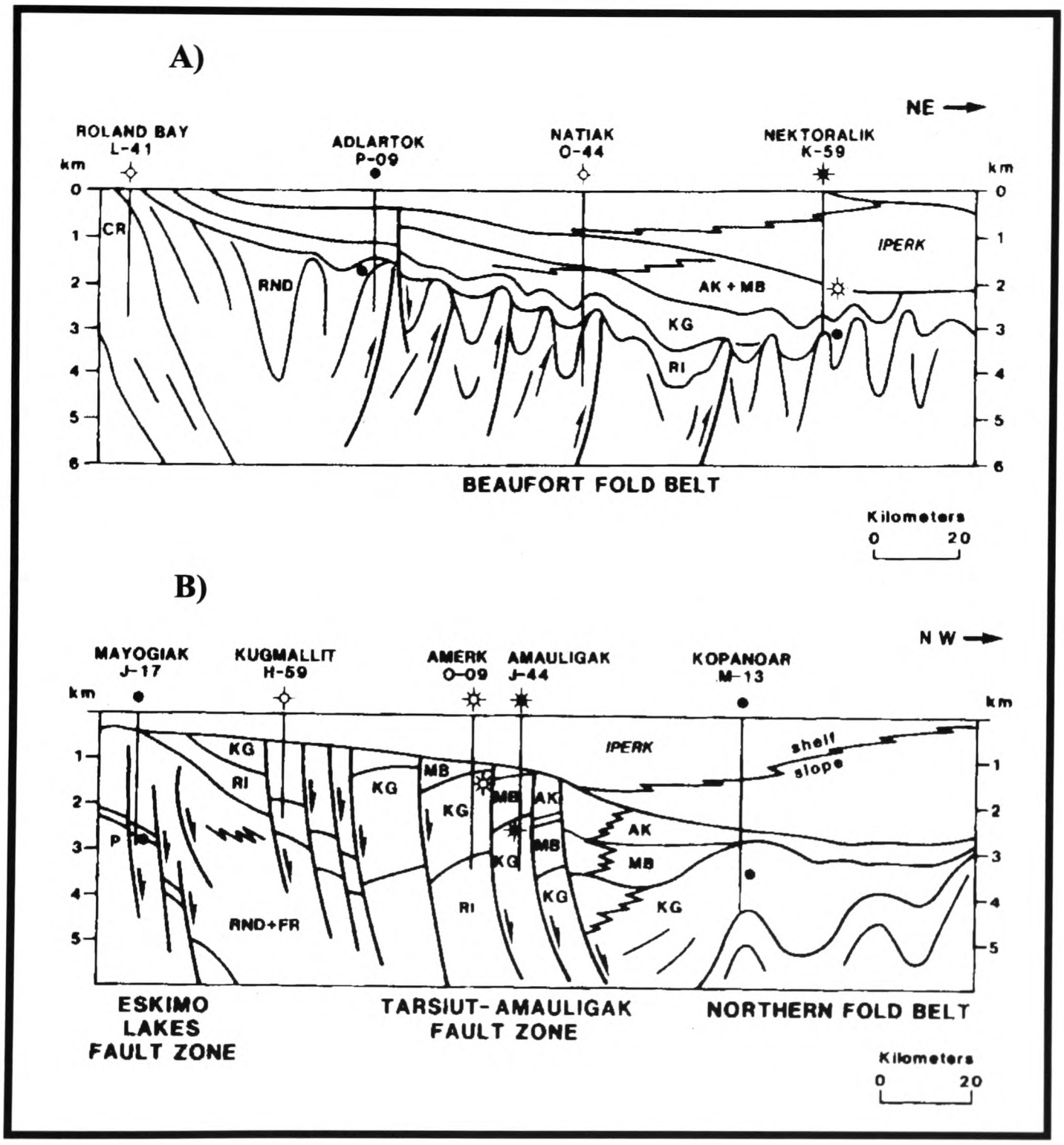

Figure 6.22: Schematic structural cross-sections of the Beaufort-Mackenzie Delta (after Dixon *et al.*, 1992). Cross-section A, across the western part and B, across the southern part of the Beaufort-Mackenzie basin. Key: AK = Akpak sequence, MB = Mackenzie Bay sequence, KG = Kugmallit sequence, RI = Richards sequence, RND = Reindeer supersequence, FR = Fish River sequence, CR = Cretaceous and P = Paleozoic and older.

four phases was ended by a tectonic episode. The four tectonostratigraphic phases are Cenomanian to Middle Maastrichtian (phase 1); Late Maastrichtian to Middle Eocene (phase 2); Middle Eocene to Late Miocene (phase 3) and Pliocene to (?)Early Pleistocene (phase 4) (Dixon *et al.*, 1992).

During phase 1 sedimentation in the basin was limited to the deposition of some thin strata of organic rich muds laid on the outer shelf and in the basinal environments on top of pre-drift sediments deposited during the early rifting and drifting in Early Cretaceous. This strata was laid in two sequences known as the Boundary Creek (Cenomanian - Turonian) and the Smoking Hills (Santonian - Campanian) sequences, the oldest sequences of the deltaic succession (Dixon *et al.*, 1992).

Before deposition of phase 2 stratigraphic sequences (Late Maastrichtian - Middle Eocene) a major northward shift in depocentres to the continental margin of the Canadian basin occured. During this phase of deposition deltaic depocentres were relocated along the southwestern margin of the Canadian Sea.

Phase 3 was deposited on top of the Middle Eocene unconformity following the end of phase 2 tectonics. Sedimentation at this time (Middle Eocene - Late Miocene) was concentrated in the central Canadian Beaufort Sea. The deposition of the strata of phase 3 represents a shift in deltaic depocentres to the northeast from the southwestern margin of the Canadian basin during deposition of the previous tectonostratigraphic phase.

The fourth and last tectono-stratigraphic phase of the Beaufort-Mackenzie deltaic succession spans from Pliocene to Recent and two stratigraphic units are deposited unconformably onto the Early Pliocene unconformity. The early Pliocene unconformity was produced by the end of phase 3 major tectonic episode. The Iperk (Pliocene - Lower Pleistocene) and the Shallow Bay (Upper Pleistocene - Holocene) sequences deposited during this phase are stratigraphically separated by a major hiatus at Early Pleistocene time. Deposition of the Iperk strata is progradational and controlled most of the modern shelf and slope topography and represented a large delta complex grading basinward into shelf, slope, and

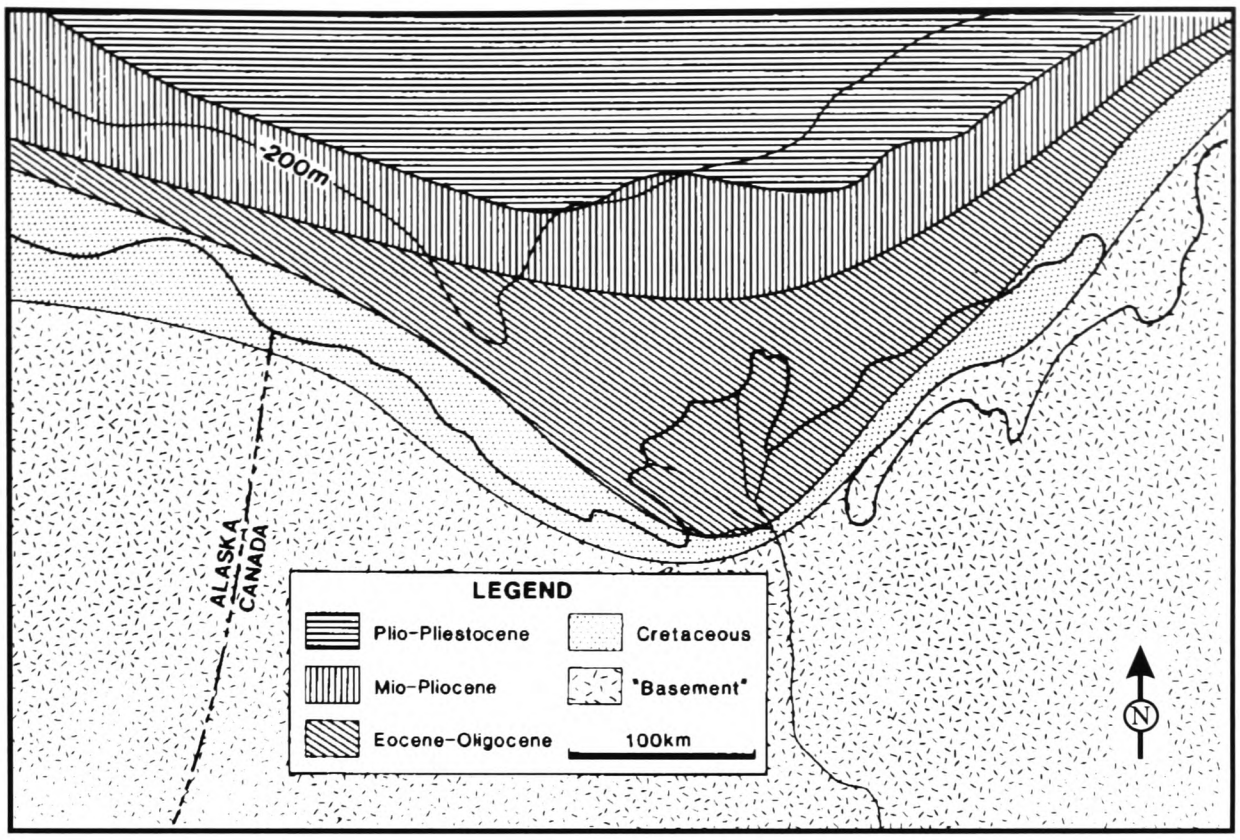

Figure 6.23: Generalized stratigraphic map of the Beaufort-Mackenzie Delta, modified from Curtis (1986).

basinal deposits (Dixon *et al.*, 1992). In contrast to the Iperk sequence, the Shallow Bay sequence is of little significance in thickness and in most cases it cannot be separated in CDP (Common Depth Point) seismic data from the underlying Iperk sequence, leading to its inclusion in the Iperk sequence. The strata of the Shallow Bay sequence is thickest in the Mackenzie trough reaching some 400 m and lies unconformably onto older eroded Tertiary strata (Dietrich *et al.*, 1985). Fig 6.23 summarizes the Cretaceous to Recent time stratigraphy of the Beaufort-Mackenzie area.

Following the dominance of the regressive patterns of deposition characterized by basinward offlapping cycles the Tertiary Beaufort-Mackenzie Delta, vertical and lateral stratigraphy compares very well to that of the Niger and the Gulf Coast basins. A core sample from the Beaufort-Mackenzie delta analysed by Curtis (1986) is virtually indistinguishable from the aggradational and progradational delta cycles with grain size sequences and sedimentary structures generally observed in other Tertiary deltas. Marine shales are overlain by pro-delta clays which in turn are overlain by delta-front sands, distributary mouth bar and distributary channel deposits of the the lower delta plain. Offshore the Canadian

Beaufort Sea, the delta prograded into the Canadian Basin, which is underlain by oceanic crust.

High sedimentation rate, virtually in balance with high basin subsidence, resulted in diachronous lithofacies units as the product of repetitive offlapping depositional cycles which placed a mobile shale facies at the base, grading upward to a massive sand facies at the top (Curtis, 1986).

6.6.5 The Western Irish Namurian Basin *(Southwest Ireland).*

The Namurian Basin of western Ireland covers a large part of West County Clare (Fig. 6.14D). It comprises a deltaic succession of alternating shales, siltstones and sandstones, deposited in repeated sequences of upward coarsening strata up to 1600 m in thickness (Rider, 1974; 1978). The sedimentological composition of the depositional sequences, ranging in thickness between 60 and 120 m, indicate that these sequences were deposited in deltas of high load sediment input from the west with low wave and some littoral drift influence which are comparable to those of the Tertiary Mississippi Delta (Rider, 1978) and with some stages of the development of the Tertiary section of the Zambezi Delta. Depositional environments change from deep water black shales and turbidites in the lower part of the Namurian sequence through a transition of slump deposits into a series of shallow water delta sequences in the upper part (Martinsen, 1989).

The stratigraphy of the Namurian deltaic succecession of Western Ireland is subdivided in two major rock groups, the Shannon Group at the base and the Central Clare Group at the top of the succession. Generally, the sequences of the Shannon Group thicken from both North Clare in the north and North Cork in the south towards the Shannon Estuary region (Martinsen, 1989). The Shannon Group comprises the Clare Shale at the base overlain by the Ross Formation with the Gull Island Formation at the top of the group. The Ross Formation is represented by thick sandy turbidites with no apparent vertical stratal definition in the central part of the basin. The Gull Island Formation lies conformably on top of the Ross formation and comprises extensivelly deformed slope sediments dominated by mud slumps and turbidites in its lower part. The upper part of

this formation is made of mud slumps and undeformed mustones (Martinsen, 1989). The three depositional units are clearly separated by chronozones (marine bands)which can be traced all over the basin (Rider, 1974; Pulham, 1989; Martinsen, 1989; Davies and Elliott 1995). The Ross Formation can reach more than 300 m while the Gull Island formation is 395 m in the southwest and central Clare Basin (Pulham, 1989).

Deposition after the Gull Island Formation is characterized by gradually upward coarsening delta front sediments of the Tullig Cyclothem (the first of a group of five cyclothems of the Central Clare Group). Within the Central Clare Group five marine bands separating cyclothems have been identified. They are from base to top the Tullig, Kilkee, Doonlicky and Cyclothems four and five (Rider, 1974; Pulham, 1989). The Central Clare Group is 915 m in the southwest and Central Clare Basin. All five cyclothems are made of deltaic basinward progradational units, each produced by the basinward progradation of a fluvial-dominated delta lobe (Rider, 1974; Pulham, 1989).

Fig. 6.24 is a geological map of the West County Clare. The Visean Limestone are the last formation deposited prior to the Namurian delta development in the area. The lowermost formation of the Namurian succession is the Clare Shales formation overlain by the Ross Sandstone formation, the Gull Island and the Tullig sand formations in a generally upward shallowing sediment succession (Rider, 1978; Pulham, 1989; Martinsen, 1989; Martinsen and Bakken 1990). The Ross formation (maximum thickness 380 m) is a turbidite sandstone succession characterized by several thick slumps in its upper part which is overlain by the highly deformed delta slope succession of the lower part of the Gull Island formation with a maximum thickness of 550 m. The deformation observed is due to soft sediment deformation processes active at the time of deposition (Martinsen, 1989). The upper Gull Island Formation is an upward coarsening succession in the bottom grading into a wave-reworked siltstone with occasional sandstone beds indicating a gradational transition into prodelta sediments of the overlying Tullig formation. The Namurian delta sediments of Western Ireland were deformed

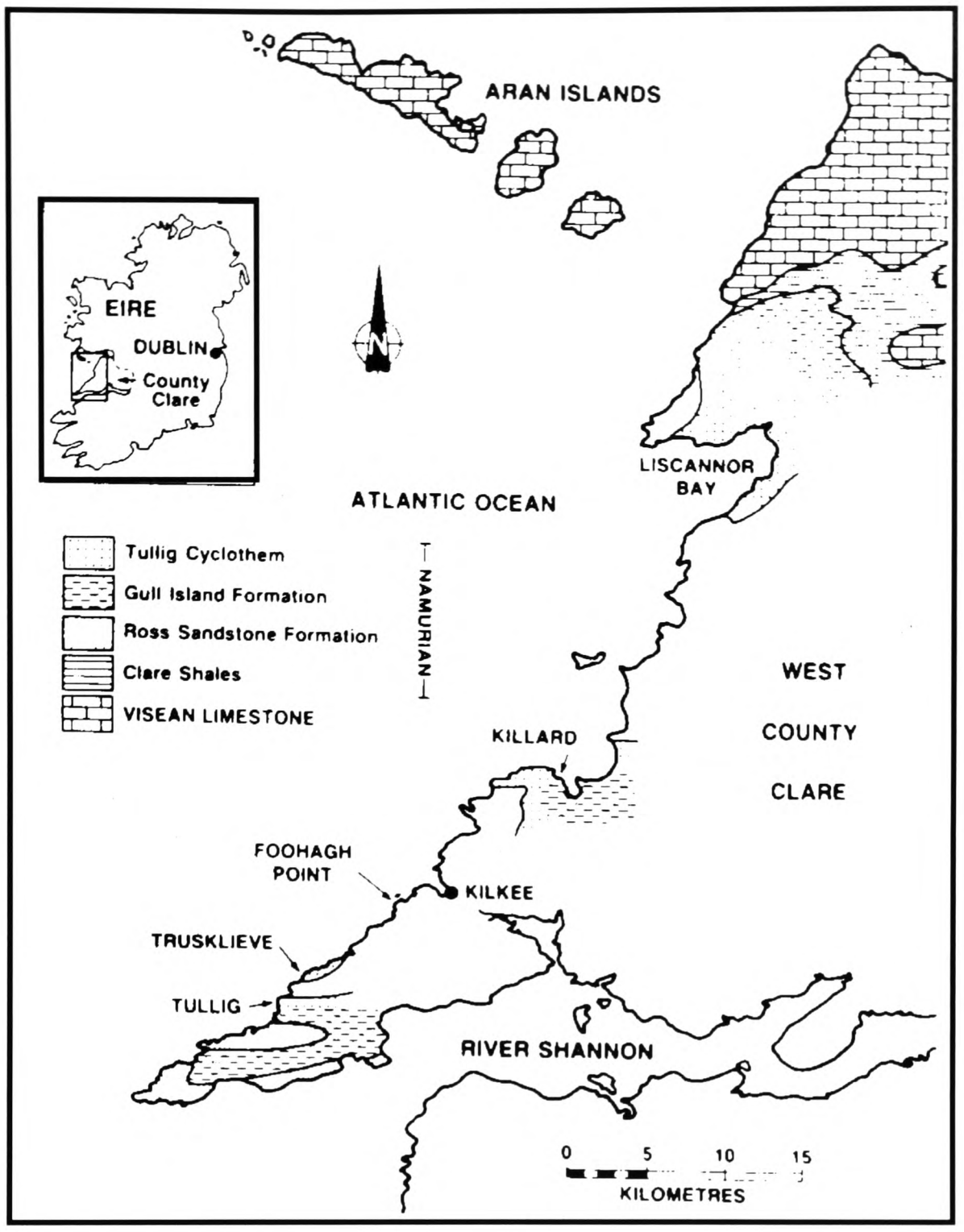

Figure 6.24: Schematic geological map of southwest County Claire, western Ireland, after Pulham (1989).

and folded by the northward migrating Variscan front during Late Carboniferous times (Cooper *et al.*, 1986). Later these sediments were exhumed during Tertiary vertical tectonics.

Syn- and post depositional soft sediment deformation characteristic on seismic data in other deltaic settings in the Mississippi, Niger, Beaufort-Mackenzie and elsewhere is observable at outcrop scale in the Namurian Delta rock exposures in western Ireland (Figs. 6.25; 6.26; 6.27). Folding, mud slides and slumping,

Figure 6.25: Mud diapir exposed off the coast of western Ireland.

mud dirpirs as well as normal and listric faulting are also charcteristic (Figs. 6.28; 6.29). Several transgressive episodes are well recorded by often clearly mappable transgressive surfaces (onlap surfaces). Sandstone bodies are often deposited on top of erosional channel surfaces cutting through older sediments.

Syn-depositional growth faulting is characteristic within the deltaic succession (Figs. 6.27; 6.28; 6.29). The faults are rotational scoop-shaped normal faults gradually transformed into listric faults generally filled in the downthrow by overthickening sequences of distributary mouth sanstones (Fig. 6.27).

Namurian deltaic deposition in the Clare Basin was influenced by a combination of various sedimentary processes of which fluvial, basinal (waves), syn-depositional deformation factors (slumping, sliding and growth and listric faults) and rapid basin subsidence are the most important (Rider, 1978; Gill, 1979; Pulham, 1989; Martinsen, 1989; Martinsen and bakken, 1990). Of all these processes, fluvial processes remained the most predominant and produced distributary channel sandstones and fluvial dominated mouth-bar deposits. Syn-sedimentary

Figure 6.26: Syn-depositional soft sediment deformation (erosion and folding) in the Namurian Delta in western Ireland.

faulting, slumping, gravity sliding and shale diapirism observed at outcrop scale in the Clare Basin are generally a good analog to similar features observed on seismic data in delta front sediments in the U.S. Gulf Coast, the Niger and the Beaufort-

Mackenzie Deltas. Single channel sandstones internal structures reflects a high energy depositional environment in relatively straight channels. Although very often syn-depositional deformation in the basin overprints depositional processes, mouth-bar sandstones internal structures do reflect a variety of frictional and buoyant river mouth typical processes (Pulham, 1989).

The southern part of the Namurian Delta of the Clare Basin is characterized by large multistorey channel sandstones suggesting major deformation across the delta plain due to rapid basin subsidence and high sediment compaction rates in contrast to the northern part of the basin with an architecture and structure consistent with a more stable fluvial dominated delta setting (Pulham, 1989). This section of the Namuriam Delta of the Clare Basin compares well to the upper section of the Zambezi Delta Basin, from Top Oligocene to Recent time.

Figure 6.27: Syn-depositional soft sediment deformation (erosion growth faulting and folding) in the Namurian Delta in western Ireland.

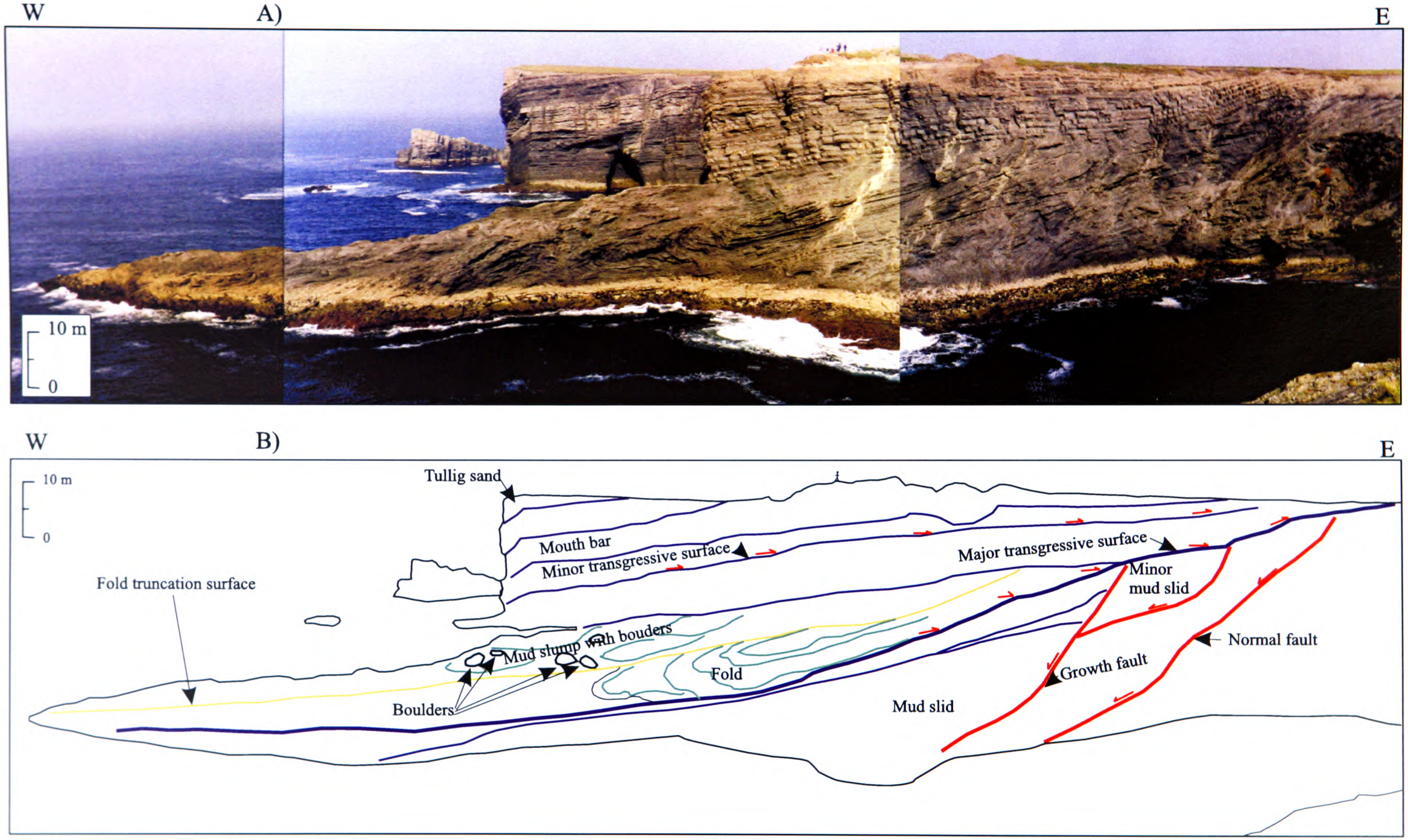

Figure 6.28: Syn- and post-depositional deformation features including normal and listric growth faults and sediment folding in the western Ireland Namurian basin.

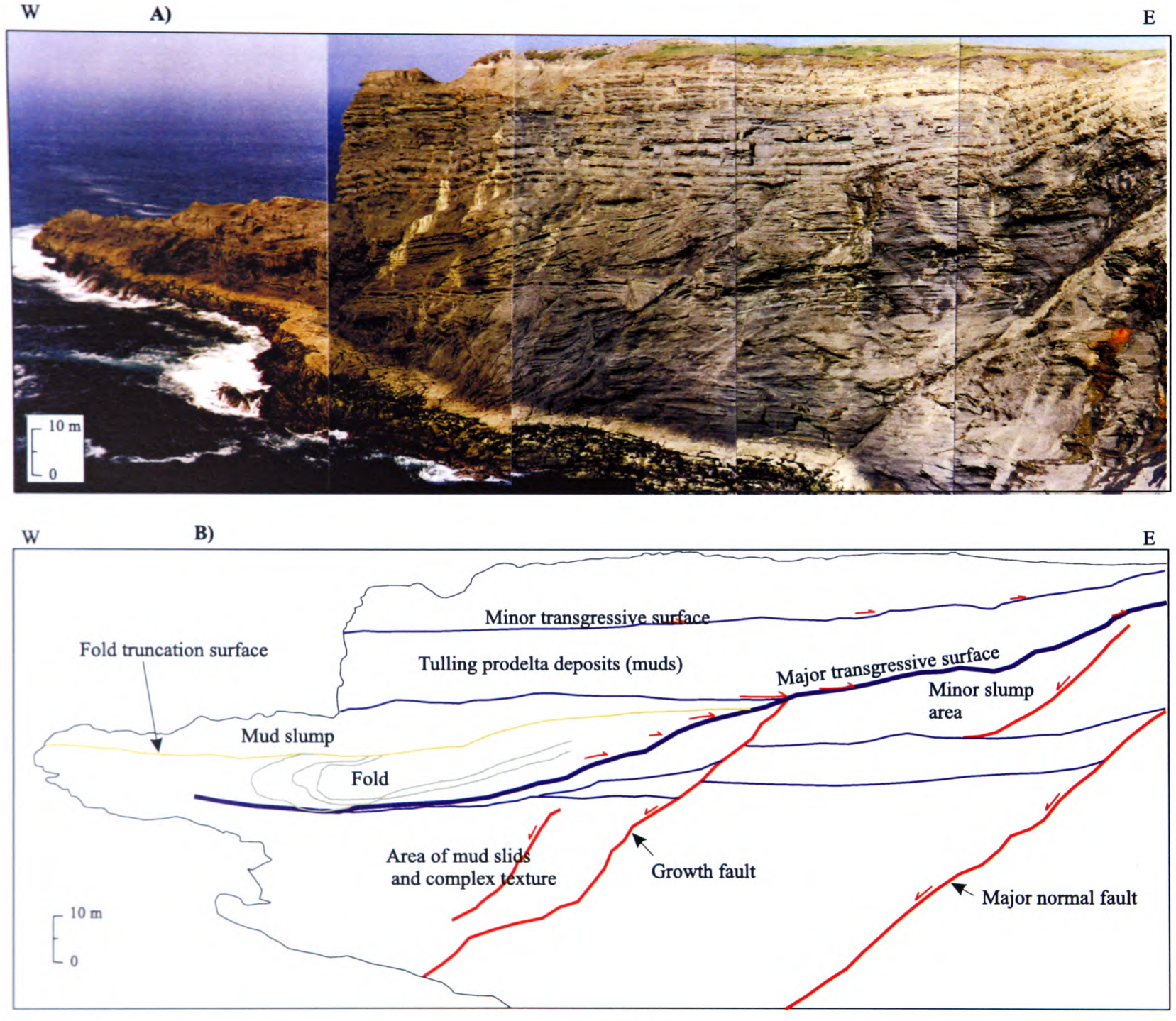

Figure 6.29: Syn- and post-depositional deformation features including normal and listric growth faults and sediment folding in the western Ireland Namurian basin.

6.6.6 Summary and comparison of regional geology.

A common characteristic in these four basins is the orderly and predictable interrelationship of sedimentation, stratigraphy, depositional environments and structure. Ages and oil producing trends are also similar for the three Tertiary deltas, the Mississippi, Niger and Beaufort-Mackenzie Deltas. These three basins contain sediments amounting up to 16 km in th Beaufort-Mackenzie Delta with vertical gross lithological sequence bearing shales at the base, overlain by interbedded sandstones and shales, overlain by thick sandstones. Generally in all three Tertiary basins progradation produced regressive wedges as the basins subsided. The vertical lithological sequence is repeated laterally from the basin landward in all three basins. The stratigraphic units of the depositional sequences generally thickening basinward across a series of normal listric faults, down to the basin syn-depositional faults (Fig. 6.30). Another important common characteristic in these basins is hydrocarbon trapping associated with diapiric (salt

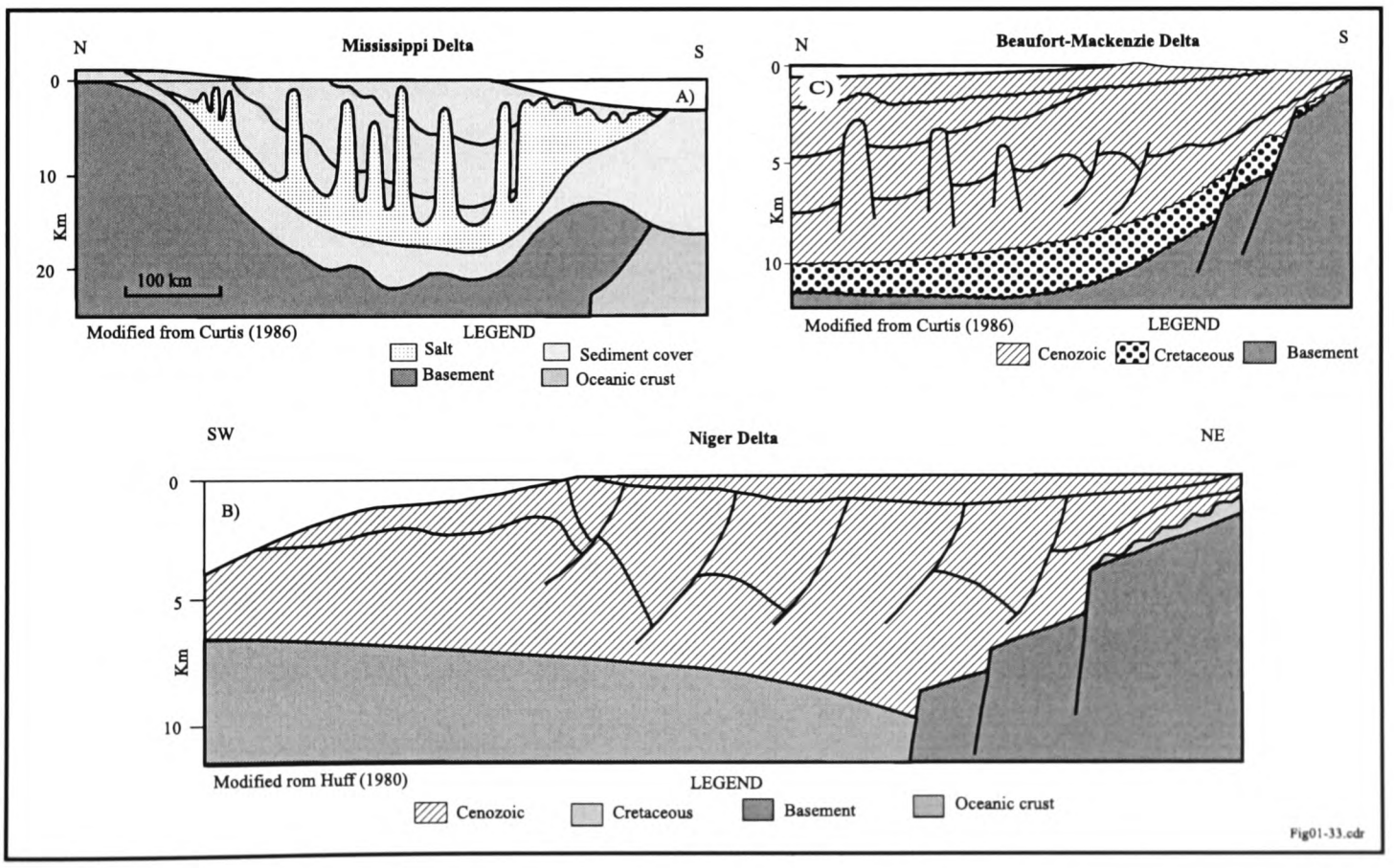

Figure 6.30: Schematic dip cross-sections of the Mississippi (A), Niger (B) and Beaufort-Mackenzie (C) after Huff (1980) and Curtis (1986). No horizontal scale is given for B and C. See Fig. 6.15 for the geographic location of section (A).

and shale diapiric) structures and abnormal pressures driving gravity mass movements.

Dispite the many similarities between these three Tertiary basins, differences lie in their geological settings and geological histories. In the Mississippi Delta the presence of salt resulted in a wide variety of salt dome structures in addition to diapirs and roll-over anticlines common to all three basins. Tectonic settings prior to Tertiary deposition is different in all three basins. Variations in delta morphology and sand bodies geometry can be attributed to variations in ratios of rates of deposition to rates of basin subsidence.

The Namurian basin of western Ireland offers good rock exposures which enable the observation and study of depositional and structural features often mapped on subsurface data in the Zambezi Delta Basin. Of particular interest are channels, channel vallies stacking, lateral migration with geological time.It is therefore used here as an analogue to the seismic expression of the above sedimentary characteristics on outcrop scale.

Some of the most important aspects with respect to deltaic development are the tectonic structural setting prior to deltaic sedimentation, along with the occurrence or not of evaporites, (mainly salt), and the broad type of deltaic development (i.e. fluvial-, wave- or tidal-dominated). Deltas developed at rifted passive margins are generally characterized by abundant sedimentation and rapid basinward regressive progradation.

The occurrence of evaporites often facilitates the development of syn- and/or post-depositional structural styles observed in some deltas. Salt and undercompacted and overpressured shales are highly mobile under the growing pressure of overlying sediments. In turn, the movement of salt and/or shale causes disturbances to the overlying sediments by intrusive salt or shale diapirs, which create syn- or post-depositional structures. These may provide potential hydrocarbon plays. Also, growth faults may develop, with the possibility of generating rollover anticlines which are some of the characteristic structures found in most deltas like the Mississippi, the Niger and the Beaufort-Mackenzie Deltas.

In the Zambezi Delta Basin the development of rollover structures is limited

to Palaeocene - early Eocene sediments which were affected by early Eocene sliding and slumping of turbidite deposits in the southwestern depocentre. It is not clear whether these reflect early signs of East African Rift fault reactivation in the area, or whether its timing is related to the long wavelength, low amplitude folding of pre-deltaic sediments in this part of the basin. Salt is not known from geological evidence in the Mozambique Basin as a whole and in the Zambezi Delta Basin in particular. However, evaporites including some salt could have been deposited in Late Jurassic to early Cretaceous, analogous to the Aptian salt layer known from the early stages of the opening of the South Atlantic Ocean (Rona, 1982) provided that salt lakes and climatic conditions existed at this time in the area. Tertiary evaporites (gypsum and anhydrite) are known in the Zambezi Delta Basin and are widespread in the northern part of the Mozambique Basin (Rona, 1982; Salman *et al.*, 1985; Abdula and Salman, 1995). They constitue the main reservoir seal in the gas fields of Temane and Pande in northeastern Inhambane province of southern Mozambique.

Some depositional features of the Zambezi Delta Basin are very similar to those observed in other deltas. As in the Gulf of Mexico, Niger and Beaufort-Mackenzie Deltas, deltaic sedimentation in the Zambezi Delta is mainly of Tertiary age and generally basinward progradation, which produced an orderly and predictable interrelationship of sedimentation, stratigraphy, depositional environments and structure.

During Tertiary deposition in the Gulf of Coast, the depocentre moved basinward, as well as eastward, producing along-strike variability (Fig. 6.31) in some way dissimilar to the multi-cyclic switch between the depocentres observed during Neogene sedimentation in the Zambezi Delta Basin. The Niger Delta structural setting prior to deltaic development is responsible for the gulfward progradation confined to the Benue Trough. The Niger Delta prograded from Miocene times steadily into the Gulf of Guinea with some slight shift in Oligocene times to the southeast (Fig. 6.32). The shoreface advance to the Gulf of Guinea amounts to more than 300km between Miocene and the present time. Along-

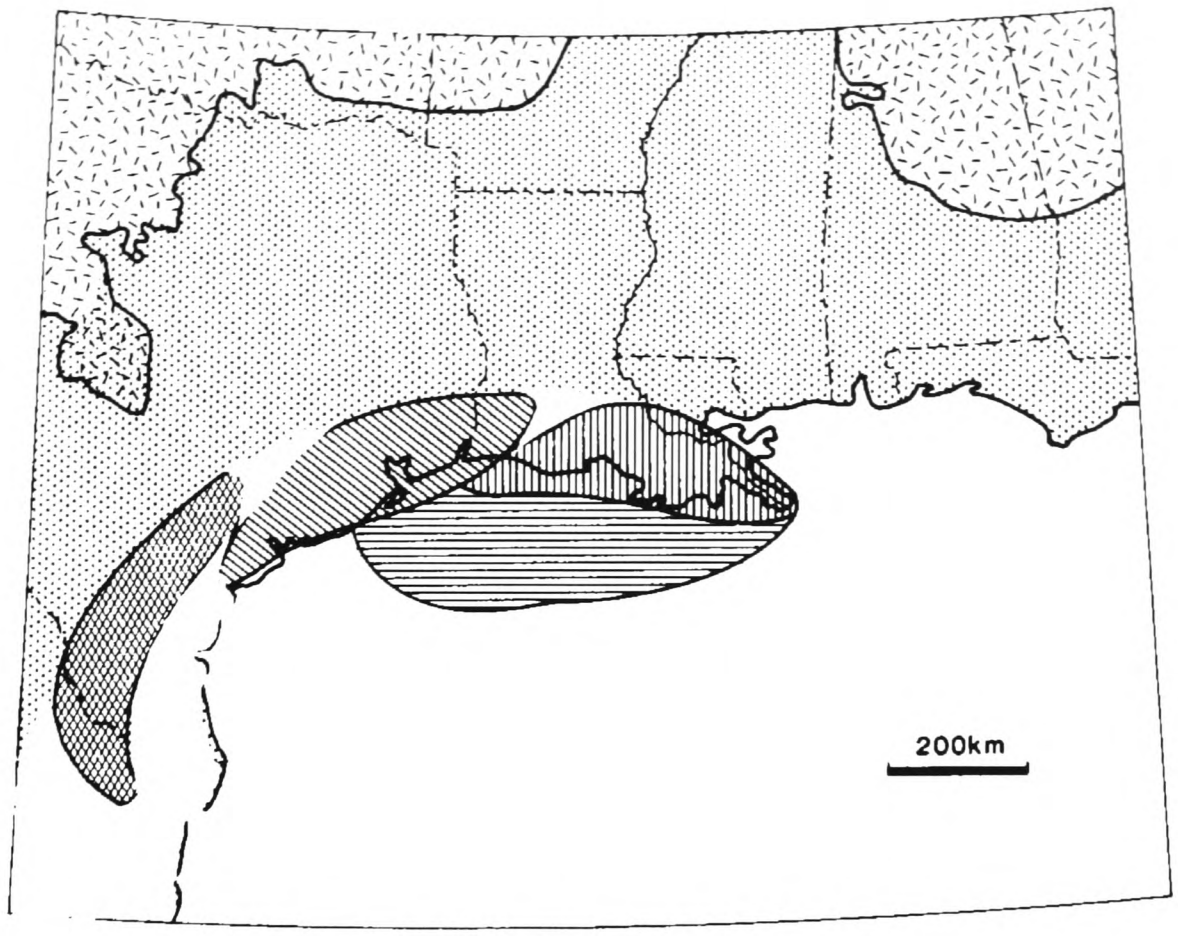

Figure 6.31: Schematic map of sediment depocentres of the Gulf Coast area showing eastward and seaward migration of sediment depocentres (after Curtis, 1986).

strike variability is minimal in the southeastern and northwestern parts of the Niger Delta Basin (Short and Staeuble, 1967).

Ages and oil producing trends are also similar for the three Tertiary deltas, the Mississippi, Niger and Beaufort-Mackenzie. These basins contain sediments amounting up to 16 km in the Beaufort-Mackenzie Delta with vertical gross lithological sequence bearing shales at the base, overlain by interbedded sandstones and shales, overlain by thick sandstones. They generally prograded in regressive basin-filling as the basins subsided. The vertical lithological sequence is repeated laterally from the basin landward in all three basins. The stratigraphic units of the depositional sequences generally thicken basinward across a series of normal

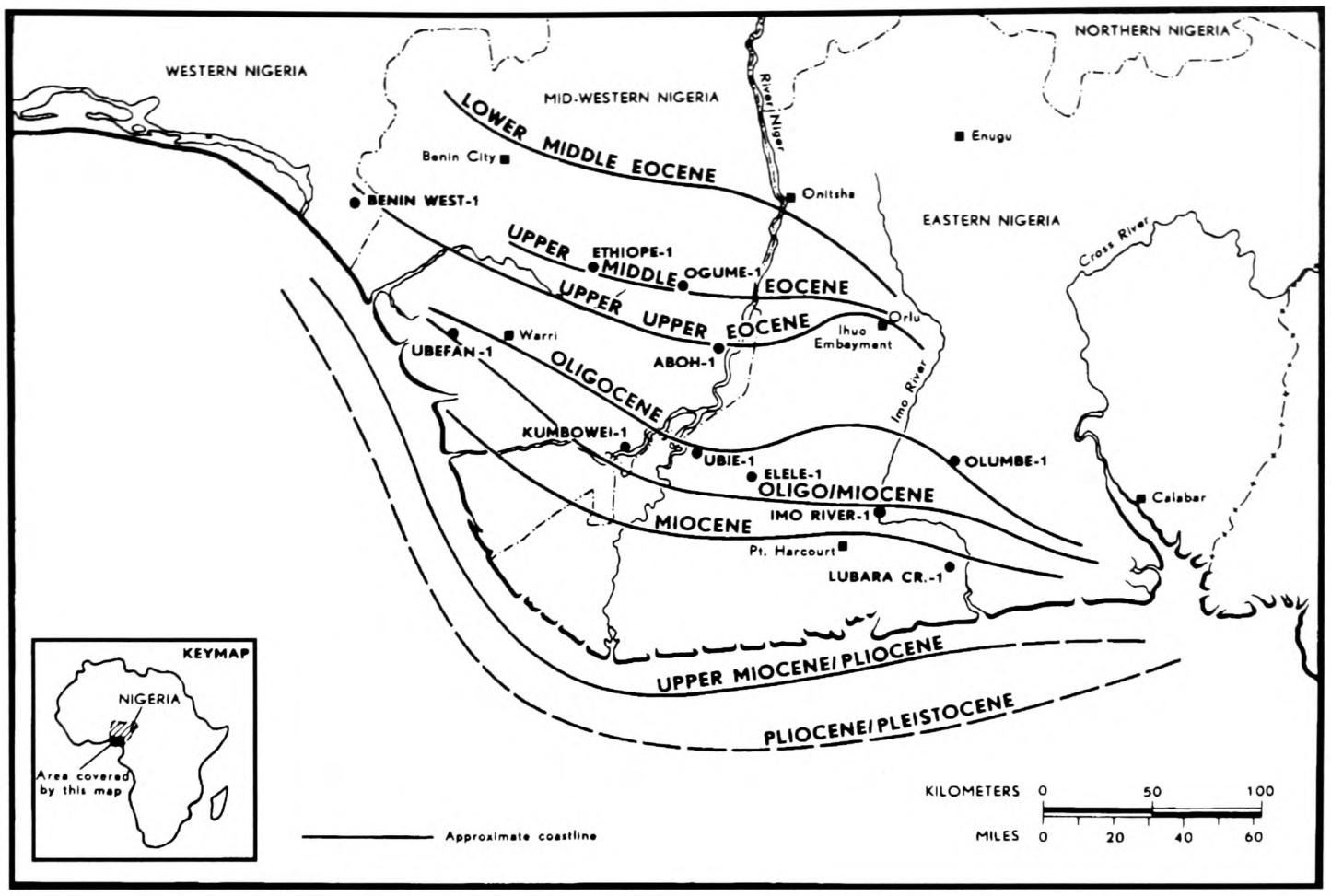

Figure 6.32: Paleogeographic map of Tertiary evolution of the Niger Delta (after Short and Staeuble, 1967).

listric down to the basin syn-depositional faults, (Fig. 6.30). Another important common characteristic in these basins is hydrocarbon trapping associated with diapiric (salt and shale diapiric) structures and abnormal pressures driving gravity mass movements.

The Namurian basin of western Ireland offers good rock exposures which enable the observational study and comparison of depositional and structural features often mapped on subsurface data. It is therefore used here as an analogue to the seismic expression of the above sedimentary characteristics on outcrop scale. Erosional channels and channel valleys observed at a larger scale in the Namurian basin reproduce in a similar way the same structures mapped on seismic data from the Zambezi Delta Basin.

6.6.7 Summary of similarities and differences.

Some similarities between the Zambezi Delta Basin and the the Mississippi, Niger, Beaufort-Mackenzie and the Namurian basin in Ireland are identi-

fied. These include: 1) generally basinward regressive depositional pattern which produced vertical and lateral deltaic depositional sequences with patterns typical of lithofacies units and syn-depositional growth faulting (limited in the Zambezi Delta Basin). However rollover and diapiric (salt and/or shale) structures common in the Mississippi, Niger, Beaufort-Mackenzie and Namurian Basin of western Ireland are not characteristic features in the Zambezi Delta Basin. However, growth faulting in the Zambezi Delta Basin is observed as a one-of event in late Eocene, which involved late Cretaceous to late Eocene successions. The amounts of sediments deposited during Tertiary to Recent times exceeds 10km in all Tertiary deltas refered to in this study.

Differences amongst these deltas lie in their geological and tectonic settings, rate of deposition to rate of basin subsidence, the palaeoenvironmental aspects concerning river, wave or tide dominance and climate and the influence of eustatic sea level variations. In the Mississippi Delta the presence of salt resulted in a wide variety of salt dome structures in addition to diapirs and roll-over anticlines common to all three basins. Tectonic settings prior to Tertiary deposition is different in all three basins. Therefore it is believed here that the tectonic setting prior to deltaic development is not as relevant as tectonic processes during and after deltaic deposition. Variations in delta morphology and sand bodies geometry can be attributed to variations in ratios of rates of deposition to rates of basin subsidence. Along-strike variability as observed in the Zambezi Delta Basin is also observed with some similarity in the Mississippi Delta where a steady eastwards shift of deltaic depocentres causes strike variability in the basin.

Chapter 7

Conclusions and recommendation for further work.

Chapter 6 is a summary of main findings of the present work. The results of this study are compared to previous work and finally some recommendations for further work are made.

7.1 Summary of main findings.

Analyses of seismic and well log data, has enabled an improved structural and seismic stratigraphic model of late Cretaceous and Tertiary evolution of the Zambezi Delta Basin to be made, which allows for a better understanding of the tectono-stratigraphic development and evolution of the basin. The results of the present work demonstrate that late Cretaceous to Recent times Zambezi Delta Basin evolution is controlled mainly by two depositional processes, fluvial and basin (wave) processes and by the variability in sediment supply in two main depocentres. The interplay of the above factors with tectonics, climate and sea level changes generated the overall late Cretaceous to Recent basin stratigraphy and depositional architecture. The basin is situated in central Mozambique at the present day Zambezi River mouth and extends from onshore to the offshore in a NW-SE direction into the waters of the Mozambique Channel over an estimated area of about 350,000 square kilometres both on- and offshore to the 2500m

isobath.

Approximately 21,700km of seismic data and logs from nine wells have been used to re-evaluate the sedimentary and geotectonic history of the Zambezi Delta Basin, offshore sector. Seismic stratigraphic methods applied to the seismic data, allow a detailed basin chronostratigraphy to be made with consequent improved understanding of the basin's fill history. Sedimentation during Tertiary and Quaternary deltaic buildout in the Zambezi Delta Basin is interpreted here as alternating between two main depocentres both of which are structurally controlled.

It is demonstrated that sedimentation alternated along a SW-NE zone between two main depocentres separated by the Beira basement high during their Tertiary development. The Zambezi Delta southwestern depocentre is bounded to the southeast by the Beira basement uplift while the East African Rift active extension in the northeast is suspected to be an active E-W graben structure. The latter is bounded to the south by the northeastern flank of the Beira basement high.

It is shown that several periods of non-deposition and erosion (hiatus) are recorded across the basin, some of which are restricted to parts of the basin while others are widespread in the basin (regional unconformities). Generally, periods of sedimentation in one depocentre mean a period of non-deposition and erosion in the other depocentre with sediment bypass and reworking and redeposition in deeper parts of the basin (not covered by seismic data used in this study). Moreover sedimentation is controlled by onshore tectonics controlling sediment sources with tectonics, eustatic sea level variations and sediment load controlling basin subsidence and accommodation space in the basin offshore.

In the early stages of major depositional cycles, sedimentation generally is restricted to small areas which with time become widespread in the depocentres and at times cover the whole basin. Lithofacies relationships are very complex in the basin due to the sedimentary architecture produced by the interplay between sea level variation, basin subsidence and sediment supply. This rendered an attempt to produce a lithofacies correlation through the well connecting profiles inpractical, due to some extent to the large distances separating the wells and

the complex stratigraphic relationships within the sedimentary strata.

Subsidence analyses confirmed observations made on seismic data on the interference of sediments from the Save River Delta with those from the Zambezi Delta. Subsidence curves reveal a common character for the wells Sangussi Marine-1, Sengo Marine-1, Zambezi-1, Zambezi-3, Micaune and Nhanguazi-1 during deltaic development in the Zambezi Delta Basin. However, the amount of basin subsidence observed is variable for each well site. This might be explained by the exploration wells relative position with respect to the main tectonic events onshore which determined sediment source position relative to the basin. This will have determined the sediment supply routes (sediment supply pathways), the amount of sediment supplied to these locations as well as the amount of time these locations were exposed to erosion during depositional hiatuses. For the wells Sofala-1, Nemo-1 and Divinhe-1 to the southwest, a different picture emerges from the subsidence analyses, probably suggesting a different dominant deltaic setting for the stratigraphy of these wells. This picture is in agreement with observations made on seismic data, which show that in general sedimentation switched to the northeastern depocentre after the last rifting episode and higher sedimentation rates are recorded in this depocentre from early Neogene times onwards (see Fig. 6.4).

The integrated study of gravity and magnetic contour maps enabled the identification of the main structural trends of the basin summarised on Fig. 5.4. The structures identified here are in line with structures and structural trends mapped on seismic data and discussed in Chap. 4 or mapped and discussed by other workers. However, it is believed from the results of this study that the southwestern depocentre is a product of rift tectonics, which opened the basinal structure right at the early stages of continental breakup. This tectonism followed pre-existing structural trends which set up the breakup geometry in Middle Jurassic for this area.

Results from 2D depth to magnetic basement on five profiles (Fig. 5.6) across chosen locations showed some correlation with results achieved with seismic data. Due to poor data quality these results can only be used qualitatively.

Nevertheless, they are in agreement with results reflecting regional structural trends in the east African continental margin achieved previously by other workers.

The Free-Air gravity model achieved in this study is a variant of the usual model achieved when crustal thinning and accumulated sediments extend seaward from the coastal area at a rifted passive continental margin. In view of the fact that oceanic magnetic anomalies lie 300km away to the south, thin crust beneath the Zambezi Delta Basin sediments is thought to be continental in origin and stretched immediately prior to breakup in Middle Jurassic times. One interpretation of the gravity modelling is that a double positive-negative anomaly pair can be loosely related to the Watts and Marr (1995) idea of a "weak margin". However, the modification to Moho depth in the final model away from local isostatic equilibrium poses questions about the accuracy of the deep structure of the model. Since the shallow structure cannot be significantly in error it raises the possibility of the existence of undetermined deep density variations. One option would be to introduce a significant thickness of crustal underplating instead of increased crustal thinning in Fig.5.13 in order to achieve a better compromise between the final gravity model and isostatic equilibrium model (Fig. 5.11 C). Alternatively, the significant Neogene-Recent layer of 5-6km thickness may be receiving some isostatic compensation flexurally because of the increasing strength of the lithosphere as the margin has aged. This would allow explanation of part of the shelf-edge gravity high without recourse to extra crustal thinning or underplating. In this case the gravity profile would reflect a "weak margin" as described by Watts and Marr (1995) and my preference, is for this latter interpretation.

7.2 Comparison with previous work.

A substantial amount of work on the geology of the Mozambique Basin on- and offshore, which includes the Zambezi Delta Basin has been published over the years. This work ranges from onshore geology to offshore marine geology and geophysics which has contributed significantly to the advances made to

date on the geotectonic evolution of the East African continental margin post-continental breakup. Some of the most valuable contributions are by Dingle and (1974), Forster (1975), Scrutton and Dingle (1976), Kamen-Kaye (1978; 1982; 1983), Segoufin (1981), Scrutton *et al.* (1981), Dingle *et al.* (1983), Flores (1970; 1973; 1983; 1984), Al-Kasim *et al.* 1985, Salman *et al.* (1985), Coffin and Rabinowitz (1987), Coster *et al.* (1989), Salman and Abdula (1995) only to mention a few. However, a summary of the petroleum geology of the Mozambique and the Rovuma Basins can be found in Salman *et al.* (1985) and Salman and Abdula (1995).

The present work makes a contribution to some aspects concerning the late Cretaceous to Recent evolution of the Zambezi Delta Basin. A detailed stratigraphic account of the Neogene to Recent section of the stratigraphy of the basin improves greatly the understanding of the degree of complexity of the deltaic succession. The integration of newly interpreted seismic and well data set, including gravity and magnetic maps and profiles, enabled a broad assessment of the structural setting of the basin. A rift and thermal subsidence situation can be suggested as the mechanism probably responsible for bringing about the southwestern depocentre, one of two main depocentres derived for the delta basin in this study. The northeastern depocentre is interpreted also for the first time as a still subsiding graben structure possibly produced during continental breakup in Middle Jurassic reactivated during the east African Rift System in Middle Tertiary. This structure is believed here to still be active, hence causing sediment disruption above what are believed to be active fault zones, a claim which is partly supported by significant seismic activity recorded during the last few decades.

For the first time the Zambezi Delta sediment succession is interpreted as switching between two main depocentre thus producing along-strike vaiability. This is of great importance for hydrocarbon prospectivity in the basin and must be taken into account when developing play concepts for hydrocarbon exploration.

7.3 Further work.

This study is an integrated geophysical and geological re-evaluation of existing seismic, well log, gravity and magnetic data with the view to producing an improved understanding of basin evolution and depositional history of the deltaic succession. The results achieved with this work not only confirm some previous findings but also provide a better understanding of the development and evolution of the basin and its depositional history.

For the first time the Zambezi Delta sediment succession is interpreted as switching between two main depocentre thus producing along-strike vaiability.

The seismic stratigraphic interpretation produced in this study has a potential not only to impact upon existing sequence stratigraphic models for deltaic settings for example in the interpretation of depositional sequences and "system tracts".

Exploration work will have to be extended to some of the deep water areas and to the itermediate area of the basin which lies between on-shore and off-shore seismic grids if more is to be known about the hydrocarbon potential of the basin. Well drilling must also be extended to unexplored areas of the basin with possible hydrocarbons potential in the deep water sector and in the northeastern depocentre. Deeper boreholes are key to probe new sections of the basin stratigraphy, which to date are only known by indirect geophysical data interpretations (structural and stratigraphic inference). The northeastern depocentre which is composed mainly of Neogene sediments and some older, deeper deposits remains underexplored.

The seismic grid of 10x10km is very wide and only allows the mapping of large structures, therefore a finer grid would be necessary to allow more detail than could be achieved here. New 3D seismic data, with a longer recording period will enable the study of the lower section of the basin. It is recommended in this work that future exploration work should contemplate the deep water environment as well as the present shallow water sector where seismic data need to be updated with better quality 3D seismic data. The deep water sector, however, will provide much needed information as to whether lowstand fans have developed

during sea level lowstand as there is evidence for sediment bypass and sediment reworking from the shoreface during times of sea level lowstand. The stratigraphic relationships between lowstand sand bodies (lowstand fans) and the transgressive muds is of great significance in determining whether stratigraphic plays can be expected in the deep water environment. It will also provide information about possible hydrocarbon prone source rocks deposited in that environment prior and during deltaic deposition.

The poor quality of well data are of great concern for accurate age dating of the sedimentary strata as mapped here. Therefore any new wells drilled in the area in the future will help to overcome the discrepancies often observed amongst the information provided by existing data acquired between 1956 and 1973.

Better gravity and magnetic data coverage could provide better gravity and magnetic maps which would yield in better assessment of the basement structure and better structural models. These could help address outstanding questions on the structural development of the Zambezi Delta Basin.

Bibliography

Abdula, I. and Salman, G., 1995. Geology, potential of Pande gas field, Mozambique Basin. Oil and Gas Journal, v. **93**, n. 43, p. 102-106.

Al-Chalabi, M., 1974. An analysis of stacking, rms, average, and interval velocities over a horizontally layered ground. Geophysical Prospecting, v. **22**, n. 3, p. 458-475.

Al-Chalabi, M., 1979. Velocity determination from seismic reflection data. In: Fitch, A. A. (Ed.), Development in geophysical exploration methods - 1. Applied Sci. Publ., London, pp. 1-68.

Al-Kasim, F., Narayanan, K. and Riis, F., 1985. Basin Evolution on the Coast of Africa and in Western Indian Ocean During/After Break of Gondwanaland. Unpublished report, NPD, Stavanger, Norway.

Allen, J. R. L., 1970. Sediments of the modern Niger delta; a summary and review. In: Deltaic sedimentation; modern and ancient. Special Publication - Society of Economic Paleontologists and Mineralogists, v. **15**, p. 138-151.

Allen, P.A. and Allen, J.R.,1992. Basin Analysis - Principles and Applications. Blackwell Scientific Publications. Oxford, London, Edinburgh, Boston, Melbourne, Paris, Berlin, Vienna, 451 pp.

Barongo, J. O., 1985. Method for depth estimation on aeromagnetic vertical gradient anomalies. Geophysics, v. **50**, n. 6, p. 963-968.

Beck, R.H., and Lehner, P., 1974. Oceans, New Frontiers in Exploration. AAPG Bull., Vol. **58**, pp. 376-395.

Beltrandi, M. and Pyre, A., 1973. Geologic evolution of South-west Somalia. In: Blant, G. (ed.) Sedimentary basins of African coast; 2, South and east coast

Besaire H., 1972. Geologie de Madagascar I. Les terrains sedimentaires. Tananarive: Malagasy Imprimerie Nationale. Ann. Geolo. Madagascar. No.35.

Blant, G., 1973. Structure et paleogeographie du littoral meridional et oriental de l'Afrique (Structure and paleogeography of the southern and eastern coast of Africa). In: Bassins Sedimentaires du Littoral Africain–Sedimentary Basins of the African Coasts, Symposium, Part 2, Littoral Austral et Oriental–South and East Coast, p. 193-231.

Brown, L. F., Jr. and Fisher, W. L., 1982. Seismic-stratigraphic interpretation of depositional systems; examples from Brazilian rift and pull-apart basins. In: **Payton, C.E. (Ed.)**, Seismic stratigraphy; applications to hydrocarbon exploration. Memoir - American Association of Petroleum Geologists, n. **26**, p. 213-248.

Castaing, C., 1991. Post-Pan-African tectonic evolution of South Malawi in relation to the Karoo and Recent East African Rift Systems. Tectonophysics, Vol. **191**, pp. 55-73.

Church, K.D. and Gawthorpe, R.L., 1994. High resolution sequence stratigraphy of the late Namurian in the Widmerpool Gulf (East Midlands, UK). Marine and Petroleum Geology, v. **11**, n. 5, p. 528-543.

Church, K.D. and Gawthorpe, R.L., 1997. Sediment supply as a control on the variability of sequences; an example from the late Namurian of northern England. Journal of the Geological Society of London, v. **154** Part 1, p. 55-60.

Clifford, A.J., 1984. African oil; past, present, and future. AAPG Bulletin, v. **68**, n. 9, p. 1200.

Clifford, A.J., 1986. African oil; past, present, and future. AAPG Memoir **40**, pp. 339-373.

Coffin, M.F. and Rabinowitz, P.D., 1987. Reconstruction of Madagascar and Africa: Evidence from the Davie Ridge Fracture Zone and Western Somali Basin. J. Geophys. Res., **92 (B9)**, pp. 9385-9406.

Cook, F.A., Coflin, K.C., Lane, L.S., Dietrich, J.R. and Dixon, J., 1987. Structure of the southeast margin of the Beaufort-Mackenzie Basin, Arctic Canada, from crustal seismic-reflection data. Geology (Boulder), v. **15**, n. 10, p. 931-935.

Cooper, M. A., Collins, D. A., Ford, M., Murphy, F. X., Trayner, P. M. and O'Sullivan, M., 1986. Structural evolution of the Irish Variscides. Journal of the Geological Society of London, v. **143**, n. 1, p. 53-61.

Coster, P.W., 1983. Mozambique Final Report: Seismic Interpretation Areas I,II,III. Report to ENH, Mozambique. Unpublished Report.

Coster, P.W., Lowrence, S.R. and Fortes, G., 1989. Mozambique: A new geological framework for hydrocarbons exploration. J. Pet. Geol., **12(2)**, pp. 205-230.

Cratchley, C. R. and Jones, G. P., 1965. An interpretation of the geology and gravity anomalies of the Benue valley, Nigeria. Great Britain, Overseas Geol. Surv., Geophys. Div., Geophys. Paper, v. **1**, 26 p.

Cruickshank, A. R. I., 1978a. Palaeontological perspectives. South African Journal of Science, v. **74**, n. 12, p. 453-454.

Cruickshank, A. R. I., 1978b. Feeding adaptations in Triassic dicynodonts. Palaeontologia Africana, v. **21**, p. 121-132.

Curtis, Doris M., 1970. Miocene deltaic sedimentation, Louisiana Gulf Coast. In: Morgan J.P. (Ed.) Deltaic sedimentation; modern and ancient. Special Publication - Society of Economic Paleontologists and Mineralogists, v. **15**, p. 293-308.

Curtis, D.M., 1986. Comparative Tertiary petroleum geology of the Gulf Coast, Niger, and Beaufort-Mackenzie Delta areas. Geological Journal, v. **21**, n. 3, p. 225-255.

Daly, M.C. and Unrug, R., 1982. The Muva Supergroup of northern Zambia: A craton to mobile belt sedimentary sequence. Trans. Geol. Soc. S. Africa, v. **85**, pp 155-165.

Darracott, B. W., Fairhead, J. D., Girdler, R. W. and Hall, S.A., 1973. The East African Rift System; Implications of Continental Drift to the Earth Sciences. Rifts and Oceans, Vol. **2**; Part 7, p. 757-766.

Davis, S.J. and Elliott, T., 1994. Spectral gamma ray charcterization of high resolution sequence stratigraphy: examples from Upper Carboniferous fluvio-deltaic systems, County Clare, Ireland. In: **Howell, J.A., and Aitken, J.F. (Eds.)**, High Resolution Sequence stratigraphy: Inovations and Applications. Geol. Soc. Special Publ. no. **104**, pp. 25-35.

Davis, B. K., 1990. Velocities for depth conversion. In: **Ala, M., Hatamian, H., Hobson, G. D., King, M. S., Williamson, I. (Eds.)**, Seventy-five years of progress in oil field science and technology. A. A. Balkema, Rotterdam, pp. 145-152.

De Buyl, M. and Flores, G., 1986. The Southern Mozambique Basin: The most promising hydrocarbon province offshore East Africa. In: **Michael T. Halbouty (Editor)**, Future Petroleum Provinces of the World. AAPG Mem. **40**, pp. 399-425.

Dietrich, J. R., Dixon, J. and McNeil, D. H., 1985. Sequence analysis and nomenclature of Upper Cretaceous to Holocene strata in the Beaufort-Mackenzie Basin. Paper - Geological Survey of Canada, v. **85-1A**, p. 613-628.

Dingle, R.V. and Scrutton, R.A., 1974. Continental Breakup and the Development of Post-Paleozoic Sedimentary Basins around Southern Africa. Geol. Soc. of America Bulletin, Vol. **85**, pp. 1467-1474.

Dingle, R.V., 1976. A review of the sedimentary history of some post-Permian continental margins of atlantic-type. In: **de Almeida, F. F. M. (Ed.)**, Simposio internacional sobre as margens continentais de tipo atlantico. Anais da Academia Brasileira de Ciencias, v. **48**, p. 67-80, Suplemento.

Dingle, R.V., 1982. Continental margin subsidence; a comparison between the east and west coasts of Africa. In: **Scrutton, Roger A., (editor)**, Dynamics of passive margins, Geodynamics Series, v. **6**, p. 59-71.

Dingle, R.V., Siesser, William G. and Newton, A. R., 1983. Mesozoic and Tertiary geology of Southern Africa. A.A. Balkema, Rotterdam, 383 p.

Dixon, J., Dietrich, J., Snowdon, Lloyd R., Morrell, G. and McNeil, D. H., 1992. Geology and petroleum potential of Upper Cretaceous and Tertiary strata, Beaufort-Mackenzie area, Northwest Canada. AAPG Bulletin, v. **76**, n. 6, p. 927-947.

DNG (Direccao Nacional de Geologia), 1987. Carta Geologica de Mocambque (Geological map of Mozambique). Scale: 1:1 000 000.

DNG (Direccao Nacional de Geologia), IGM (Instituto Geologico Mineiro de Portugal) 1999. Carta Geologica da Margem continental de Mocambque (Geological map of the continental margin of Mozambique). Scale: 1:2 000 000.

Dobrin, Milton B. and Savit, Carl H., 1988. Introduction to geophysical prospecting. McGraw-Hill Book Co., New York, Fourth Edition, 867 p.

Droz, L. and Mougenot, D., 1987. Mozambique Upper Fan: Origin of Depositional Units. AAPG Bull., Vol. **71**, No. 11, pp. 1335-1365.

Du Toit, A.L., 1937. Our Wandering Continents. Oliver and Boyd, Edinburgh, 366 p.

Ebinger, C.J., Crow, M.J., Rosendahl, B.R., Livingstone, D.A. and Le Fournier, J., 1984. Structural evolution of Lake Malawi, Africa. Nature (London), v. **308**, n. 5960, p. 627-629.

Ebinger, C.J., Rosendahl, B. R. and Reynolds, D. J., 1987. Tectonic model of the Malawi Rift, Africa. Tectonophysics, v. **141**, n. 1-3, p. 215-235.

Elliott, T., 1986. Deltas. In: **H.G. Reading (Ed.)**, Sedimentary Environments and Facies, 2nd Edition, Blackwell Scientific Publications, Oxford.

Flores, G., 1984. The SE Africa triple junction and the drift of Madagascar. Journal of Petroleum Geology, Vol. **7**, No. 4, pp. 403-418.

Flores, G., 1973. The Cretaceous and Tertiary sedimentary basins of Mozambique and Zululand. In: **G. Blant (Editor)**, Sedimentary basins of African Coasts. pt. 2, South and East Coasts. Assoc. African Geol. Surveys, Paris, pp. 81-111.

Flores, G., 1970. Suggested origin of the Mozambique Channel. Trans, Geol. Soc. S. Afr., Vol. **73**, No. 1, pp. 1-16.

Forster, R., 1975. The geological history of the sedimentary basin of southern Mozambique, and some aspects of the origin of the Mozambique Channel. Palaeogeogr. Palaeoecol., Vol. **17**, No. 4, pp. 267-287.

Fortes, G. and Kihle, R., 1983. The petroleum geology and hydrocarbon prospectivity of Mozambique. ENH. Archives,Maputo.

Galloway, W.E., 1975. Process framework for describing the morphologic and stratigraphic evolution of deltaic depositional systems. In: **Broussard, M.L. (Ed.)**, Deltas, models for exploration, p. 87-98.

Galloway, W.E., 1987. Depositional and structural architecture of prograding clastic continental margins; tectonic influence on patterns of basin filling. Norsk Geologisk Tidsskrift. Vol. **67**, No. 4, pp. 237-251.

Galloway, W.E., 1989a. Genetic stratigraphic sequences in basin analysis; I, Architecture and genesis of flooding-surface bounded depositional units. AAPG Bulletin, v. **73**, n. 2, p. 125-142.

Galloway, W.E., 1989b. Genetic stratigraphic sequences in basin analysis; II, Application to Northwest Gulf of Mexico Cenozoic basin. AAPG Bulletin, v.textbf73, n. 2, p. 143-154.

Galloway, W.E., 1990. Clastic facies models, depositional systems, sequences, and correlation; a sedimentologist's view of the dimentional and temporal resolution of lithostratigraphy. In: **Cross, Tomothy A. (Ed.)**, Quantitative dynamic stratigraphy, p. 459-477.

Gardner, G. H. F., Gardner, L. W. and Gregory, A. R., 1974. Formation velocity and density; the diagnostic basics for stratigraphic traps. Geophysics, v. **39**, n. 6, p. 770-780.

GECO, 1983. Reports by Geophysical Co., Norway to ENH, Mozambique. Unpublished reports.

GECO, 1985. Reports by Geophysical Co., Norway to ENH, Mozambique. Unpublished reports.

Gill, W. D., 1979. Syn-depositional sliding and slumping in the West Clare Namurian basin, Ireland. Special Paper - Geological Survey of Ireland, n. 4, 31 p.

Gill, J. R. and Cobban, W. A., 1973. Stratigraphy and geologic history of the Montana Group and equivalent rocks, Montana, Wyoming, and North and South Dakota. U. S. Geological Survey Professional Paper, 37 p.

Haq, B.U., Hardenbol, J. and Vail, P.R., 1987. Chronology of Fluctuating sea levels since the Triassic. Science, v. **235**, n. 4793, p. 1156-1167.

Haq, B.U., Hardenbol, J. and Vail, P.R., 1988. Mesozoic and Cenozoic chronostratigraphy and cycles of sea-level change. In: **Wilgus, C.K., Hastings, B.S., Ross, C.A., Posamentier, H.W., Van Wagoner, J. and Kendall, C.G. St. C. (Eds.)**, Sea-level changes; an integrated approach. Special Publication - Society of Economic Paleontologists and Mineralogists, v. **42**, p. 72-108.

Hawkings, T.J. and Hatfield, W.G., 1975. The regional setting of the Taglu field. In: **Yorath, C.J., Parker J.R., and Glass, D.J. (Ed.)**, Canada's continental margins. Mem. Can. Soc. Petrol. Geol., v. **4**, pp. 633-648.

Hubard, R.J., 1988. Age and Significance of Sequence Boundaries on Jurassic and Early Cretaceous Rifted Continental Margins. AAPG Bull., Vol. **72**, No. 1, pp. 49-72.

Hubard, R.J., Pape, J. and Roberts, D., G., 1986a. Depositional sequence mapping to illustrate the evolution of a passive continental margin. In: **Berg, O.R., Woolverton, D.G. (Eds.)**, Seismic stratigraphy II; an integrated approach to hydrocarbon exploration. AAPG Memoir, v. **39**, p. 93-115.

Hubard, R.J., Pape, J. and Roberts, D., G., 1986b. Depositional sequence mapping as a technique to establish tectonic and stratigraphic framework and evaluate hydrocarbon potential on a passive continental margin. In: **Berg, O.R., Woolverton, D.G. (Eds.)**, Seismic stratigraphy II; an integrated approach to hydrocarbon exploration. AAPG Memoir, v. **39**, p. 79-91.

Huff, K. F., 1980. Frontiers of world exploration. In: **Miall, A. D. (Ed.)**, Facts and principles of world petroleum occurrence. Memoir - Canadian Society of Petroleum Geologists, n. **6**, p. 343-362.

Iliffe, J.E., DeBuyl, M., Kendall, C.G.S. and Lerche, I., 1986. Two dimensional restoration of seismic-reflection profiles from Mozambique - Technique for assessing rift extention histories. AAPG Bull., Vol. **70**, No. 5, p. 603. (Meeting abstract).

Iliffe, J.E., Lerche, I. and DeBuyl, M., 1991. Basin analysis and hydrocarbon generation of the South Mozambique Graben using extensional models of heat flow. Marine and Petroleum Geology, v. **8**, n. 2, p. 152-162.

Kajato, K., 1986. The Geology and Hydrocarbon Potential of Tanzania. Oil and Gas Exploration in the SADCC Region, pp. J1-J38.

Kajato, K., 1994. Rovuma Basin, Mozambique and Tanzania. Proposed Regional Seismic Su rvey and Stratigraphic Well. In: Petroleum exploration in southern Africa: Proceedings of SADCC Energy Sector Petroleum conference, Windhoek, 19-21 October 1993, pp. 259-298.

Kamen-Kaye, M., 1978. Permian to Tertiary faunas and palaeogeography: Somalia, Kenya, Tanzania, Mozambique, Madagascar, South Africa. J. Pet. Geol., v. **1**, n. 1, pp. 79-101.

Kamen-Kaye, M., 1982. Mozambique Madagascar Geosyncline I: Deposition and Architecture. Jour. Pet. Geol. Vol. **5**, No. 1, pp. 3-30.

Kamen-Kaye, M., 1983. Mozambique Madagascar Geosyncline II: Petroleum Geology. Jour. Pet. Geol. Vol. **5**, No. 3, pp. 287-308.

Kearey, P. and Vine, F.J., 1996. Global tectonics. Second edition, Blackwell Science, Oxford, 333 p.

Kihle, R., 1983. Recent surveys outline new potential for offshore Mozambique. Oil and Gas Journal, v. **81**, n. 9, p. 126-134.

King, L., 1973. An improved reconstruction of Gondwanaland; In: Implications of Continental Drift to the Earth Sciences. Palaeogeographic Implications. Academic Press, London, Vol. **2**, Part 8, pp. 851-864.

King, N.W., 1958. Basic palaeogeography of Gondwanaland during the Late Palaeozoic and Mesozoic Eras. Quart. J. Geol Soc. London, Vol. **114**, Part 1, n. 453, pp. 44-70.

Lawrence, S.R., 1989. Prospects for petroleum in Late Proterozoic/Early Palaeozoic Basins of Southern-Central Africa. Journal of Petroleum geology, Vol. **12**, No. 2, pp. 231-242.

Le Roux, J.P., 1985. Tectonic and sedimentological environments of sandstone-hosted uranium deposits, with special reference to the Karoo Basin of South Africa. In: **Finch, W.I.; Davis, J.F. (Eds.)**, Geological environments

of sandstone-type uranium deposits, p. 279-290. 27A - Economic geology, geology of ore deposits.

Le Roux, J. P., Toens, P. D., 1986. A review of the uranium occurrence in the Karoo Sequence, South Africa. In: **Anhaeusser, C. R., Maske, S. (Eds.)**, Mineral deposits of Southern Africa, p. 2119-2134. 27A - Economic geology, geology of ore deposits.

Le Roux, J. P. and Toens, P. D., 1987. The Permo-Triassic uranium deposits of Gondwanaland. In: **McKenzie, Garry D. (Eds.)**, Gondwana Six; Stratigraphy, sedimentology, and paleontology. Geophysical Monograph, v. **41**, p. 139-146. AGU.

Lehner, P. and de Ruiter, P. A. C., 1977. Structural history of Atlantic margin of Africa. AAPG Bulletin, v. **61**, n. 7, p. 961-981.

Lort, J.M., Limond, W.Q., Segoufin, J. and Patriat, Ph., 1979. New seismic data in the Mozambique Channel. Mar. Geophys. Res., Vol. **4**, pp. 71-89.

Martin, A.K., 1984. Plate tectonic status and sedimentary basin infill of the Natal Valley. (S.W. Indian Ocean). PhD Thesis, Bull. 14, M.G.U. Univ. of Cape Town.

Martin, A. K., 1987. Comment on "Relative positions of Africa and Antarctica in the Upper Cretaceous; evidence for non-stationary behaviour of fracture zones", by Ph. Patriat, J. Segoufin, J. Goslin and P. Beuzart. Earth and Planetary Science Letters, v. **81**, n. 2-3, p. 312-316.

Martinsen, O.J., 1989. Styles of soft-sediment deformation on a Namurian (Carboniferous) delta slope, western Irish Namurian Basin, Ireland. In: **Whateley, M. K. G., Pickering, K. T. (Eds.)**, Deltas; sites and traps for fossil fuels. Geological Society Special Publications, v. **41**, p. 167-177.

Martinsen, Ole J. and Bakken, B., 1990. Extensional and compressional

zones in slumps and slides in the Namurian of County Clare, Ireland. Journal of the Geological Society of London, v. **147**, n. 1, p. 153-164.

Martinsen, O.J., 1993. Namurian (Late Carboniferous) depositional systems of the Craven-Askrigg area, northern England; implications for sequence-stratigraphic models. In: **Posamentier, H.W., Summerhayes, C.P., Haq, B.U.; Allen, G.P. (Eds.)**, Sequence stratigraphy and facies associations. Special Publication of the International Association of Sedimentologists, v. **18**, p. 247-281.

Martinsen, O.J. and Helland-Hansen, W., 1995. Strike variability of clastic depositional systems; does it matter for sequence-stratigraphic analysis?. Geology (Boulder), v. **23**, n. 5, pp. 439-442.

Mascle, J., 1976. Atlantic-type continental margins; distinction of two basic structural types. In: **de Almeida, F. F. M. (Ed.)**, Simposio internacional sobre as margens continentais de tipo atlantico (Continental Margins of Atlantic Type). Anais da Academia Brasileira de Ciencias, v. **48**, p. 191-197, Suplemento.

Mascle, J., Mougenot, D., Blarez, E. Marinho, M and Virlogeux, P., 1987. African transform continental margins: examples from Guinea, the Ivory Coast and Mozambique. Geol. Jour. Vol. **22**, pp. 537-561.

Miall, A.D., 1997. The geology of stratigraphic sequences. Springer-Verlag, Berlin. 433 p.

Militzer, H. und Weber, F., 1984. Angewandte Geophysik - Band 1 - Granimetrie und Magnetik. Springer-Verlag, Vienna, Akad.-Verlag, Berlin, 353 p.

Militzer, H., Schoen, J. und Stoetzner, U., 1986. Angewandte Geophysik im Ingenieur- und Bergbau. Ferdinard Enke Verlag, Stuttgart, 419 p.

Mitchum, R. M., Jr., Vail, P. R. and Thompson, S., III, 1977a. Seismic stratigraphy and global changes of sea level; Part 2, The depositional se-

quence as a basic unit for stratigraphic analysis. In: **Payton, C. E. (Ed.)**, Seismic stratigraphy; applications to hydrocarbon exploration. Memoir - American Association of Petroleum Geologists, n. **26**, p. 53-62.

Mitchum, R.M., Vail, P.R. and Sangre, J.B., 1977b. Seismic stratigraphy and global changes of sea level; Part 6, Stratigraphic interpretation of seismic reflection patterns in depositional sequences. In: **Payton, C. E. (Ed.)**, Seismic stratigraphy; applications to hydrocarbon exploration. Memoir - American Association of Petroleum Geologists, n. **26**, p. 117-133.

Mitchum, R. M., Jr. and Vail, P. R., 1977c. Seismic stratigraphy and global changes of sea level; Part 7, Seismic stratigraphic interpretation procedure. In: **Payton, C. E. (Ed.)**, Seismic stratigraphy; applications to hydrocarbon exploration. Memoir - American Association of Petroleum Geologists, n. **26**, p. 135-143.

Mougenot, D., Recq, M., Virlogeux, P., and Lepvrier, C., 1985. Une ramification sous-marine du Rift East-Africain: Les Grabens Kerimbas et Lacerda (marge continetale nod-mozambique). Reunion soc. Geol. France, Geologie des Oceans, Bordeaux, 2 et 3 Decembre. (Abstract)

Mougenot, D., Recq, M., Virlogeux, P. and Lepvrier, C., 1986a. Seaward extension of the East African Rift. Nature, Vol. **321**, No. 6070, pp. 599-603.

Mougenot, D., Vanney, J.R., and Vilogeux, P., 1986b. La Marge Continentale Nord-Mozambique et la Chaine Davie: Presentation d'une novelle Carte Bathymetrique et de son interpretation geomorphologique. Soc. Geol. Fr., "Geologie et Geophysique des Oceans".

Mougenot, D., Virlogeux, P., Vanney, J.R., and Malod, J., 1986c. La marge continentale au Nord du Mozambique: resultats preliminaires de la campagne md40/macamo. Bull. Soc. Geol. France, V. **(8)**, t. II, no. 3, pp. 419-422.

Mougenot, D., Hernandes, J. and Virlogeaux, P., 1989. Tectonic and Volcanism in the submarine Kerimbas Graben (Northern Mozambique

Continental-Margin). Bulletin de la Societe Geologique de France, Vol. **5**, No. 2, pp. 401-409.

Nairn, A. E.M., Lerche, I. and Iliffe, J.E., 1991. Geology, basin analysis and hydrocarbon potential of Mozambique and the Mozambique Channel. Earth Sci. Rev., Vol. **30**, pp. 81-123

Narayanan, K. and Weier, H.L., 1980. Tanzania Oil Prospects: a new approach to oil and gas exploration. Report of UNIDO/UNDP Project URT/74/028 to Gov of Tanzania. Unpublished report.

Narayanan, K. and Vollset, J., 1980. Geological evolution of southern and eastern Africa before and after the break up of Gondwanaland. NPD, Stavanger, Norway. Unpublished report.

Narayanan, K. and Pederson, T., 1984. Seismic stratigraphic interpretation of the Zambezi Basin, Mozambique. Report OD-84-17, Norwegian Petroleum Directorate, Stavanger. Unpublished report.

Nicols, G.J. and Daly, M.C., 1989. Sedimentation in an intracratonic extensional basin: The Karoo of the central Morondava basin, Madagascar. Geol. Mag. v. **126**, pp. 339-354.

Parasnis, D. S., 1979. Principles of applied geophysics. 3rd. edition, Capman and Hall, New York, 275 p.

Partington, M. A., Copestake, P., Mitchener, B. C. and Underhill, J. R., 1993. Biostratigraphic calibration of genetic stratigraphic sequences in the Jurassic-lowermost Cretaceous (Hettangian to Ryazanian) of the North Sea and adjacent areas. In: **Parker, J. R. (Ed.)**, Petroleum geology of Northwest Europe; Proceedings of the 4th conference. Petroleum Geology of Northwest Europe: Proceedings of the 4th Conference, v. **4**, p. 371-386.

Patriat, P., Segoufin, J., Goslin, J., and Beuzart, P., 1985. Relative positions of Africa and Antarctica in the Upper Cretaceous: evidence for

non-stationary behavior of fracture zones. Earth Planet. Sci. Lett., Vol. **75**, p. 204-214.

Patriat, P. and Segoufin, J., 1987. Reply to the comment on "Relative positions of Africa and Antarctica in the Upper Cretaceous; evidence for non-stationary behaviour of fracture zones", by A. K. Martin. Earth and Planetary Science Letters, v. **81**, n. 2-3, p. 317-318.

Pedley, R.C, Busby, J.P., Dabek, Z.K., 1993. GRAVMAG, Vol. **1.1** User Manual - Interactive, 2.5D gravity and magnetic modelling. British Geological Survey, Technical Report WK/93/26/R, 77p.

Pedley, R.C, Phillips, M.W., Williamson, J.P., 1994. GRAVMAG Toolkit, Vol. **1.1** User Manual. British Geological Survey, Technical Report WK/94/1/R, 55p.

Peters, L.J., 1949. The direct approach to magnetic interpretation and its practical application. Geophysics, v. **14**, n. 3, p. 290-320.

Petters, S.W., 1991. Regional Geology of Africa. Springer-Verlag, Berlin, New York, London.

Picha, F.J., 1988. Sedimentary provinces of Africa, Middle East, and South America; classification and hydrocarbon potential. AAPG Bulletin, v. **72**, n. 2, p. 236.

Posamentier, H.W. and Vail, P.R., 1988. Eustatic controls on clastic deposition; II, Sequence and systems tract models. In: **Wilgus, C.K., Hastings, B.S., Ross, C.A., Posamentier, H.W., Van Wagoner, J. and Kendall, C.G.St.C. (Eds)**, Eustatic controls on clastic deposition; II, Sequence and systems tract models. Special Publication - Society of Economic Paleontologists and Mineralogists, v. **42**, p. 125-154.

Pulham, A. J., 1989. Controls on internal structure and architecture of sandstone bodies within Upper Carboniferous fluvial-dominated deltas, County Clare, western Ireland. In: **Whateley, M. K. G. and Pickering, K. T.**

(Eds.), Deltas; sites and traps for fossil fuels. Geological Society Special Publications, v. **41**, p. 179-203.

Qiu, X., Priestley, K. and McKenzie, D., 1996. Average lithospheric structure of Southern Africa. Geophysical Journal International, v. **127**, n. 3, p. 563-587.

Rabinowitz, P.D., 1971. Gravity anomalies across the East African continental margin. J. Geophys. Res., Vol. **76**, pp. 7107-7117.

Rabinowitz, P.D.; Coffin, M.F. and Falvey, D., 1981. The Madagascar-Africa separation. Eos, Transactions, American Geophysical Union, Vol. **62**, n. 17, p. 297-298.

Rabinowitz, P.D.; Coffin, M.F.; Falvey, D., 1982. Salt diapirs bordering the continental margin of Northern Kenya and Southern Somalia. Science, Vol. 215, n. 4533, p. 663-665.

Rabinowitz, P.D.; Coffin, M.F. and Falvey, D., 1983. The separation of Madagascar and Africa. Science, Vol. **220**, n. 4592, p. 67-69.

Rao, D. A. and Ram Babu, H. V., 1984. On the half-slope and straight-slope methods of basement depth determination. Geophysics, v. **49**, n. 8, p. 1365-1368.

Rider, M.H., 1974. The Namurian of west County Clare. Proceedings of the Royal Irish Academy, Section B: Biological, Geological and Chemical Science, v. **74**, n. 9, p. 125-142.

Rider, M.H., 1978. Growth faults in Carboniferous of western Ireland.AAPG Bulletin, v. **62**, n. 11 Part 1, , p. 2191-2213.

Rona, P.A., 1982. Evaporites at passive margins. In: **Scrutton, R.A. (Ed.)**, Dynamics of passive margins. Geodynamics Series, v. **6**, p. 116-132.

Salman, G., Vissotski, N.I. and Vedrintsev, A.B., 1985. The Geology and Hydrocarbon Prospectivity of Mozambique. Vol.**I** and **II**, ENH Archives, Maputo, Mozambique.

Salman, G. and Abdula, I., 1995. Development of the Mozambique and Ruvuma sedimentary basins, offshore Mozambique. Sedimentary Geology, v. **96**, n. 1-2, p. 7-41.

Schneider, F., Bouteca, M. and Vasseur, G., 1994. Validity of the porosity/effective-stress concept in sedimentary basin modelling. Fist Break, Vol. **12**, no. 6, p. 321-326.

Schon, J., 1983. Petrophysik. Akademie-Verlag. Berlin, 405 p.

Schon, J., 1996. Physical properties of rocks - Fundamentals and principles of petrophysics. Pergamon, London, 583 p.

Sclater, J. G. and Christie, P. A. F., 1980. Continental stretching; an explanation of the post-Mid-Cretaceous subsidence of the central North Sea basin. Journal of Geophysical Research, v. **85**, n. B7, p. 3711-3739.

Scotese, C.R., 1991. Jurassic and Cretaceous plate tectonic reconstructions. Palaeogeography, Palaeoclimatology, Palaeoecology, v. **87**, n. 1-4, p. 493-501.

Scrutton, R.A., 1976a. Continental breakup and deep crustal structure at the margins of southern Africa. In: **Almeida, F.M. (Editor)**, Proceedings of the International Symposium on Continental Margins of Atlantic Type, sao Paulo. Ann. Brazil Acad. Sci., **48** (Supplement), pp. 275-286.

Scrutton, R.A., 1976b. Crustal structure at the continental margin south of South Africa. The Geophysical Journal of the Royal Astronomical Society, v. **44**, n. 3, p. 601-623.

Scrutton, R.A., Dingle, R. V., 1976. Observations on the processes of sedimentary basin formation at the margins of southern Africa. Tectonophysics, v. 36, n. 1-3, p. 143-156.

Scrutton, R.A., 1978. Davie Fracture Zone and the movement of Madagascar. Earth and Plan. Sci. Letts., Vol. **39**, pp. 84-88.

Scrutton, R.A., 1979. On sheared passive continental margins. Tectonophysics, v. **59**, n. 1-4, p. 293-305.

Scrutton, R.A., Heptonstall, W.B. and Peacock, H.J., 1981. Constraints on the motion of Madagascar with respect to Africa. Mar.-Geol., Vol. **43**, No.1-2, pp. 1-20.

Scrutton, R.A., 1982a. Dynamic of passive margins. Geodynamics Series v. **6**, AGU, Geol. Soc. Am., Boulder, Colorado.

Scrutton, R.A., 1982b. Passive continental margins; a review of observations and mechanisms. In: **Scrutton, Roger A. (Ed.)**, Dynamic of passive margins. Geodynamics Series v. **6**, p. 5-11.

Segoufin, Jacques, 1981. Morphologie et structure du canal Mozambique. Univ. Strasbourg 1, Strasbourg 1, France (Doctoral, Th.: Sci. phys. Degree), 162 p.

Segoufin, J., 1978. Anomalies magnetiques mesozoiques dans le bassin de Mozambique. Acad. Sci., Paris , C. R., Ser. D., Vol. **287**. No. 3, pp. 109-112.

Selley, R. C., 1976. Subsurface facies analysis. The Log Analyst, v. **17**, n. 1, p. 3-11.

Selley, R. C., 1992. Ancient Sedimentary Environments. 3rd edition, Chapman and Hall, London, New York, Tokyo, Melbourne, Madras.

Serra, O., 1986. Fundamentals of Well-log Interpretation: 2. The Interpretation of Logging Data. Developments in Petroleum Science, v. **15B**, 684 p. Elsevier, Amsterdam, Netherlands.

Sheriff, R. E., 1991. Encyclopedic Dictionary of Exploration Geophysics. Geophysical references series. Soc. Explor. Geophys., Third Edition, 376 p., Tulsa, OK, United States.

Short, K. C. and Staeuble, A. J., 1967. Outline of geology of Niger delta. AAPG Bulletin, v. **51**, n. 5, p. 761-799.

Skeels, D.C., 1947. Ambiguity in gravity interpretation. Geophysics, v. **12**, n. 1, p. 43-56.

Sloss, L. L., 1963. Sequences in the cratonic interior of North America. Geological Society of America Bulletin, v. **74**, n. 2, p. 93-113.

Smith, R.M.H., 1990. A review of stratigraphy and sedimentary environments of the Karoo Basin of South Africa. In: **Kogbe, C. A. and Lang, J. (Eds)**, Major African continental Phanerozoic complexes and dynamics of sedimentation. Journal of African Earth Sciences, v. **10**, n. 1-2, p. 117-137.

Smith, A.G. and Hallam, A., 1970. The fit of the southern continents. Nature, Vol. **225**, n. 5228, pp. 139-144.

Smith, R.A., 1959. Some depth formulae for local magnetic and gravity anomalies. Geophysical prospecting, Vol. **7**, pp. 55-63.

Smith, R.A., 1961. Some theorems concerning local magnetic anomalies. Geophysical prospecting, Vol. **9**, pp. 399-410.

Steckler, M. S. and Watts, A. B., 1978. Subsidence of the Atlantic-type continental margin off New York. Earth and Planetary Science Letters, v. **41**, n. 1, p. 1-13.

Stuart, G. W. and Zengeni, T. G., 1987. Seismic crustal structure of the Limpopo mobile belt, Zimbabwe. Tectonophysics, v. **144**, n. 4, p. 323-335.

Tankard, A.J., Jackson, M.P.A., Eriksson, K.A., Hobday, D.K., Hunter, D.R. and Minter, W.E.L. 1982. Crustal evolution of southern Africa; 3.8 billion years of Earth history. Springer-Verlag, New York, 523 p.

Telford, W. M., Geldart, L. P. and Sheriff, R.E., 1990. Applied geophysics. Cambridge Univ. Press, Cambridge, 770 p.

Underhill, J.R., 1991. Controls on Late Jurassic seismic sequences, Inner Moray Firth, UK North Sea; a critical test of a key segment of Exxon's original global cycle chart. Basin Research, v. **3**, n. 2, p. 79-98.

Underhill, J. R. and Partington, M. A., 1993. Jurassic thermal doming and deflation in the North Sea; implications of the sequence stratigraphic evidence. In: **Parker, J. R. (Ed.)**, Petroleum geology of Northwest Europe; Proceedings of the 4th conference. Petroleum Geology of Northwest Europe: Proceedings of the 4th Conference, Vol. **4**, p. 371-386.

Vail, P.R., Mitchum, R. M., Jr. and Thompson, S., III, 1977a. Seismic stratigraphy and global changes of sea level; Part 3, Relative changes of sea level from coastal onlap. In: **Payton, C. E. (Ed.)**, Seismic stratigraphy; applications to hydrocarbon exploration. Memoir - American Association of Petroleum Geologists, n. **26**, p. 63-81.

Vail, P.R., Mitchum, R. M., Jr. and Thompson, S., III, 1977b. Seismic stratigraphy and global changes of sea level; Part 4, Global cycles of relative changes of sea level. In: **Payton, C. E. (Ed.)**, Seismic stratigraphy; applications to hydrocarbon exploration. Memoir - American Association of Petroleum Geologists, n. **26**, p. 83-97.

Vail, P.R., Todd, R. G. and Sangree, J. B., 1977c. Seismic stratigraphy and global changes of sea level; Part 5, Chronostratigraphic significance of seismic reflections. In: **Payton, C. E. (Ed.)**, Seismic stratigraphy; applications to hydrocarbon exploration. Memoir - American Association of Petroleum Geologists, n. **26**, p. 99-116.

Vail, P.R., Hardenbol, J. and Todd, R. G., 1984. Jurassic unconformities, chronostratigraphy, and sea-level changes from seismic stratigraphy and biostratigraphy. In: **Schlee, J.S. (Ed.)** Interregional unconformities and hydrocarbon accumulation. AAPG Memoir, v. **36**, p. 129-144.

Vail, P.R., 1987. Seismic stratigraphy interpretation using sequence stratigraphy; Part 1, Seismic stratigraphy interpretation procedure. In: **Bally, A.W.**

(Ed.), Atlas of seismic stratigraphy. AAPG Studies in Geology, v. **27**, n. 1, p. 1-10.

Van Wagoner, J. C., Mitchum, R. M., Jr., Posamentier, H.W. and Vail, P. R., 1987. Seismic stratigraphy interpretation using sequence stratigraphy; Part 2, Key definitions of sequence stratigraphy. In: **Bally, A. W. (Ed.)**, Atlas of seismic stratigraphy. AAPG Studies in Geology, v. **27**, n. 1, p. 11-14.

Van Wagoner, J.C., Mitchum, R.M., Campion, K.M. and Rahmanian, V.D., 1990. Siliciclastic sequence stratigraphy in well logs, cores, and outcrops; concepts for high-resolution correlation of time and facies. American Association of Petroleum Geologists, Tulsa, OK, United States. Methods in Exploration Series, v. **7**, pp. 1-55.

Veevers, J.J., Powell, C.M. and Johnson, B.D., 1980. Seafloor constraints on the reconstruction of Gondwanaland. Earth Planet. Sci. Lett. Vol. **51**, No. 2, pp. 275-278.

Walker, K. R., 1992. The marine flooding interval between the Moccasin and overlying "Martinsburg" formations; a 3rd order sequence boundary. In: **Driese, S.G., Mora, C.I., Walker, K.R. (Eds.)**, Paleosols, paleoweathering surfaces, and sequence boundaries. Studies in Geology (Knoxville), v. **21**, p. 26-33.

Watts, A.B. and Marr, C., 1995. Gravity anomalies and the thermal and mechanical structure of rifted continental margins. In: **Banda *et al.* (Eds.)**, Rifted ocean-continent boundaries, p. 65-94.

Wescott, W.A., 1988. A Late Permian fan-delta system in the southern Morondava Basin, Madagascar. In: **Nemec, W., Steel, R. J. (Eds.)**, Fan deltas; sedimentology and tectonic settings, p. 226-238.

Worzel, J.L. and Shurbet, G. L., 1955. Gravity interpretations from standard oceanic and continental crustal Sections. Special Paper - Geological Society of America, , p. 87-100.

Worzel, J.L., 1974. Standard oceanic and continental structure. In: **Burk, C.A. and Drake, C.L. (Eds.)**, The geology of continental margins, v. **39**, p. 59-66.

Wright, R. P.and Askin, R. A., 1987. The Permian-Triassic boundary in the southern Morondava Basin of Madagascar as defined by plant microfossils. In: **McKenzie, G.D. (ed.)**, Gondwana Six; Stratigraphy, sedimentology, and paleontology. Geophysical Monograph, v. **41**, p. 157-166.